

UCSF

UC San Francisco Electronic Theses and Dissertations

Title

Examining the regulation of hepatic drug disposition and metabolism by organic anion transporting polypeptide, P-glycoprotein and multidrug resistance-associated protein 2

Permalink

<https://escholarship.org/uc/item/9gp2s0gp>

Author

Lau, Yvonne Yi-Yang

Publication Date

2006

Peer reviewed|Thesis/dissertation

Examining the Regulation of Hepatic Drug Disposition and Metabolism by Organic Anion Transporting Polypeptide, P-glycoprotein and Multidrug Resistance-associated Protein 2

by

Yvonne Yi-Yang Lau

B.Sc. Biomedical Engineering, Johns Hopkins University, Baltimore, Maryland

DISSERTATION

Submitted in partial satisfaction of the requirements for the degree of

DOCTOR OF PHILOSOPHY

in

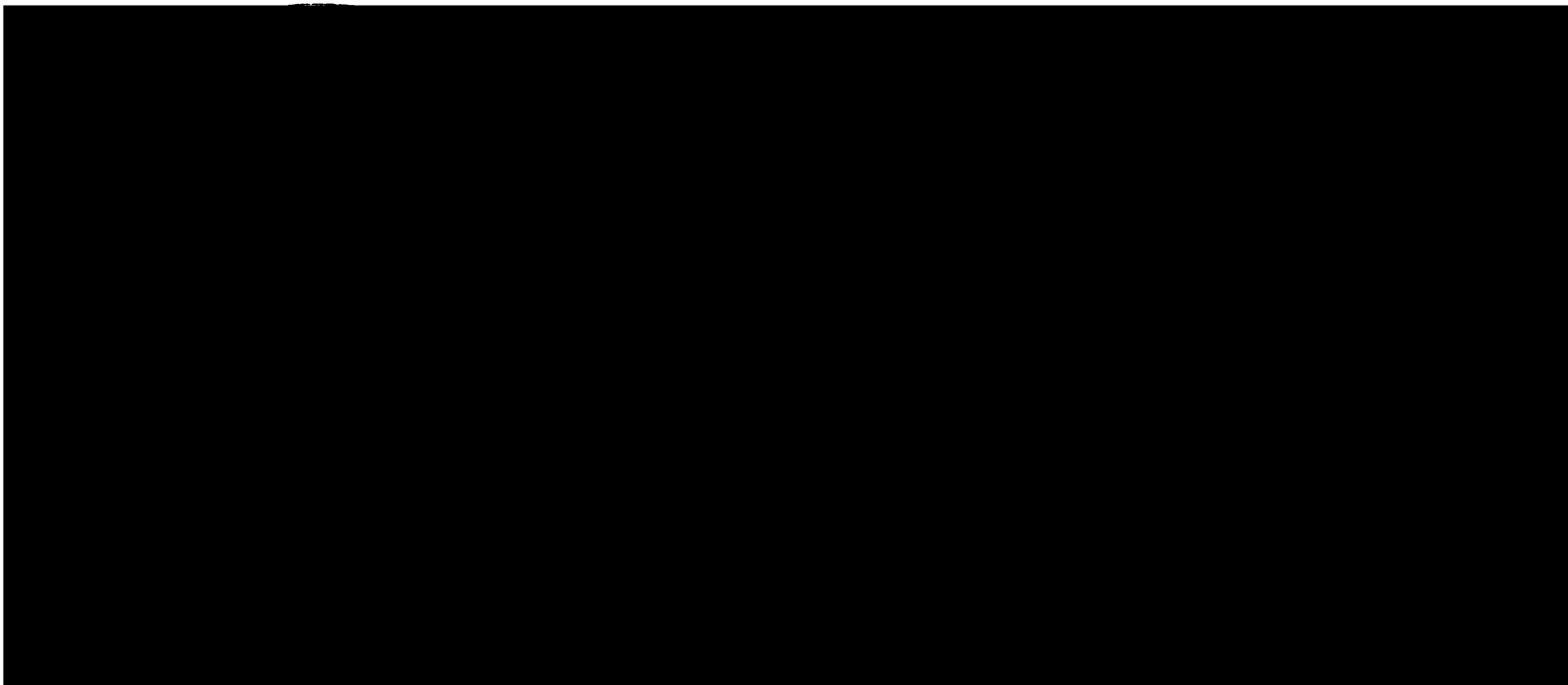
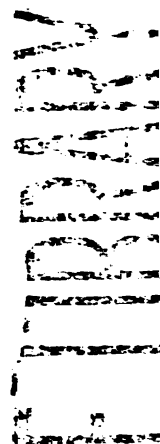
PHARMACEUTICAL SCIENCES AND PHARMACOGENOMICS

in the

GRADUATE DIVISION

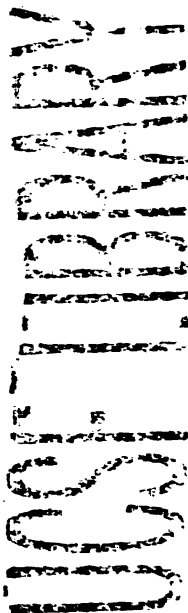
of the

UNIVERSITY OF CALIFORNIA, SAN FRANCISCO



This dissertation is dedicated to:

My parents, C.P. Lau and Marilyn Yu



ACKNOWLEDGEMENTS

This thesis is the result of four and a half years of work whereby I have been accompanied and supported by many people. It is a pleasure to now have the opportunity to express my gratitude to all of them.

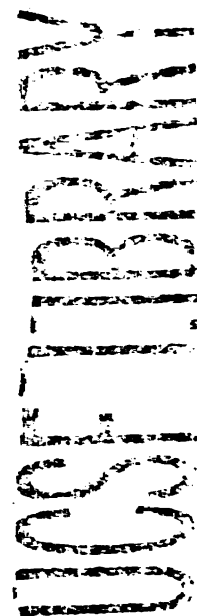
First of all, I would like to express my deepest gratitude to my supervisor, Dr. Leslie Z. Benet, for his support and patience throughout my study. It has been quite a rewarding experience for me, from not knowing who “Leslie Benet” was when I first came to UCSF, to becoming one of his students and now approaching graduation. I am constantly amazed by Les’ ability to provide guidance to students and postdoctoral scholars despite his hectic schedule, and his ability to see the big picture of a research problem and navigate the research focus of the lab while still giving each of us enough room to think independently and pursue our own interests. In particular, his openness to and support of students, as well as his devoted attitude to science, have made a deep impression on me and will remain with me lifelong.

I am also grateful for the thorough reviews and excellent comments received from my thesis committee, Drs Kathleen Giacomini and Betty-ann Hoener. Special thanks to Dr. Yong Huang for his analytical expertise, who helped me a great deal in developing the LC/MS-MS assays for animal and clinical samples, and also Dr. Emil Lin, for his kindness to students and generosity in providing me with the use of equipment at the Drug Studies Unit, UCSF. Sincere thanks to Dr. Lynda Frassetto from the General Clinical Research Center for her assistance and involvement with the many aspects related to my clinical study; Dr. Antony McDonagh from the UCSF Liver Center for

providing me with the TR⁺ rats for conducting perfused rat liver studies and Wendy Chan from the Genotyping Core Facility, UCSF, for genotyping my clinical samples. I would like to especially acknowledge Dr. Hideaki Okochi for the help extended to me, not only his excellent assistance in animal studies, but also for our many rewarding scientific discussions regarding study design.

I would like to thank former group members; I am obliged especially to Drs Chi-Yuan Wu, Carolyn Cummins, Hong Sun, Muhammad Baluom, Winnie Kim, Jae Chang, Nobuaki Watanabe and Ms. Sumiko Hirai for their assistance, valuable discussions and friendship. I would also like to thank Mike Goldenberg, Frances Peterson, Alan Wolfe and fellow graduate students and labmates, Justine Lam, Joseph Custodio, Sara Shugarts, Dr. HongXia Zheng and Dr. Selma Sahin, all of whom have made U66 a really pleasant place to work.

This acknowledgement would not be complete without mentioning my relatives and friends. Thanks to my cousins, Kai-Yeung Lau from UCSF and Janice Hui from Hong Kong, for consistently being there to support me and going through graduate school together with me. My buddy, Janie Zhou, has been my most trusted friend since freshman year. I am grateful that she constantly reminds me of how to enjoy life and always stay true to myself. Thanks to my Hopkins friends from the east coast, Dulles, Shugi and Brian, my Bay Area friends, Bik, Sherry, Helen, Alan and Adam, for sharing many happy moments with me. A special thanks goes to my elder cousin, Dr. Kong Loh, for all the advice that he has given to me regarding school and career for the past five years. I want to extend my sincere gratitude to my boyfriend, Wilbur Lee, for his unwavering and unconditional support for the past three years. Without him, I would be a less happy



person today. Lastly, I would like to thank my younger brother, Walter, who is unaware of how much his carefree lifestyle inspired me to see the lighter side of everything.

Finally and most importantly, I would like to thank my father, Dr. C.P. Lau and my mother, Marilyn Yu, who taught me the good things that really matter in life. Both scientists, they inspired me to pursue science as a profession and doing a PhD is definitely one of the best decisions I have made so far in my life. I would like to share this moment of happiness with my parents and my brother. They provided me enormous support during the whole period of my research.

UNIVERSITY OF CALIFORNIA LIBRARY

Abstract

EXAMINING THE REGULATION OF HEPATIC DRUG DISPOSITION AND METABOLISM BY ORGANIC ANION TRANSPORTING POLYPEPTIDE, P-GLYCOPROTEIN AND MULTIDRUG RESISTANCE-ASSOCIATED PROTEIN 2

Yvonne Yi-Yang Lau

There are many examples of clinical drug interactions at the level of metabolizing enzymes such as cytochrome P450 and much effort during drug development has been focused on determining the potential interactions between new drug molecules with enzymes. However, it now appears that members of the OATP uptake transporter family, as well as certain efflux pumps including P-glycoprotein (P-gp) and multidrug resistance-associated protein 2 (MRP2) are also key players in affecting drug disposition in the liver besides enzymes. We hypothesized that inhibition of hepatic uptake or efflux transporters would modify the disposition and metabolism of drugs.

My dissertation research primarily used the isolated perfused rat liver (IPRL) system, which retains all the relevant transporters and enzymes, to examine the pharmacokinetic changes at the organ level. The results from IPRL studies with digoxin with and without transporter inhibitors showed that inhibition of Oatp1a4 by rifampicin and P-gp by quinidine affects CYP3A metabolism significantly by decreasing and increasing clearance, respectively. The same perfused liver system was also applied to

atorvastatin, a compound that acts as a substrate of multiple transporters including Oatp, P-gp and Mrp2, as validated by cellular assays. Our data suggested that the Oatp-mediated uptake of both atorvastatin and its metabolites was inhibited by rifampicin. However, the extent of metabolism was significantly reduced as reflected by the reduced amounts of metabolites detected in rifampicin-treated livers.

Following an *in vivo* study examining the influence of rifampicin in reducing the clearance and metabolism of atorvastatin in rats, a clinical study was conducted to determine if the liver-specific transporter, OATP1B1, represents the major hepatic uptake system for atorvastatin and its active metabolites in humans. Our results demonstrated that acute inhibition of OATP1B1 caused a 6-fold increase in the exposure of atorvastatin and its metabolites. These data emphasize the relevance of OATP in affecting the hepatic elimination of atorvastatin. Metabolites of atorvastatin undergo similar disposition pathways as the parent drug.

Overall, the results from the IPRL study correlates well with *in vivo* studies and support our hypothesis that transporters are the major players in hepatic drug elimination, even for substrates that undergo extensive metabolism.

1
2
3
4
5
6
7
8
9
10
11
12
13
14
15
16
17
18
19
20
21
22
23
24
25
26
27
28
29
30
31
32
33
34
35
36
37
38
39
40
41
42
43
44
45
46
47
48
49
50
51
52
53
54
55
56
57
58
59
60
61
62
63
64
65
66
67
68
69
70
71
72
73
74
75
76
77
78
79
80
81
82
83
84
85
86
87
88
89
90
91
92
93
94
95
96
97
98
99
100

TABLE OF CONTENTS

ACKNOWLEDGEMENTS	iv
ABSTRACT	vii
LIST OF TABLES	xvi
LIST OF FIGURES	xviii

CHAPTER 1

INTRODUCTION: FACTORS AFFECTING THE HEPATIC DRUG ELIMINATION PATHWAY

1.1. Introduction	1
1.2. Significance of hepatic transport systems in drug disposition	3
1.3. Factors affecting hepatic drug elimination	5
1.3.1. Physiological factors	6
1.3.1.1. Anatomical considerations	6
1.3.1.2. Hepatic blood flow	8
1.3.2. Physicochemical factors	8
1.3.2.1. Lipophilicity	8
1.3.2.2. Ionization	9
1.3.3. Transmembrane factors	10
1.3.3.1. Transporters	12
1.3.3.2. Drug metabolizing enzymes	26
1.4. Relationship between hepatic drug transport and metabolic systems	32

1.4.1. Transporters affect the intrinsic ability of enzymes to metabolize drug	32
1.4.2. Overlap of substrate specificities between various hepatic transporters	34
1.4.3. Overlap of substrate specificities and regulation between hepatic transporters and drug metabolizing enzymes	35
1.4.4. Hypothesis and rationale	39
1.4.5. Specific aims	39

CHAPTER 2

EX SITU INHIBITION OF HEPATIC UPTAKE AND EFFLUX SIGNIFICANTLY CHANGES METABOLISM: HEPATIC ENZYME-TRANSPORTER INTERPLAY

2.1 Introduction	41
2.2 Materials and methods	44
2.2.1 Chemicals	44
2.2.2 Surgery and perfusion of isolated rat livers	44
2.2.3 Experimental design	45
2.2.4 Sample preparation	45
2.2.5 Measurement of digoxin and its metabolites	46
2.2.6 Measurement of rifampicin and quinidine levels in perfusate samples	47
2.2.7 Data analysis	48
2.3 Results	48
2.3.1 Effects of rifampicin and quinidine on digoxin disposition	48

2.3.2	Effects of rifampicin and quinidine on digoxigenin bisdigitoxoside disposition	51
2.3.3	Levels of digoxin and digoxigenin bisdigitoxoside in rifampicin- and quinidine-treated liver tissues	52
2.4	Discussion	54

CHAPTER 3

MULTIPLE TRANSPORTERS AFFECT THE DISPOSITION OF ATORVASTATIN AND ITS TWO ACTIVE HYDROXY METABOLITES: APPLICATION OF IN VITRO AND EX SITU SYSTEMS

3.1	Introduction	60
3.2	Materials and methods	63
3.2.1	Materials	63
3.2.2	Transient transfection and uptake transport assays	64
3.2.3	Preparation of cell culture monolayers and transport studies	65
3.2.4	Metabolism by rat liver microsomes	66
3.2.5	Surgery and perfusion of isolated rat livers	67
3.2.6	LC/MS-MS measurement of atorvastatin and metabolites	68
3.2.7	HPLC measurement of rifampicin	69
3.2.8	Data analysis	69
3.3	Results	71
3.3.1	Uptake studies in HEK293 cells with transient expression of uptake transporters	71
3.3.2	Transport studies of atorvastatin in MII, MII-cMOAT, and M-MDR1 cell systems	76
3.3.3	Metabolic studies of atorvastatin by rat microsomes	79

UNIVERSITY OF
 BRISTOL
 LIBRARY

3.3.4	Isolated perfused rat liver studies of atorvastatin	80
3.3.4.1	Atorvastatin-rifampicin interaction study	80
3.3.4.2	Wild-type Sprague-Dawley and TR ⁻ rats study	87
3.4	Discussion	88

CHAPTER 4

CYP3A4-TRANSFECTED CACO-2 CELLS AS A TOOL FOR UNDERSTANDING THE EFFLUX-METABOLISM INTERPLAY OF ATORVASTATIN IN THE INTESTINE AND THE LIVER

4.1	Introduction	94
4.2	Materials and methods	97
4.2.1	Materials	97
4.2.2	Cell culture growth conditions	97
4.2.3	Transport studies of atorvastatin across CYP3A4-transfected Caco-2 cells	98
4.2.4	Transport studies of 2-hydroxy atorvastatin and 4-hydroxy atorvastatin across M-MDR1 cells	99
4.2.5	LC/MS-MS measurement of atorvastatin and metabolites	100
4.2.6	Data analysis	100
4.3	Results	101
4.3.1	Transport of atorvastatin across CYP3A4-transfected Caco-2 cells	101
4.3.2	Metabolism of atorvastatin across CYP3A4-transfected Caco-2 cells	104
4.3.3	Extraction ratios of atorvastatin across CYP3A4-transfected Caco-2 cells	106
4.3.4	Atorvastatin metabolites transport across M-MDR1 cells	107
4.4	Discussion	110

CHAPTER 5

PHARMACOKINETICS OF ATORVASTATIN AND ITS HYDROXY METABOLITES IN RATS AND THE EFFECTS OF CONCOMITANT RIFAMPICIN SINGLE DOSES: RELEVANCE OF FIRST-PASS FROM HEPATIC UPTAKE TRANSPORTERS, INTESTINAL AND HEPATIC METABOLISM

5.1	Introduction	115
5.2	Materials and methods	118
5.2.1	Materials	118
5.2.2	Pharmacokinetic experiments in rats	118
5.2.3	Calculation of blood to plasma concentration ratio of atorvastatin in rats	119
5.2.4	Metabolism by rat small intestine microsomes	120
5.2.5	LC/MS-MS measurement of atorvastatin, 2-hydroxy-atorvastatin, 4-hydroxy-atorvastatin and rifampicin	121
5.2.6	Pharmacokinetic analysis	121
5.3	Results	123
5.3.1	Effect of rifampicin on the pharmacokinetics of atorvastatin under intravenous dosing	123
5.3.2	Effect of rifampicin on the pharmacokinetics of atorvastatin under oral dosing	127
5.3.3	Effect of rifampicin on the oral bioavailability, gut and liver metabolic extractions of atorvastatin	130
5.3.4	Metabolic studies of atorvastatin by rat small intestinal microsomes	131
5.4	Discussion	132

CHAPTER 6

**THE EFFECT OF OATP1B1 ON THE DISPOSITION OF
ATORVASTATIN IN HEALTHY VOLUNTEERS**

6.1	Introduction	138
6.2	Methods	142
6.2.1	Clinical study	142
6.2.1.1	Subjects and study design	142
6.2.1.2	Sequencing analysis for <i>SLCO1B1</i> polymorphisms identification	143
6.2.1.3	Analytical drug assays	145
6.2.1.4	Pharmacokinetic analysis	146
6.2.1.5	Statistical analysis	147
6.2.2	In vitro study	148
6.2.2.1	Materials	148
6.2.2.2	Transient transfection and uptake transport studies	148
6.2.2.3	Data analysis	149
6.3	Results	150
6.3.1	Clinical study	150
6.3.1.1	Effect of rifampicin on the pharmacokinetics of atorvastatin acid and lactone	150
6.3.1.2	Effect of rifampicin on the pharmacokinetics of atorvastatin metabolites in acid and lactone forms	154
6.3.1.3	Effect of rifampicin on the AUC ratios of each hydroxy-atorvastatin to atorvastatin (acid and lactone)	158
6.3.1.4	Rifampicin plasma concentrations	160

6.3.1.5 Comparisons of allelic and genotypic frequencies in study subjects	160
6.3.1.6 Effects of OATP1B1 polymorphisms on the pharmacokinetics of atorvastatin and its metabolites with and without rifampicin treatment	162
6.3.2 In vitro study	166
6.3.2.1 In vitro uptake kinetics of atorvastatin acid and rifampicin inhibitory effect on the uptake of atorvastatin in HEK293 cells transiently transfected with OATP1B1	166
6.3 Discussion	169

CHAPTER 7

Conclusion and perspectives

7.1 Overview	178
7.2 Cellular studies	179
7.3 Ex situ studies	180
7.4 In vivo studies	182
7.5 Clinical study	183
7.6 Concluding remarks	185

CHAPTER 8

References	188
-------------------	-----

LIST OF TABLES

Table 1.1	Organic anion transporting polypeptides	20
Table 1.2	Substrates of CYP3A4, P-gp, Mrp2 and OATPs/Oatps	37
Table 2.1	Comparison of parameters between control livers perfused with digoxin only and livers co-perfused with rifampicin or quinidine	50
Table 2.2	Comparison of relative volume of distribution steady-state values between control livers perfused with digoxin only and livers co-perfused with transporter inhibitors	53
Table 3.1	Atorvastatin transport and inhibition across MII and MII-cMOAT cell monolayers	77
Table 3.2	Effects of rifampicin on the microsomal metabolism of atorvastatin	79
Table 3.3	Comparison of parameters between control rat livers perfused with atorvastatin alone and livers co-perfused with rifampicin	83
Table 3.4	Percentage of the dose recovered as atorvastatin or hydroxy atorvastatin from rat livers perfused with atorvastatin alone and livers co-perfused with rifampicin	85
Table 3.5	Comparison of parameters between Sprague-Dawley and TR ⁻ rat livers perfused with atorvastatin	87
Table 4.1	Atorvastatin transport across CYP3A4-transfected Caco-2 cell monolayers in the absence and presence of GG918 and cyclosporine	102
Table 4.2	2-Hydroxy atorvastatin and 4-hydroxy atorvastatin transport across M-MDR1 cell monolayers in the absence and presence of GG918	108
Table 5.1	Pharmacokinetic variables for atorvastatin and its metabolites in rats after a single oral dose or intravenous dose of atorvastatin with and without rifampicin given as a bolus intravenous dose	126

Table 5.2	Summary of derived pharmacokinetic parameters of atorvastatin after single oral dose or intravenous dose of atorvastatin with and without rifampicin given as a bolus intravenous dose	130
Table 5.3	Measures of atorvastatin bioavailability and calculated hepatic and gut metabolic extraction	131
Table 5.4	Effects of rifampicin on the intestinal microsomal metabolism of atorvastatin	132
Table 6.1	Single-nucleotide polymorphism primers for identification of <i>SLCO1B1</i> polymorphisms using sequencing	145
Table 6.2	Pharmacokinetic variables of atorvastatin acid and lactone in 12 healthy volunteers after a single oral dose of 40 mg atorvastatin with and without intravenous rifampicin	153
Table 6.3	Pharmacokinetic variables of 2- and 4-hydroxy-atorvastatin acid and lactone in 12 healthy volunteers after a single oral dose of 40 mg atorvastatin with and without intravenous rifampicin	157
Table 6.4	Haplotypes of <i>OATP1B1</i> gene in 11 subjects	161
Table 6.5	AUC values of atorvastatin and its metabolites after a single dose of atorvastatin with and without intravenous rifampicin in two <i>OATP1B1</i> genotypic groups : <i>OATP1B1</i> *1a/*1a and *1a/*15	163
Table 7.1	Pharmacokinetics of tacrolimus, digoxin and atorvastatin in perfused rat liver preparation with and without transporter inhibitors	181

LIST OF FIGURES

Figure 1.1	Schematic representation of a cross section of liver	7
Figure 1.2	Human hepatic canalicular transport proteins	12
Figure 1.3	Human hepatic basolateral transport proteins	13
Figure 1.4	Transmembrane topology of OATP1B1 with two major allelic variants	22
Figure 2.1	Influence of rifampicin and quinidine on concentrations of digoxin in perfusate following addition of 10 µg of digoxin to the perfusate	49
Figure 2.2	Perfusate time course of rifampicin and quinidine	50
Figure 2.3	Influence of rifampicin and quinidine on concentrations of digoxigenin bisdigitoxoside in perfusate following addition of 10 µg of digoxin to the perfusate	51
Figure 2.4	Amounts of digoxin and digoxigenin bisdigitoxoside recovered in control, rifampicin-treated and quinidine-treated liver tissues	53
Figure 3.1	Uptake of atorvastatin in HEK293 cells with transient expression of Oatp uptake transporters	72
Figure 3.2	Concentration-dependent uptake of atorvastatin into Oatp1a4 and Oatp1b2 transiently transfected HEK293 cells	73
Figure 3.3	Inhibitory effect of rifampicin on the uptake of atorvastatin by Oatp1a4 and Oatp1b2 transient transfected HEK293 cells	74
Figure 3.4	Uptake of 2-hydroxy atorvastatin and 4-hydroxy atorvastatin in HEK293 cells with transient expression of Oatp1b2 in the presence and absence of rifampicin	75
Figure 3.5	Cis-inhibition of atorvastatin uptake in HEK293 cells with transient expression of Oatp1b2 by 2-hydroxy atorvastatin and 4-hydroxy atorvastatin	76

Figure 3.6	Effects of efflux transport inhibitors on atorvastatin transport: rifampicin across M-MDR1 cells and GG918 across M-MDR1 cells	78
Figure 3.7	Influence of rifampicin on concentrations of atorvastatin, 2-hydroxy atorvastatin and 4-hydroxy atorvastatin in perfusate	81
Figure 3.8	Time profile of cumulative amount of atorvastatin and total hydroxy atorvastatin detected in bile in control and rifampicin-treated perfused rat livers	86
Figure 4.1	The spatial relationship between the enzyme and transporters in the intestine and the liver as mimicked by the cellular system	96
Figure 4.2	Bidirectional transport of atorvastatin across CYP3A4-transfected Caco-2 cell monolayers in the absence and presence of P-gp inhibitors, GG918 and cyclosporine	103
Figure 4.3	Intracellular levels of atorvastatin in CYP3A4-transfected Caco-2 cells after an apical or basolateral dose in the absence and presence of the inhibitors, GG918 and cyclosporine	104
Figure 4.4	2-Hydroxy atorvastatin and 4-hydroxy atorvastatin found inside the CYP3A4-transfected Caco-2 cells at 3 hours after an apical or basolateral atorvastatin dose	105
Figure 4.5	Extraction ratio of atorvastatin after an apical dose or basolateral dose of atorvastatin in CYP3A4-transfected Caco-2 cells	107
Figure 4.6	The intracellular amounts of 2-hydroxy atorvastatin or 4-hydroxy atorvastatin detected inside M-MDR1 cells at 3 hour after an apical or basolateral dose of either 2-hydroxy atorvastatin or 4-hydroxy atorvastatin	109
Figure 5.1	Mean plasma concentrations of atorvastatin, 2-hydroxy atorvastatin and 4-hydroxy atorvastatin in rats after a single intravenous dose of 2 mg/kg atorvastatin with and without rifampicin given as a bolus intravenous dose (20 mg/kg)	124

Figure 5.2	Mean plasma concentrations of atorvastatin, 2-hydroxy atorvastatin and 4-hydroxy atorvastatin in rats after a single oral dose of 10 mg/kg atorvastatin with and without rifampicin given as a bolus intravenous dose (20 mg/kg)	128
Figure 5.3	Mean plasma concentration of rifampicin following a single intravenous dose in an atorvastatin rat pharmacokinetic study with rifampicin co-administration	132
Figure 6.1	The proposed metabolic pathways of atorvastatin	139
Figure 6.2	Mean plasma concentration of atorvastatin acid and atorvastatin lactone in 12 healthy volunteers after a single oral dose of 40 mg atorvastatin with and without intravenous rifampicin	151
Figure 6.3	Individual AUC ratios of atorvastatin lactone to atorvastatin acid in 12 healthy volunteers after a single oral dose of 40 mg atorvastatin with and without intravenous rifampicin	152
Figure 6.4	Mean plasma concentration of 2-hydroxy-atorvastatin acid, 2-hydroxy-atorvastatin lactone; 4-hydroxy-atorvastatin acid, and 4-hydroxy-atorvastatin lactone in 12 healthy volunteers after a single oral dose of 40 mg atorvastatin with and without intravenous rifampicin	155
Figure 6.5	Individual AUC ratios of 2-hydroxy-atorvastatin lactone to 2-hydroxy-atorvastatin acid and 4-hydroxy-atorvastatin lactone to 4-hydroxy-atorvastatin acid in 12 healthy volunteers after a single oral dose of 40 mg atorvastatin with and without intravenous rifampicin	156
Figure 6.6	Individual AUC ratios of 2-hydroxy-atorvastatin acid to atorvastatin acid; 4-hydroxy-atorvastatin acid to atorvastatin acid; 2-hydroxy-atorvastatin lactone to atorvastatin lactone; and 4-hydroxy-atorvastatin lactone to atorvastatin lactone in 12 healthy volunteers after a single oral dose of 40 mg atorvastatin with and without intravenous rifampicin	159

Figure 6.7	Mean plasma concentration of a single intravenous infusion of rifampicin given half an hour before a single oral dose of atorvastatin in 12 healthy volunteers	160
Figure 6.8	Mean plasma concentrations of atorvastatin acid and metabolites in 11 healthy volunteers after a single oral dose of 40 mg atorvastatin with and without intravenous rifampicin in two OATP1B1 genotypic groups: <i>OATP1B1</i> *1a/*1a and *1a/*15	164
Figure 6.9	Uptake of atorvastatin and hydroxy-atorvastatin acids at 1 μ M into HEK293 cells with transient expression of OATP1B1 or vector control	167
Figure 6.10	Concentration-dependent uptake of atorvastatin into OATP1B1 transiently transfected HEK293 cells	167
Figure 6.11	Inhibition of the uptake of atorvastatin by rifampicin into OATP1B1 transiently transfected HEK293 cells	168

Chapter 1

INTRODUCTION: FACTORS AFFECTING THE HEPATIC DRUG ELIMINATION PATHWAY

1.1 Introduction

The human body is constantly exposed to a wide array of xenobiotics, ranging from food components, environmental toxins to pharmaceuticals, and has developed complex mechanisms to detoxify these substances. Historically, enzymatic metabolism is regarded as the major process for drug detoxification and the liver has traditionally been considered as the major site for drug metabolism. Hepatic metabolism is mainly driven by oxidative (Phase I) and conjugative (Phase II) drug metabolizing enzymes. After entering the liver, drug molecules are generally oxidized by cytochrome P450 (CYP) enzymes prior to undergoing conjugation, as the oxidized functional group is usually the target for Phase II enzymes, which mediate conjugation by adding endogenous polar or ionic groups to make the compound more hydrophilic for elimination.

In recent years, clear evidence has emerged to suggest that membrane transporters localized in the liver are critical factors in determining drug disposition. For instance, the role of ATP-driven efflux transporters such as P-glycoprotein (P-gp) and multidrug resistance-associated protein 2 (MRP2/Mrp2; human/rodent), in mediating biliary excretion at the canalicular (i.e. apical) border of hepatocytes (the parenchymal cells of the liver) has been widely studied (Keppler and Arias, 1997; Schinkel, 1997; Borst et al.,

1999). At the sinusoidal (basolateral) border, the more recently discovered uptake transporters such as the organic anion-transporting peptides (OATP/Oatp; human/rodent) are present to facilitate transport of organic ions and endogenous compounds, such as bile acids, into the liver (Meier et al., 1997; Hagenbuch and Meier, 2004; Mikkaichi et al., 2004). Based on the localization of drug uptake and efflux transporters in the hepatocytes, it appears that the directional movement of compounds across the liver requires the coordinated activity of both types of transporters.

For the past decade, our laboratory has conducted a series of cellular, animal and human studies to investigate the interplay between intestinal P-gp and CYP3A in changing overall drug absorption and metabolism (Wacher et al., 1998; Cummins et al., 2002a, 2004). These studies reveal that the role of P-gp in the intestine extends beyond simply limiting parent drug absorption but also includes increasing the access of drug to intestinal metabolism by CYP3A through repeated cycles of absorption and efflux between the gut lumen and the enterocytes (epithelial cells of the intestine). Along this line of thinking, we hypothesized that hepatic metabolism can also be altered by changes that occur only in transporters residing in the basolateral and apical border of hepatocytes, which control the entrance and the exit of drug compounds, respectively.

The overall goal of this dissertation research was to examine the effects of hepatic transporters, both uptake (OATP) and efflux (P-gp and MRP2), on drug disposition and the metabolism process. Using *in vitro* and *ex situ* models, hepatic transport and CYP3A-mediated metabolism were examined in microsomal systems, CYP3A4-transfected Caco-2 cells and isolated perfused rat livers in the presence and absence of transporter inhibitors. The influence of individual transporters in modulating drug disposition was

also studied by applying various transporter-overexpressing cellular systems. To investigate the effect of hepatic transporter inhibition upon systemic drug disposition, first-pass elimination and overall bioavailability, both animal and clinical studies were conducted.

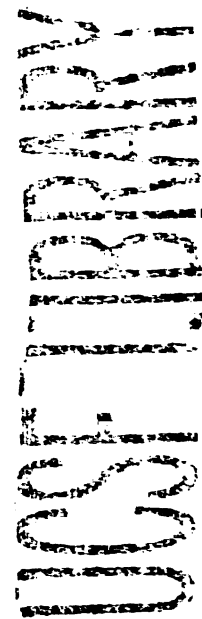
1.2 Significance of hepatic transport systems in drug disposition

The liver functions as a clearance organ responsible for the elimination of a large variety of drugs and metabolic products. Two carrier-mediated processes govern the sequential transport across hepatocytes: sinusoidal (basolateral) uptake from the portal/arterial circulation and canalicular (apical) efflux into the bile. Canalicular efflux transporters P-gp, MRP2, breast cancer resistance protein (BCRP) and the bile salt export pump (BSEP) are the major ATP-dependent efflux pumps for excretion of drugs and metabolites into the bile (Chandra and Brouwer, 2004). Uptake transporters such as OATP, located at the basolateral membrane of hepatocytes, are responsible for the influx of bulky amphipathic and hydrophilic compounds (Meier et al., 1997). The expression of transporters at both hepatocyte membranes plays a critical role in determining the net transcellular transport and ultimately governs the pharmacokinetic and metabolism profiles of drug compounds in the body. During the past decade, there has been widespread interest in understanding the transport aspects of hepatic clearance of drugs among pharmaceutical scientists for several reasons:

1. **Oral bioavailability.** Good oral bioavailability is often an important consideration for the development of bioactive molecules as therapeutic

agents. Oral bioavailability of drug molecules is often limited by first-pass effects due to metabolism. However, a reduction in the availability of drugs after oral administration may also occur as a result of alteration in drug transport systems. Liver is an important organ for first-pass elimination. In some cases, enhanced hepatic uptake and/or biliary excretion due to induction of uptake and efflux transporters may reduce the systemic exposure of certain drugs and enhance their biotransformation to polar metabolites, thus limit their pharmacological activity. In other situations, extensive hepatic uptake may be beneficial to drug efficacy for drugs whose main target is in the liver, such as the HMG-CoA reductase inhibitors (i.e. statins).

2. **Systemic toxicity.** Inhibition of hepatic uptake and/or biliary excretion may be desirable for drug candidates as it enhances their systemic levels and availability. However, in some situations, inhibition of hepatic uptake transporter may increase the drug concentration and lead to systemic toxicity, causing adverse events. In other situations, inhibition of hepatic efflux transporters can lead to toxicity in hepatocytes.
3. **Drug-drug interactions.** Clinically relevant drug-drug interactions are often reported at the level of hepatic metabolism as co-administration of drug metabolizing enzyme inhibitors can increase the blood or plasma concentrations of drugs and the risk of adverse events. However, interactions can also occur by inhibition of the relevant hepatic transporters that are located both upstream and downstream of hepatic

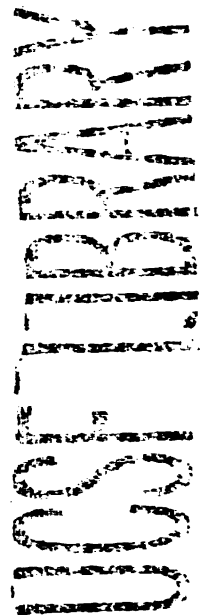


enzymes. For instance, the significant increase in drug exposure of the non-metabolizing rosuvastatin in transplant recipients on an antirejection regimen was attributed to the co-administration of cyclosporine, which is an inhibitor of OATP1B1 (previously known as OATP-C), a liver specific uptake transporter (Simonson et al., 2004).

4. **Drug-disease interactions.** Endogenous compounds may interact with hepatic transport proteins resulting in impaired transport activity. Such interactions may be direct or indirect in nature and may involve the up or down-regulation of protein expression. For instance, with the development of renal failure, certain uremic toxins inhibit the liver uptake of drugs and organic anions, such as bromosulphophthalein (BSP), indocyanine green (ICG), and thyroxine, where hepatic OATPs are the major transporters and cause a decrease in their hepatic clearance (Sun et al., 2006).

1.3 Factors affecting hepatic drug elimination

How well a drug compound traverses the polarized cell membranes of hepatocytes is governed by (A) physiological factors such as anatomy and blood flow, (B) the compound's physicochemical characteristics such as lipophilicity and the extent of ionization as well as (C) transmembrane factors such as transporters and drug-metabolizing enzymes. It is also important to note whether a carrier protein required for drug transport is in some way related to the physicochemical properties of the drug compound.



1.3.1 Physiological factors

When drug compounds enter the liver compartment, various anatomical and physiological variables control the fate of the drug elimination process.

1.3.1.1 Anatomical considerations

The liver is a highly perfused organ. Blood delivery to the liver is supplied by two major blood vessels: the hepatic artery (~20 % of the hepatic blood supply) and the portal vein (~ 80 % of the hepatic blood supply) (Fig. 1.1). Venous blood from the entire gastrointestinal tract (containing nutrients from the intestines) is brought to the liver by the hepatic portal vein. The hepatic portal vein branches within the liver to form the hepatic acinus, a complex capillary bed intimately associated with the hepatocytes. Blood from the hepatic artery and portal vein mix, and then travel through the liver sinusoids, which are specialized capillaries that have a unique endothelial system (Evans, 1980).

From the sinusoids, the blood enters the central vein, and then the hepatic veins are eventually drained directly into the inferior vena cava. The bile produced in the liver is collected into the bile canaliculi, which merge to form the bile ducts. These eventually drain into the right and left hepatic ducts, which in turn merge to form the common hepatic duct.

The hepatocytes are arranged in cords of one-cell thickness, surrounded by sinusoids on both sides, which bathe the hepatocytes in blood. Hepatocytes make up 60-80% of the cytoplasmic mass of the liver. They display membrane polarity: the sinusoidal membrane represents the basolateral surface, while the bile canalicular membrane only accounts for 15% of the total hepatocyte surface area, but is specialized for excretion

USF
LIBRARY

with the help of ATP-dependent efflux pumps (Evans, 1980). The basolateral and canalicular membranes differ in their biochemical composition and functional characteristics and are separated by tight junctions that seal off the bile canaliculi and hence form the only anatomical barrier maintaining the concentration gradients between the blood and the bile. The endothelial cells line the sinusoids but contain large holes (fenestrations) that allow direct contact between constituents of plasma, the sinusoids and the lateral surface membranes. This structural arrangement facilitates contact between plasma protein-bound drug and transporters on the hepatocytes surface membrane (Boyer, 1980).

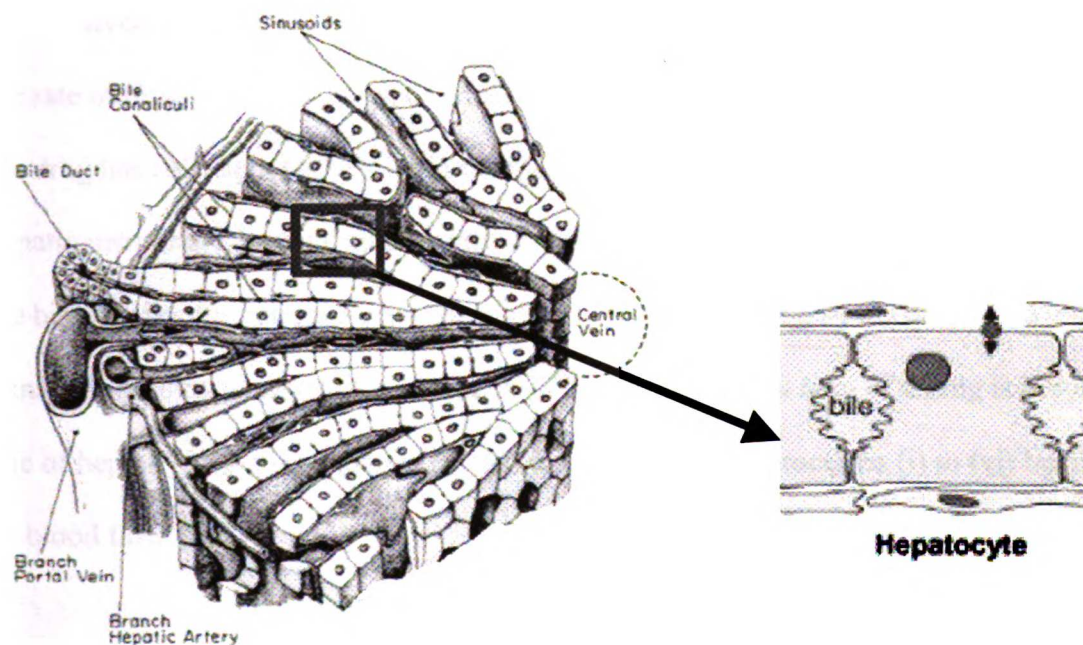


Fig. 1.1 Schematic representation of a cross section of liver. The adjoining hepatocytes illustrating the locations of the sinusoidal and canalicular membranes are also shown (from Molecular Biology of the Cell, 3rd edition, Alberts et al. New York, Garland Publishing).

1.3.1.2 Hepatic blood flow

The concentration gradient created between hepatic portal blood and hepatocytes drives the diffusion of drugs across the vascular endothelium, the Space of Disse, and finally, the sinusoidal plasma membrane of the hepatocytes. Processes such as (i) entrance of drug into the hepatocytes either by diffusion or carrier-mediated mechanisms, (ii) exit of drug from hepatocytes by biliary excretion, (iii) metabolism of drug in the hepatocytes and (vi) binding of drug to plasma protein or blood cells, are in competition with the bulk flow of blood that removes drug from the sinusoidal space into the hepatic venules.

Even when a drug has a high hepatic extraction ratio (ER_H ; a parameter relating the rate of drug extraction by an organ to the rate at which it is presented to the organ), the drug has sufficient time while in the liver to become unbound, pass through the hepatic membrane, be catalyzed by drug-metabolizing enzymes and/or transported into the bile. Under this condition, hepatic elimination is rate-limited by perfusion and not by transport, binding or metabolic processes. When the extraction ratio of a drug is low, the rate of hepatic drug elimination is limited by one or more of processes (i) to (vi) but not by blood flow.

1.3.2 Physicochemical factors

1.3.2.1 Lipophilicity

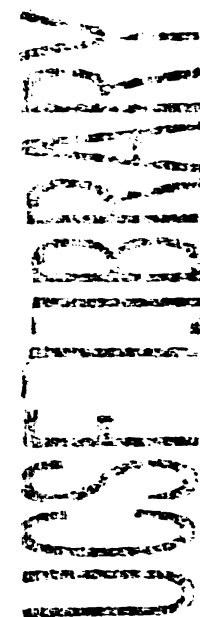
Lipophilicity is the key parameter in determining the ability of a drug to bind to plasma proteins and to cross lipid membrane barriers. Increasing lipophilicity of a

compound usually increases its protein binding, volume of distribution and permeability across cell membranes. At the same time, solubility and renal extraction decrease as well. Lipophilicity is measured by Log P (the log partition coefficient between octanol and water at neutral pH); Log D is used when the pH is specified.

Lipophilic compounds may move from sinusoidal plasma into the hepatic cytosol by passive diffusion. Their high permeability will allow them to cross the lipid membrane barrier efficiently without the aid from transporters *in vivo*. There is a positive correlation between the lipophilicity of drugs and the affinity towards drug metabolizing P450 enzymes (Lewis et al., 2004a). Besides, structure-activity relationship studies have shown that less lipophilic (more hydrophilic) compounds are often less likely to interact with the substrate binding site of efflux transporters such as P-gp (Klopman et al., 1997; Litman et al., 1997). For instance, pravastatin, which is more hydrophilic than other members of the statin family, exhibits weaker inhibitory properties toward P-gp mediated transport (Chen et al., 2005).

1.3.2.2 Ionization

The extent of ionization is determined by the relative pK_a (the acid dissociation constant) value of drug and the pH of the aqueous environment. A majority of the drugs currently on the market are either weak acids or weak bases. Each weak acid/base has a pK_a value. The value affects the proportion of drug molecules in the ionized and unionized forms. The ratio of ionized over unionized form affects the drug's solubility, permeability and the candidacy for uptake transporters.



The Henderson-Hasselbalch equation describes the derivation of pH as a measure of acidity in biological and chemical systems. Two equivalent forms of the equation are,

$$\text{pH} - \text{pK}_a = \log_{10} [\text{A}^-] / [\text{HA}] \quad \text{--- for acid}$$

$$\text{pH} - \text{pK}_a = \log_{10} [\text{B}] / [\text{BH}^+] \quad \text{--- for base}$$

where A^- is the conjugate base of the acid HA and BH^+ is the conjugate acid of the base B. Thus, when $\text{pH} - \text{pK}_a$ is equal to 1 for acids and equal to -1 for bases, $\sim 90\%$ of drug compounds exist in the ionized form.

The unionized form of a weak acid or weak base is the predominant form that can traverse the lipid bilayer of the cell plasma membrane or hepatocytes or other cell types. The ionized form of acid or base usually requires a carrier-mediated process to be transported across the plasma membrane. However, even compounds that are highly ionized can diffuse across the membrane in their unionized form, because of shifting equilibria.

1.3.3 Transmembrane factors

After a drug arrives in the systemic circulation following either oral or intravenous administration, it can enter the hepatocytes from sinusoidal capillaries and exit from hepatocytes into the bile canaliculi by multiple pathways: (i) passive diffusion, (ii) paracellular transport (between the cell junctions) and (iii) transcellular transport mediated by uptake carriers (facilitated diffusion) and active efflux pumps.

Many drugs are transported by a combination of pathways. For example, the kinetics of uptake of a drug molecule into hepatocytes can be described by the following equation,

$$v_0 = \underbrace{(V_{\max} \cdot C)/(K_m + C)}_{\text{Carrier-mediated uptake}} + \underbrace{P \cdot C}_{\text{Passive diffusion}}$$

where v_0 is the initial uptake rate, C is the substrate concentration, K_m is the Michaelis-Menten constant, V_{\max} is the maximal uptake rate, and P is the nonsaturable uptake clearance, also known as the permeability constant.

If multiple transporters are involved, multiple terms for carrier-mediated uptake are needed:

$$v_0 = \sum_i^n (V_{\max, i} \cdot C)/(K_{m, i} + C) + P \cdot C$$

where i represents the i th carrier-mediated uptake process of n processes.

There are two components in the equation, the saturable carrier-mediated uptake $[(V_{\max} \cdot C)/(K_m + C)]$ and the nonsaturable diffusion portion ($P \cdot C$), which follows Fick's law:

$$\frac{dQ}{dt} = \left(\frac{DAK_p}{h} \right) (C_1 - C_2)$$

dQ/dt - rate of diffusion D - diffusion coefficient
 A - surface area of membrane K_p - partition coefficient
 h - membrane thickness
 $C_1 - C_2$ = concentration difference for solute
 Generally, $C_1 \gg C_2$

UNIVERSITY OF
 SOUTH ALABAMA
 LIBRARY

Since D , A , K_p and h are constants, given a certain drug and membrane, and given that $C_1 \gg C_2$, then,

$$\frac{dQ}{dt} = PC_1$$

Where P - permeability constant

1.3.3.1 Transporters

Many studies have revealed the importance of transporters in drug disposition in the body. There is increasing recognition that transporters play a major role in drug absorption and elimination, as well as toxicity and efficiency. In this section, we summarize the various types of transporters that are known to be present at the sinusoidal and canalicular membranes of hepatocytes and involved in hepatobiliary excretion. Their locations in the liver are illustrated in Fig. 1.2 (canalicular transporters) and Fig. 1.3 (basolateral transporters).

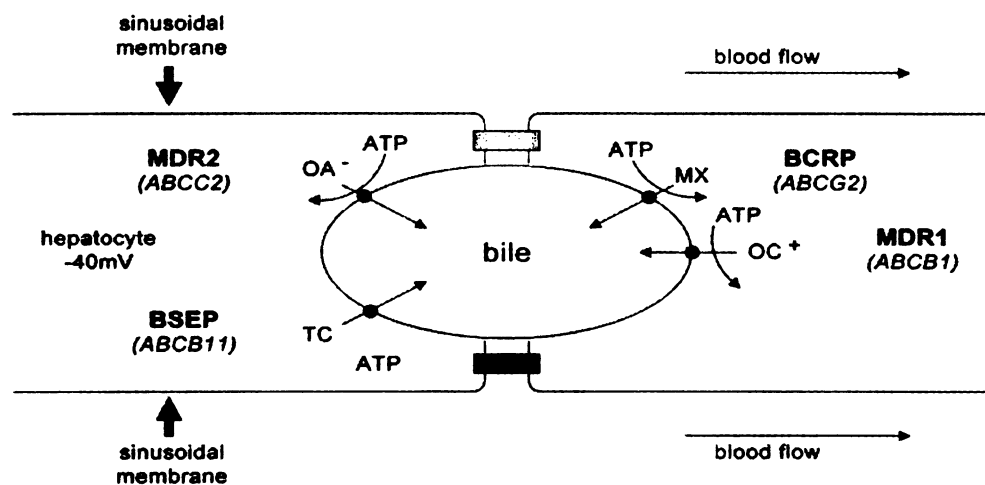


Fig 1.2 Human hepatic canalicular transport proteins. (OA^- : organic anions; OC^+ : organic cations; TC: taurocholate); Modified from Chandra and Brouwer (2004).

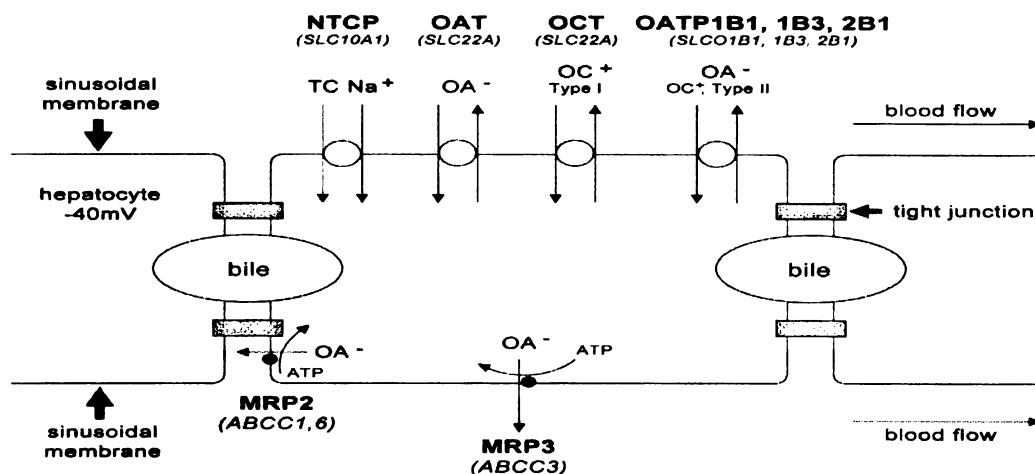


Fig 1.3 Human hepatic basolateral transport proteins. (OA⁻: organic anions; OC⁺: organic cations; TC: taurocholate); Modified from Chandra and Brouwer (2004).

(1) Drug transporters at the hepatic canalicular membrane

(1A) ABCB1 (P-gp):

The P-gp efflux pump belongs to the ATP-binding cassette transporter superfamily (Gottesman and Pastan, 1993). In humans, P-gp is encoded by the *MDR1* gene (or ABCB1), whereas in mice and rat two multidrug resistance proteins are encoded by the genes *mdr1a* and *mdr1b* (Gottesman and Pastan, 1993; Schinkel et al., 1997). Both genes encode for drug transporting functionality but have different tissue expression and substrate specificities. The P-gp substrate spectrum covers a wide range of structurally diverse compounds. Typically, the substrates are lipophilic (LogP > 1 and preferentially > 2), neutral or positively charged at physiological pH, bulky (molecular weight > 400) and exhibit one or more planar aromatic rings that enable interaction with a hypothesized

“flat” hydrophobic region of the MDR1 drug-binding domain (Seelig, 1998; Schmid et al., 1999).

Although the endogenous function of P-gp is not known, P-gp is predominantly recognized for its function as an efflux pump that removes xenobiotics from the interior of cells. In terms of its tissue distribution, P-gp is strategically expressed in organs and tissues that are involved in the defense mechanism against harmful xenobiotics. It is found on the luminal surface of the intestinal epithelia, the renal proximal tubule, the bile canalicular membrane of hepatocytes, the placenta and the blood-brain barrier (BBB) (Thiebaut et al., 1987; Cordon-Cardo et al., 1989).

In the liver, P-gp is expressed at the bile canalicular border of hepatocytes. Interference with P-gp mediated biliary secretion may affect drug clearance, cellular drug concentration in the liver, and hence the extent of hepatic metabolism. As demonstrated by a clinical study in which healthy volunteers were administered oral doses of digoxin for 8 consecutive days either with or without quinidine, followed by catheterization with a duodenal triple-lumen perfusion catheter to measure biliary clearance of digoxin on the 8th day, quinidine significantly decreased digoxin biliary clearance by 35% (Hedman et al., 1990). These studies indicate that alterations in biliary clearance caused by P-gp efflux are evident under experimental and clinical settings.

In addition to drug-drug interactions caused by P-gp inhibition, induction of P-gp has also been demonstrated in studies with pregnane X receptor (PXR) ligands, such as rifampicin and St. John’s Wort (Greiner et al., 1999). A 3.5-fold increase in intestinal P-gp expression and a decrease in the oral bioavailability of digoxin was observed when a

single oral dose of digoxin was administered in the presence and absence of rifampicin given 600 mg per day for 10 days (Greiner et al., 1999).

(1B) ABCG2 (BCRP):

Breast cancer resistance protein (BCRP) is an ABC half transporter, which was first detected in breast cancer cell lines (Doyle et al., 1998). It is primarily expressed in the small intestine, the placenta, the BBB and the hepatic canalicular membrane but not the kidney. In contrast to humans, mice display the highest expression of Bcrp1 in the kidney with moderate expression in the placenta (Allikmets et al., 1998; Doyle et al., 1998).

BCRP is a relatively novel transporter and its involvement in drug absorption and disposition has not been completely characterized. However, it has been suggested that BCRP plays a role in the secretion of drugs such as pitavastatin (Hirano et al., 2005b), and topotecan (Jonker et al., 2000). There is a certain level of substrate/inhibitor overlap between BCRP and P-gp. For example, cerivastatin is transported by both P-gp and BCRP (Matsushima et al., 2005); GG918, a potent inhibitor of both BCRP and P-gp increases the bioavailability of topotecan significantly in P-gp deficient mice. Given that topotecan is a selective substrate for BCRP and only weakly interacts with P-gp, these data suggest that the pharmacokinetics changes were due to BCRP inhibition (Jonker and Schinkel, 2004).

It has also been demonstrated that BCRP preferentially transports sulfated conjugates over glucuronide conjugates (Suzuki et al., 2003; Matsushima et al., 2005)

and that biliary excretion of the sulfated steroid was maintained even in the Mrp2-deficient rat (Takenaka et al., 1995).

(1C) ABCC2 (MRP2):

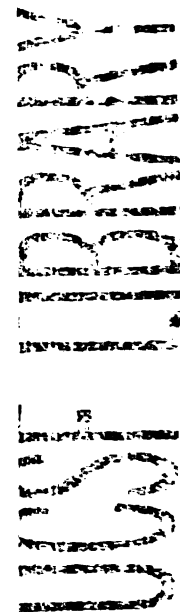
The multidrug resistance-associated protein 2 (MRP2), the most widely studied apical membrane transporter of the MRP/Mrp (human/rodent) family, previously known as canalicular multispecific organic anion transporter (cMOAT), is another major canalicular transporter responsible for the biliary excretion of both endogenous and exogenous compounds. It was originally cloned from rat liver as cMRP (Buchler et al., 1996) and from human liver named as cMOAT (Paulusma et al., 1996). MRP2 is mainly located on the apical membrane of the liver, intestine and kidney tubules (Buchler et al., 1996; Schaub et al., 1999; Fromm et al., 2000). Despite some overlap in substrate specificity between MRP2 and P-gp (Cole et al., 1994), MRP2 is mostly involved in the unidirectional biliary excretion of organic anions and drug conjugates such as phase II glutathione and glucuronide conjugates, bile acids, bilirubin and unconjugated drug compounds such as pravastatin (Sasaki et al., 2002), vincristine (Kawabe et al., 1999) and the fluorescent dye carboxy-2',7'-dichlorofluorescein (CF) (Fardel et al., 2005). Active efflux of unconjugated drugs and toxins has obvious implications for detoxification, since conjugated metabolites are generally regarded as less reactive. However, active efflux of conjugated products prevents cellular accumulation, thereby limiting reformation of the active parent compound either spontaneously or by enzymatic hydrolysis. MRP2 has been shown to act synergistically with several phase II conjugating enzymes including the GSH S-transferases (GSTs) and UDP-glucuronosyl transferases (UGTs) to minimize

toxicity of several electrophilic drugs including cytotoxic agents (Depeille et al., 2004; Smitherman et al., 2004). Mutations that disrupt MRP2 function cause bilirubin accumulation and jaundice in rats (Paulusma et al., 1996; Ito et al., 1997) and in patients. Clinically this diagnosis is called Dubin-Johnson syndrome (Paulusma et al., 1997). In rat strains such as EHBR (Esai hyperbilirubinemic rat) and TR-/GY rat lacking Mrp2, impaired biliary secretion of glutathione, glutathione conjugates and bilirubin glucuronides was observed (Buchler et al., 1996; Konig et al., 1999; Keitel et al., 2003).

(1D) ABCB11 (SPgp/BSEP):

BSEP, the bile salt export pump, also known as sister gene of P-glycoprotein, was first cloned from porcine liver (Childs et al., 1995) and exhibits expression predominantly in the canalicular membrane of liver hepatocytes. It is mainly responsible for mediating the hepatobiliary excretion of conjugated and unconjugated bile salts (Gerloff et al., 1998). Strautnieks et al. (1998) demonstrated that mutations in the human BSEP gene resulted in type 2 progressive familial intrahepatic cholestasis (PFIC2), a disease characterized by an interference in the hepatic secretion of bile salts.

Besides playing a critical role in mediating the secretion of endogenous compounds, studies using a cell line transfected with murine Bsep have shown that Bsep was capable of transporting drug compounds such as vinblastine and calcein-acetoxymethyl ester (Lecureur et al., 2000). Significant ATP-dependent uptake of pravastatin was also observed using membrane vesicles expressing human BSEP and rat Bsep (Hirano et al., 2005a). The xenobiotic substrate spectrum covered by BSEP still has not been fully explored, but based on its inability to transport many P-gp substrates such



as rhodamine 123, vincristine, daunorubicin, paclitaxel and digoxin, its role in drug disposition may be considerably more limited than that of its close relative, P-gp.

(2) Drug transporters at the hepatic sinusoidal membrane

(2A) SLCO (OATP):

The organic anion transporting polypeptides (OATP/Oatp; human/rodent) are encoded by the gene family SLCO (SLC21) (Hagenbuch and Meier, 2004) and are basolateral transporters that play an important role in hepatic clearance. OATPs mediate sodium-independent transport of a diverse array of endogenous and exogenous compounds that are mostly bulky, amphipathic anions as well as type II cations (bulky molecules with cationic groups located near the ring, e.g. quinidine) and neutral steroids. Typical substrates include bile acids, steroid conjugates, thyroid hormone, anionic oligopeptides and drugs such as digoxin, pravastatin and methotrexate (Hagenbuch and Meier, 2004; Mikkaichi et al., 2004). The transport mechanism for OATP is not yet fully understood but studies have demonstrated that rat Oatp1a1 (previously known as Oatp1) may function as a bi-directional transporter: hepatic uptake of substrates could be driven by the efflux of bicarbonate (Satlin et al., 1997) and countertransport of reduced glutathione that exists at high concentrations within hepatocytes (Li et al., 1998).

Eleven human OATP genes have been described in the literature. Hagenbuch and Meier (2004) have recently proposed a new species-independent nomenclature system for the OATP family, in which OATPs/Oatps are subdivided into families ($\geq 40\%$: family; $\geq 60\%$: subfamily). For instance, OATP1A2 belongs to family OATP1 and subfamily OATP1A. The old and new symbols as well as tissue location for OATP/oatp

(human/rodent) are listed in Table 1.1. Within this family, OATP1A2, OATP1B1, OATP1B3 and OATP2B1, previously known as OATP-A, -C, 8 and -B, respectively, are the proteins predominantly expressed on the sinusoidal membrane of human liver (Konig et al., 2000a; Kullak-Ublick et al., 2001).

11
12
13
14
15
16
17
18
19
20
21
22
23
24
25
26
27
28
29
30
31
32
33
34
35
36
37
38
39
40
41
42
43
44
45
46
47
48
49
50
51
52
53
54
55
56
57
58
59
60
61
62
63
64
65
66
67
68
69
70
71
72
73
74
75
76
77
78
79
80
81
82
83
84
85
86
87
88
89
90
91
92
93
94
95
96
97
98
99
100

Table 1.1 Organic anion transporting polypeptides (OATPs/Oatps; human/rodent).

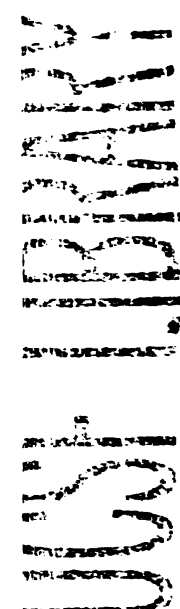
Modified from Hagenbuch and Meier (2004).

Novel protein name	Novel gene symbol	Old protein name	Old gene symbol	Expression
Human OATP				
OATP2A1	<i>SLCO2A1</i>	PGT	<i>SLC21A2</i>	Widely
OATP1A2	<i>SLCO1A2</i>	OATP-A	<i>SLC21A3</i>	Brain, Liver
OATP1B1	<i>SLCO1B1</i>	LST-1/OATP-C/OATP2	<i>SLC21A6</i>	Liver only
OATP1B3	<i>SLCO1B3</i>	LST-2/OATP8	<i>SLC21A8</i>	Liver only
OATP2B1	<i>SLCO2B1</i>	OATP-B	<i>SLC21A9</i>	Widely
OATP3A1	<i>SLCO3A1</i>	OATP-D	<i>SLC21A11</i>	Widely
OATP4A1	<i>SLCO4A1</i>	OATP-E	<i>SLC21A12</i>	Widely
OATP1C1	<i>SLCO1C1</i>	OATP-F	<i>SLC21A14</i>	Brain, testis
OATP5A1	<i>SLCO5A1</i>	OATP-J/OATP-RP4	<i>SLC21A15</i>	?
OATP6A1	<i>SLCO6A1</i>	GST/OATP-1	<i>SLC21A19</i>	Testis
OATP4C1	<i>SLCO4C1</i>	OATP-R	<i>SLC21A20</i>	Kidney
Rat Oatp				
Oatp1a1	<i>Slco1a1</i>	Oatp1	<i>Slc21a1</i>	Liver, kidney
Oatp2a1	<i>Slco2a1</i>	RPGT	<i>Slc21a2</i>	Widely
Oatp1a3-v1 Oatp1a3-v2	<i>Slco1a3</i>	OAT-K1 OATP-K2	<i>Slc21a4</i>	Kidney
Oatp1a4	<i>Slco1a4</i>	Oatp2	<i>Slc21a5</i>	Retina, liver, brain
Oatp1a5	<i>Slco1a5</i>	Oatp3	<i>Slc21a7</i>	Retina, brain, liver, kidney
Oatp1b2	<i>Slco1b2</i>	Oatp4/rst-1	<i>Slc21a9</i>	Liver only
Oatp2b1	<i>Slco2b1</i>	mOat1/Oatp-B	<i>Slc21a10</i>	Widely
Oatp3a1	<i>Slco3a1</i>	Oatp-D	<i>Slc21a11</i>	Widely
Oatp4a1	<i>Slco4a1</i>	Oatp-E	<i>Slc21a12</i>	Widely
Oatp1a6	<i>Slco1a6</i>	Oatp5	<i>Slc21a13</i>	Kidney
Oatp1c1	<i>Slco1c1</i>	Oatp14	<i>Slc21a14</i>	Brain
Oatp6b1	<i>Slco6b1</i>	RGST-1/Oatp16	<i>Slc21a16</i>	Testis
Oatp6c1	<i>Slco6c1</i>	RGST-2/Oatp18	<i>Slc21a18</i>	Testis
Oatp4c1	<i>Slco4c1</i>	Oatp-R		Kidney

OATP1B1:

Among the hepatically expressed OATP members, OATP1B1, consisting of 670 amino acids with 12 putative membrane spanning domains (Fig. 1.4), represents the major OATP in the liver exhibiting the most abundant and exclusive expression on the basolateral plasma membrane of hepatocytes (Abe et al., 1999; Hsiang et al., 1999; Tamai et al., 2000). Many structurally diverse anionic compounds are substrates of this protein, including hydrophilic pravastatin (Nishizato et al., 2003) as well as albumin-bound lipophilic drugs that are metabolized such as cerivastatin (Shitara et al., 2003) and repaglinide (Niemi et al., 2005a). Blockage of OATP1B1 has been implicated in certain clinically relevant drug-drug interactions. For instance, Shitara et al. (2003) have demonstrated that the OATP1B1-mediated transport of cerivastatin is significantly inhibited by cyclosporine, suggesting that the increased exposure of cerivastatin by co-administered cyclosporine as observed in humans can be partly explained by inhibition of hepatic uptake, in addition to inhibition of CYP3A4-mediated metabolism by cyclosporine.

In recent years, several single nucleotide polymorphisms (SNP) in the *SLCO1B1* (gene symbol of OATP1B1) have been reported. A number of the identified alleles were associated with marked changes in the intrinsic clearance values associated with a reduction in OATP1B1 function. For instance, reduced surface expression due to a sorting error was observed in the Val174Ala mutant (caused by SNP T521C) in HeLa cells, where V174 is located in the fourth transmembrane domain (Fig. 1.4). T521C (Val174Ala) is a common SNP across various ethnic groups. Its genotypic frequency is 14-15% in European American, 16% in Japanese and 2% in African American (Tirona et



al., 2001; Nishizato et al., 2003; Mwinyi et al., 2004). These genetic polymorphisms have been linked to clinically significant changes in drug clearance. Two clinical studies that were designed to examine the impact of OATP1B1 SNPs on the pharmacokinetics of pravastatin, carried out in both Japanese and Caucasian volunteers, have shown that the nonrenal clearance of pravastatin was significantly reduced in healthy volunteers with OATP1B1*15/*15 (130D 174A) homozygotes compared with groups with OATP1B1*1b/*15 heterozygotes alone (130D 174V/130D 174A) (Nishizato et al., 2003; Niemi et al., 2004).

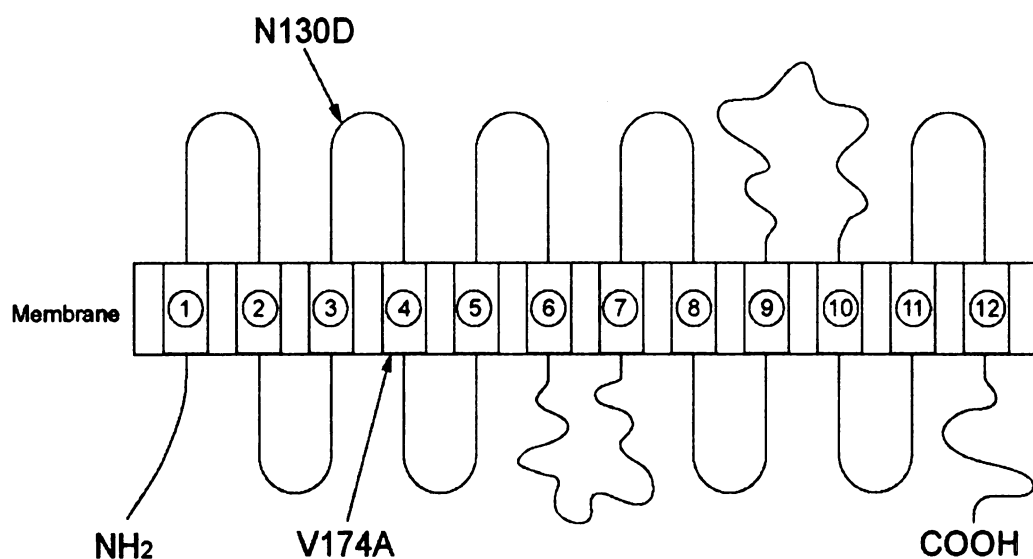


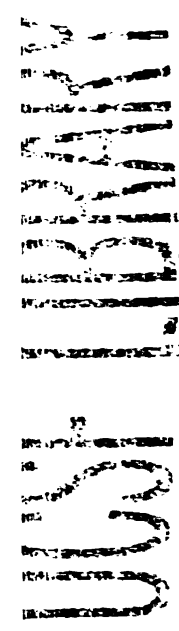
Fig. 1.4 Transmembrane topology of OATP1B1 with two major allelic variants (N130D and V174A). Modified from Tirona et al. (2001).

OATP1B3:

OATP1B3 was also cloned from human liver and encodes a glycoprotein of 702 amino acids, which shares 80% amino acid identity with OATP1B1 (Konig et al., 2000a). Under normal physiological conditions, OATP1B3 is predominantly expressed at the basolateral membrane of hepatocytes (Konig et al., 2000a; Abe et al., 2001). However, OATP1B3 has also been shown to be expressed in various cancer tissues as well as in tumor cell lines derived from certain cancers including gastric, colon and pancreas (Konig et al., 2000a). The substrate specificity of OATP1B3 commonly overlaps that of OATP1B1 (Ismair et al., 2001; Kullak-Ublick et al., 2001). OATP1B3 is unique in that it is the only human OATP capable of transporting the cardiotonic drugs, digoxin and amiodarone (Kullak-Ublick et al., 2001).

Rat Oatps:

In general, the transport properties of the rat Oatps cannot be directly translated to that of the human OATPs due to the fact that the *Slco* gene products of rat are not exact one-to-one orthologs of the human OATP proteins (Tamai et al., 2000). It becomes challenging when cross-species extrapolation need to be done to predict hepatic clearance or explain certain drug-drug interactions considering that distinct proteins exhibit different substrate specificities. For example, OATP1B1 only shares 64-65% identity with its rat and mouse ortholog Oatp1b2; The cardiotonic drug, digoxin is a specific substrate for human OATP1B3 (Kullak-Ublick et al., 2001), yet it is an exclusive substrate for Oatp1a4 (previously known as Oatp2) in rat (Meier et al., 1997).

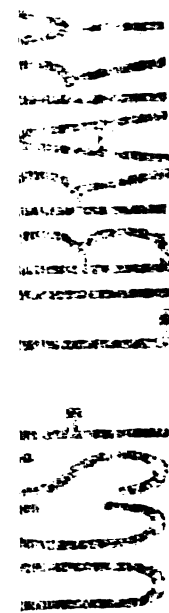


(2B) SLC22A7 (OAT2):

The organic anion transporters (OATs/Oats; human/rodent) are encoded by the gene family SLC22 and were first cloned in kidney. Among which, Oat2 (*Slc22a7*) acts as a sodium-independent facilitative transporter expressed predominantly in the rat kidney and liver; it transports prototypical anionic substrates such as paraaminohippurate (PAH) (Sekine et al., 1998; Cha et al., 2000). Oat2 also transports dicarboxylates, indomethacin, methotrexate and nucleoside derivatives (Sekine et al., 1998).

(2C) SLC22A1 (OCT1):

The hepatic uptake of small hydrophilic type I organic cations, with size ranging from 60 to 350 Daltons and at least one positively charged amino moiety at physiological pH, is mediated by the electrogenic organic cation transporter 1, OCT1/Oct1 (human/rodent; *SLC22A1*) (Grundemann et al., 1994; Zhang et al., 1999). Human OCT1 was first identified and cloned by Zhang et al. (1997) from liver. Rat Oct1 is expressed in the basolateral membrane of hepatocytes as well (Meyer-Wentrup et al., 1998). OCT1 is the primary transporter for the hepatic uptake of organic cationic compounds in humans. Substrates for which transport has been directly demonstrated include the prototypical substrate tetraethylammonium (TEA), the neurotoxin 1-methyl-4-phenylpyridinium (MPP⁺), drugs such as cimetidine and metformin, biogenic amines including dopamine, norepinephrine and several other endogenous compounds (e.g. choline and creatinine) (Shu et al., 2001; Jonker and Schinkel, 2004).

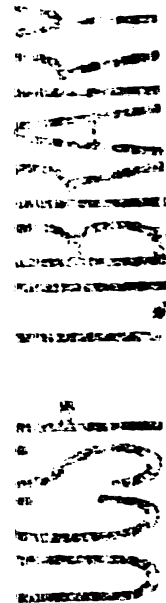


(2D) SLC10A1 (NTCP):

Sodium-taurocholate co-transporting polypeptide (NTCP) is involved in the sodium-dependent uptake of bile acids (Trauner and Boyer, 2003). This protein transports taurocholate (TC) with sodium in a stoichiometry of 1 to 2 and it preferentially mediates the transport of conjugated bile salts such as TC, taurochenodeoxycholate, but also transports unconjugated bile salts to a lesser extent. Some non-bile salt substrates include dehydroepiandrosterone sulfate (DHEAS), 3, 3', 5-triiodo-L-thyronine (T3), thyroxine (T4), bromosulfophthalein (BSP), and estrone-3-sulfate (Meier et al., 1997; Friesema et al., 1999).

(2E) ABCC3 (MRP3):

Multidrug resistance protein 3 (MRP3) is an ABC efflux pump present in the basolateral membrane of human hepatocytes, considered to be responsible for the secretion of drug metabolites into the bloodstream for subsequent urinary elimination (Zelcer et al., 2005). König et al. (1999) have reported high expression of MRP3 in the livers of patients whose MRP2 function is deficient (Dubin-Johnson syndrome). It is likely that MRP3 might play a role in compensating for the impaired function of MRP2 in the liver. In rat, Mrp3 was first cloned from the liver of MRP2-deficient rats (EHBR) as an inducible protein under cholestatic conditions (Hirohashi et al., 1998). Recently, Zelcer et al. (2005) have demonstrated that rat Mrp3 mediates the transport of morphine-3-glucuronide and morphine-6-glucuronide by using both *in vitro* cellular assay and Mrp3(-/-) mice, suggesting that Mrp3 plays a significant role in the hepatic elimination of



glucuronidated metabolites. It is likely that many glucuronidated compounds are preferentially excreted in the urine and not in the bile, presumably to circumvent the exposure of these metabolites to the intestine that may result in their deglucuronidation and reabsorption. Other MRP3/Mrp3 substrates include anticancer drugs such as methotrexate (Kool et al., 1999) and bile salts, both sulfated and nonsulfated (Hirohashi et al., 2000).

1.3.3.2 Drug metabolizing enzymes

Liver is an organ with the highest drug metabolizing capacity in the body. Drug metabolism is classified into Phase I and Phase II reactions. Drug metabolizing enzymes including both Phase I enzymes such as cytochromes P450 and Phase II enzymes such as UDP-glucuronosyl transferases (UGTs), glucuronosyl transferases (GST) and sulfotransferases are abundantly expressed in the liver. In this section, we summarize the various types of Phase I, specifically the cytochromes P450 3A and 2C families, and the Phase II enzyme UGT that are highly expressed in the liver and involved in the biotransformation of xenobiotics.

(1) Phase I enzymes: cytochrome P450

The Phase I detoxification system, composed mainly of oxidative processes mediated by the cytochrome P450 supergene family of enzymes, is generally the first enzymatic defense against foreign compounds, although other enzymes such as flavin monooxygenases, peroxidases and amine oxidases are also present and involved in Phase I metabolism. It has been estimated that the entire endoplasmic reticulum of the liver,

which comprises approximately 5% of total body weight, contains about 25,000 nanomole of cytochrome P450 enzymes (Iwatsubo et al., 1997). Cytochrome P450 enzymes, previously known as mixed function oxidase enzymes, are heme-containing enzymes responsible for reactions, mainly oxidation and hydroxylation, that do not result in a significant change in molecular weight or water solubility of the substrate, but are of great importance as oxidative reactions add or expose sites where phase II metabolism can subsequently occur.

Among all the cytochrome P450s, six subfamilies appear to play a significant role for the first-pass metabolism of drugs and exogenous toxins: CYP1A2, CYP2C9, CYP2C19, CYP2D6, CYP2E1 and CYP3A4. It has been estimated that 90% of drug oxidation can be attributed to these six enzymes (Tanaka, 1998), which exhibit broad and overlapping substrate and/or inhibitor specificities. However, it is not unusual for a compound to be metabolized by several CYP isoforms simultaneously.

(1A) CYP3A:

Cytochrome P450 3A4 (CYP3A4) is the most abundantly expressed drug metabolizing enzyme in man. This isoform of the CYP family is of particular interest as it is responsible for the degradation of approximately 60% of all pharmaceutical agents (Benet et al., 1996a) thus an important area of interest with respect to enzyme based drug interactions. CYP3A4 metabolizes more drug molecules than all other isoforms combined. Among the drugs metabolized are sedatives such as midazolam; the antiarrhythmics, quinidine and amiodarone; cancer chemotherapeutic agents paclitaxel and vinblastine; cholesterol lowering agents such as atorvastatin and simvastatin;

calcium channel antagonists such as diltiazem and nifedipine and various antimicrobials and HIV protease inhibitors (Tanaka, 1998). Also of particular interest and significance is the localization of CYP3A4 in the intestinal tract and the liver (Watkins et al., 1985; Watkins et al., 1987), where it serves a primary defense mechanism. The relative abundance of CYP3A4 in human liver and intestine are estimated to be 30% and 70%, respectively, of the total P450 in each organ (de Waziers et al., 1990).

From a structural perspective, CYP3A4 enzyme has a relatively large and open channel near the heme binding site, greater than that found in other P450s (Lewis et al., 1996, 2004b). Due to the flexibility in the active site cavity of CYP3A4, a certain level of promiscuity exists for substrate binding, which allows more than one substrate to access the enzyme at one time and explains the broad substrate spectrum covered by CYP3A4. For substrates and/or inhibitors that are metabolized by CYP3A4 or act on CYP3A4, a certain level of compound lipophilicity is of key importance to P450 binding affinity and enzyme selectivity (Lewis et al., 2004a).

CYP3A5 is another member of the CYP3A gene family and its levels in liver and intestine may exceed those of CYP3A4 in some individuals. However, CYP3A5 is highly polymorphic and its expression level is correlated to the frequency of its *CYP3A5*1* allele (Kuehl et al., 2001; Schuetz et al., 2004). Only people with at least one *CYP3A5*1* allele express large amounts of CYP3A5. This isoform is more frequently expressed in livers of African Americans (60%) than in those of Caucasians (33%). Because CYP3A5 represents at least 50% of the total hepatic CYP3A content in subjects polymorphically expressing CYP3A5, this isoform may be the most important contributor to genetic

interindividual variability and interracial differences in CYP3A-dependent drug clearance and in response to many medicines (Kuehl et al., 2001).

(1B) CYP2C:

The human CYP2Cs are an important subfamily of P450 enzymes. Collectively, these enzymes metabolize approximately 20% of clinically used drugs (Gray et al., 1995; Evans and Relling, 2004). There are four members of the subfamily, CYP2C8, CYP2C9, CYP2C19, and CYP2C18. Of these CYP2C8, CYP2C9, and CYP2C19 are of clinical importance. The CYP2C enzymes are all genetically polymorphic and have differences with regard to the type of substrates recognized (Gray et al., 1995). CYP2C9 is widely considered to be the most important member of the CYP2C family because of its relatively high concentration in the liver and its activity towards numerous drugs with low therapeutic indices such as S-warfarin, phenytoin, tolbutamide, losartan and many non-steroidal anti-inflammatory drugs (NSAIDs) (Lasker et al., 1998; Miners and Birkett, 1998). CYP2C9 has the ability to metabolize several drug classes including protein pump inhibitors and antidepressants (Rendic and Di Carlo, 1997). Polymorphisms in the coding region of the CYP2C9 gene produce variants at amino acid residues Arg144Cys (*2) and Ile359Leu (*3). Individuals homozygous for Leu359 have markedly diminished metabolic capacities for most CYP2C9 substrates, although the prevalence of this allele is relatively low. The cholesterol lowering agent, fluvastatin, a substrate of CYP2C9, has been proposed as a marker of differences in pharmacokinetics in humans having the CYP2C9*3 alleles (Kirchheiner et al., 2003).

CYP2C8 is another major human hepatic P450, constituting around 7% of total microsomal CYP content in the liver (Shimada et al., 1994). The prototypical substrate of CYP2C8 is paclitaxel (Rahman et al., 1994). Other drugs for which CYP2C8 contributes to metabolism include the antidiabetic drugs troglitazone, rosiglitazone and repaglinide (Baldwin et al., 1999; Bidstrup et al., 2003) and the HMG-CoA reductase inhibitors, cerivastatin, fluvastatin and atorvastatin (Jacobsen et al., 2000; Wang et al., 2002). The lipid-lowering drug, gemfibrozil, has been recognized as a CYP2C8 inhibitor (Wang et al., 2002). CYP2C8-dependent metabolism of cerivastatin is believed to be inhibited by gemfibrozil *in vivo* and possibly cause serious adverse effects leading to rhabdomyolysis, a complication responsible in good part for cerivastatin being taken off the market in 2001 (Wang et al., 2002), even though it has also been reported that OATP1B1, the hepatic uptake transporter that mediates the uptake of cerivastatin into the liver could also be partially inhibited by gemfibrozil *in vitro* (Shitara et al., 2004).

(2) Phase II enzymes

Sulfation, glucuronidation, and glutathione conjugation represent the three most prevalent phase II metabolism processes that may occur directly on parent compounds [e.g. acetaminophen (Gram and Gillette, 1971)] that contain appropriate structural motifs, or, as is usually the case, on functional groups added or exposed by phase I oxidation. These three conjugation reactions increase the molecular weight and water solubility of the compound, in addition to adding a negative charge to the molecule. The conjugation of polar compounds occurs via a number of reactions involving N-acetyltransferases (NAT-1, 2), methyl transferases, glutathione transferase and most commonly, by

sulfotransferases (SULTs), glucuronosyl transferases such as uridine-diphospho (UDP) glucuronosyl-transferases (UDPGTs), also known as UGTs.

(2A) UDP-glucuronosyl transferases (UGTs):

Glucuronidation, mediated by UGTs, is a major detoxification pathway for endogenous and exogenous compounds in mammals that results in the intracellular formation of polar metabolites. The UGTs are the only phase II enzymes found in the smooth endoplasmic reticulum and they catalyze the transfer of a glucuronic acid moiety from uridine-5'-diphospho- α -D-glucuronic acid (UDP-GA) to hydroxyl, carboxyl or amino functional groups of a drug molecule. The majority of UGTs, like other drug-metabolizing enzymes, display broad and often overlapping substrate specificities. To date, about 24 human UGT genes have been identified.

UGT enzymes are subdivided into two families: UGT1 and UGT2. Nine functional isoforms comprise the UGT1A subfamily (Tukey and Strassburg, 2000; Guillemette, 2003). UGT1A1 is of particular interest because it is responsible for the detoxification of the hepatic heme breakdown product, bilirubin (Bosma et al., 1994) and for glucuronidation of numerous drug compounds such as simvastatin (Prueksaritanont et al., 2002). It has been proposed that glucuronide conjugates of the acid form of statins can undergo spontaneous cyclization *in vivo* to form statin lactones, which are the relevant substrates for CYP3A4-mediated metabolism (Prueksaritanont et al., 2002).

Glucuronide conjugation is a reversible process. Glucuronide conjugates can be deconjugated *in vivo* via enzymatic process mediated by β -glucuronidases. Unlike the liver, β -glucuronidase activity is highly present in the duodenum, hence, many

glucuronide conjugates excreted in the bile are subsequently deconjugated to the aglycone, which may be reabsorbed, resulting in enterohepatic cycling of that compound (Roberts et al., 2002).

1.4 Relationship between hepatic drug transport and metabolic systems

1.4.1 Transporters affect the intrinsic ability of enzymes to metabolize drug

Models of hepatic elimination have been developed in order to quantify clearance changes when plasma protein binding, enzymatic activity or hepatic perfusion are altered. The most commonly used model is the well-stirred model described by equation (1.1) (Wilkinson and Shand, 1975). This model assumes that there is instantaneous and complete mixing occurring within the liver and can be readily applied to summarize alterations of the changes mentioned above:

$$CL_H = \frac{Q \times f_u \times CL_{int}}{Q + f_u \times CL_{int}} \quad \text{Eqn. (1.1)}$$

CL_H is the hepatic blood clearance, Q is the hepatic blood flow, f_u is the fraction unbound in blood and CL_{int} is the intrinsic clearance that relates the rate of metabolism to the unbound concentration at the enzymatic site.

Besides changing clearance by altering metabolic enzymes, changes in transporter function can also change CL_{int} without apparently affecting the enzymatic activity, by changing the exposure of unbound concentration of substrate to the enzymes.

Transporters, both uptake and efflux, can lead to alternations in the apparent volume of distribution at the site of enzymatic reaction, for instance, the hepatocytes.

The intrinsic clearance (CL_{int}) concept was first defined by Rowland et al. (1973):

$$CL_{int} = K_p \times V_L \times k_{e,u} \quad \text{Eqn. (1.2)}$$

where K_p , the apparent partition coefficient is defined as the unbound drug concentration between the liver and the emergent venous blood ($K_p = C_{L,u} / C_{out,u}$); V_L is the volume of the liver compartment; $k_{e,u}$ is the first-order rate constant for unbound drug elimination by both biliary excretion (biliary rate constant = k_b) and metabolism (metabolic rate constant = k_m , which for saturable systems can be written in terms of a *Michaelis-Menten* process). The ($K_p \times V_L$) term is defined as the apparent volume of distribution in the liver.

From our study results using digoxin as a model substrate as described in chapter 2, we demonstrated that inhibition of uptake and efflux transporters alone could decrease and increase the apparent volume of distribution in the liver, respectively (see Table 2.2). Hence, the extent of metabolism changed accordingly due to alterations in drug concentration at the enzymatic site caused by changes in the apparent volume, given that k_m remained constant.

Since hepatic clearance is related to intrinsic clearance, except for high hepatic extraction ratio drugs where clearance is limited by blood flow [i.e. ($f_u \times CL_{int}$) \gg Q], changes in intrinsic clearance caused by inhibition of transporters can be translated into changes in hepatic clearance and are reflected as changes in the area under the concentration-time curve (AUC).

1.4.2 Overlap of substrate specificities between various hepatic transporters

It is generally accepted that the uptake of various anionic compounds is mediated by OATPs and OATs, while their canalicular excretion is mediated by the anionic MRP2 and BSEP efflux pumps. Human OATP1B1 and MRP2 have been implicated in the hepatobiliary transport of many endogenous and exogenous anionic compounds such as hormones and the anionic drugs rifampicin and pravastatin (Nishizato et al., 2003; Sasaki et al., 2004; Spears et al., 2005). However, several reports have demonstrated that many known P-gp substrates such as paclitaxel and doxorubicin, the neutral digoxin and the zwitterionic fexofenadine are also recognized by OATPs/Oatps (Cvetkovic et al., 1999; Shitara et al., 2002; Smith et al., 2005). On the other hand, some anionic compounds such as estradiol-17 β -glucuronide and atorvastatin can also be transported by P-gp in human (Huang et al., 1998; Lau et al., 2006a).

An excellent study conducted by Hirano et al. (2005b) used various doubly-transfected cell systems with co-expression of OATP1B1/MDR1, OATP1B1/MRP2 and OATP1B1/BCRP to evaluate the involvement of multiple transporters in regulating the vectorial transport of compounds. They investigated only poorly metabolized substrates, such as pitavastatin, to illustrate that the multiplicity of transport mechanisms in hepatic elimination is a common phenomenon. Thus, it is necessary to consider various types of uptake and efflux transporters together to better understand the drug elimination process in the liver.

1.4.3 Overlap of substrate specificities and regulation between hepatic transporters and drug metabolizing enzymes

In 1995, Wachter et al. (1995), on the basis of an extensive literature review, revealed a striking overlap in substrate specificities between P-gp and CYP3A systems. The co-localization and co-induction of these two proteins are important for drug delivery as the up-regulation of both proteins through the steroid and xenobiotic receptor (SXR) and PXR pathways (Synold et al., 2001) can lead to extensive drug clearance and metabolism in both intestine and liver. This is of particular concern to chemotherapy since many anti-cancer agents that are dual substrates of P-gp and CYP3A, including paclitaxel, are potent SXR agonists, so an auto-induction mechanism can effect their clearance (Synold et al., 2001; Gottesman et al., 2002).

Co-induction does not occur only for the P-gp and CYP3A system. Recently, it has been suggested and demonstrated that the expression of certain hepatic Oatp uptake transporters and CYP450 enzymes are coordinately regulated in the rat liver via induction by PXR ligands such as pregnenolone-16 α -carbonitrile (PCN) (Cheng et al., 2005). Bile acid-induced repression of OATP1B1 (OATP-C) was also found to be dependent on both PXR and constitutive androstane receptor (CAR)-mediated pathways (Stedman et al., 2005). This evidence suggests that OATPs and CYPs might share a common induction mechanism in the liver.

Since OATP is an important player in controlling the transcellular movement of compounds into the liver, where they may be subject to CYP3A-mediated metabolism and subsequent biliary excretion mediated by P-gp and MRP2, we compiled a table consisting of common substrates among these three players involved in the hepatic

elimination pathway (Table 1.2): (1) CYP3A; (2) efflux transporters P-gp and MRP2, and (3) uptake transporters (OATP/Oatp; human/rodent). Unlike CYP3A, P-gp and MRP2, there is a poor correlation for OATP across species due to the low amino acid sequence homology, hence it is necessary to consider the substrate specificities of human and rodent forms of OATP separately.

The list encompasses various drug types ranging from clinically used drugs to fluorescent dyes and endogenous substrates. Since this thesis describes studies with atorvastatin, it is intriguing to note that nearly all HMG-CoA reductase inhibitors (both non-CYP3A and CYP3A substrates) are substrates for both uptake and efflux transporters except for the highly lipophilic lovastatin and simvastatin, which are administered in the prodrug lactone form in clinics. This is most likely due to the amphipathic nature of the hydroxy acid form of statins. The acid form of statins is a surface-active molecule, since it consists of a lipophilic part and a more hydrophilic portion. It is believed that the surface activity of a molecule is an important physicochemical property, as it will affect its partition and diffusion into and across biological membranes, and thus a compound's susceptibility for the OATP transporters (Lindahl et al., 1999), which usually uptake hydrophilic compounds. As mentioned in the previous section (1.3.2.1), affinity towards CYP3A4 and P-gp requires a certain level of lipophilicity. This explains why most statins are affected by CYP-mediated metabolism and P-gp mediated efflux.

Table 1.2

Substrates of CYP3A4, P-gp, Mrp2 and OATPs/Oatps (human/rodent).

Key: Black, yes; grey, no; striped, controversial; white, unknown.

Compound	CYP3A4	P-gp	MRP2	OATP1B1	OATP1B3	Oatp1a1	Oatp1a4	Oatp1b2
Anticancer drugs								
Vinblastine	Black	Black	Black	White	White	White	White	White
Vincristine	Black	Black	Black	White	White	White	White	White
Daunorubicin	Grey	Black	White	White	White	White	White	White
Doxorubicin	Grey	Black	White	White	White	White	White	White
Methotrexate	Grey	Grey	Black	Black	Black	White	White	White
Docetaxel	Black	Black	Black	Grey	Black	White	White	White
Paclitaxel	Black	Black	Black	Grey	Black	White	White	White
Topotecan	Black	Black	White	White	White	White	White	White
Irinotecan	Black	Black	White	Grey	White	White	White	White
SN-38*	Black	Black	White	Black	White	White	White	White
HIV Protease Inhibitor								
Amprenavir	Black	Black	White	White	White	White	White	White
Indinavir	Black	Black	Black	White	White	White	White	White
Nelfinavir	Black	Black	White	White	White	White	White	White
Ritonavir	Black	Black	Black	White	White	White	White	White
Saquinavir	Black	Black	Black	White	White	White	White	White
Antibiotics								
Erythromycin	Black	Black	White	Grey	White	White	Black	White
Troleandomycin	Black	White	White	White	White	White	White	White
Clarithromycin	Black	White	White	White	White	White	White	White
Azithromycin	Grey	Black	White	White	White	White	White	White
Rifampicin	Grey	Striped	Black	Black	Black	White	Black	White
HMG-CoA Reductase Inhibitor								
Atorvastatin	Black	Black	Black	Black	White	Grey	Black	Black
Cerivastatin	Black	Black	Black	Black	White	White	Black	Black
Lovastatin	Black	Black	White	Grey	White	Grey	Grey	Grey
Simvastatin	Black	Black	White	Grey	White	White	Grey	Grey
Pravastatin	Grey	Grey	Black	White	White	Striped	Black	White
Rosuvastatin	Grey	Black	White	White	White	White	White	Black
Pitavastatin	Grey	Black	Black	Black	Black	Black	Black	Black

U.S. LIBRARY

Compound	CYP3A4	P-gp	MRP2	OATP1B1	OATP1B3	Oatp1a1	Oatp1a4	Oatp1b2
Immunosuppressants								
Cyclosporine								
Tacrolimus								
Sirolimus								
Antiarrhythmic								
Quinidine								
Digoxin**								
Amiodarone								
Ouabain								
Angiotensin receptor antagonist								
Olmesartan								
Valsartan								
Telmisartan								
Endothelin receptor antagonist								
Bosentan								
Atrasentan								
BQ123								
Others								
Repaglinide								
Gemfibrozil								
Fexofenadine								
Enalapril								
Fluorescent dyes								
Calcein AM								
Rhodamine 123								
Sulfobromophthalein (BSP)								
Indocyanine green								
Endogenous substrates								
Estrone-3-sulfate								
Estradiol-17beta-glucuronide								
T3								
T4								
Bilirubin								
Bilirubin-mono-glucuronide								
Taurocholate								

* Active metabolite (7-ethyl-10-hydroxy camptothecin) of the anticancer drug, irinotecan.

** Digoxin is affected by metabolism mediated by rat CYP3A but not human CYP3A.

WAT LIBRARY

1.4.4 Hypothesis and rationale

The overall goal of this project is to test the hypothesis that inhibition of uptake and efflux transporters not only alter blood levels by blocking the hepatic elimination pathway but also modify the partition of drug molecules into the liver, hence the exposure of drug molecules to the metabolizing enzymes, provided that transporter inhibitors have no or minimal inhibitory effects on enzymatic activity. We expect to see a decrease in metabolism when uptake transporters are inhibited and an increase in metabolism when efflux transporters are inhibited. Increased knowledge of the interplay between OATP uptake transporter, P-gp and MRP2 efflux transporters as well as CYP3A4 enzyme in the liver will allow a greater understanding of hepatic drug disposition and metabolism. Better predictions can be made for the changes in pharmacokinetic profiles, especially for drugs that are eliminated mostly by hepatobiliary excretion, upon inhibition of any of these proteins in humans.

1.4.5 Specific aims

The objectives of this study are as follows:

1. Determine the kinetic parameters of the OATP/Oatp mediated uptake, P-gp and MRP2 mediated transport and the metabolite formation profile using atorvastatin as a model compound in cell culture and microsomes (Chapter 3).

2. Examine the changes in hepatic disposition and the extent of metabolism of model compounds digoxin and atorvastatin at the organ level using the isolated perfused rat liver (IPRL) system (Chapter 2 & 3).

3. Examine the P-gp-Cyp3A interplay for atorvastatin in the intestine and the liver using CYP3A4-transfected Caco-2 cells (Chapter 4).

4. (a) Test whether inhibiting Oatp hepatic uptake in whole animals (rats) changes the disposition and metabolism of atorvastatin (Chapter 5).
(b) Determine the effect of OATP1B1 inhibition on the disposition of atorvastatin and its active metabolites in humans (Chapter 6).

11
12
13
14
15
16
17
18
19
20
21
22
23
24
25
26
27
28
29
30
31
32
33
34
35
36
37
38
39
40
41
42
43
44
45
46
47
48
49
50
51
52
53
54
55
56
57
58
59
60
61
62
63
64
65
66
67
68
69
70
71
72
73
74
75
76
77
78
79
80
81
82
83
84
85
86
87
88
89
90
91
92
93
94
95
96
97
98
99
100

Chapter 2

EX SITU INHIBITION OF HEPATIC UPTAKE AND EFFLUX SIGNIFICANTLY CHANGES METABOLISM: HEPATIC ENZYME- TRANSPORTER INTERPLAY¹

2.1 Introduction

Liver plays a crucial role in the disposition and elimination of a wide variety of physiological substrates and xenobiotics. The uptake of compounds into hepatocytes is primarily mediated by members of the solute carrier superfamily (SLCO) located at the basolateral side of the plasma membrane of hepatocytes (Meier et al., 1997). Sodium and ATP-independent transporters involved in the hepatic uptake of anionic compounds can be categorized into two major families: the organic anion transporting polypeptide (OATP/Oatp; human/rodent) and the organic anion transporter (OAT/Oat; human/rodent). Members of the OATP/Oatp (gene symbol, *SLCO/slco*; human/rodent) family are predominantly expressed in the liver and are responsible for mediating the hepatocellular uptake of a wide spectrum of substrates including bile salts, conjugates of

¹ This chapter was modified from a published manuscript entitled "Ex situ inhibition of hepatic uptake and efflux significantly changes metabolism: hepatic enzyme-transporter interplay" Y.Y. Lau, C.Y. Wu, H Okochi, and L.Z. Benet, *J Pharmacol Exp Ther* (2004) 308: 1040-1045

steroids, hormones and other large amphiphilic organic anions (Kanai et al., 1996a; Kanai et al., 1996b; Meier et al., 1997; Ambudkar et al., 1999; Eckhardt et al., 1999; Suzuki and Sugiyama, 1999). The substrate specificities of various OATPs/Oatps overlap considerably, although unique features of individual transporters have been demonstrated. For example, it has been shown that the cardiovascular drug digoxin is specifically transported with high affinity by Oatp1a4 (*slco1a4*), previously known as Oatp2 (Noe et al., 1997; Kodawara et al., 2002; Shitara et al., 2002). Since digoxin is also known to be a substrate for the ATP-dependent drug efflux pump, P-glycoprotein (P-gp), which is located in the canalicular membrane of hepatocytes (de Lannoy and Silverman, 1992; Cavet et al., 1996; Keppler and Arias, 1997; Stieger and Meier, 1998), it is reasonable to postulate that digoxin is actively taken up across the sinusoidal membrane into hepatocytes via Oatp1a4 and secreted into biliary canaliculi via P-gp. In order to estimate the contribution of Oatp1a4 to the hepatic disposition of digoxin, an inhibitor for Oatp1a4, rifampicin, was used to block the uptake function of Oatp1a4. Rifampicin has been shown to effectively block Oatp1a4-mediated transport of digoxin in Oatp1a4-transfected LLC-PK₁ cells with a K_i value of 1.46 μM (Shitara et al., 2002). On the basis of recent *in vivo* brain uptake studies, Zong and Pollack (2003) suggest that rifampicin at concentrations of 500 μM or greater could inhibit P-gp mediated efflux. Earlier studies have also shown that rifampicin can inhibit P-gp activity *in vitro* (Fardel et al., 1995). However, the degree to which rifampicin inhibits P-gp mediated efflux is dependent on the substrate molecule and rifampicin inhibition on P-gp mediated efflux of digoxin has not been specifically investigated. The antiarrhythmic agent quinidine, a well-known P-

1
2
3
4
5
6
7
8
9
10
11
12
13
14
15
16
17
18
19
20
21
22
23
24
25
26
27
28
29
30
31
32
33
34
35
36
37
38
39
40
41
42
43
44
45
46
47
48
49
50
51
52
53
54
55
56
57
58
59
60
61
62
63
64
65
66
67
68
69
70
71
72
73
74
75
76
77
78
79
80
81
82
83
84
85
86
87
88
89
90
91
92
93
94
95
96
97
98
99
100

2.2 Materials and methods

2.2.1 Chemicals

Digoxin, quinidine, rifampicin and corticosterone were purchased from Sigma-Aldrich (St. Louis, MO). The powder form of digoxigenin bisdigitoxoside (Dg2) was extracted and purified by HPLC in our laboratory.

2.2.2 Surgery and perfusion of isolated rat livers

Male Sprague-Dawley rats (300-400g, Bantin and Kingman, San Leandro, CA) were anesthetized with ketamine/xylazine (80mg, 12 mg/ml) prior to surgery. The hepatic portal vein and superior vena cava were cannulated following approval of protocols by the Committee on Animal Research, UCSF. The livers were isolated for perfusion *ex situ* as previously described from our laboratory (Prueksaritanont et al., 1992). Oxygenated Krebs-Henseleit buffer (pH 7.4), supplemented with sodium taurocholate (220 nmole/min), 1 % bovine serum albumin and glucose (10 mM) was pumped through the liver at a flow rate of 40 ml/min via a catheter inserted in the portal vein. We chose the commonly employed red blood cell free perfusion technique, which requires higher flow rates than the physiological flow rate in order to provide sufficient oxygen carrying capacity. Perfusion was performed at 37°C in a recirculatory manner, from a reservoir containing 110 ml of perfusate, through a 10 µm in-line filter, oxygenator and bubble trap placed before the liver. The perfusate in the reservoir was oxygenated directly using carbogen, 95% O₂ / 5% CO₂, and stirred continuously. Liver viability was judged on the basis of its appearance (uniformly pink to brown), oxygen consumption, portal vein

pressure (20-30 mmHg) and pH (in the range of 7.35-7.45), as well as metabolic capability.

After allowing time for the liver to stabilize for 20 min, the inhibitors (quinidine or rifampicin) were added to the reservoir 10 min prior to digoxin addition. Perfusate samples (0.5 ml) were collected immediately (0 min) and at 2, 5, 10, 15, 20, 30, 45 and 60 min after the addition of digoxin. At the end of experiment, the liver was removed, blotted dry and weighed. An aliquot of liver was homogenized with ice-cold Krebs-Henseleit buffer in a 1:2 ratio and maintained frozen at -80°C prior to analysis. No attempt was made to quantitate digoxin and Dg2 in the bile due to fluctuating bile flow rate from cannulated common bile duct after liver isolation.

2.2.3 Experimental design

To examine the influence of rifampicin and quinidine on the hepatic disposition of digoxin, 18 rats were divided equally into 3 groups and each group was perfused with $10\mu\text{g}$ of digoxin solution diluted in normal saline, added directly into the reservoir to yield an initial concentration of $\sim 110\text{ nM}$. While one group served as the control, the other two groups served as treatments. For inhibition studies, rifampicin or quinidine with a final perfusate concentration of $100\mu\text{M}$ or $10\mu\text{M}$, respectively, was administered 10 min prior to digoxin addition.

2.2.4 Sample preparation

Liquid-liquid extraction was performed for sample preparation. As a first step, $200\mu\text{l}$ of each perfusate sample and $100\mu\text{l}$ of each liver homogenate sample

supplemented with 100µl perfusate buffer was transferred into glass tubes. The internal standard, corticosterone (50 ng/ml), and 2 ml of methyl tertiary butyl ether (MTBE) were added to each tube. The final sample/internal standard/organic solvent mixtures were then mixed briefly followed by centrifugation at 4000 rpm for 10 min. Afterwards, a methanol ice-bath was prepared to freeze the bottom aqueous layers of each centrifuged sample so that the upper organic layers could be easily separated out. The organic layer of each sample was then evaporated under nitrogen. The dried solutes were reconstituted with 200 µl of methanol and transferred into HPLC screw cap vials with 250 µl inserts (Hewlett-Packard, Palo Alto, CA, USA).

Calibration control samples for digoxin and digoxigenin bisdigitoxoside (Dg2) with final concentrations ranging from 1 nM to 1µM were extracted and prepared the same way as experimental samples. A calibration control sample set was prepared for each type of sample using perfused blank perfusate buffer and blank liver homogenate solutions, respectively.

2.2.5 Measurement of digoxin and its metabolites

Samples were analyzed on a LC/LC-mass selective detector system (Hewlett-Packard) consisting of the 1100 HPLC components HPLCI and HPLCII as previously described (Christians et al., 2000). The two HPLC systems were connected via a 7240 Rheodyne six-port switching valve mounted on a step motor (Rheodyne, Cotati, CA). The system was controlled and data were processed using ChemStation Software Revision A.06.01 (Hewlett-Packard).

Samples (50 μ l) were injected onto a 10 \times 2-mm extraction column (Keystone Scientific, Bellefonte, PA) filled with Hypersil ODS-1 of 10 μ m particle size (Shandon, Chadwick, UK). Samples were washed with a mobile phase of 20% methanol and 80% 0.1% formic acid supplemented with 1 mmol/L sodium acetate. The flow was 2 ml/min and the temperature for the extraction column was set to 65°C. After 0.75 min, the switching valve was activated and the analytes were eluted in the backflush mode from the extraction column onto a 50 \times 4.6-mm C₈, 3.5 μ m analytical column (Zorbax XDB, C₈, Hewlett-Packard). The mobile phase consisted of methanol and 0.1% formic acid supplemented with 1 mmol/L sodium acetate. The following gradient was run: time 0 min, 55% methanol; 6 min, 100% methanol. The flow rate was 0.7 ml/min. The analytical column was also maintained at 65 °C. Two minutes after sample injection, the mass-selective detector was activated.

2.2.6 Measurement of rifampicin and quinidine levels in perfusate samples

The HPLC system used was described above. Rifampicin was resolved on a 250 \times 4.6- μ m C₈, 4.0 100 Å analytical column (Microsorb-MV, C₈, Varian, Walnut Creek, CA). The mobile phase was composed of 0.05 M potassium dihydrogen phosphate: acetonitrile (55:45, v/v) with a flow rate of 1ml/min. The UV absorbance was monitored at a wavelength of 340nm. Quinidine was chromatographed on a 150 \times 4.6- μ m C₈, 4.0 100 Å analytical column (Microsorb-MV, C₈, Varian) with a mobile phase of 0.5% acetic acid and 0.25% tetraethylamine: acetonitrile (75:25; v/v) with a flow rate of 1.5 ml/min. The UV absorbance was monitored at a wavelength of 245 nm.

2.2.7 Data analysis

Values for area under the concentration-time curve (AUC) were calculated using the linear trapezoidal method. For the inhibition studies, concentrations in perfusate and homogenized liver at 60 min were used to calculate the ratios of the amount of digoxin to Dg2 recovered in liver, the ratio of the concentrations of rifampicin in liver to perfusate and the ratio of the concentrations of quinidine in liver to perfusate. Student's two-tailed *t* test was used to assess statistical significance. Differences between groups were considered significant if $p < 0.05$.

2.3 Results

2.3.1 Effects of rifampicin and quinidine on digoxin disposition

Utilizing the perfusion system described above in the absence of a liver, perfusate concentrations of digoxin remained relatively constant (Fig.2.1), indicating that little drug is lost in the system. In all experiments, Dg2 was the only digoxin metabolite detected.

Fig. 2.1 illustrates the decline of digoxin concentrations in perfusate over time in the absence and presence of rifampicin or quinidine. In control livers perfused with digoxin only, digoxin concentrations in perfusate declined in a bi-exponential manner in which they dropped rapidly within the first 20 min and decreased steadily throughout the 60 min perfusion period (Fig. 2.1).

Digoxin concentrations at all sampling times were elevated by the addition of rifampicin (Fig.2.1), which is reflected by the significant 34 % increase in AUC from 3880 ± 210 nM·min to 5200 ± 240 nM·min ($p < 0.01$) as shown in Table 2.1. In contrast,

concurrent perfusion with quinidine decreased the concentration of digoxin markedly with a 14% decrease in the AUC to 3220 ± 340 nM·min ($p < 0.05$) (Table 2.1). *In vitro* rat hepatic microsome studies showed no effect for these concentrations of the two inhibitors on digoxin metabolism (data not shown). Figs. 2.2 (A) and 2.2 (B) show the concentrations of rifampicin and quinidine in perfusate, respectively. Immediately after administration, rifampicin levels declined rapidly within the first 10 min (before digoxin was dosed) and decreased only slightly afterwards. A similar pattern was observed for quinidine, indicating rapid hepatic uptake during the initial distribution phase.

Fig. 2.1 Influence of rifampicin and quinidine on concentrations of digoxin in perfusate following addition of 10 µg of digoxin to the perfusate. Values are mean \pm SD, n = 6 per group; no liver, n = 3. * $p < 0.05$; ** $p < 0.01$ for values compared with control.

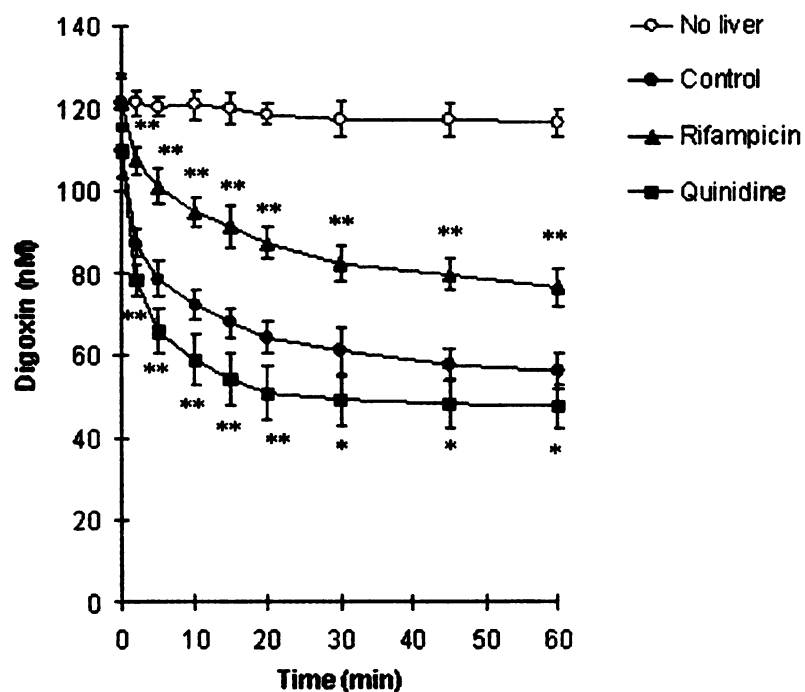


Table 2.1 Comparison of parameters between control livers perfused with digoxin only and livers co-perfused with rifampicin or quinidine.

Parameter ^a	Treatment group		
	Control	Quinidine	Rifampicin
Digoxin AUC ^b (nM·min)	3880 ± 210	3220 ± 340*	5200 ± 240**
Dg2 AUC ^b (nM·min)	1480 ± 90	1690 ± 120*	1130 ± 200*
Dg2 AUC/digoxin AUC	0.382 ± 0.029	0.530 ± 0.076**	0.217 ± 0.037*
Dg2/digoxin in liver ^c	0.131 ± 0.023	0.488 ± 0.192**	0.136 ± 0.045
Liver/Perfusate (inhibitor) ^d	N/A	8.08 ± 0.72	13.3 ± 3.0

N/A, not applicable

^a Mean ± SD, n = 6 per group

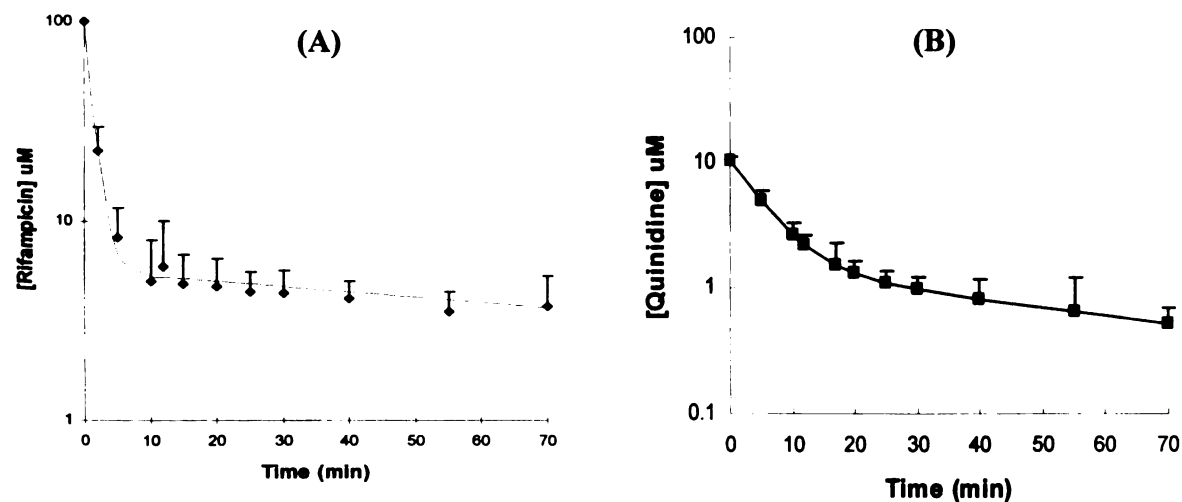
^b AUC calculated using the linear trapezoidal method up to 60 min.

^c Ratio of amount of Dg2 formed to amount of digoxin retained in liver at 60 min.

^d Ratio of concentrations of quinidine or rifampicin in liver to perfusate at 60 min.

* $p < 0.05$; ** $p < 0.01$ significantly different from control.

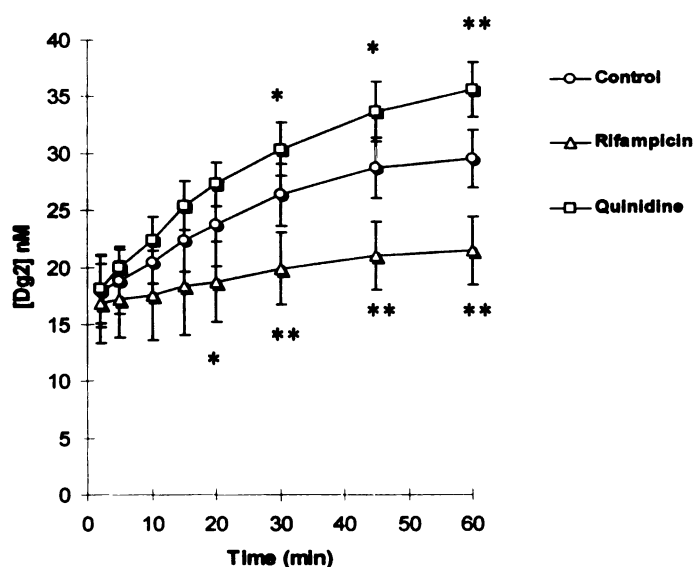
Fig. 2.2 Perfusate time course of rifampicin (A) and quinidine (B). Values are mean ± SD, n = 3.



2.3.2 Effects of rifampicin and quinidine on digoxigenin bisdigitoxoside disposition

The concentration of digoxigenin bisdigitoxoside (Dg2) was detectable 2 min after the start of perfusion and increased steadily up to 60 min (Fig. 2.3), indicating that hepatic enzymatic activity of CYP3A was functional throughout the perfusion period. Comparing the AUC of the control group and the treatment groups (Table 2.1), the AUC of Dg2 was decreased 24% by rifampicin ($p < 0.05$) and increased 14% by quinidine ($p < 0.05$). The ratio of the metabolite AUC to parent AUC (Dg2 AUC/digoxin AUC) was also calculated and was significantly increased by quinidine (0.530 ± 0.076 vs. 0.382 ± 0.029 in control; $p < 0.01$) and significantly decreased by rifampicin (0.217 ± 0.037 vs. 0.382 ± 0.029 in control; $p < 0.05$).

Fig. 2.3 Influence of rifampicin and quinidine on concentrations of Dg2 in perfusate following addition of 10 μg of digoxin to the perfusate. Values are mean \pm SD, $n = 6$ per group. * $p < 0.05$; ** $p < 0.01$ for values compared with control.



2.3.3 Levels of digoxin and digoxigenin bisdigitoxoside in rifampicin- and quinidine-treated liver tissues

The amount of digoxin and Dg2 recovered in liver tissue (expressed as % of original dose) for control, rifampicin and quinidine-treated livers are shown in Fig. 2.4. Approximately 17% of digoxin was retained in control livers after 60 min of perfusion, while 12% and 13% of digoxin dose, respectively, were detected in rifampicin and quinidine-treated groups.

Dg2 in liver exhibits a significant increase of 168% in the quinidine-treated group ($p < 0.01$) versus control while it is decreased by 31% in the rifampicin-treated group ($p < 0.01$). The ratios of Dg2 to digoxin retention in liver were comparable for control and rifampicin-treated livers whereas that for quinidine-treated livers showed a highly significant increase by ~ 4-fold (0.488 ± 0.192 vs. 0.131 ± 0.023 in control; $p < 0.01$) (Table 2.1). Mass balance calculations (digoxin and Dg2 in perfusate and liver) show no significant differences between the three studies ($90.5 \pm 9.8\%$ for control; $89.3 \pm 6.6\%$ with rifampicin; $88.9 \pm 5.1\%$ with quinidine).

We also observed a significant decrease in the calculated volume of distribution at steady state (V_{ss}) when Oatp1a4 was inhibited by rifampicin (Table 2.2). The increase in the V_{ss} value of digoxin upon P-gp inhibition by quinidine agrees directionally with the previous study results using tacrolimus as a model compound when canalicular P-gp was inhibited by GG918 in the IPRL system (Wu and Benet, 2003).

Fig. 2.4 Amounts of digoxin and Dg2 recovered in control, rifampicin-treated and quinidine-treated liver tissues. Values are mean \pm SD, $n = 6$ per group. * $p < 0.05$; ** $p < 0.01$ for values compared with control.

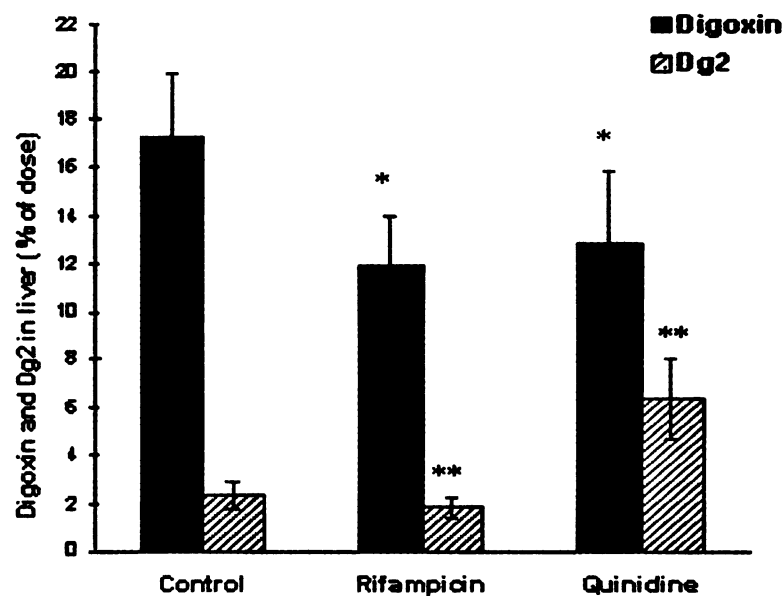


Table 2.2 Comparison of relative volume of distribution steady-state values between control livers perfused with digoxin only and livers co-perfused with transporter inhibitors.

Relative V_{ss} values calculated from the IPRL studies

Drug ^a	Control	Efflux inhibition	Uptake inhibition
Digoxin	1.00 \pm 0.03	1.30 \pm 0.07**	0.82 \pm 0.05*
Tacrolimus (Wu and Benet, 2003)	1.00 \pm 0.13	2.53 \pm 0.27**	N/A

^a Each value represents mean \pm SD, $n = 6$.

* $p < 0.05$; ** $p < 0.01$ significantly different from control.

2.4 Discussion

In the present study, we investigated the *ex vivo* disposition and excretion of digoxin (Dg3) and its metabolite, digoxigenin bisdigitoxoside (Dg2), in the isolated rat perfused liver system in the presence of inhibitors for Oatp1a4 and P-gp. Dg2 was the only metabolite detected during the perfusion period. This is consistent with previous data from our laboratory where rat liver microsome studies showed that the formation of Dg2 from digoxin is rapid ($CL_{int} = 2.92 \mu\text{l}/\text{min}/\text{mg}$ protein) and is much faster (~ 20-fold higher) than the cleavage of Dg2 to digoxigenin mono-digitoxoside and the aglycone digoxigenin (Salphati and Benet, 1999).

Rifampicin has been shown to be a potent inhibitor of Oatp1a4 in LLC-PK₁ cells (Shitara et al., 2002) and rat hepatocytes (Fattinger et al., 2000). At 100 μM , rifampicin substantially inhibits Oatp1a4-mediated transport of digoxin by 60 % (Shitara et al., 2002). In microsomal incubations, no effect of 100 μM rifampicin on digoxin was observed (data not shown). Our results indicate that a single bolus dose of rifampicin at the same concentration, significantly increased the AUC of digoxin in perfusate (Table 2.1) and decreased the amount of recovered digoxin in liver (Fig. 2.4), suggesting that rifampicin markedly reduced digoxin's sinusoidal uptake. We also monitored the disposition of rifampicin itself in perfusate (Fig. 2.2A) and observed higher concentrations of rifampicin in liver versus perfusate (Table 2.1). Given that the hepatocellular uptake of digoxin was reduced in the presence of rifampicin, we would expect a reduction in its hepatic metabolism since the bulk of drug entering the hepatocytes is reduced and the availability to CYP3A is decreased subsequently. Consequently, in our results, significantly less Dg2 was detected in liver tissues (Fig.

2.4). There was also a significant decrease in the calculated volume of distribution at steady state (V_{ss} , which is a term equal to the sum of perfusate volume and the apparent volume of the liver in the IPRL system) of digoxin following rifampicin treatment (Table 2.2), indicating that inhibition of the uptake transporter resulted in a decrease in the apparent volume of distribution of digoxin in the liver (Table 2.2). The change of Dg2 in liver seems to be reflective of what is observed in the perfusate (Fig. 2.3). The ratio of Dg2 to digoxin retention in liver is consistent between the control and the rifampicin-treated group, suggesting linear kinetics in which reduction in digoxin entry into liver leads to a proportional reduction in Dg2 formed. These results support our hypothesis that an uptake transporter such as Oatp1a4 may control the access of dual Oatp1a4/CYP3A substrates to the enzyme in the liver. Since the Dg2 to parent ratio in the liver did not change in the presence of rifampicin versus control (Table 2.1), we believe that any potential rifampicin inhibition of P-gp as reported by Zong and Pollack (2003) is not significant here.

P-gp functions as an energy-dependent drug efflux pump and prevent the accumulation of drugs in various organs including intestine and liver. Wu and Benet (2003) have performed an IPRL study using a known potent Pgp inhibitor, GG918 (1 μ M), to inhibit the P-gp mediated efflux of a dual CYP3A and P-gp substrate, tacrolimus. The AUC of tacrolimus was significantly decreased from control (2260 ± 430 ng-min/ml) by GG918 (1730 ± 270 ng-min/ml, $p < 0.05$), indicating the importance of P-gp in affecting CYP3A metabolism.

Quinidine is another potent inhibitor of this efflux pump. Fromm et al. (1999) have shown that 5 μ M of quinidine effectively inhibits P-gp-mediated transport of

digoxin by approximately 57 % in the Caco-2 MDR1 transfected cell line. Kakumoto et al. (2002) also demonstrated that quinidine inhibits the transport of digoxin in MDR1-overexpressing LLC-GA5-COL150 cells with an estimated IC_{50} value of 9.52 μ M. Here, we tested whether co-perfusion of quinidine in isolated perfused rat livers could inhibit the P-gp-mediated transport of digoxin. In the liver, absorbed compounds enter the hepatocytes from the sinusoidal blood, then the drugs are either biotransformed, transported/diffused back into blood or eliminated via biliary secretion. Since P-gp is located on the canalicular membrane of hepatocytes, drug molecules confront CYP3A prior to P-gp efflux, in an opposite manner to the Oatp1a4/CYP3A interaction. Since quinidine can inhibit P-gp from pumping drug molecules out to the bile canaliculi, the parent drug will have a prolonged intracellular residence time in liver tissue, as reflected by the increase in the V_{ss} value (Table 2.2), thereby, increasing its availability to CYP3A for metabolism; as a result, an increase in metabolite formation is expected with a relative decrease in parent compound compared to control. Others have shown that Oatp1a4-mediated transport of digoxin is inhibited by quinidine with a K_i value of $120 \pm 27 \mu$ M in Oatp1a4-stably expressing LLC-PK₁ cells (Shitara et al., 2002). This is not surprising since often inhibitors that alter P-gp transport activity also affect the function of uptake transporters. To overcome this complication, choosing an appropriate concentration of quinidine to serve as a specific inhibitor of P-gp becomes crucial. In our study, an initial perfusate concentration of 10 μ M of quinidine was used based on its inhibition constants (K_i) for Oatp1a4 and P-gp-mediated transport of digoxin, respectively. As depicted in Fig. 2.2B, quinidine perfusate concentrations affecting Oatp1a4 rapidly fell to 15 % of this value, about one-hundredth of the K_i for Oatp1a4. However, intracellular

concentrations affecting P-gp were probably maintained at or above the 10 μ M concentration due to the preferential intracellular accumulation of quinidine (Table 2.1), where the liver to perfusate concentration ratio at 60 min is \sim 8.

A significant increase in digoxin metabolism could also be observed in the liver tissues as reflected by the 3.7-fold increase in the ratio of Dg2 to digoxin retention in the quinidine treated group (Table 2.1), as compared to the 1.4-fold increase in perfusate AUCs. An efflux transport study utilizing MDCK expressing MDR1 cells demonstrated that Dg2, which is structurally similar to digoxin, is a substrate for P-gp (data not shown), explaining the increased Dg2 in liver relative to perfusate. Since mass balance was the same for all three groups, the significant decrease in liver digoxin concentrations in the quinidine group (Fig. 2.4) may be explained by a marked increase in metabolite formation in the liver, while the significant decrease in liver digoxin concentrations in the rifampicin (Fig. 2.4) group is explained by decreased hepatic uptake.

The working concentration of digoxin was carefully chosen based on its metabolic parameter to assure that the metabolizing enzyme does not reach saturation. Here, 110 nM of digoxin was selected, which is well below the K_m value (125 μ M) for the CYP3A catalysis of Dg2 from digoxin reported by our laboratory (Salphati and Benet, 1999). Quinidine had no effect on digoxin metabolism up to 100 μ M (Salphati and Benet, 1999) suggesting that it is unlikely that quinidine inhibits CYP3A in the perfused rat liver. The present study suggests that 10 μ M of quinidine is an appropriate concentration with minimal inhibitory effects on Oatp1a4 and CYP3A.

The mechanism of the clinically important drug interaction between digoxin and quinidine is well documented in the literature (Leahey et al., 1978; Bussey, 1982; Mordel

et al., 1993) When administered concomitantly, quinidine is known to increase the plasma concentrations of digoxin in both humans and rats (Bigger and Leahey, 1982; Sakai et al., 1988). *In vitro* studies addressing the digoxin-quinidine interaction suggest that P-gp is involved (Tanigawara et al., 1992; Su and Huang, 1996; Fromm et al., 1999). P-gp is highly expressed in the apical membrane of epithelial cells of small intestine (Su and Huang, 1996), the apical canalicular membrane of hepatocytes (Keppler and Arias, 1997), and the renal tubular cells of the kidney (Hori et al., 1993). The orientation of P-gp in these locations allows the rapid efflux of substrates from the basolateral surface to the lumen of small intestine, renal tubules, and into the bile. Hence, it is likely that the reported increase in digoxin plasma levels in rats is caused by the inhibitory effect of the co-administered quinidine on the basolateral to apical transport of digoxin across the enterocytes, hepatocytes and renal tubules (Hori et al., 1993; Su and Huang, 1996). However, since digoxin is extensively metabolized by CYP3A in rat, our data demonstrate that quinidine increases the extent of digoxin metabolism by blocking the P-gp mediated biliary secretion of digoxin, yielding lower *in vivo* digoxin concentrations in the hepatic compartment alone. Thus, our results point out a caution, as we have noted previously for P-gp knockout animals (Cummins et al., 2002b): although inhibition of P-gp may decrease overall systemic drug clearance, it would always be expected to increase hepatic metabolism of P-gp substrates.

Studies from our laboratory (Cummins et al., 2002a, 2002b, 2003) have examined the interplay between transporters and metabolic enzymes, proposing that transporters may control the access of drug molecules to the enzymes, and that therefore changes in transporter function can change intestinal and hepatic metabolism without apparently

Chapter 3

MULTIPLE TRANSPORTERS AFFECT THE DISPOSITION OF ATORVASTATIN AND ITS TWO ACTIVE HYDROXY METABOLITES: APPLICATION OF IN VITRO AND EX SITU SYSTEMS¹

3.1 Introduction

Atorvastatin (ATV), a member of the class of 3-hydroxy-3-methylglutaryl-coenzyme A (HMG-CoA) reductase inhibitors, also known as statins, is one of the most potent drugs for treatment of hypercholesterolemia (Nawrocki et al., 1995). ATV undergoes extensive metabolism primarily by cytochrome P450 (CYP) 3A in the liver to form two active metabolites, *ortho*-hydroxy atorvastatin and *para*-hydroxy atorvastatin (Jacobsen et al., 2000). Black et al. (1999) demonstrated that ATV undergoes a similar metabolic pathway in rats, where both parent and metabolite compounds were exclusively excreted in the bile, indicating that hepatic metabolism and biliary excretion are the major routes of elimination.

¹ This chapter was published in a manuscript entitled "Multiple transporters affect the disposition of atorvastatin and its two active hydroxy metabolites: application of in vitro and ex situ systems" Y.Y. Lau, H Okochi, Y Huang and L.Z. Benet, J Pharmacol Exp Ther (2006) 316: 762-771

Drug-drug interactions of ATV are often reported at the level of hepatic Phase I or Phase II enzymes (Kantola et al., 1998; Lennernas, 2003). Co-administration of ATV and an inhibitor for CYP3A or UDP-glucuronosyltransferase may increase ATV blood concentrations and the risk of rhabdomyolysis (Jacobson, 2004). However, interactions can also occur by inhibition of the relevant hepatic transporters that are located both upstream and downstream of hepatic enzymes. Our group has demonstrated previously, using digoxin and erythromycin as examples, that the ratio of intracellular drug concentrations of parent to metabolite may change when hepatic transporters (both uptake and efflux) are inhibited since the amount of drug available to the enzyme varies with transporter activity (Chapter 2; Lam and Benet, 2004; Lau et al., 2004; Sun et al., 2004).

Two carrier-mediated processes govern the sequential transport across the hepatocytes: the sinusoidal (basolateral) uptake from portal/arterial circulation and the canalicular (apical) efflux into the bile. Canalicular efflux transporters P-glycoprotein (P-gp) and multidrug resistance associated protein 2 (MRP2/Mrp2; human/rodent) are the two major ATP-dependent efflux pumps for excretion of drugs into the bile (Keppler and Arias, 1997). At the basolateral membrane of hepatocytes, uptake transporters such as the organic anion transporting polypeptide (OATP/Oatp) are responsible for the influx of bulky amphipathic and hydrophilic compounds (Meier et al., 1997).

ATV has been shown to be a P-gp substrate in various transport studies (Wu et al., 2000; Hochman et al., 2004; Chen et al., 2005). ATV can inhibit MRP2-mediated efflux (Chen et al., 2005) but whether or not it is a substrate of MRP2 had not been confirmed, though other statins, such as pravastatin, have been shown to be substrates of

MRP2 (Sasaki et al., 2002; Nezasa et al., 2003). Structurally, ATV consists of a lipophilic region and a more hydrophilic part (see Fig. 6.1). Its lipophilicity makes it a good substrate for CYP3A as well as for efflux transporters. In contrast, its hydrophilicity makes it a likely candidate for uptake transporters such as OATP/Oatp. *In vitro* studies have demonstrated that ATV, as well as other statins such as cerivastatin, pravastatin and rosuvastatin, are transported by, and inhibitors of, the liver specific OATP1B1 (previously known as OATP-C or OATP2) (Hsiang et al., 1999; Tokui et al., 1999; Shitara et al., 2003; Simonson et al., 2004; Chen et al., 2005).

Prior to this study, there was no published information on the influence of rat Oatps on the hepatic uptake of ATV and its two hydroxy metabolites. To estimate the contribution of Oatps on the hepatic disposition and metabolism of ATV, rifampicin (RIF) was chosen as a general inhibitor for Oatps since it has been shown to effectively inhibit the OATP/Oatp mediated uptake of various anionic compounds including taurocholate, estrone sulfate, as well as the neutral digoxin, with relatively low K_i values (1-2 μM) (Fattering et al., 2000; Shitara et al., 2002; Vavricka et al., 2002; Tirona et al., 2003). On the basis of *in vitro* studies using MRP2-overexpressing cells, Cui et al. (2001a) showed that RIF can also inhibit the MRP2-mediated efflux of bromosulfophthalein and leukotriene C_4 at high concentrations. Moreover, RIF has also demonstrated an inhibitory effect on P-gp radiolabeling by the photo-activable P-gp ligand azidopine (Fardel et al., 1995). This is not surprising, since OATP and MRP2 and/or P-gp often work in a concerted manner for drug elimination and share similar substrate and inhibitor specificity, even though the affinity and inhibition potency for uptake and efflux transporters might differ.

In this study, we evaluated the influence of individual hepatic uptake and efflux transporters on the disposition of ATV and its metabolites and characterized the effects of RIF on the hepatic uptake and efflux, as well as metabolism of ATV using cellular systems and rat microsomes. To directly observe how the dynamic interplay between transporters and enzymes contributes to alterations in ATV pharmacokinetics, the isolated perfused rat liver (IPRL) system was used. Mrp2-deficient TR rats were also studied to assess the involvement and influence of Mrp2 in the hepatobiliary transport and metabolism of ATV in the IPRL system.

3.2 Materials and methods

3.2.1 Materials

Atorvastatin (ATV), *para*-hydroxy atorvastatin (4-OH ATV) (PD142542, BMS-241423-01) and *ortho*-hydroxy atorvastatin (2-OH ATV) (PD152873, BMS243887-01) were kindly supplied by Parke-Davis (Ann Arbor, MI) and Bristol-Myers Squibb (Princeton, NJ). Fluvastatin (Novartis, Cambridge, MA) and GG918 (GF120918; GlaxoSmithKline, Research Triangle Park, NC) were kind gifts from the manufacturers. Rifampicin, NADPH and sodium butyrate were purchased from Sigma-Aldrich (St. Louis, MO). All other chemicals were reagent grade and purchased from either Sigma or Fisher Scientific (Pittsburg, PA, USA). Human OATP1B1 and rat Oatp1a1 (Oatp1), Oatp1a4 (Oatp2), Oatp1b2 (Oatp4) cDNA plasmids were kindly provided by Professor Richard Kim (Vanderbilt University, Nashville, Tennessee). The MRP-2 overexpressing cell line (MII-cMOAT) as well as the respective wildtype cell line MDCKII (MII) were a

generous gift from Professor Piet Borst and Dr. Raymond Evers (The Netherland Cancer Institute). MDCK and MDCK-MDR1 (M-MDR1) cell lines were generously provided by Dr. Ira Pastan (National Cancer Institute). Human embryonic kidney cells (HEK293) and all cell culture media were obtained from the UCSF Cell Culture Facility (San Francisco, CA). Six-well plates were obtained from Corning Life Sciences (Acton, MA). Transwell inserts and poly-D-lysine coated 12-well plates were obtained from BD Bioscience (Bedford, MA). The Lipofectamine 2000 transfection system was purchased from Invitrogen (Carlsbad, CA).

3.2.2 Transient transfection and uptake transport assays

All OATP/Oatp expression plasmids were sequence verified and when expressed in cells were shown to be transport competent toward prototypical substrates (estrone sulfate for Oatp1a1 and OATP1B1, digoxin for Oatp1a4, CCK8 for Oatp1b2) (data not shown). HEK293 cells were cultured in Eagle's minimal essential medium with Eagle's balanced salt solution and l-glutamine plus 10% heat-inactivated fetal bovine serum (FBS), non-essential amino acids, sodium pyruvate, streptomycin and penicillin. Cells were seeded into poly-D-lysine coated 12-well plates at a density of 0.5×10^6 cells/well one day prior to transient transfection with OATP1B1, Oatp1a1, 1a4 and 1b2 plasmids or pEF/V5-His vector control (Invitrogen, Carlsbad, CA) using the Lipofectamine 2000 transfection system according to the manufacturer's directions. Culture medium was replaced 24 hour before the uptake studies with the same medium containing 10 mM sodium butyrate to induce the expression of transporters. Before initiation of the uptake study, cells were washed once with phosphate buffered saline (PBS) pre-warmed at 37

°C. The uptake study was initiated by adding 0.5 ml of OptiMEM buffer (Invitrogen) containing substrates and incubating at 37 °C for 3 min. Preliminary experiments had shown that the uptake rate was linear over this time period (data not shown). For the inhibition studies, inhibitors and substrates were added simultaneously. At designated times, buffer was removed to terminate the reaction and the cells were washed three times with ice-cold PBS. The homogenate was centrifuged for 5 min at 13,000g and the resulting supernatant was analyzed by LC/MS-MS. The protein concentrations in cell experiments were determined by the method of Lowry et al. (1951) using bovine serum albumin as a standard.

3.2.3 Preparation of cell culture monolayers and transport studies

MII-cMOAT and MII cells were cultured at 37 °C and humidified, 5% CO₂-atmosphere in Dulbecco's modified Eagle's medium (DMEM) supplemented with 10% heat-inactivated FBS and 100 U/ml penicillin and 100 U/ml streptomycin. M-MDR1 cells were cultured in the same medium containing 80 mg/ml colchicine for selected growth of transfected cells (Pastan et al., 1988). Cells grown to confluence in culture flasks were harvested and seeded into transwell inserts in 6-well plates at a density of $\sim 10^6$ cells/insert. Studies were conducted 5 to 6 days post-seeding for the two cell lines. Media was changed once every 2 days and 24 hours before the experiment.

The transport experiments were adapted with modifications from Flanagan et al. (2002) and Cummins et al. (2004). Briefly, cell monolayers were preincubated in transport buffer (Hanks' balanced salt solution containing 25 mM HEPES and 1% FBS, pH 7.4) for 20 min at 37 °C. Transepithelial electrical resistance (TEER) was measured in

each well using a Millicell ERS voltohmmeter (Millipore Corporation, Bedford, MA) to assess the integrity of monolayers. The average TEER values obtained from MII, MII-cMOAT and M-MDR1 cells were $170 \pm 15 \text{ Ohm} \cdot \text{cm}^2$ (n=12), $160 \pm 10 \text{ Ohm} \cdot \text{cm}^2$ (n=12) and $1780 \pm 20 \text{ Ohm} \cdot \text{cm}^2$ (n=12), respectively. For measuring drug secretion (B)asolateral \rightarrow (A)apical, 2.5 ml of transport buffer containing ATV ($5 \mu\text{M}$) was put into the B side and 1.5 ml of buffer was put into the A side. At selected times (1, 2 and 3 hr), 150- μl samples were taken from the A side and replaced with fresh buffer. For measuring drug absorption (A \rightarrow B), the drug solution was put into the A side and samples were taken from the B side. For inhibition studies, the inhibitors, RIF ($50 \mu\text{M}$) or GG918 ($0.5 \mu\text{M}$), were put into both the A and B sides. During the studies, the cells were incubated in a shaking incubator (Boekel Scientific, Feasterville, PA). After the last time point (3 hr), the apical solutions were removed by suction, and each filter was dipped twice in ice-cold PBS. Intracellular measurements of ATV were obtained by solubilizing the cells on each culture insert with 0.4 ml of ice-cold MeOH/H₂O [7/3 (v/v)] and sonicating for 10 min. The homogenate was centrifuged for 5 min at 13,000g and the resulting supernatant was analyzed by LC/MS-MS.

3.2.4 Metabolism by rat liver microsomes

Rat liver microsomes were isolated and incubated as described previously by our laboratory (Jacobsen et al., 2000). In brief, microsomal proteins (0.75 mg/ml), 0.1 M phosphate buffer (pH 7.4) and ATV (in methanol, final concentration $1 \mu\text{M}$) were pre-incubated for 5 min. NADPH (1 mM) was added to start the reaction at $37 \text{ }^\circ\text{C}$. To assess the effects of RIF on ATV metabolism, RIF (in dimethyl sulfoxide, final concentration

10-250 μM) was added to the liver microsomal preparations. The reaction was stopped by protein precipitation by addition of an equal volume of ice-cold acetonitrile containing the internal standard, fluvastatin (0.5 μM). The supernatants were stored at -80 °C for LC/MS-MS measurement.

3.2.5 Surgery and perfusion of isolated rat livers

Male Sprague-Dawley rats (300-400 g; Bantin and Kingman, San Leandro, CA) were anesthetized with ketamine/xylazine (80mg; 12mg/ml) before surgery. The hepatic portal vein and superior vena cava were cannulated following approval of protocols by the Committee on Animal Research, University of California, San Francisco. The livers were isolated for perfusion *ex situ* using standard techniques as described previously by our laboratory (Chapter 2; Wu and Benet, 2003; Lau et al., 2004). Briefly, recirculating perfusion was performed at 37 °C from a reservoir containing 110 ml of perfusate composed of Krebs-Henseleit buffer (pH 7.4), supplemented with sodium taurocholate (220 nmole/min), 1% bovine serum albumin, and glucose (10 mM), through the liver via a catheter inserted in the portal vein. The perfusate in the reservoir was oxygenated directly using carbogen, 95% O₂/5% CO₂, and stirred continuously. Measures of liver viability included oxygen consumption, portal vein pressure (20-30 mmHg), pH (7.35-7.45) and metabolic capability. Livers were allowed to stabilize for 20 min. RIF was added to the reservoir 5 min before ATV addition. Perfusate samples (0.5 ml) were collected immediately (0 min) and at 3, 5, 10, 15, 20, 30, 45 and 60 min after the addition of ATV and accumulative bile samples were collected for up to 60 min. At the end of experiment, the liver was removed, blotted dry, and weighed. An aliquot of liver was

homogenized with ice-cold PBS in a 1:2 ratio and maintained frozen at -80 °C before analysis. To examine the effects of RIF on ATV hepatic disposition, 20 rats were divided equally into four groups, and each group was perfused with a bolus dose of ATV to yield an initial perfusate concentration of ~ 1 µM. Whereas one group served as the control, the other three groups served as treatment groups for inhibition studies, with three different final perfusate concentrations of RIF (5, 10 and 50 µM). Samples were prepared by liquid-liquid extraction as described previously (Chapter 2; Lau et al., 2004). In brief, 3 ml of methyl tertiary butyl ether (MTBE) with internal standard, fluvastatin (0.5 µM), was added to each liver, bile and perfusate sample. After centrifugation, separation of the organic layer in a methanol dry ice-bath and evaporation of the organic layer under nitrogen gas, the dried solutes were reconstituted with methanol for analysis by LC/MS-MS.

For studies using the TR⁻ rats, the same IPRL procedures were applied. Six TR⁻ rats were kindly provided by Dr. Antony McDonagh (School of Medicine, UCSF) and were used for IPRL study together with 6 male Sprague-Dawley (SD) rats, which are the wild-type counterparts of TR⁻ rats. Each rat liver was perfused with a bolus dose of ATV to yield an initial perfusate concentration of ~ 5 µM. ATV and metabolites disposition were compared between these two strains of rats at the end of the experiment (60 min).

3.2.6 LC/MS-MS measurement of atorvastatin and metabolites

A Micromass Quattro Ultima instrument (Waters, Milford, MA) with electrospray-positive ionization was used. The multiple reaction monitor (MRM) was set at 559.6 – 440.8 *m/z* for ATV, 575.2 – 440.5 *m/z* for 2-OH ATV and 4-OH ATV and

412.3 – 265.9 *m/z* for the internal standard, fluvastatin. The cone voltage and collision energy were set at 30 V and 20 eV, respectively. The analytical column was an Agilent, XDB C18 (4.6 x 50 mm, 5 µm particle size, Agilent Technologies). The mobile phase consisted of 46% acetonitrile containing 0.05% acetic acid and 5 mM ammonium acetate. Five-microliter aliquots were injected, and the flow rate was set at 1.0 ml/min with ¼ split into the mass system.

3.2.7 HPLC measurement of rifampicin

The HPLC method for analyzing RIF was described previously (Chapter 2; Lau et al, 2004). Briefly, liver samples were analyzed on a HP1100 HPLC-system (Hewlett-Packard, Palo Alto, CA). RIF was resolved on a Microsorb-MV, C₈ analytical column (4.6 x 250 mm, 4 µm particle size; Varian, Walnut Creek, CA). The mobile phase was composed of 0.05 M potassium dihydrogen phosphate/acetonitrile [55/45(v/v)] at a flow rate of 1 ml/min. The UV absorbance was monitored at a wavelength of 340 nm.

3.2.8 Data analysis

The kinetics parameters for the uptake of ATV in the transporter-expressing HEK293 cells were obtained by using the following equation:

$$v_0 = (V_{\max} \cdot S)/(K_m + S) + P_{\text{dif}} \cdot S \quad \text{Eqn. (3.1)}$$

where v_0 is initial uptake rate, S is the substrate concentration, K_m is the Michaelis constant, V_{\max} is the maximal uptake rate, and P_{dif} is the nonsaturable uptake clearance.

The above equation was fitted to the data, using a nonlinear least squares method by SigmaPlot (Version 5.0; SPSS Inc., Chicago, IL). To obtain the IC₅₀ value of RIF inhibition on ATV uptake, the data were fitted using WinNonlin (Version 3.1; Pharsight Corporation, Mountain View, CA). For transport studies, the permeability (P_{app}) values were calculated as follows where the rate of transport was measured from the flux of drug across the cells:

$$P_{app} = \text{rate of transport}/(\text{surface area} \times \text{initial donor concentration}) \quad \text{Eqn. (3.2)}$$

For the IPRL studies, values for area under the concentration –time curve (AUC) were calculated using the linear trapezoidal method. Biliary clearance (CL_b) was the quotient of the cumulative biliary amount of ATV and the AUC of ATV. Student's t test was used to analyze differences between two groups. Analysis of variance was used to analyze differences among more than two groups, and the significance of difference between two means in these groups was evaluated using Tukey's post hoc test. The *p* value for statistical significance was set at < 0.05.

3.3 Results

3.3.1 Uptake studies in HEK293 cells with transient expression of uptake transporters

The uptake of ATV into various rat Oatps (Oatp1a1, 1a4, 1b2) and human OATP1B1 transfected cells and vector-transfected cells is shown in Fig. 3.1. The uptake of ATV was significantly higher in Oatp1a4, Oatp1b2 and OATP1B1 transfected cells relative to that into vector-transfected cells (Fig. 3.1). Oatp1a4 also showed a lower apparent transport efficiency compared with Oatp1b2 using prototypical substrates (data not shown). The concentration-dependent uptake of ATV was examined in Oatp1a4 and Oatp1b2 transfected cells (Fig. 3.2A and 3.2B, respectively). Both a saturable and a nonsaturable component were observed as demonstrated by the Eadie-Hofstee plots (insets of Fig. 3.2A and 3.2B). The obtained K_m , V_{max} and P_{dif} values for the uptake of ATV in Oatp1a4- transfected cells were $22.2 \pm 11.9 \mu\text{M}$, $106.0 \pm 49.7 \text{ pmole/min/mg protein}$ and $0.80 \pm 0.59 \mu\text{l/min/mg protein}$, respectively. The saturable component estimated by V_{max}/K_m accounts for about 86 % of the total uptake. The corresponding values for the uptake of ATV in Oatp1b2-transfected cells were $7.12 \pm 3.10 \mu\text{M}$ for K_m , $37.1 \pm 11.1 \text{ pmole/min/mg protein}$ for V_{max} and $1.50 \pm 0.15 \mu\text{l/min/mg protein}$ for P_{dif} . Saturable uptake accounts for about 79 % of the total uptake. Oatp1a4- and 1b2-mediated uptake of ATV was inhibited by RIF in a concentration-dependent manner (Fig. 3.3). The K_i value was estimated by $IC_{50}/[1 + S/K_m]$. The estimated IC_{50} and K_i values for RIF inhibition on Oatp1a4-mediated uptake of ATV were $3.05 \pm 1.44 \mu\text{M}$ and $2.88 \pm 1.33 \mu\text{M}$ respectively. The corresponding values for RIF inhibition on Oatp1b2-mediated uptake of

ATV were $0.95 \pm 0.25 \mu\text{M}$ and $0.79 \pm 0.13 \mu\text{M}$. In addition, Oatp1b2 was capable of transporting 2-OH ATV and 4-OH ATV (Fig. 3.4). In the presence of excess RIF ($50 \mu\text{M}$), the uptake of these metabolites were reduced to almost the same level as that in vector-transfected cells (Fig. 3.4). ATV ($1 \mu\text{M}$) uptake was inhibited by both 2-OH ATV and 4-OH ATV at concentrations of $1 \mu\text{M}$ and $10 \mu\text{M}$ (Fig. 3.5).

Fig. 3.1 Uptake of ATV ($1 \mu\text{M}$) in HEK293 cells with transient expression of Oatp uptake transporters. Data are shown as the mean \pm SD ($n = 4$). **, $p < 0.01$; ***, $p < 0.001$ versus vector control.

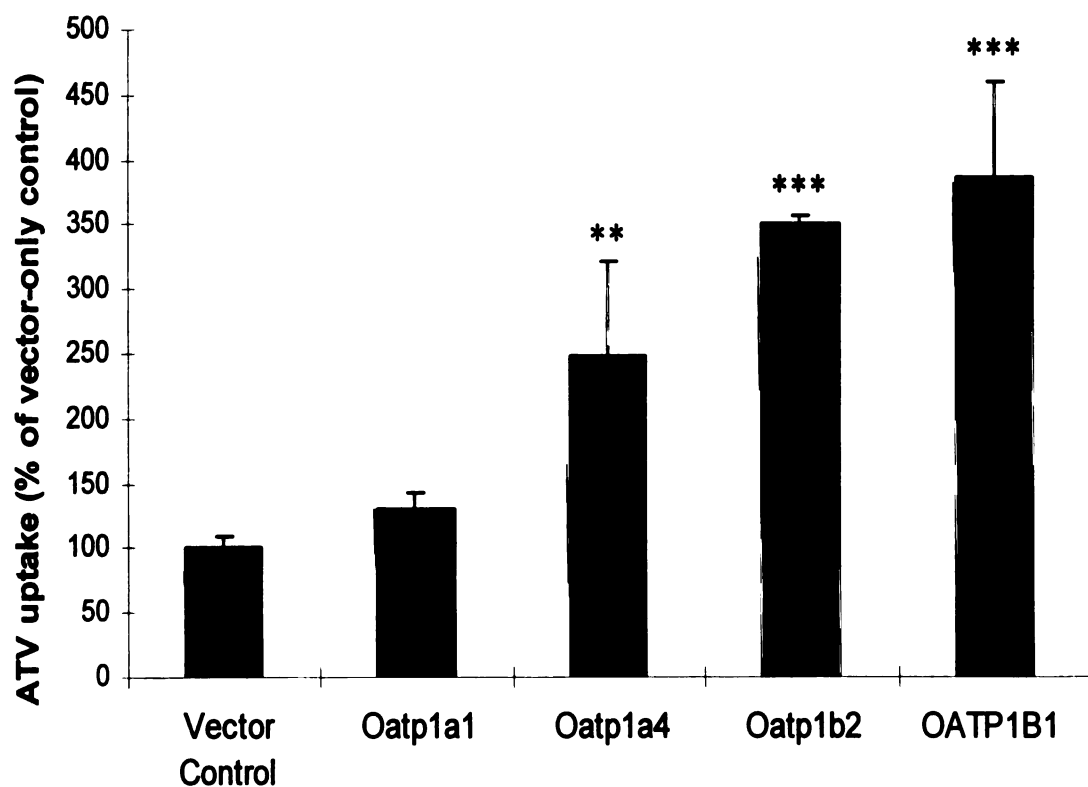


Fig. 3.2 Concentration-dependent uptake of ATV into (A) Oatp1a4 and (B) Oatp1b2 transiently transfected HEK293 cells. Insets show the Eadie-Hofstee plots of the uptake of ATV. Each value represents mean \pm SD ($n = 4$).

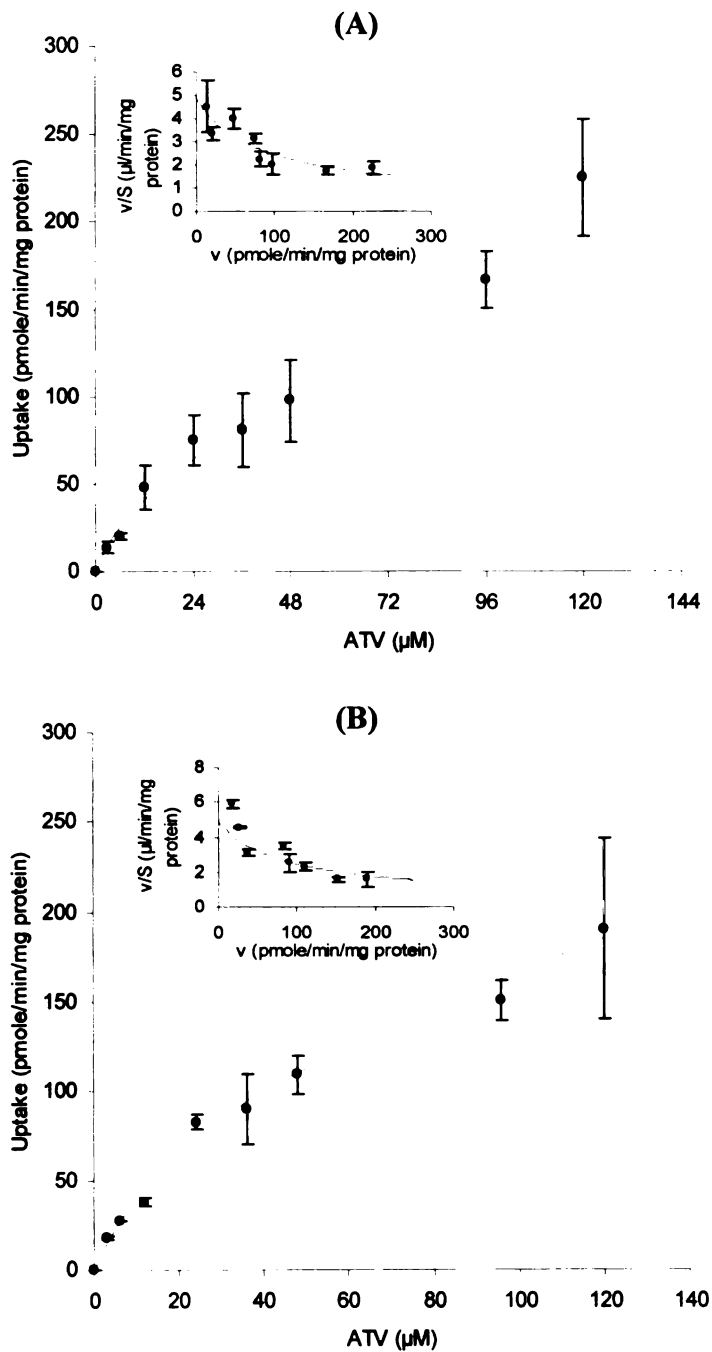


Fig. 3.3 Inhibitory effect of RIF on the uptake of ATV (1 μ M) by Oatp1a4 (triangles) and Oatp1b2 (circles) transiently transfected HEK293 cells. Each value represents mean \pm SD ($n = 4$). Net Oatp1a4 and Oatp1b2-mediated uptakes were calculated by subtracting values obtained with vector-only HEK293 cells from those obtained with transfected HEK293 cells.

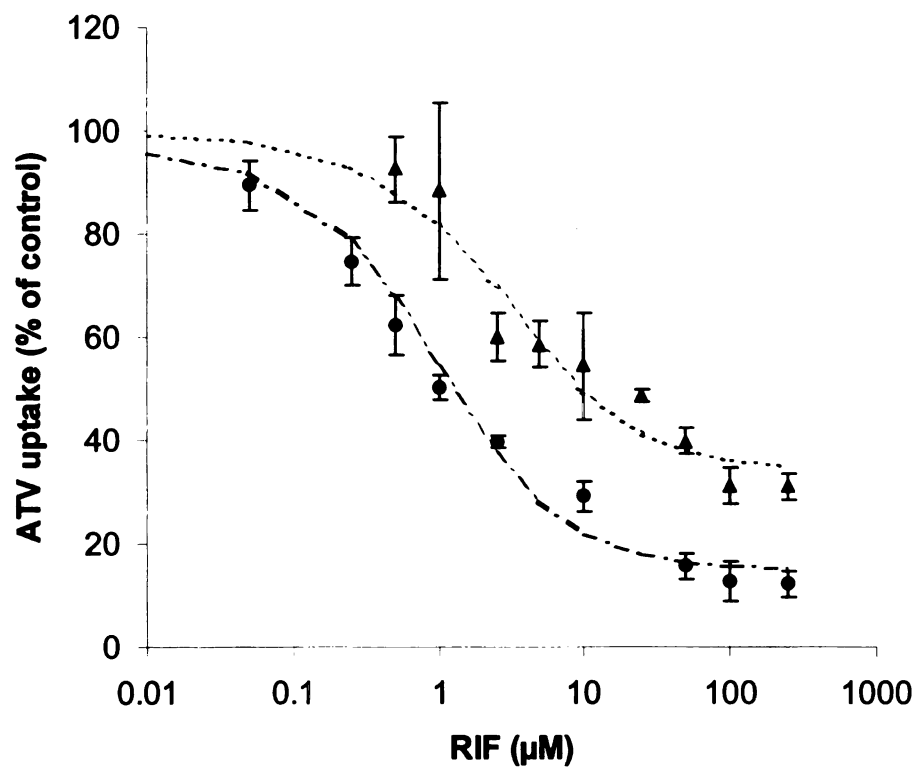


Fig. 3.4 Uptake of 2-OH ATV and 4-OH ATV in HEK293 cells with transient expression of *Oatp1b2* in the presence and absence of RIF (50 μ M). Cellular uptakes of 2-OH ATV (1 μ M) and 4-OH ATV (1 μ M) were determined at 3 min. Data are shown as the mean \pm SD ($n = 4$). **, $p < 0.01$; ***, $p < 0.001$ versus vector control.

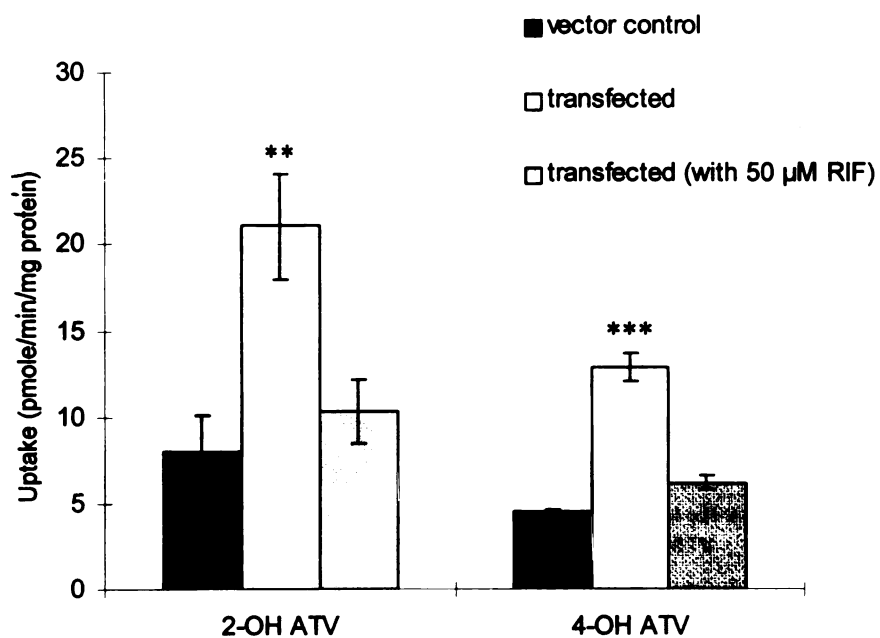
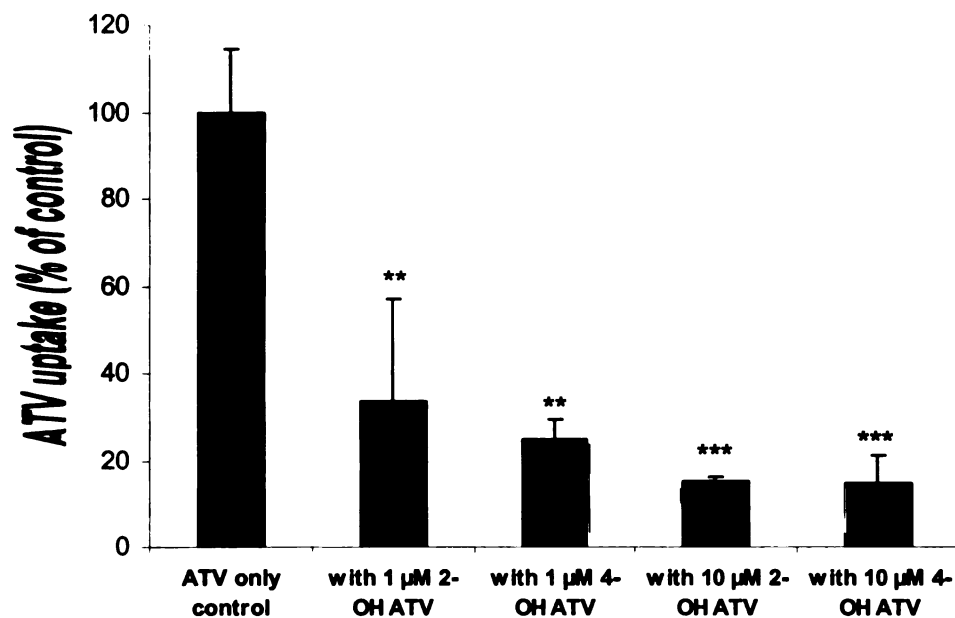


Fig. 3.5 Cis-inhibition of ATV uptake in HEK293 cells with transient expression of *Oatp1b2* by 2-OH ATV and 4-OH ATV. Cellular uptakes of ATV (1 μM) were determined in the absence and presence of 2-OH ATV (1 and 10 μM) and 4-OH ATV (1 and 10 μM) and reported as a percentage of ATV only control. Data are shown as the mean \pm SD ($n = 4$). **, $p < 0.01$; ***, $p < 0.001$ versus control.



3.3.2 Transport studies of atorvastatin in MII, MII-cMOAT, and M-MDR1 cell systems

A significantly ($p < 0.01$) higher B \rightarrow A transport of ATV across MII-cMOAT cells ($P_{\text{app}} = 2.65 \times 10^{-6} \text{ cm sec}^{-1}$) than across MII cells ($P_{\text{app}} = 1.52 \times 10^{-6} \text{ cm sec}^{-1}$) was observed resulting in a net flux ratio (B \rightarrow A/A \rightarrow B) ratio of 3.03 ± 0.43 for MII-cMOAT cells (Table 3.1). In MII cells, the net flux ratio was also higher than 1. This could be explained by the presence of endogenous canine P-gp as well as MRP2 present in the cells, as previously shown in our lab (Flanagan et al., 2002) by Western blot, which

would be expected to generate partial transepithelial transport of ATV. With the addition of RIF (50 μ M), the B \rightarrow A permeability of ATV across MII-cMOAT was significantly reduced by ~ 50 %, resulting in a 3-fold decrease in the net flux ratio (Table 3.1). The intracellular ATV accumulation also significantly increased ($p < 0.05$) compared to the MII-cMOAT control (Table 3.1). In MII cells, the B to A transport of ATV was also decreased by RIF due to the presence of modest expression levels of endogenous MRP2 (Flanagan et al., 2002). RIF demonstrated no inhibitory effect on P-gp at 50 μ M using P-gp over-expressing M-MDR1 cells (Fig. 3.6A), but GG918, a relatively specific inhibitor for P-gp (Cummins et al., 2004), at 0.5 μ M completely eliminated the bidirectional difference in transport (Fig. 3.6B).

Table 3.1 ATV (5 μ M) transport and inhibition across MII and MII-cMOAT cell monolayers.

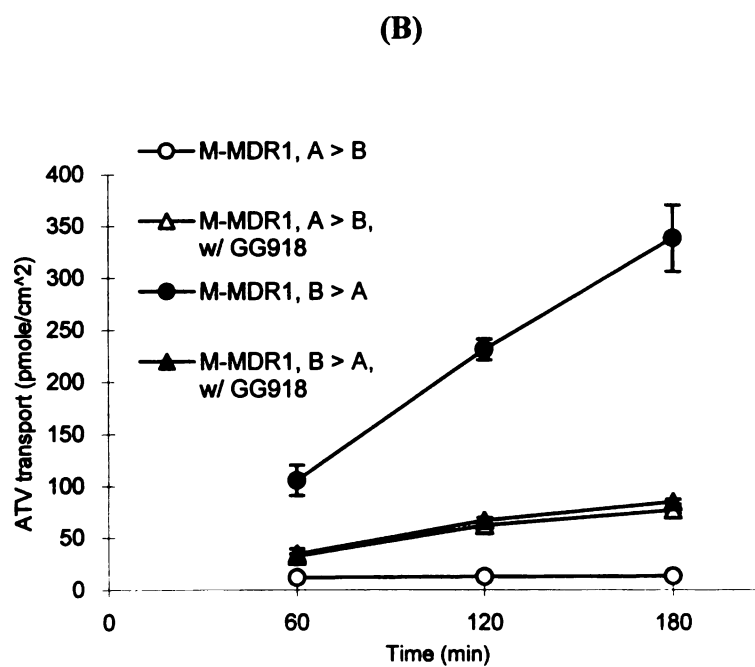
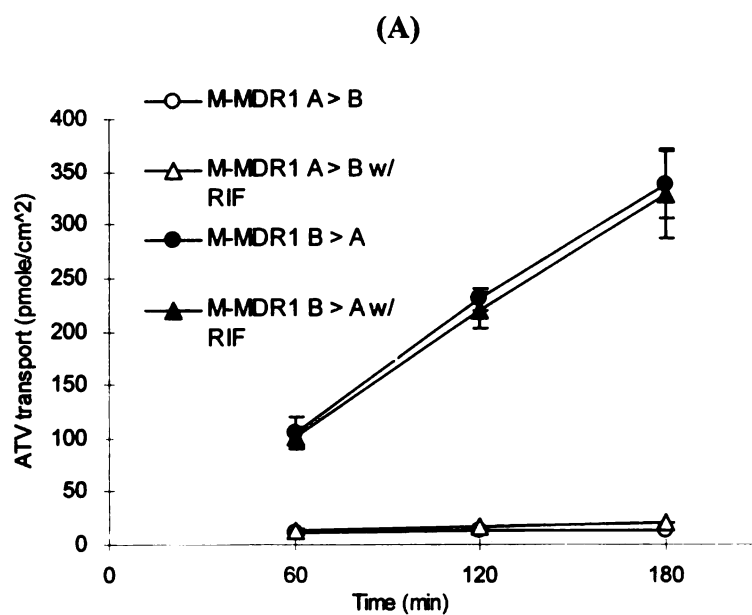
	<i>Condition</i>	P_{app} (B \rightarrow A) \times 10^{-6} (cm sec $^{-1}$) ^a	Net flux ratio (B \rightarrow A/ A \rightarrow B) ^a	Intracellular ATV (B \rightarrow C) ^b (pmole) ^a
MII	control	1.52 \pm 0.23	1.94 \pm 0.43	70.7 \pm 15.5
	w/ RIF (50 μ M)	1.22 \pm 0.09*	1.10 \pm 0.24	87.0 \pm 11.7
MII- cMOAT	control	2.65 \pm 0.23	3.03 \pm 0.43	81.7 \pm 16.6
	w/ RIF (50 μ M)	1.26 \pm 0.09**	0.95 \pm 0.24**	118.5 \pm 9.4*

*, $p < 0.05$; **, $p < 0.01$, RIF treated groups significantly different from ATV only controls.

^a Each value represents mean \pm SD, $n = 4$.

^b Intracellular accumulation of ATV at 3 hr after basolateral doses of ATV to the donor side.

Fig. 3.6 Effects of efflux transport inhibitors on ATV (5 μ M) transport: (A) RIF (50 μ M) across M-MDR1 cells and (B) GG918 (0.5 μ M) across M-MDR1 cells. Values are means \pm SD, $n = 4$.



3.3.3 Metabolic studies of atorvastatin by rat microsomes

The inhibitory effects of RIF (0-250 μM) on the metabolism of ATV were examined (Table 3.2). RIF did not alter the metabolic formation of 2-OH ATV up to a concentration of 25 μM and reduced it to 57% of the control value at 250 μM . RIF did not significantly affect the formation of 4-OH ATV at concentrations lower than 100 μM .

Table 3.2 Effects of RIF on the microsomal metabolism of ATV (1 μM).

Concentrations	2-OH ATV ^a	4-OH ATV ^a
μM	% of control	
0	100.0 \pm 3.9	100.0 \pm 2.4
10	94.5 \pm 2.3	101.8 \pm 1.2
25	92.4 \pm 5.4	99.8 \pm 3.9
50	87.5 \pm 6.9*	91.4 \pm 5.7
100	76.3 \pm 7.6**	80.3 \pm 5.0*
250	57.1 \pm 1.2****	75.0 \pm 1.5**

^a Each value represents mean \pm SD ($n = 4$).

*, $p < 0.05$; **, $p < 0.01$; ***, $p < 0.001$ significantly different from control.

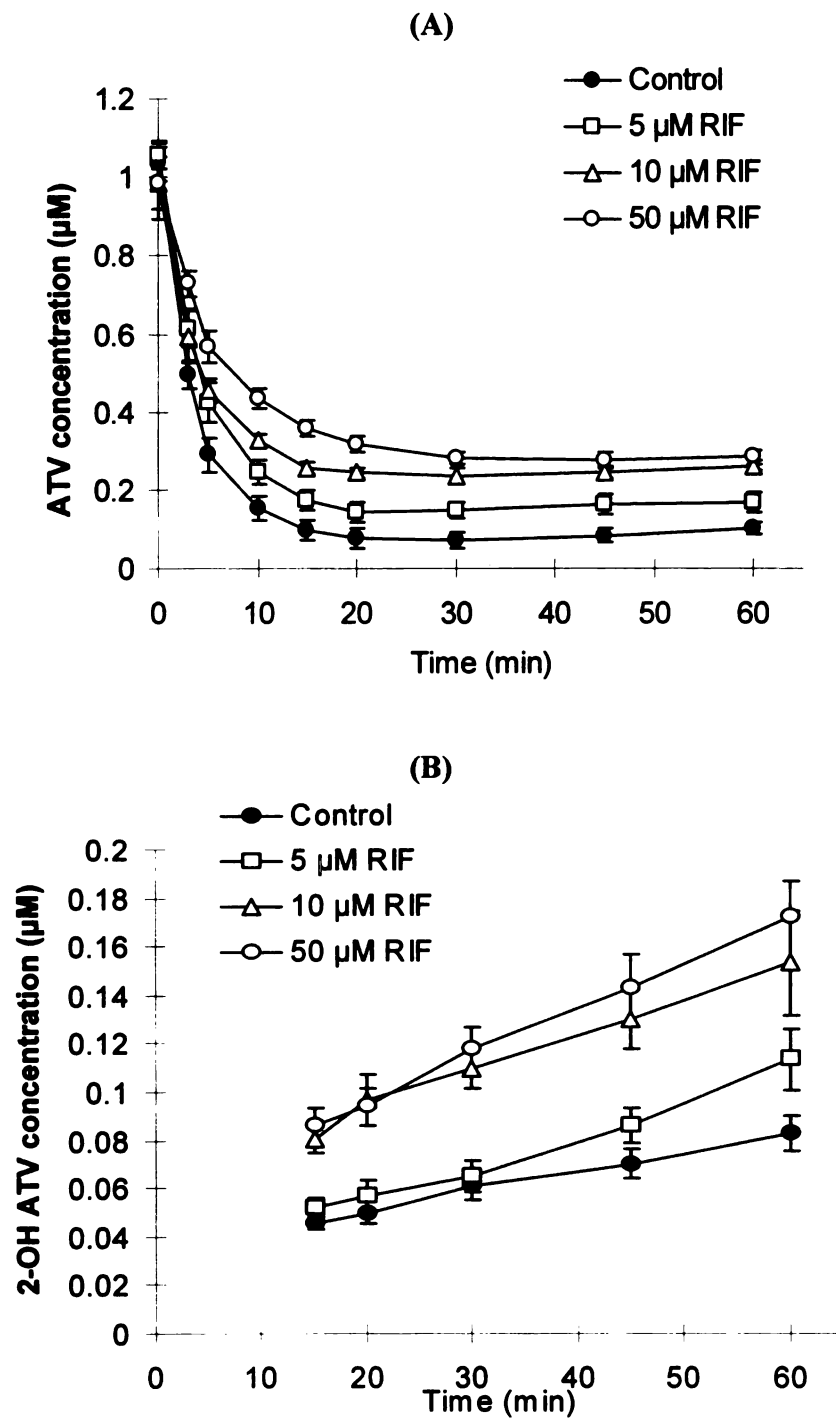
3.3.4 Isolated perfused rat liver studies of atorvastatin

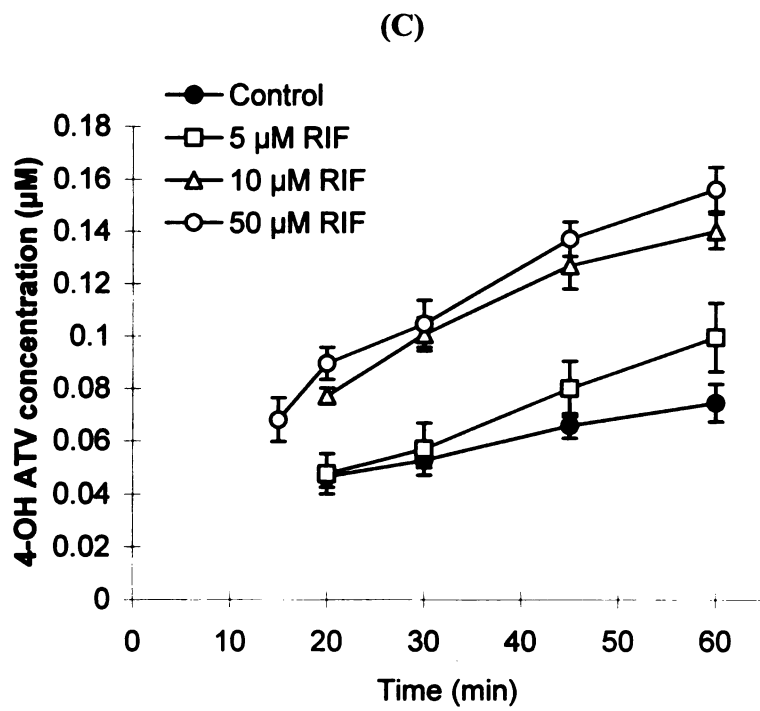
3.3.4.1 Atorvastatin-rifampicin interaction study

Figure 3.7A illustrates the disposition of ATV in perfusate over time in the absence (control) and presence of various concentrations of RIF (5, 10 and 50 μ M). In all RIF-treated groups, ATV concentrations at all sampling times were elevated. The AUC of ATV over the 1-hr sampling period was significantly increased by 56%, 108% and 151% for 5 μ M, 10 μ M and 50 μ M RIF-treated groups, respectively, as shown in Table 3.3. The concentrations of 2-OH ATV and 4-OH ATV were detectable 15 min after the start of perfusion and increased steadily up to 60 min (Figs. 3.7B & 3.7C), indicating that hepatic enzymatic activity of CYP3A was functional throughout the perfusion period. The observed increase in metabolites perfusate concentrations without a concomitant decrease in ATV perfusate concentrations after the rapid initial distribution phase might be due to significant evaporation from perfusate or cis-inhibition of ATV uptake by the metabolites accumulated in the perfusate. Both metabolites could inhibit ATV uptake at the same or 10-fold higher molar concentration of ATV in cellular uptake studies (Fig. 3.5).

The AUCs of both hydroxy metabolites were increased by ~ 20% for 5 μ M RIF, ~ 80% for 10 μ M RIF ($p < 0.01$) and ~ 100% by 50 μ M RIF ($p < 0.001$) treated groups (Table 3.3). The ratio of the sum of the metabolite AUCs to parent AUC (OH ATV AUC/ATV AUC) was comparable for all RIF-treated groups and control group.

Fig. 3.7 Influence of RIF (5, 10, 50 μ M) on concentrations of (A) ATV, (B) 2-OH ATV and (C) 4-OH ATV in perfusate. Each value represents mean \pm SD, $n = 5$ per group.





1
2
3
4
5
6
7
8
9
10
11
12
13
14
15
16
17
18
19
20
21
22
23
24
25
26
27
28
29
30
31
32
33
34
35
36
37
38
39
40
41
42
43
44
45
46
47
48
49
50
51
52
53
54
55
56
57
58
59
60
61
62
63
64
65
66
67
68
69
70
71
72
73
74
75
76
77
78
79
80
81
82
83
84
85
86
87
88
89
90
91
92
93
94
95
96
97
98
99
100

Table 3.3 Comparison of parameters between control rat livers perfused with ATV alone and livers co-perfused with RIF.

Parameter ^a	<i>Treatment group</i>			
	Control	RIF 5 μ M	RIF 10 μ M	RIF 50 μ M
ATV AUC ^b (μ M·min)	8.55 \pm 1.89	13.3 \pm 1.7*	17.8 \pm 3.1***	21.4 \pm 3.0***
2-OH ATV AUC ^b (μ M·min)	2.93 \pm 0.48	3.51 \pm 0.75	5.33 \pm 0.64 **	5.84 \pm 0.71***
4-OH ATV AUC ^b (μ M·min)	2.44 \pm 0.36	2.90 \pm 0.92	4.44 \pm 0.06**	5.23 \pm 0.08***
OH ATV AUC/ATV AUC	0.66 \pm 0.18	0.48 \pm 0.08	0.56 \pm 0.09	0.53 \pm 0.08
OH ATV/ATV in liver ^c	0.43 \pm 0.16	0.35 \pm 0.15	0.28 \pm 0.11	0.17 \pm 0.05*
CL _b (ml/min) ^d	1.31 \pm 0.50	0.64 \pm 0.18**	0.21 \pm 0.06***	0.064 \pm 0.019***
bile/liver (ATV) ^e	0.21 \pm 0.04	0.26 \pm 0.10	0.10 \pm 0.05	0.026 \pm 0.019***
bile/liver (OH ATV) ^f	0.14 \pm 0.06	0.27 \pm 0.15	0.42 \pm 0.31	0.059 \pm 0.017
RIF in liver ^g (μ M)	N/A	11.2 \pm 2.1	18.4 \pm 3.6	121 \pm 19

^a Mean \pm SD, $n = 5$ per group.

^b AUC calculated using the linear trapezoidal method up to 1 hr.

^c Ratio of amount of total OH ATV formed to amount of ATV retained in liver at 1 hr.

^d Biliary clearance (quotient of the cumulative amount of ATV excreted into bile and the ATV AUC)

^e Ratio of amount of ATV in bile to that in liver at 1 hr.

^f Ratio of amount of total OH ATV in bile to that in liver at 1 hr.

^g Concentration of RIF detected in liver at 1 hr.

*, $p < 0.05$; **, $p < 0.01$; ***, $p < 0.001$ significantly different from control.

The amounts of ATV and metabolites recovered in various matrices from IPRL studies in the absence and presence of RIF are presented in Table 3.4. The amounts of RIF recovered in the liver homogenate increased linearly with the RIF dose administered ($y=2.49x - 3.71$; $r^2 = 0.998$). The majority of the dose recovered was present in the liver homogenate as ATV at the end of the experiment (1hr). ATV amount was significantly decreased in 5 μM RIF-treated livers and slightly decreased in 10 μM RIF-treated livers. In 50 μM RIF-treated livers, however, there was an increase in ATV amount, although not significant. Liver retention of metabolites was reduced, with a significant decrease of ~50 % for total metabolites (sum of 2-OH ATV and 4-OH ATV) in all RIF-treated groups. The ratios of total metabolites to parent retention in liver were calculated for all groups (Table 3.3). There was a gradual decrease of the ratios with increasing RIF concentration (19%, 35% and 60 % decrease for 5, 10, and 50 μM RIF, respectively). However, only the 50 μM RIF-treated group exhibited a significant decrease.

RIF exhibited a concentration dependent inhibitory effect on the biliary excretion of ATV and metabolites, in which the cumulative amounts were significantly reduced in the 10 and 50 μM RIF-treated groups (Table 3.4; Fig. 3.8A & 3.8B). The biliary clearance of ATV was significantly decreased 51%, 84% and 95% by 5, 10 and 50 μM RIF, respectively. The ratios of amounts of ATV in bile/liver were statistically unchanged for 5 and 10 μM RIF treated groups, but was significantly decreased 88% by 50 μM RIF (Table 3.3). The bile/liver ratio for total OH ATV was not significantly changed between groups. Mass balance calculations (ATV, 2-OH ATV and 4-OH ATV in perfusate, liver and bile) show no statistical significant differences between the four studies (79.3 ± 8.4 % for control, 70.0 ± 6.5 % with 5 μM RIF, 79.4 ± 8.2 % with 10 μM

RIF, 93.1 ± 13.9 % with $50 \mu\text{M}$ RIF). Furthermore, the 5 and $10 \mu\text{M}$ RIF treatment groups, where we expect no effects on the enzymatic process, the increase in perfusate drug and metabolite amounts appear to be balanced by the decreased amounts in the liver so that the total percentage of metabolites is essentially the same as for control (28.7% for control, 26.4% for $5 \mu\text{M}$ RIF and 30.8% for $10 \mu\text{M}$ RIF) (Table 3.4). This unexpected finding differs from our previous digoxin reports (Chapter 2; Lam and Benet, 2004; Lau et al., 2004).

Table 3.4 Percentage of the dose recovered as ATV or OH ATV from rat livers perfused with ATV alone and livers co-perfused with RIF.

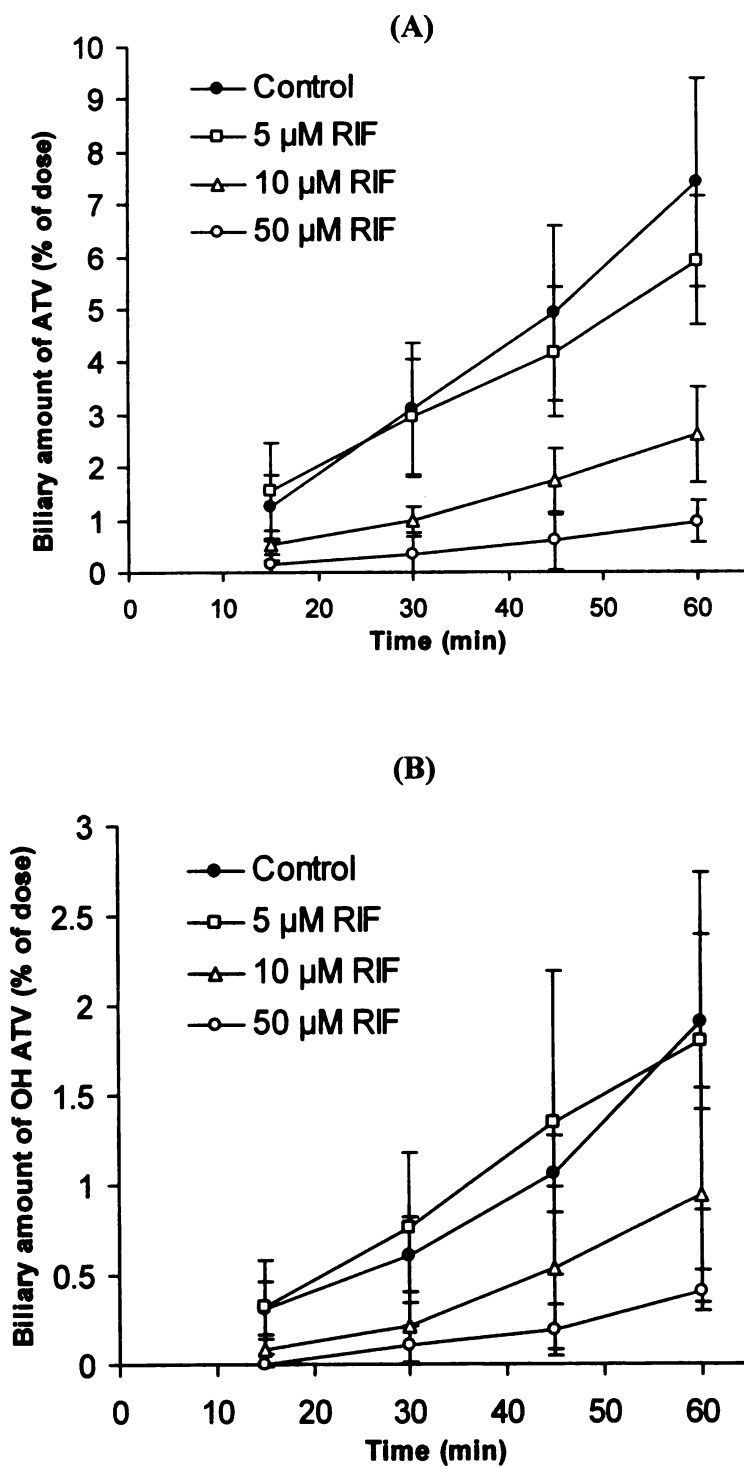
Treatment ^a	Matrix						Total
	Perfusate		Liver		Bile		
	ATV	OH ATV ^b	ATV	OH ATV ^b	ATV	OH ATV ^b	
Control	7.58 ± 3.08	11.4 ± 1.7	35.7 ± 5.6	15.4 ± 5.8	7.41 ± 2.00	1.90 ± 0.49	79.3 ± 8.4
RIF $5 \mu\text{M}$	$13.2 \pm 1.6^*$	$17.1 \pm 2.5^{**}$	$24.5 \pm 4.1^*$	$7.52 \pm 3.31^*$	5.92 ± 1.23	1.80 ± 0.94	70.0 ± 6.5
RIF $10 \mu\text{M}$	$19.4 \pm 4.5^{***}$	$22.6 \pm 3.3^{***}$	26.7 ± 4.7	$7.21 \pm 1.91^*$	$2.60 \pm 0.90^{***}$	$0.94 \pm 0.59^{**}$	79.4 ± 8.2
RIF $50 \mu\text{M}$	$20.7 \pm 2.5^{***}$	$23.1 \pm 1.6^{***}$	41.2 ± 10.7	$6.75 \pm 0.97^{**}$	$0.96 \pm 0.29^{***}$	$0.41 \pm 0.12^{***}$	93.1 ± 13.9

^a Mean \pm SD, $n = 5$ per group.

^b OH ATV is the sum of 2-OH ATV and 4-OH ATV.

*, $p < 0.05$; **, $p < 0.01$; ***, $p < 0.001$ significantly different from control.

Fig. 3.8 Time profile of cumulative amount of (A) ATV and (B) total OH ATV (sum of 2-OH ATV and 4-OH ATV) detected in bile in control and RIF-treated perfused rat livers. Values are mean \pm SD, $n = 5$ per group.



3.3.4.2 Wild-type Sprague-Dawley and TR⁻ rats study

There was no statistically significant difference between the AUC_{0-60 min} values for the SD and TR⁻ rats (Table 3.5). The cumulative biliary excretion of ATV and total hydroxy metabolites in SD rats was significantly higher than the biliary excretion in TR⁻ rats. The biliary clearance (CL_b) value in TR⁻ rats was about one tenth of that in SD rats (Table 3.5).

Table 3.5 Comparison of parameters between Sprague-Dawley (SD) and TR⁻ rat livers perfused with ATV.

Strain ^a	ATV AUC ^b ($\mu\text{M}\cdot\text{min}$)	Cumulative ATV biliary excretion (nmole) ^c	Cumulative OH ATV biliary excretion (nmole) ^c	CL _b (ml/min) ^d
SD	43.0 \pm 19.9	62.4 \pm 14.2	4.45 \pm 3.33	1.63 \pm 0.64
TR ⁻	48.2 \pm 20.0	7.18 \pm 6.35***	0.47 \pm 0.44*	0.16 \pm 0.13**

^a Mean \pm SD, $n = 5$ per group.

^b AUC calculated using the linear trapezoidal method up to 1 hr.

^c Cumulative biliary amounts up to 1 hr.

^d Biliary clearance (quotient of the cumulative amount of ATV excreted into bile and the ATV AUC).

*, $p < 0.05$; **, $p < 0.01$; ***, $p < 0.001$ significantly different from SD rats.

3.4 Discussion

It is now well recognized that the hepatic drug elimination process is mainly regulated by three distinct groups of proteins: uptake transporters, metabolizing enzymes and efflux transporters, arranged in a sequential manner. The goal of the present study was to investigate the complex interplay between these groups of proteins by applying the IPRL as a proof of concept model, complemented by cellular studies to examine individually the relevance of the potential players in the disposition of ATV. In all cases, the ability of RIF to inhibit transporters and enzymes was tested.

Our uptake study results demonstrate that ATV is a substrate of OATP1B1 and Oatp1a4 as well as Oatp1b2 (Fig. 3.1), the rat ortholog of OATP1B1 (Kakyo et al., 1999; Cattori et al., 2001). RIF is capable of inhibiting ATV uptake mediated by both Oatps in a concentration dependent manner (Fig. 3.3). Recently, it has been demonstrated that RIF is a substrate of Oatp1b2 (Tirona et al., 2003), which is liver specific and exhibits the highest amino acid sequence identity with OATP1B1 (Cattori et al., 2001). It is likely that RIF competitively reduces the sinusoidal uptake of ATV via this transporter as well as the more well studied Oatp1a4 (Fattering et al., 2000; Shitara et al., 2002).

Similar to P-gp, MRP2 is an efflux transporter, expressed at high levels in the canalicular domains of hepatocytes (Evers et al., 1998). Transport studies were used as a tool to evaluate the influence of MRP2 on drug export since the cellular B → A transport mimics the orientation of apical efflux transporters in the liver. The results generated from the MII-cMOAT cells indicate that ATV is a co-substrate of both P-gp (Fig. 3.6B) and MRP2 (Table 3.1), with a net flux ratio of 3 using the MII-cMOAT cells, a value that reflects the leaky nature of this cell line. Incubation with 50 μM of RIF results in

decreased P_{app} ($B \rightarrow A$), a change in the flux ratio to approximately unity, along with a significant increase in intracellular ATV accumulation (Table 3.1). These results support the report of Cui et al. (2001a) in that RIF is capable of inhibiting MRP2 as well as OATP.

The working concentration of ATV was carefully chosen at 1 μM in the IPRL study, which is well below the K_m values (23.8 μM and 19.8 μM for 2-OH ATV and 4-OH ATV formation, respectively) obtained from microsomal studies (data not shown) and uptake studies (Fig. 3.2A & 3.2B), to prevent saturation of both enzyme and Oatp transporters. As expected, RIF significantly increased the AUC of ATV in the IPRL studies at all three tested concentrations (5, 10 and 50 μM).

The influence of Oatps on hepatic transport of the two ATV active hydroxy metabolites has not been reported previously. In the present IPRL studies, we observed an increase in AUC for both metabolites by RIF in a concentration dependent manner. This phenomenon is consistent with the uptake study in which both metabolites are substrates of Oatp1b2 and that RIF significantly inhibits their uptake (Fig. 3.4). Our previous digoxin IPRL study (Chapter 2; Lau et al., 2004) showed that inhibition of digoxin hepatic uptake led to an increase in parent drug AUC but a decrease in metabolite AUC; hence a decrease in metabolite/parent AUC ratio was observed. We suspect that this decrease in ratio is a result of the metabolite not being a substrate, at least, not as good a substrate for the uptake transporter as the parent drug. In the present study, the metabolite/parent AUC ratios remain statistically unchanged, indicating that the disposition of the two ATV metabolites were inhibited by RIF to a similar extent as the parent ATV.

Overlap in inhibitor selectivity for enzyme versus transporter makes it difficult to differentiate the roles of uptake transporter and enzyme in drug disposition since inhibition of either can lead to an increase in drug exposure. We therefore examined the inhibitory effect of RIF on CYP-mediated metabolism of ATV in microsome. RIF appears to have only a moderate effect on metabolism, showing inhibition only at higher concentrations ($\geq 50 \mu\text{M}$) (Table 3.2). RIF liver concentrations reached values of 11.2 and 18.4 μM for the 5 and 10 μM RIF doses, respectively (Table 3.3), concentrations well below 50 μM . Consequently, less ATV and metabolites were detected in liver tissues for 5 and 10 μM RIF doses (Table 3.4), indicating that RIF has an inhibitory effect on uptake but no effect on metabolism at concentrations less than 50 μM in the liver. Although not statistically significant, the metabolites/parent liver ratios between the control and the 5 and 10 μM RIF-treatment groups appear to decrease gradually with increasing RIF concentration (Table 3.3). Since the metabolites appear to be more susceptible than the parent to Oatp mediated uptake, more metabolites would stay in the perfusate as opposed to the liver (Fig. 3.7B & 3.7C), and hence the extent of decrease in liver retention for metabolites would be greater than that for parent drug.

A greater and significant decrease in the metabolite/parent liver ratio was observed for the 50 μM RIF-treatment group (Table 3.3). Here, RIF liver concentration reached a value of 120 μM , a concentration high enough to inhibit the formation of both metabolites (Table 3.2). However, the increase in ATV retention in liver cannot be attributed to enzymatic inhibition only. Note that the bile/liver amount ratio for ATV was relatively constant across control and the 5 and 10 μM RIF-treatment groups (Table 3.3), suggesting that the change of parent drug and metabolites in bile is reflective of

what is observed in the liver. However, the ratio was significantly decreased in the 50 μ M RIF-treatment group (Table 3.3), suggesting that apical transporters mediating the efflux of ATV might be inhibited at this concentration. Determining whether the metabolites are substrates of P-gp and Mrp2 is the subject of continuing studies in our lab. However, it is likely that increased ATV retention in liver is partially caused by Mrp2 inhibition based on our present transport study results (Table 3.1). On the basis of the results obtained from TR⁻ rats (Table 3.5), Mrp2 is likely to play a dominant role in the biliary excretion of ATV as indicated by the fact that the biliary amount of ATV was significantly lower in the experiments using TR⁻ rats, which have inherited the Mrp2 deficiency, as compared to the results obtained from SD rats. It is unclear as to why there was no significant increase in AUC_{0-60 min} in TR⁻ rats when the CL_b of TR⁻ rats was about one-tenth the value of SD rats. We speculate that reduction in the expression of other transporter proteins such as Oatp1a4 (Kuroda et al., 2004) might cause greater accumulation of ATV in the liver of TR⁻ rats and is responsible for the relatively small increase in the perfusate exposure. We also tested the potential for 50 μ M RIF to inhibit P-gp, using P-gp over-expressing cells. No inhibition of transport activity could be detected (Fig 3.6A). Obviously, to unambiguously characterize the pharmacokinetics of ATV, the contributions of other transporters such as Bcrp and Bsep at the canalicular border and Mrp3 and Ntcp on the basolateral side should be further examined.

It has been suggested that the concerted action of uptake and efflux transporters govern the movement of drugs across hepatocytes and that combined inhibition of both types of transporters may account for the observed drug interactions *in vivo* (Cvetkovic et al., 1999; Cui et al., 2001a; Sasaki et al., 2004). However, it is essential to recognize

that uptake and efflux transporters may exert opposing effects on liver drug concentrations of both parent drug and metabolites. Recent studies from our laboratory have shown that decreased and increased metabolism of digoxin were observed when Oatp1a4 and P-gp were inhibited, respectively (Chapter 2; Lam and Benet, 2004; Lau et al., 2004). When efflux is blocked, more drug is available to be metabolized by the enzyme whereas less drug can access the enzyme when uptake is inhibited. In the present study, inhibition of Oatp-mediated uptake also reduced the partition of ATV in the liver, as reflected by the decrease in parent drug and metabolites detected in liver in the 5 and 10 μ M RIF groups. However, the extent of metabolism remained unaltered as demonstrated by the similar OH ATV recovered in the entire system between control and 5, 10 μ M RIF treatment groups (Table 3.4), which we cannot explain at the present time. Although ATV liver retention was increased due to a combination of inhibition of enzyme and efflux transporter at 50 μ M RIF, the perfusate AUC changes still suggest that uptake inhibition was in effect.

Inhibition of ATV hepatic uptake has implications beyond pharmacokinetics since the liver is the site of action for ATV, as well as its two active metabolites. Considering that significant hydroxy metabolites are formed before reaching the liver due to intestinal CYP3A-mediated metabolism (Lennernas, 2003), a decrease in HMG-CoA reductase inhibitory effect will likely occur under Oatp inhibition since hydroxy metabolites are substrates for Oatp and are equipotent as the parent drug.

A recent study examining the relationship between an OATP1B1 variant and ATV and pravastatin induced rhabdomyolysis found that the OATP-C*15 mutant allele is significantly higher in patients who experienced statin-induced myopathy, suggesting

the significance of OATP1B1 down-regulation to statin exposure (Morimoto et al., 2004). It has also been previously demonstrated that OATP/Oatp could be the major determinant in causing clinical drug-drug interactions between cerivastatin and cyclosporine (Shitara et al., 2003) and between bosentan and cyclosporine (Treiber et al., 2004). This study further confirms the dominance of Oatp in mediating the interactions between ATV and the Oatp inhibitor, RIF. RIF is a much weaker inhibitor of CYP3A compared to cyclosporine and therefore a better compound for differentiating uptake versus metabolism. Based on the results of the present study, we conclude that inhibition of hepatic uptake might be one of the major mechanisms for drug-drug interaction, particularly for metabolized compounds such as ATV. In the following chapters the ATV-RIF interaction in whole animal and clinical studies will be presented.

Chapter 4

CYP3A4-TRANSFECTED CACO-2 CELLS AS A TOOL FOR UNDERSTANDING THE EFFLUX-METABOLISM INTERPLAY OF ATORVASTATIN IN THE INTESTINE AND THE LIVER

4.1 Introduction

Drug absorption from the gastrointestinal (GI) tract is a very complex process and is influenced by many factors, including physiochemical properties (i.e. solubility, permeability) of drug compounds as well as carrier-mediated processes. Efflux transporters located in the intestine, including P-glycoprotein (P-gp), the multidrug resistant-associated protein family (MRP) and breast cancer resistant protein (BCRP) might all play a role in modulating the rate and extent of intestinal drug absorption and metabolism (Takano et al., 2006).

Cytochrome P450 3A4 (CYP3A4) and P-gp are present at high levels in the villus tips of enterocytes in the GI tract (Watkins et al., 1987; Zhang and Benet, 2001) and have been considered to work cooperatively in limiting the availability of xenobiotics (Benet and Cummins, 2001; Zhang and Benet, 2001). Our laboratory has previously hypothesized and demonstrated that by inhibiting the activity of intestinal P-gp, the extent of gut metabolism for compounds that are bi-substrates of P-gp and CYP3A4 were reduced as the repeated cycling of drugs mediated by P-gp at the apical membrane of

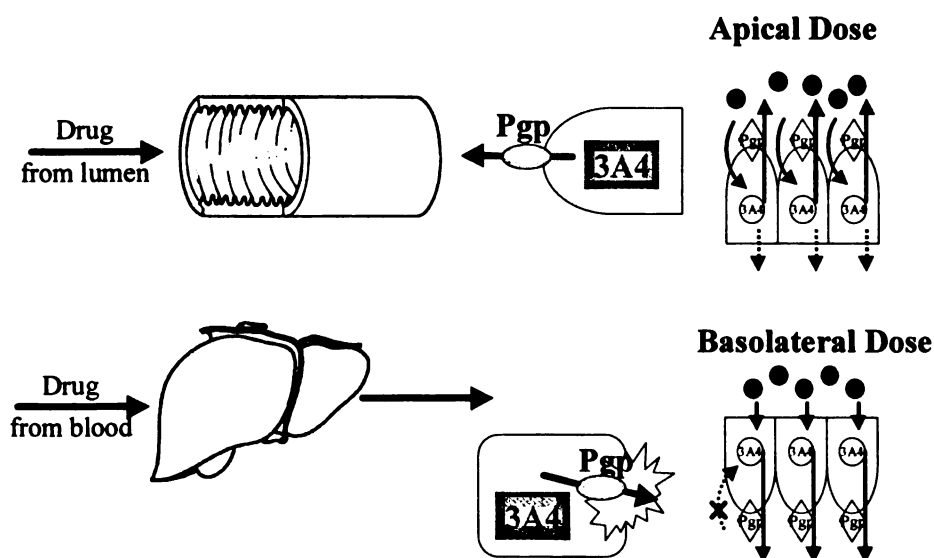
enterocytes was inhibited, hence, leading to an increase in oral bioavailability (Benet et al., 2004). By adopting a cell-based model using the CYP3A4 cDNA-transfected Caco-2 cells, the metabolic extraction ratio (ER), a measurement of the extent of metabolism, of extensively metabolized drug compounds such as the immunosuppressant, sirolimus, and the cysteine protease inhibitor, *N*-methyl piperazine-Phe-homoPhe-vinylsulfone phenyl (K77), was found to be reduced in the presence of GG918, an inhibitor of P-gp but not CYP3A4 (Cummins et al., 2002a, 2004), when drugs were dosed on the apical (A) side. However, the basolateral ER was increased when these compounds were dosed at the basolateral (B) side. In the case of reverse direction transport (i.e. B to A direction), the enzyme topographically precedes the efflux transporter, which mimics the relationship between these two proteins in the liver compartment (Benet et al., 2004).

In 1995, Amidon and co-workers proposed the Biopharmaceutics Classification System (BCS), in which they suggested that aqueous solubility and GI permeability of drug compounds are the fundamental properties for controlling the rate and extent of oral drug absorption (Amidon et al., 1995). Wu and Benet (2005) recognized the importance of these physicochemical properties and proposed a new system, the Biopharmaceutics Drug Disposition Classification System (BDDCS), with the objective of predicting the effects of influx and efflux transporters on drug pharmacokinetics and metabolism.

In the present study, we used atorvastatin (ATV), an extensively metabolized drug categorized as a Class II compound in the BDDCS system (Wu and Benet, 2005), exhibiting low solubility and high permeability, as a model compound to evaluate if P-gp can modulate its extent of metabolism with and without two inhibitors, GG918 (an inhibitor of P-gp) and cyclosporine A (CsA, a dual inhibitor of P-gp and CYP3A4).

P-gp-mediated efflux of ATV was validated by comparing the difference in net flux ratio in MDCK-MDR1 (M-MDR1) cell system with and without GG918, as presented in Chapter 3 (Fig. 3.6B). Metabolic ER from both A to B and B to A directions were monitored in all studies, as the topographical relationship between CYP3A4 and P-gp in the intestine and the liver was represented by A to B and B to A transport, respectively (Benet et al., 2004) (Fig. 4.1). The intracellular drug levels were also measured at the end of the experiments to estimate the influence of inhibitors on cellular disposition of parent drug and its metabolites. It was the purpose of this study to model possible efflux-metabolism interplay in both gut and liver as they might contribute to the low bioavailability (F) of ATV in humans (Gibson et al., 1997).

Fig. 4.1. The spatial relationship between the enzyme and transporter in the intestine and the liver as mimicked by the cellular system of Cummins et al. (2001). From Benet et al. (2004).



4.2 Materials and methods

4.2.1 Materials

Atorvastatin (ATV), *para*-hydroxy atorvastatin (4-OH ATV) and *ortho*-hydroxy atorvastatin (2-OH ATV) were kindly supplied by Parke-Davis (Ann Arbor, MI) and Bristol-Myers Squibb (Princeton, NJ). Fluvastatin (Novartis, Cambridge, MA) and GG918 (GF120918; GlaxoSmithKline, Research Triangle Park, NC) were kind gifts from the manufacturers. Transwell inserts with 0.4 μ M-pore size were obtained from BD Bioscience (Bedford, MA). Six-well plates were obtained from Corning Life Sciences (Acton, MA). Sodium butyrate, 12-*O*-tetradecanoylphorbol 13-acetate (TPA) and cyclosporine (CsA) were purchase from Sigma-Aldrich (St. Louis, MO). All other chemicals were of reagent grade and purchased from either Sigma-Aldrich or Fisher Scientific Co. (Pittsburg, PA).

4.2.2 Cell culture growth conditions

CYP3A4-transfected Caco-2 cells (Gentest, Woburn, MA; passages 3) were grown using Dulbecco's modified Eagle's medium containing 8.5 g/l glucose, 25 mM HEPES, and 2.2 g/l NaHCO₃ and nonessential amino acids (custom made by the UCSF Cell Culture Facility, San Francisco, CA) containing 15% heat-inactivated FBS (Invitrogen, Carlsbad, CA), 100 U/ml penicillin and 100 mg/ml streptomycin as well as 100 μ g/ml hygromycin B (Invitrogen). Cells grown to confluence in culture flasks were harvested and seeded into transwell inserts in 6-well plates at a density of $\sim 3 \times 10^5$ cells/insert and grown to confluence for 13-14 days. Media was changed once every 2

days. Twenty-hour hours before the experiment, the cell culture media was replaced with growth media containing 4 mM sodium butyrate and 100 nM TPA for CYP3A4 protein induction (Cummins et al., 2002a, 2004).

The MDCK-MDR1 (M-MDR1) cell line was generously provided by Dr. Ira Pastan (National Cancer Institute, National Institutes of Health, Bethesda, MD). M-MDR1 cells were cultured in Dulbecco's modified Eagle's medium supplemented with 10% heat-inactivated FBS, 100 U/ml penicillin and 100 mg/ml streptomycin, containing 80 mg/ml colchicine for selected growth of MDR1 transfected cells (Pastan et al., 1988). Cells grown to confluence in culture flasks were harvested and seeded into transwell inserts in 6-well plates at a density of $\sim 10^6$ cells/insert and grown to confluence for 5 to 6 days.

4.2.3 Transport studies of ATV across CYP3A4-transfected Caco-2 cells

The transport experiments were adapted with modifications from Flanagan et al. (2002) and Cummins et al. (2004). Briefly, cell monolayers were preincubated in transport buffer (Hanks' balanced salt solution containing 25 mM HEPES and 1% FBS, pH 7.4) for 20 min at 37 °C. Transepithelial electrical resistance (TEER) was measured in each well using a Millicell ERS voltohmmeter (Millipore Corporation, Bedford, MA) to assess the integrity of monolayers. The average TEER values obtained from the cells were $320 \pm 15 \text{ Ohm} \cdot \text{cm}^2$ ($n = 12$). For measuring drug secretion (B)asolateral \rightarrow (A)pical, 2.5 ml of transport buffer containing ATV (20 μM) was put into the B side and 1.5 ml of buffer was put into the A side. At selected times (1, 2 and 3 hr), 150- μl samples were taken from the A side and replaced with fresh buffer. For measuring drug

absorption (A → B), the drug solution was put into the A side and samples were taken from the B side. For inhibition studies, the inhibitors, CsA (10 μM) or GG918 (0.5 μM), were put into both A and B sides. During the studies, the cells were incubated in a shaking incubator (Boekel Scientific, Feasterville, PA). After the last time point (3 hr), 150-μl samples were collected from the donor side as well. The apical solutions were removed by suction, and each filter was dipped twice in ice-cold phosphate buffered saline. Intracellular measurements of ATV were obtained by solubilizing the cells on each culture insert with 0.4 ml of ice-cold MeOH/H₂O [7/3 (v/v)] and sonicating for 10 min. The homogenate was centrifuged for 5 min at 13,000g and the resulting supernatant was analyzed by LC/MS-MS.

4.2.4 Transport studies of 2-OH ATV and 4-OH ATV across M-MDR1 cells

The transport experiment procedures were the same as that for CYP3A4-transfected Caco-2 cells. In brief, cell monolayers were preincubated in transport buffer followed by measurement of TEER values. The average TEER values for M-MDR1 cells were $1700 \pm 18 \text{ Ohm} \cdot \text{cm}^2$ (n = 12). For measuring drug secretion B → A, 2.5 ml of transport buffer containing 2-OH ATV or 4-OH ATV (1 μM) was put into the B side and 1.5 ml of buffer was put into the A side. For measuring drug absorption (A → B), the drug solution was put into the A side and samples were taken from the B side. For the inhibition study, GG918 (0.5 μM), was put into both A and B sides. At the end of the experiment (3 hr), solutions were removed by suction from both sides. Intracellular measurements of ATV were obtained by solubilizing the cells on each culture insert with 0.4 ml of ice-cold MeOH/H₂O [7/3 (v/v)] and sonicating for 10 min. The homogenate

was centrifuged for 5 min at 13,000g and the resulting supernatant was analyzed by LC/MS-MS.

4.2.5 LC/MS-MS measurement of ATV and metabolites

The method was described in the Section 3.2.6 (Chapter 3).

4.2.6 Data analysis

Calculation of the ER of ATV was performed as described previously by Cummins et al. (2002a, 2004). The ER is a measure of the extent of metabolism, i.e., the fraction of drug that was metabolized relative to the amount of drug coming in contact with the CYP3A4. All values used in the calculation of the extraction ratios are in amounts.

$$ER = \Sigma \text{metabolites}_{(d+r+i)} / (\Sigma \text{metabolites}_{(d+r+i)} + \Sigma \text{parent}_{(r+i)}) \quad \text{Eqn. (4.1)}$$

(d = donor compartment; r = receiver compartment; i = intracellular compartment)

This extraction ratio calculation incorporates in the denominator the intracellular amounts of unchanged drug, because it is reasoned that drug inside the cell can interact with CYP3A4.

$$P_{app} = \text{rate of transport} / (\text{surface area} \times \text{donor concentration}) \quad \text{Eqn. (4.2)}$$

For comparing the inhibitor-treatment groups with the control, one-way analysis of variance followed by Tukey's post hoc test was used to determine the significance of the data. The level of significance was set at $p < 0.05$.

4.3 Results

4.3.1 Transport of ATV across CYP3A4-transfected Caco-2 cells

ATV transport across CYP3A4-transfected Caco-2 cells were found to be 1.9-fold greater in the B → A direction compared with that in the A → B direction (Table 4.1, Figs. 4.2A & 4.1B) due to the higher permeation rate of ATV in the efflux direction.

The net flux of ATV was completely abolished in the presence of 0.5 μM GG918 and 10 μM CsA, in which the net flux ratios became less than unity (Table 4.1). The resulting transport profiles were found to be inverted in which the A → B transport exceeded that of B → A in the presence of inhibitors (Figs. 4.2A & 4.2B). The absorptive permeability (A → B) of ATV was significantly increased by 43% when P-gp was inhibited by GG918, but when both P-gp and CYP3A4 were inhibited simultaneously in the presence of CsA, the value was significantly increased by 79% (Table 4.1). The efflux permeability (B → A) of ATV was decreased significantly in the presence of GG918 by 48% ($p < 0.05$) whereas the value was also moderately decreased by 22% in the presence of CsA, though not significantly (Table 4.1).

The intracellular levels of ATV (Fig. 4.3) after an apical dose were also affected more by CsA compared with GG918 where a 2.5-fold increase ($p < 0.001$) versus a 50% increase ($p < 0.01$) was observed for CsA and GG918-treatment groups, respectively.

After a basolateral dose, the intracellular amounts of ATV was increased markedly by 3.2-fold in the presence of CsA ($p < 0.001$) whereas the levels of ATV was decreased by 40% in the presence of GG918 ($p < 0.01$).

Table 4.1 ATV (20 μM) transport across CYP3A4-transfected Caco-2 cell monolayers in the absence and presence of GG918 and CsA.

Condition	P_{app} (A \rightarrow B) $\times 10^{-6}$ cm / s	P_{app} (B \rightarrow A) $\times 10^{-6}$ cm / s	Net flux ratio (B \rightarrow A / A \rightarrow B)
ATV alone (20 μM)	1.4 \pm 0.2	2.7 \pm 0.4	1.9 \pm 0.4
ATV (20 μM) + CsA (10 μM)	2.5 \pm 0.1**	2.1 \pm 0.4	0.8 \pm 0.2*
ATV (20 μM) + GG918 (0.5 μM)	2.0 \pm 0.3*	1.4 \pm 0.5*	0.7 \pm 0.4*

*, $p < 0.05$; **, $p < 0.01$, inhibitors treatment group significantly different from ATV only controls.

Data are presented as the mean \pm SD ($n = 3$).

Fig. 4.2 Bidirectional transport of ATV (20 μ M) across CYP3A4-transfected Caco-2 cell monolayers in the absence and presence of P-gp inhibitors, 0.5 μ M GG918 (A) and 10 μ M CsA (B). Data are presented as the mean \pm SD ($n = 3$).

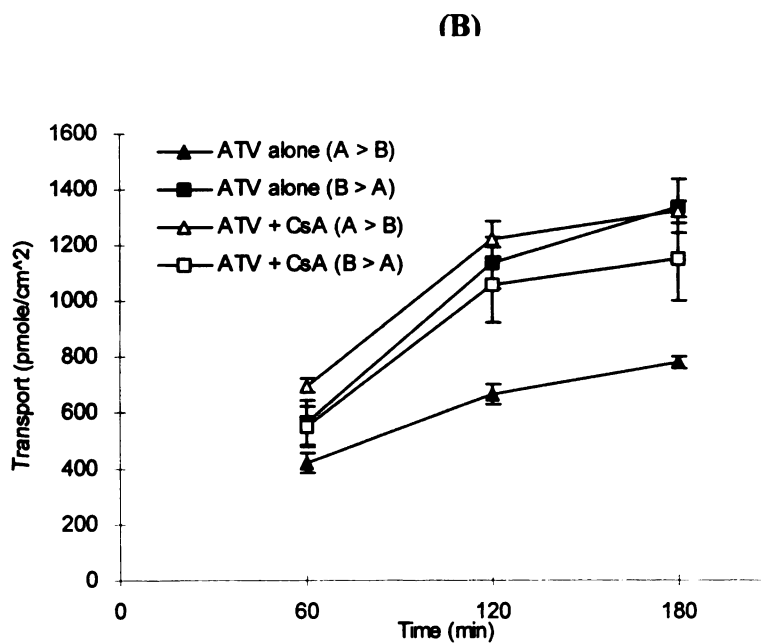
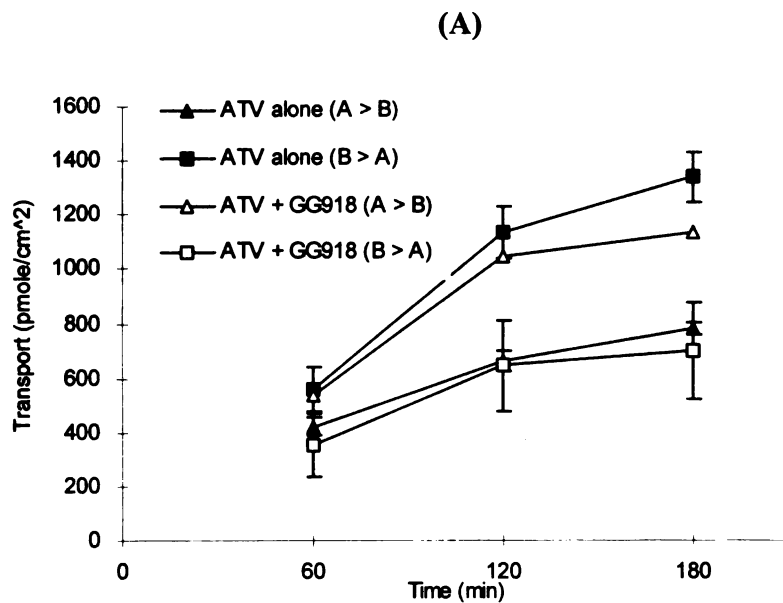
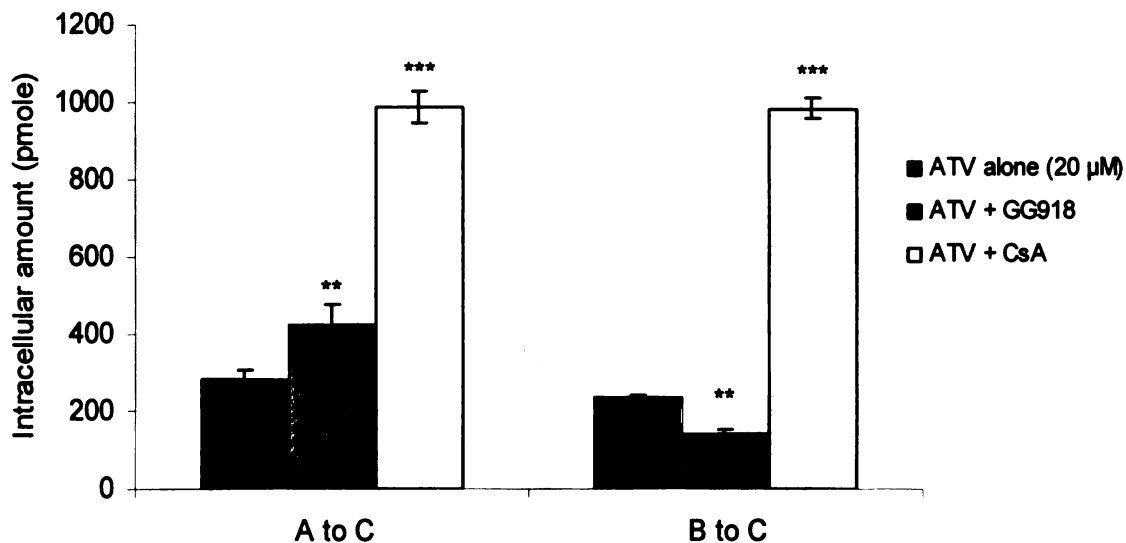


Fig. 4.3 Intracellular levels of ATV (20 μ M) in CYP3A4-transfected Caco-2 cells after an apical [A(pical) to C(ellular)] or basolateral [B(asolateral) to C(ellular)] dose (measure at 3 hr) in the absence and presence of the inhibitors, GG918 and CsA. **, $p < 0.01$; ***, $p < 0.001$, inhibitors treatment groups significantly different from ATV alone controls.

Data are presented as the mean \pm SD ($n = 3$).



4.3.2 Metabolism of ATV across CYP3A4-transfected Caco-2 cells

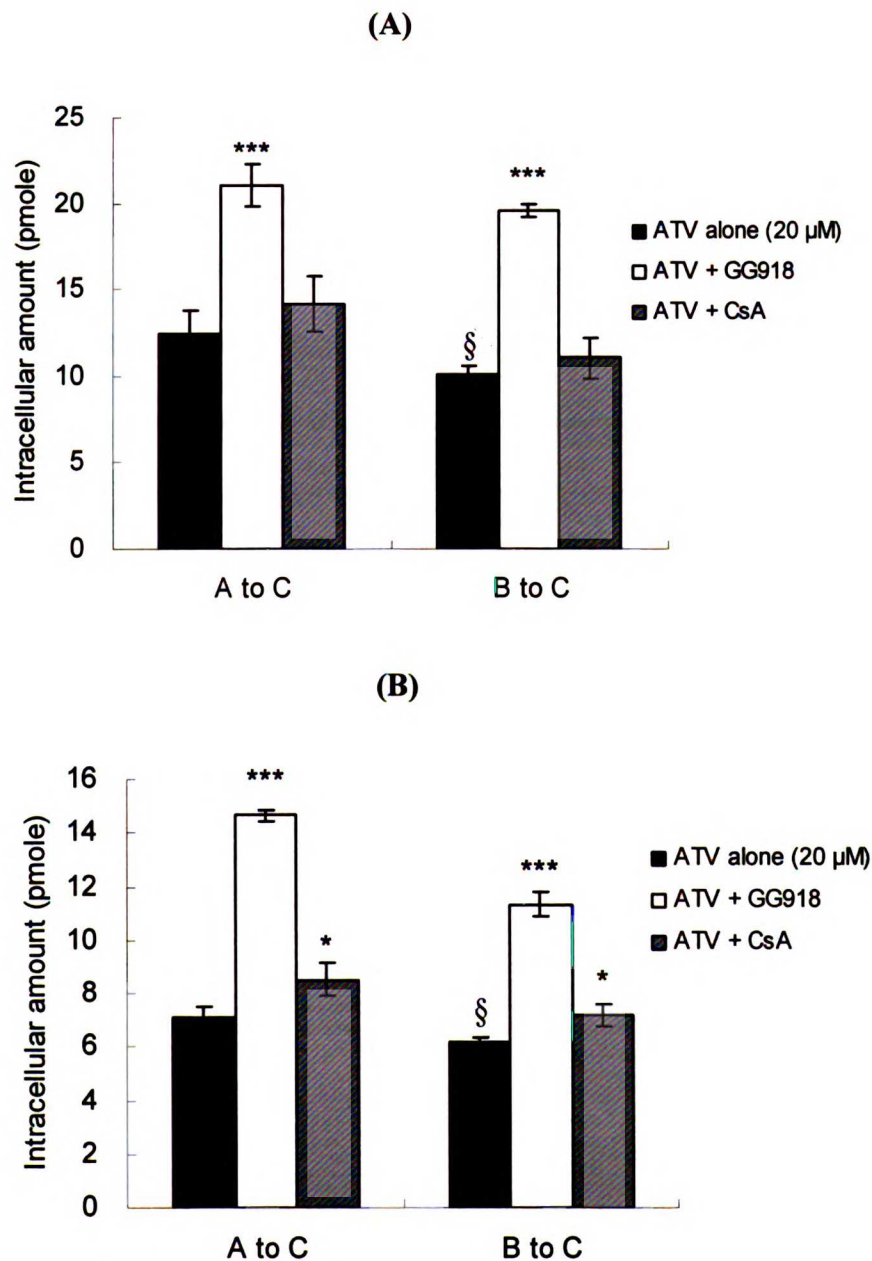
The intracellular levels of the two primary ATV metabolites, 2-OH ATV and 4-OH ATV, were monitored after incubation of ATV with the cells for 3 hrs. Lower levels of 2-OH ATV (by 18%) and 4-OH ATV (by 12%) were detected intracellularly after basolateral doses compared with apical doses (Figs. 4.4A & 4.3B), indicating the preferential efflux of metabolites in the direction of B to A, which followed the orientation of P-gp. The intracellular levels of metabolites were increased significantly in the presence of GG918 regardless of direction of dosing (Figs. 4.4A & 4.3B).

Fig. 4.4 2-OH ATV (A) and 4-OH ATV (B) found inside the cells at 3 hr after an apical [A(pical) to C(ellular)] or basolateral [B(asolateral) to C(ellular)] ATV dose (20 μ M).

***, $p < 0.001$, inhibitors treatment groups significantly different from ATV alone

controls. §, $p < 0.05$, ATV amount following basolateral dosing significantly different

from that following apical dosing. Data are presented as the mean \pm SD ($n = 3$).

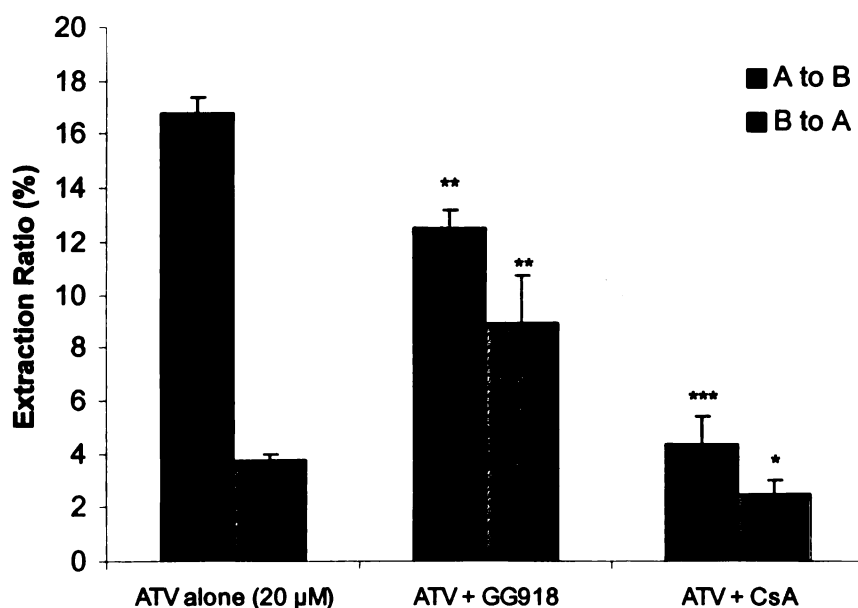


CsA only modestly increased the intracellular amounts of 2-OH ATV compared to ATV alone control, when ATV was dosed from either direction, whereas it significantly increased the corresponding values of 4-OH ATV (Fig. 4.4A & 4.3B).

4.3.3 Extraction ratios of ATV across CYP3A4-transfected Caco-2 cells

The extent of metabolism of ATV occurring upon transport across the CYP3A4-transfected Caco-2 monolayer was measured by using Eqn. (4.1). As shown in Fig. 4.5, ATV has an apical extraction ratio (ER) of 16.8%. The value was significantly decreased by 24% in the presence of GG918, demonstrating the influence of P-gp in increasing the exposure of ATV to CYP3A4 after an apical dose. From a basolateral dose, the ER was increased by 140% in the presence of GG918 ($p < 0.01$), indicating the opposite role of P-gp in mediating drug removal from the cell. CsA (10 μ M) decreased the ER following either apical or basolateral dose of ATV by 74% ($p < 0.01$) and 32% ($p < 0.05$), respectively, indicating that CYP3A4 was significantly inhibited at this concentration.

Fig. 4.5 Extraction ratio (ER) of ATV after an apical dose or basolateral dose of ATV (20 μ M) in CYP3A4-transfected Caco-2 cells. The effect of inhibiting P-gp on the ER was elucidated by incubation with GG918, whereas the dual effect of inhibiting CYP3A4 and P-gp on the ER was found by incubation with CsA. *, $p < 0.05$; **, $p < 0.01$; ***, $p < 0.001$, inhibitors-treatment groups significantly different from ATV alone controls. Data are presented as the mean \pm SD ($n = 3$).



4.3.4 ATV metabolites transport across M-MDR1 cells

To determine if the hydroxy metabolites of ATV were subject to P-gp mediated efflux, the P-gp overexpressing cell line, M-MDR1, was used to monitor the transport and intracellular accumulation of 2-OH ATV and 4-OH ATV upon GG918 treatment. As shown in Fig. 4.6, the intracellular levels of both metabolites following dosing from either side showed an increase with concomitant GG918 ($p < 0.01$). The A to B and B to A permeability values for 2-OH ATV and 4-OH ATV with and without GG918 were

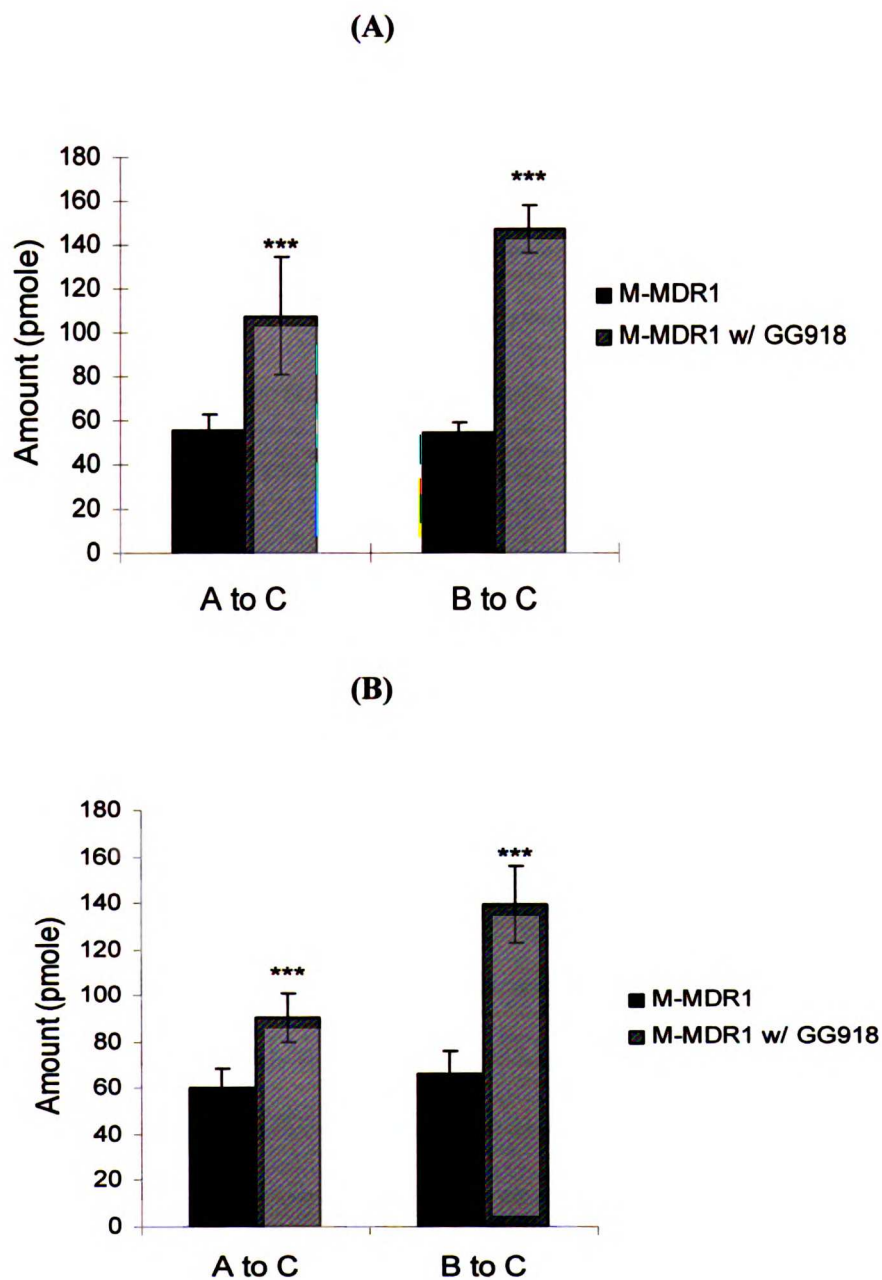
tabulated in Table 4.2. There was no significant difference between permeability from either direction. GG918 did not cause significant decreases in the net flux ratio for either metabolite. These results were likely due to the hydrophilic nature of the metabolites, which did not allow large quantities of them to traverse the cell membranes, resulting in low and variable amounts of metabolites measured at the receiver sides. Permeabilities in the A → B direction are < 40% that of the parent drug, and ≤ 20% in the B → A direction (Tables 4.1 and 4.2).

Table 4.2 2-OH ATV and 4-OH ATV (1 μM) transport across M-MDR1 cell monolayers in the absence and presence of GG918.

Condition	$P_{app} (A \rightarrow B)$ $\times 10^{-7} \text{ cm / s}$	$P_{app} (B \rightarrow A)$ $\times 10^{-7} \text{ cm / s}$	Net flux ratio (B → A/ A → B)
2-OH ATV alone (1 μM)	5.5 ± 2.4	8.5 ± 2.6	1.6 ± 0.4
+ GG918 (0.5 μM)	7.0 ± 0.1	8.9 ± 2.5	1.3 ± 0.7
4-OH ATV alone (1 μM)	4.9 ± 2.8	7.7 ± 2.0	1.6 ± 0.7
+ GG918 (0.5 μM)	5.2 ± 0.7	7.8 ± 1.2	1.5 ± 0.3

Each value represents mean ± SD, $n = 3$.

Fig. 4.6 The intracellular amounts of 2-OH ATV (A) or 4-OH ATV (B) detected inside M-MDR1 cells at 3 hr after an apical (A to C) or basolateral (B to C) dose of either 2-OH ATV or 4-OH ATV. ***, $p < 0.001$, GG918 treatment groups significantly different from metabolites alone controls. Data are presented as the mean \pm SD ($n = 3$).



4.4 Discussion

The permeation of a drug across the intestinal barrier is a complex process and involves transport mechanisms mediated by ATP-dependent efflux proteins such as P-gp. After passage across the apical enterocyte membrane, drugs may be subject to metabolism by oxidative enzymes such as CYP3A4. Our laboratory has previously applied the CYP3A4-transfected Caco-2 cell system, which expresses both P-gp and CYP3A4, as an investigational tool to study how P-gp can affect intestinal metabolism by controlling the access of drug to the intracellular metabolizing enzymes (Cummins et al., 2002a, 2004). Benet et al. (2004) have also hypothesized that the same cellular system can be applied to mimic the interactive nature between hepatic P-gp and CYP3A4 and predict potential drug-drug interactions. In the present study, we chose a dual P-gp and CYP3A4 substrate, ATV, to model how the interplay between efflux transporter and enzyme can alter the metabolic extraction in both the gut and the liver.

The working ATV concentration in this study was chosen at 20 μM in order to yield quantifiable metabolite concentrations. Our study indicated that there was a preferential transport of ATV in the (B)asolateral to (A)pical direction and this polarized efflux was completely abolished when P-gp was inhibited (Fig. 4.2A). In the presence of GG918, a potent P-gp blocker, there was a significant increase in permeability (P_{app}) in the absorptive (A to B) direction (Table 4.1; Fig. 4.2A), suggesting that more ATV was able to traverse to the B side when P-gp-mediated transport in the A to B direction was blocked. When ATV was dosed on the B side, as expected, we observed a significant decrease in B \rightarrow A transport (Table 4.1; Fig. 4.2A), indicating that there was reduced movement of ATV across the cell monolayer. Together these changes in ATV transport

from both directions led to a 63% significant decrease in the net flux ratio (Table 4.1). These results are consistent with our transport data in a less leaky cellular system obtained from M-MDR1 cells in which the net flux ratio of ATV decreased dramatically from 142 to 1 with concomitant GG918 (Chapter 3, Fig. 3.6B), and agree with literature reports, in which transport of ATV in the B to A direction was about 3-6-fold and 7-fold higher compared with that in the A to B direction in MDR1-transfected LLC-PK1 cells (Wu et al., 2000) and Caco-2 cells (Hochman et al., 2004), respectively. To examine if inhibition of CYP3A4 could also limit ATV absorption, we compared the changes of A → B transport for GG918 and CsA-treatment groups (Table 4.1; Fig. 4.2). The permeability was significantly increased 43% by GG918 and 79% by CsA, a dual inhibitor for P-gp and CYP3A4 (Table 4.1), suggesting that P-gp and CYP3A4 contribute almost equally in limiting ATV absorption.

The net flux ratio of ATV was reduced to less than unity when P-gp was inhibited, suggesting that the net efflux of ATV across CYP3A4-transfected Caco-2 cells became net absorptive transport either with GG918 or CsA (Table 4.1). This change in the net direction of transport suggests that ATV might also be a substrate of an influx transporter such as H⁺-monocarboxylic acid transporter (MCT) (Wu et al., 2000) on the apical border that may contribute to the higher transport in the A to B direction versus that in B to A direction and the higher apical ER versus basolateral ER after P-gp was inhibited by GG918 (Fig. 4.5).

The accumulation of parent ATV and its metabolites in CYP3A4-transfected Caco-2 cells were also monitored at the end of the experiment (3hr). Upon GG918 treatment, the intracellular levels of both 2-OH ATV and 4-OH ATV (Fig. 4.4), along

with that of the parent drug (Fig. 4.3), were significantly increased following an apical dose, indicating that the metabolite removal was inhibited by P-gp mediated efflux as well. Experiments in M-MDR1 cells using 2-OH ATV and 4-OH ATV directly as substrates demonstrated that both of these oxidative metabolites, which are structurally similar to the parent compound, are subject to P-gp-mediated efflux as indicated by their increased cellular accumulation when coadministered with GG918 (Fig. 4.6).

Unlike the case with P-gp alone inhibition, CsA only slightly raised the level of 2-OH ATV (Fig. 4.4A), most likely due to the stronger inhibition of CYP3A4 than that of P-gp by CsA. On the other hand, 4-OH ATV levels were significantly increased by CsA (Fig. 4.4B), though the increase was still much less extensive than the increase caused by GG918. This might be due to 4-OH ATV being a better P-gp substrate compared with 2-OH ATV, which is not obvious based on the bidirectional transport rates (Table 4.2). The substantial increase in ATV intracellular amount by CsA is expected as an additive effect since inhibition of both P-gp and CYP3A4 would lead to a reduction in ATV elimination from the cells (Fig. 4.3).

The ER of ATV (20 μ M) after an apical dose decreased significantly when P-gp alone was inhibited (Fig. 4.5). These data were consistent with previous results from Cummins et al. (2002a, 2004) using K77 and sirolimus as model compounds, in which the extent of metabolism was reduced after intestinal efflux was blocked. It has been proposed by Tam et al. (2003) that P-gp functions as an efflux pump that brings about desaturation and keeps the drug concentration low in the cellular compartment. Cummins et al. (2002a), on the other hand, proposed that P-gp brings about increased metabolism since it allows the drug to have increased mean residence time to the enzyme relative to

the amount of drug crossing the cell through repeated cycles of absorption and efflux. It can be argued that the decrease in the ER with P-gp inhibition in the A to B direction resulted from saturation of the CYP3A enzyme (Suzuki and Sugiyama, 2000; Tam et al., 2003) due to increased cellular concentrations as noted in Fig. 4.3. However, the marked decrease in the ER value of ATV from 16.8% to 4.3% when the drug was co-administered with CsA was clearly due to the inhibitory effect of CsA on CYP3A4 in addition to P-gp that reduced the rate of metabolite formation directly.

The synergistic interplay between CYP3A4 and P-gp can also be extrapolated from the B to A transport in this cell model to the situation occurring in the liver. After entering the hepatocytes from the blood circulation, drug compounds are exposed to CYP3A4 before reaching P-gp for subsequent biliary excretion. As shown in Fig. 4.3, intracellular levels of ATV decreased significantly following basolateral dosing with GG918 treatment, along with marked increases in the amounts of 2-OH ATV (Fig. 4.4A) and 4-OH ATV (Fig. 4.4B). These results are in agreement with our previous digoxin IPRL data present in Chapter 2, in which blockage of hepatic canalicular P-gp (by quinidine) caused a decrease in the amounts of digoxin in the liver tissues due to a significant increase in metabolite formation (Lau et al., 2004). In the presence of 10 μ M CsA, there was a 4-fold increase in the intracellular ATV level following basolateral dosing (Fig. 4.3), indicating CsA was directly inhibiting CYP3A4-mediated metabolism. The modest increase in the intracellular levels of 2-OH ATV by 9% and 4-OH ATV by 16% in the presence of CsA relative to control (Fig. 4.4) was in large contrast to the 93% and 82% increase in the corresponding values for the GG918-treatment groups, which explains why there was a great decrease in the ER of ATV with CsA coincubation (Fig.

4.5). These results were consistent with the findings obtained from apical dosing and suggest that inhibition of CYP3A4 by CsA did occur and was more important than CsA inhibition of P-gp mediated efflux regardless of the direction of transport.

There was a significant increase in the ER of ATV upon GG918 treatment following a basolateral dose, opposite to what was found in the absorptive transport direction (Fig. 4.5). These data agree with our digoxin IPRC study results where we showed a 3.7-fold increase in the metabolite to parent digoxin ratio in the liver tissues by quinidine (P-gp inhibition) treatment (Chapter 2; Lau et al., 2004). Although, as explained above, enzyme saturation of CYP3A4 could possibly be an explanation for the change in the ER in the A → B direction with P-gp inhibition, this cannot explain the results in the B → A direction where decreases in intracellular concentrations with P-gp (Fig. 4.3) led to increased ER values. This is because there is always an increase in drug intracellular concentrations when decreased P-gp clearance occurs following a basolateral dose, hence an increase in metabolite formation.

In conclusion, the data obtained with ATV from CYP3A4-transfected Caco-2 cells support our hypothesis and previous findings that P-gp could increase presystemic metabolism of drugs by CYP3A4 likely via repeated cycling of the drug at the apical membrane (Cummins et al., 2002a, 2004). The results obtained from the B to A transport of ATV also led us to recognize that the same system can be used to predict the interactive nature of metabolism and efflux in the liver. P-gp and CYP3A4 might be one of the major efflux-metabolism pairs, other alliances that can cause similar effect on metabolism might also exist such as that between MRP2 and UGTs (Chang and Benet, 2005) or BCRP and CYP3A4.

Chapter 5

PHARMACOKINETICS OF ATORVASTATIN AND ITS HYDROXY METABOLITES IN RATS AND THE EFFECTS OF CONCOMITANT RIFAMPICIN SINGLE DOSES: RELEVANCE OF FIRST-PASS EFFECT FROM HEPATIC UPTAKE TRANSPORTERS, INTESTINAL AND HEPATIC METABOLISM¹

5.1 Introduction

Bioavailability of orally administered drugs is often limited by first-pass effects due to metabolism and transporter-mediated processes. In clinical studies, significant interactions between the cholesterol-lowering agent, atorvastatin (ATV), and cytochrome P450 3A (CYP3A) inhibitors such as itraconazole (Kantola et al., 1998) and erythromycin (Siedlik et al., 1999) were observed, with increased area under the plasma concentration-time curve (AUC) of ATV and reduction in the AUC values of its active metabolites 2-hydroxyatorvastatin (2-OH ATV) and 4-hydroxyatorvastatin (4-OH ATV). These results suggest extensive contribution of CYP3A towards ATV metabolism *in vivo*,

¹ This chapter was modified from a published manuscript entitled "Pharmacokinetics of atorvastatin and its hydroxy metabolites in rats and the effects of concomitant rifampicin single doses: relevance of first-pass effect from hepatic uptake transporters, intestinal and hepatic metabolism" Y.Y. Lau, H Okochi, Y Huang and L.Z. Benet, Drug Metab Dispos [Fast Forward April 19, 2006]

even though other isoforms such as CYP2C8 has also been shown to metabolize ATV at a slower rate (Jacobsen et al., 2000). In humans, the absolute bioavailability of ATV is only 12% (Gibson et al., 1997) possibly due to substantial metabolism in both gut and liver by CYP3A4, the most abundant cytochrome P450 enzymes expressed in both tissues. Our laboratory has noted that the two major active oxidative metabolites of ATV were formed during incubation with both human intestinal and hepatic microsomes (Christians et al., 1998; Jacobsen et al., 2000).

Various cell-based studies have suggested that multiple transporters (both uptake and efflux) located in the intestine and liver have the potential to affect the disposition of ATV *in vivo* (Chapter 3 and 4; Hsiang et al., 1999; Wu et al., 2000; Hochman et al., 2004; Chen et al., 2005; Kameyama et al., 2005; Lau et al., 2006a). As previously hypothesized and demonstrated by our laboratory, interplay between transporters and metabolic enzymes may control the access of drug molecules to the enzymes and changes in transporter function can modulate intestinal and hepatic metabolism without directly changing enzyme activity (Chapter 2, 3 and 4; Cummins et al., 2002a, 2004; Wu and Benet, 2003; Lam and Benet, 2004; Lau et al., 2004; Lau et al., 2006a). It is likely that ATV may experience considerable transporter-enzyme interplay *in vivo* that could contribute to its low oral bioavailability.

The role of hepatic transporters, organic anion transporting polypeptides (Oatps), in modulating the disposition and biliary excretion of ATV and OH ATVs has been previously examined in our laboratory by applying the isolated perfused rat liver (IPRL) system (Chapter 3; Lau et al., 2006a). Rifampicin (RIF), a known potent inhibitor of various Oatps (Fattinger et al., 2000; Shitara et al., 2002), effectively reduced the Oatp-

mediated hepatic uptake of ATV in a dose-dependent manner, whereby lesser amounts of ATV were available for subsequent hepatic metabolism, as reflected by reduced metabolite formation detected in liver tissues and bile. However, inhibitory effects on hepatic Cyp3a and efflux transporter multidrug resistance-associated protein 2 (Mrp2) became measurable at high RIF concentrations.

It is well recognized that cytochrome P450 enzymes expressed in the intestine significantly contribute to oxidative gut wall extraction for many orally administered drugs such as sirolimus (Lampen et al., 1998) and cyclosporine (Gomez et al., 1995; Wu et al., 1995). These intestinal enzymes might act to reduce the oral bioavailability of ATV during the intestinal absorption phase before reaching the liver, where further first-pass hepatic metabolism can occur.

We present here a pharmacokinetic study performed in rats to examine the influence of hepatic uptake inhibition on ATV exposure and its metabolic extraction *in vivo*. The rat model was used since ATV undergoes similar metabolic pathways to that in humans, both oxidative metabolites and parent drug are predominantly excreted in the bile of human (Lennernas, 2003) and rats (Black et al., 1999) and only minimally in urine (< 2 %). Here, ATV was administered to rats either as intravenous bolus doses or orally, with and without a concomitant intravenous dose of RIF. We expected to observe a lower hepatic metabolic extraction with concomitant RIF when the amount of ATV available for metabolism is reduced, leading to an increase in drug exposure. We also hypothesized that extensive intestinal extraction would occur for this highly permeable, poorly soluble Class 2 drug (Wu and Benet, 2005), where the access of ATV to the enzymes would be enhanced due to efflux transporter-intestinal enzyme interplay. The purpose of this study

was two-fold: (1) investigation of the contribution of Oatps towards hepatic clearance of ATV and (2) differentiation of the extent of ATV first-pass metabolism of the intestine from that of the liver.

5.2 Materials and methods

5.2.1 Materials

Atorvastatin (ATV), *para*-hydroxy atorvastatin (4-OH ATV) and *ortho*-hydroxy atorvastatin (2-OH ATV) were kindly supplied by Parke-Davis (Ann Arbor, MI) and Bristol-Myers Squibb (Princeton, NJ). Fluvastatin (Novartis, Cambridge, MA) was a kind gift from the manufacturer. Rifampicin (RIF) powder for injection (Rifadin I.V.) was obtained from Sanofi-Aventis (Bridgewater, NJ) and was reconstituted with sterile saline for injection. All other chemicals and solvents for the analysis were of analytical grade and used as supplied commercially. Male Sprague-Dawley rats with jugular vein pre-cannulation were purchased from Charles River Laboratories (Wilmington, MA).

5.2.2 Pharmacokinetic experiments in rats

All experiments with rats were performed in accordance with the NIH guidelines and approved by the Committee on Animal Research, University of California San Francisco. Pharmacokinetic experiments with ATV, either alone or in combination with RIF, were performed in male Sprague-Dawley rats weighing 250 to 300 g, with jugular vein pre-cannulation ($n = 5$ per group). Access to water was maintained during the experiment, but animals were fasted beginning the night before the experiment and

through the 4 hr of the experiments. Rats were orally dosed with ATV that was formulated in 0.5% methylcellulose suspension, by gavage. Pilot studies indicated that dose-normalized ATV AUC values were unchanged for 1 mg/kg, 3 mg/kg and 10 mg/kg oral doses. For intravenous application, ATV was dissolved in physiological saline with 20% methanol to obtain a concentration of 1 mg/ml and given by tail-vein injection. Pilot studies indicated that dose-normalized ATV AUC values were unchanged for 1 mg/kg, 2 mg/kg and 4 mg/kg intravenous doses. The 10 mg/kg oral dose and 2 mg/kg intravenous dose were chosen for detailed study so as to yield quantifiable metabolite concentrations. RIF dissolved in saline was also given by tail-vein injection at a dose of 20 mg/kg, 5 min before the administration of ATV. Animals receiving ATV alone were injected with an equivalent volume of vehicle. Blood samples of about 300 μ l volume were drawn at predefined time points over a period of 24 hrs. Plasma was generated by centrifugation at $10,000 \times g$ for 5 min. Samples were stored at $-20\text{ }^{\circ}\text{C}$ pending analysis.

5.2.3 Calculation of blood to plasma concentration ratio (B/P) of ATV in rats

Samples of rat blood were obtained from four rats weighing 250-300 g, placed in pre-heparinized tubes and were used within 1 hr after collection. Aliquots (1 ml) of blood were transferred to glass tubes and were spiked with ATV and placed in a $37\text{ }^{\circ}\text{C}$ shaking water bath for 30 min. Five hundred microliter were withdrawn from the incubation tubes and kept at $-80\text{ }^{\circ}\text{C}$ for 5 min to achieve complete hemolysis. The remaining blood fraction was centrifuged for 5 min at $3,000 \times g$ to separate plasma and erythrocyte suspension. Calibration curves for ATV were prepared by spiking various concentrations of ATV to different matrices (whole blood, plasma and erythrocyte). Four hundred microliters of

acetonitrile were added to each sample (200 μ l) for precipitation followed by 1 min vortex mixing and centrifugation at $13,000 \times g$ for 10 min. The supernatants were injected onto the LC/MS-MS for measurement as detailed below. Drug recovery from plasma and erythrocyte fractions should equal the amount of ATV detected in whole blood by mass balance, assuming hematocrit was 0.46 in rats (Davies and Morris, 1993), which was confirmed.

5.2.4 Metabolism by rat small intestine microsomes

Rat small intestinal microsomes were isolated and incubated as described previously by our laboratory (Lampen et al., 1998; Lau et al., 2006a). In brief, microsome proteins (0.75 mg/ml), 10 mM $MgCl_2$, 0.1 M phosphate buffer, pH 7.4, and ATV (in methanol, final concentration 0.1 μ M) were preincubated for 5 min. The initial concentration of ATV was chosen at 0.1 μ M so that it mimicked the *in vivo* ATV concentration following oral administration at 10 min, when RIF first caused an elevated increase in the plasma level of ATV. NADPH (1 mM) was added to start the reaction at 37°C. To assess the effects of RIF on ATV metabolism, RIF (in dimethyl sulfoxide, final concentration 10-50 μ M) was added to the intestinal microsomal preparations. Metabolism blanks with no NADPH and heat-inactivated microsomes were run in parallel to serve as negative controls. The reaction was stopped by protein precipitation by the addition of an equal volume of ice-cold acetonitrile containing the internal standard fluvastatin (0.1 μ M). In all assays, the final methanol and dimethyl sulfoxide concentrations were < 0.5%. The supernatants were stored at $-80^\circ C$ for LC/MS-MS analysis.

5.2.5 LC/MS-MS measurement of ATV, 2-OH ATV, 4-OH ATV and RIF

The method for measurement of ATV, 2-OH ATV and 4-OH ATV was described in the Section 3.2.6 (Chapter 3). The quantitation limits for ATV and the metabolites (2-OH ATV and 4-OH ATV) were 5 nM and 1 nM, respectively.

The multiple reaction monitor (MRM) was set at 823.5 – 791.5 m/z for RIF, using a LC/MS/MS system described in Chapter 3. The sample cone voltage and collision energy were set at 30 V and 18 eV, respectively. The analytical column was a BDS C18 (50 x 4.6 mm) from Hypersil-Keystone (Bellefonte, PA). The mobile phase consisted of 36 % acetonitrile containing 0.05% acetic acid and 5 mM ammonium acetate. The flow rate was 1.0 ml/min and $\frac{1}{4}$ was split into the mass system. The lower limit of quantitation was 50 nM.

5.2.6 Pharmacokinetic analysis

Peak plasma concentrations (C_{max}) and the time to reach peak plasma concentrations (t_{max}) were directly obtained by inspection. Pharmacokinetic parameters were estimated using the WinNonLin software package (Professional version 3.1; Pharsight, Mountain View, CA). Total intravenous blood clearance of ATV (CL_{iv}) was calculated as $D/[AUC_{0-\infty, iv} \times (B/P)]$, with D as dose and $AUC_{0-\infty, iv}$ as the area under the plasma concentration-time curve calculated by the linear/logarithmic trapezoidal rule (for up/down portions of the curve, respectively) and extrapolated to infinity using the apparent terminal disposition rate constant λ_z , determined by regression analysis of the linear terminal portion of the log plasma concentration-time curve. The apparent terminal half-life ($t_{1/2}$) was estimated from the terminal rate constant with $t_{1/2} = \ln 2/\lambda_z$. For

intravenous dosing, the steady-state volume of distribution (V_{ss}) was calculated as $V_{ss} = \text{MRT} \times \text{CL}_{iv}$ with the mean residence time (MRT) being defined as the area under the first moment curve $\text{AUMC}_{0-\infty, iv}$ divided by $\text{AUC}_{0-\infty, iv}$ (Benet and Galeazzi, 1979). Because of assay limitations, ATV concentrations following oral dosing without RIF could only be measured up to 4 - 8 hrs and half-life could not be accurately determined. Since, as will be discussed later, no significant changes in ATV terminal half-life ($t_{1/2}$) were observed between i.v. dosing with and without RIF and oral dosing with RIF, it appears that RIF and route of administration do not affect $t_{1/2}$. Therefore, for bioavailability calculations, $\text{AUC}_{0-\infty}$ values following oral dosing were all calculated by extrapolating from the last quantifiable concentration using a half-life of 245 min. This seemed to be a reasonable approach since extrapolated areas for ATV following oral dosing were less than 5 % of total area. Comparisons of 2-OH ATV and 4-OH ATV metabolites to parent drug AUC ratios were only determined from 0-2 hr and 0-4 hr, respectively, since these were the time intervals that both metabolites and parent ATV could be measured in all rats.

Oral bioavailability (F) was calculated by the ratios of dose-normalized $\text{AUC}_{0-\infty}$ after oral and intravenous dosing:

$$F = \text{AUC}_{0-\infty, \text{oral}} / \text{AUC}_{0-\infty, \text{iv}} \times \text{Dose}_{iv} / \text{Dose}_{\text{oral}} \quad \text{Eqn. (5.1)}$$

Hepatic blood clearance was assumed to equal CL_{iv} , that is, all ATV elimination following intravenous dosing is hepatic.

Hepatic extraction ratio (ER_H) was estimated as:

$$\text{ER}_H = \text{CL}_{iv} / Q_H; \quad \text{Eqn. (5.2)}$$

where rat hepatic blood flow (Q_H) was assumed to be 55.2 ml/min/kg (Naritomi et al., 2001).

Since oral bioavailability is a function of: F_H [hepatic availability ($F_H = 1 - ER_H$)], F_G [gut availability ($F_G = 1 - ER_G$)], and F_{abs} [fraction absorbed] as given in Eq. 5.3 (Wu et al., 1995):

$$F = F_{abs} \times F_G \times F_H \quad \text{Eqn. (5.3)}$$

it is possible to estimate the product of $F_{abs} \times F_G$ as:

$$F_{abs} \times F_G = F / F_H \quad \text{Eqn. (5.4)}$$

Comparison of $F_{abs} \times F_G$ calculated values give an estimate of the effects of RIF on the gut processes affecting ATV availability.

Total drug blood intrinsic clearance ($f_u \times CL_{int}$) was calculated based on the well-stirred hepatic clearance model (Wilkinson, 1983):

$$f_u \times CL_{int} = CL_{iv} \times Q_H / (Q_H - CL_{iv}) \quad \text{Eqn. (5.5)}$$

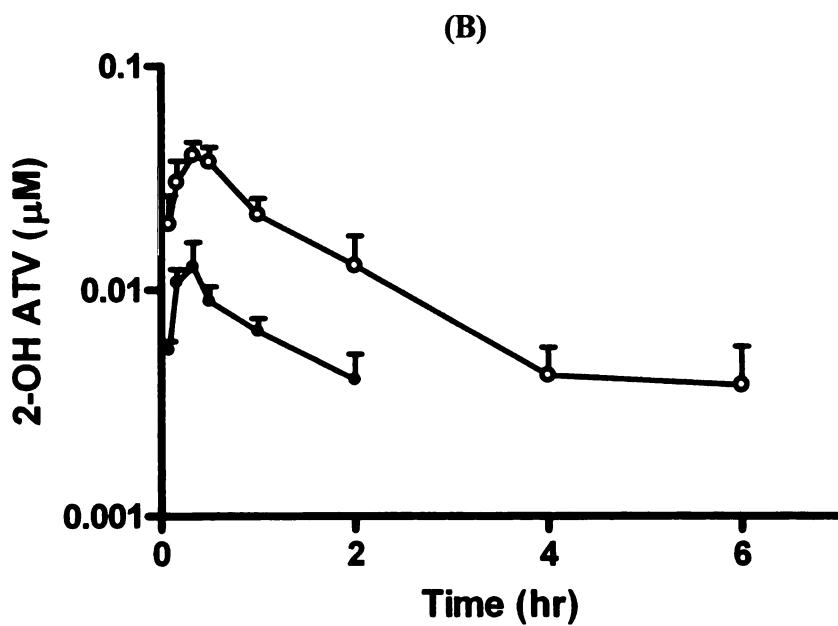
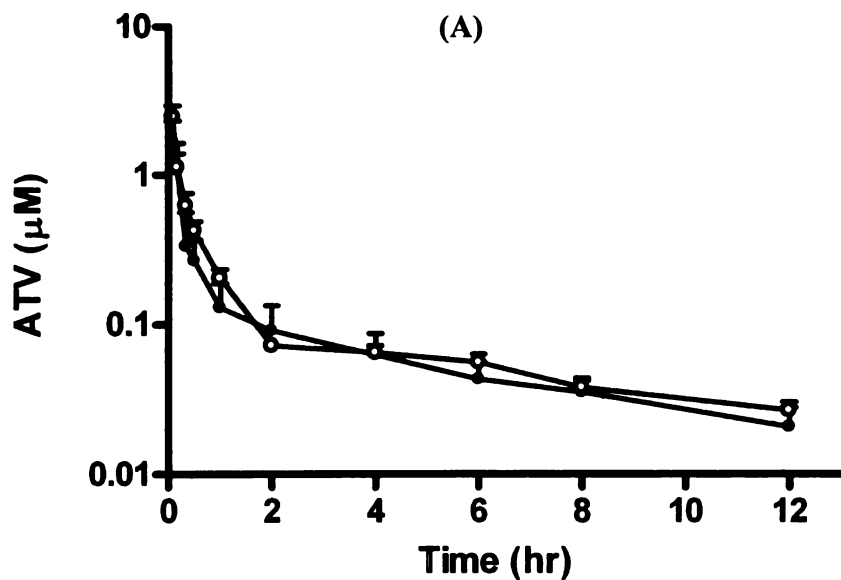
Student's t test was used to analyze difference between two groups. The p value for statistical significance was set at < 0.05 .

5.3 Results

5.3.1 Effect of RIF on the pharmacokinetics of ATV under intravenous dosing

ATV was detectable in plasma up to 12 hr after dosing, although sampling was carried out for 24 hr (Fig. 5.1A). The two active metabolites reached the 1 nM limit of detection at even earlier times (Figs. 5.1B and 5.1C). Single intravenous doses of RIF increased the $AUC_{0-\infty}$ of ATV and its two metabolites (Table 5.1). The $AUC_{0-\infty}$ of ATV

Fig. 5.1 Mean (\pm SD) plasma concentrations of (A) ATV, (B) 2-OH ATV and (C) 4-OH ATV in rats ($n = 5$) after a single intravenous dose of 2 mg/kg ATV with and without RIF given as a bolus intravenous dose (20 mg/kg). Solid circles indicate ATV alone control group; open circles indicate RIF-treatment group. Data are depicted on a semilogarithmic scale.



(C)

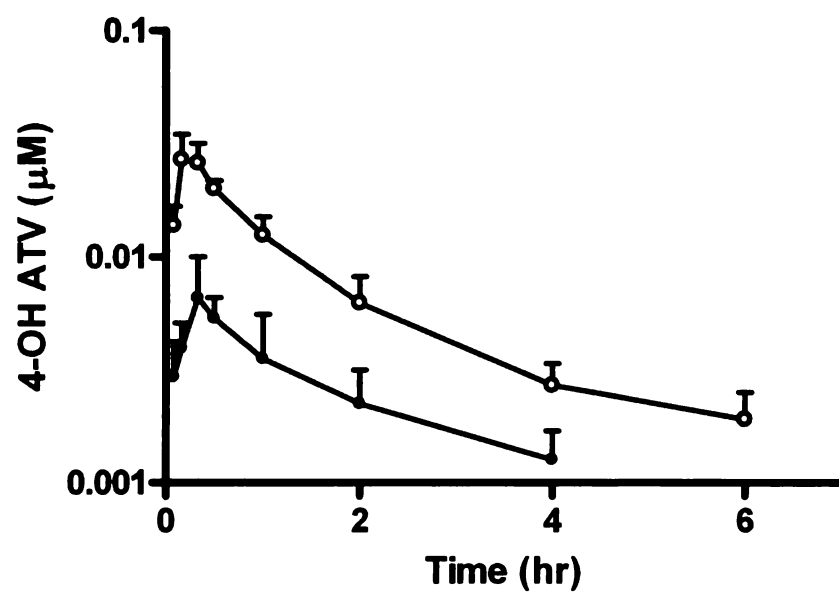


Table 5.1 Pharmacokinetic variables for ATV and its metabolites in rats ($n = 5$) after a single oral dose (10 mg/kg) or intravenous dose (2 mg/kg) of ATV with and without RIF given as a bolus intravenous dose (20 mg/kg).

Variable	Intravenous		Oral	
	ATV alone	with RIF	ATV alone	with RIF
ATV				
C_{max} (μM)	1.69 ± 0.63^a	2.48 ± 1.10^a	0.21 ± 0.36	$0.65 \pm 0.46^*$
t_{max} (min)	a	a	20 (10-60)	30 (30-120)
$t_{1/2}$ (min)	288 ± 83	292 ± 128	ND	245 ± 122
$AUC_{0-12 \text{ hr}}$ ($\mu\text{M} \cdot \text{min}$)	68.1 ± 16.2	89.7 ± 23.5	19.6 ± 8.8	$68.2 \pm 26.3^{**}$
$AUC_{0-\infty}$ ($\mu\text{M} \cdot \text{min}$)	78.7 ± 18.9	$107 \pm 19^*$	20.6 ± 8.8	$71.8 \pm 26.5^{**}$
2-OH ATV				
C_{max} (μM)	0.013 ± 0.008	$0.040 \pm 0.015^{**}$	0.021 ± 0.011	$0.055 \pm 0.048^*$
t_{max} (min)	10 (10-30)	20 (10-30)	60 (20-60)	30 (30-120)
$AUC_{0-2 \text{ hr}}$ ($\mu\text{M} \cdot \text{min}$)	0.71 ± 0.27	$2.84 \pm 0.91^{**}$	1.72 ± 1.21	$5.19 \pm 2.91^*$
4-OH ATV				
C_{max} (μM)	0.004 ± 0.001	$0.027 \pm 0.021^{**}$	0.012 ± 0.020	$0.030 \pm 0.031^*$
t_{max} (min)	10 (10-30)	10 (10-30)	30 (10-60)	60 (30-120)
$AUC_{0-4 \text{ hr}}$ ($\mu\text{M} \cdot \text{min}$)	0.64 ± 0.31	$2.22 \pm 0.52^{***}$	0.81 ± 0.61	$5.52 \pm 3.59^*$

Data are mean values \pm SD ($n = 5$); t_{max} data are given as median and range.

^a For intravenous parent ATV dosing, first measured time point at 5 min;

* $p < 0.05$; ** $p < 0.01$; *** $p < 0.001$ as compared to values for the same dosing route without RIF.

ND: not determinable due to assay limits of quantitation.

was increased by 36% ($p < 0.05$) with concomitant RIF compared with ATV alone. The AUC values of the active metabolites for 2-OH ATV and 4-OH ATV were respectively 4-fold greater ($p < 0.01$) and 3.5-fold greater ($p < 0.001$) for the RIF-treatment group than the control group over comparable time periods. C_{\max} of 2-OH ATV was increased by 3.1-fold ($p < 0.01$), whereas that of 4-OH ATV was increased by 6.8-fold ($p < 0.01$).

The intravenous clearance (CL_{iv}) and steady-state volume of distribution (V_{ss}) in blood were calculated using the measured blood to plasma ratio (B/P) of 1.47. There was a 28% significant decrease in CL_{iv} ($p < 0.05$). The 26% decrease in V_{ss} by RIF treatment did not reach statistical significance (Table 5.2). Parallel changes in CL_{iv} and V_{ss} often result from changes in protein binding, but here this would suggest RIF increased protein binding, a highly unlikely outcome and our *in vitro* measures showed no change of RIF on ATV binding (data not shown). The calculated total drug intrinsic clearance ($f_u \times CL_{int}$) using Eqn. (5.5) decrease significantly by 53% from 88.0 ± 42.6 to 41.4 ± 11.6 ml/min/kg for this intermediate extraction ratio drug. There was a marked 3-fold increase ($p < 0.01$) in the AUC ratio of metabolites to parent drug (AUC_M/AUC_P) by RIF (Table 5.2). When calculating ($f_u \times CL_{int}$), we assumed that RIF has no effect on hepatic blood flow.

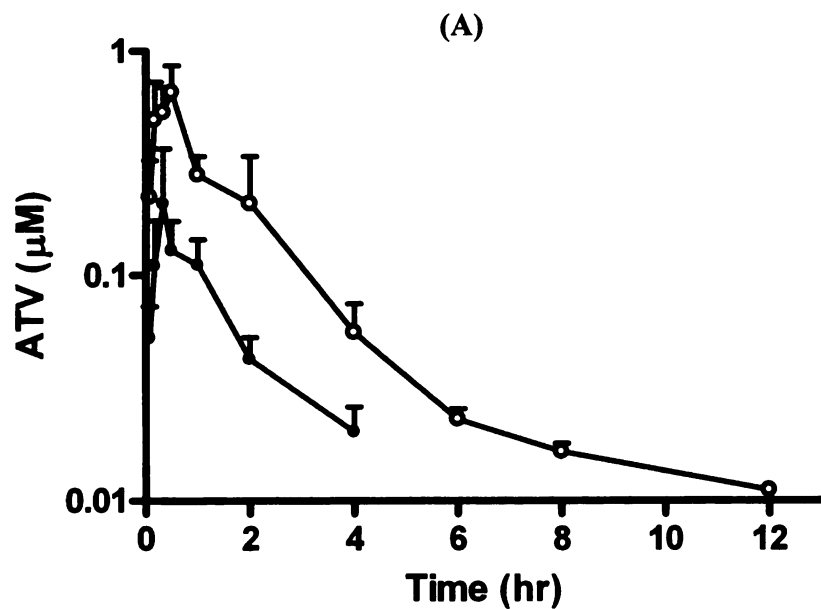
5.3.2 Effect of RIF on the pharmacokinetics of ATV under oral dosing

RIF raised the plasma concentrations of ATV, 2-OH ATV and 4-OH ATV after oral administration (Figs. 5.2A-C). The AUC values over comparable time periods were increased by approximately 3 to 3.5-fold for both ATV ($p < 0.01$) and 2-OH ATV ($p < 0.05$), and 6.8-fold for 4-OH ATV ($p < 0.05$). Furthermore, RIF significantly increased

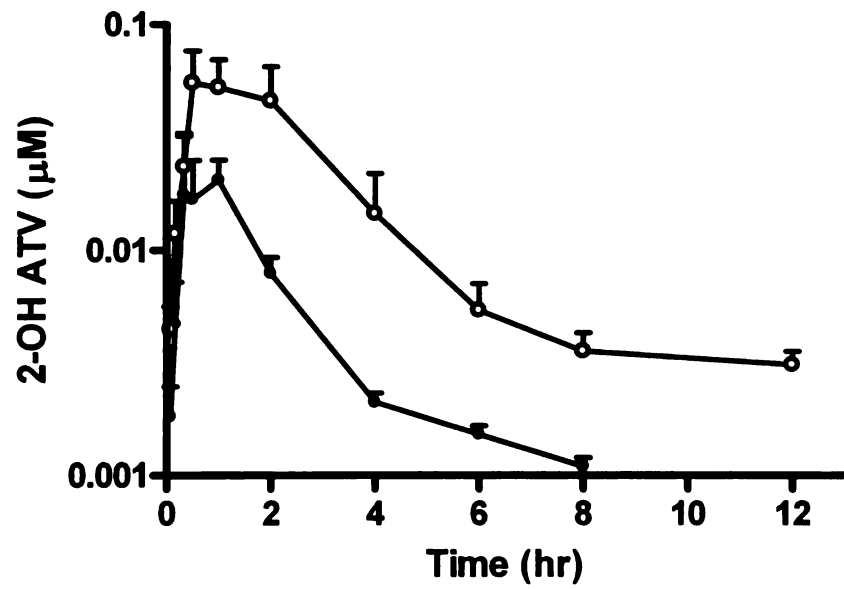
the C_{max} of ATV and metabolites by approximately 2.5 to 3-fold ($p < 0.05$) (Table 5.1).

The AUC ratio of metabolites to parent drug (AUC_M/AUC_P) was virtually unchanged in the absence or presence of RIF (Table 5.2).

Fig. 5.2 Mean (\pm SD) plasma concentrations of (A) ATV, (B) 2-OH ATV and (C) 4-OH ATV in rats ($n = 5$) after a single oral dose of 10 mg/kg ATV with and without RIF given as a bolus intravenous dose (20 mg/kg). Solid circles indicate ATV alone control group; open circles indicate RIF-treatment group. Data are depicted on a semilogarithmic scale.



(B)



(C)

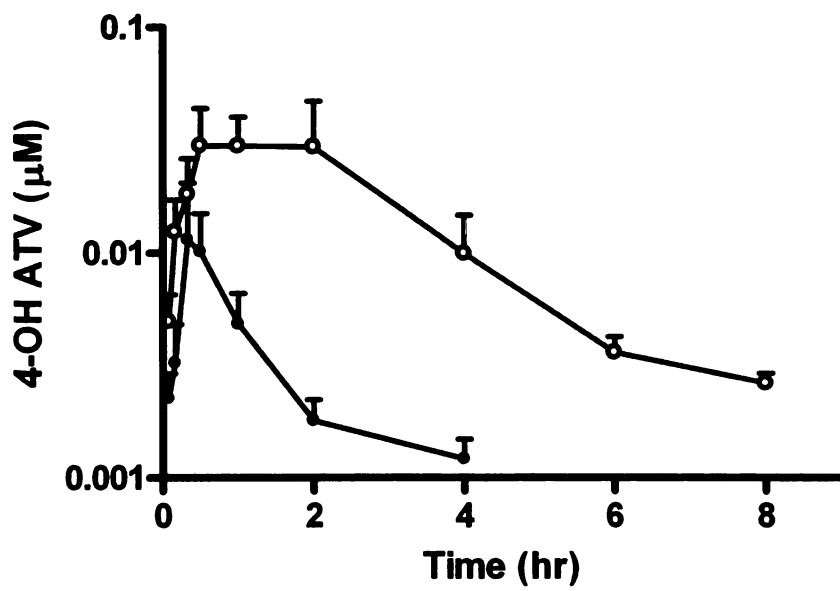


Table 5.2 Summary of derived pharmacokinetic parameters of ATV in rats ($n = 5$) after single oral dose (10 mg/kg) or intravenous dose (2 mg/kg) of ATV with and without RIF given as a bolus intravenous dose (20 mg/kg).

	CL _{iv} ^a (ml/min/kg)	(f _u × CL _{int}) ^a (ml/min/kg)	V _{ss} ^a (L/kg)	AUC _M /AUC _P ^b i.v.	AUC _M /AUC _P ^b oral
ATV alone	32.3 ± 7.1	88.0 ± 42.6	10.2 ± 3.4	0.033 ± 0.006	0.22 ± 0.12 [§]
with RIF	23.3 ± 3.9*	41.4 ± 11.6*	7.5 ± 5.1	0.11 ± 0.04**	0.20 ± 0.09 [§]

Data are mean values ± SD ($n = 5$); the level of significance was set at $p < 0.05$.

^a Blood values following intravenous dosing.

^b AUC_{0-2hr} ratio of ATV metabolites (sum of 2-OH ATV and 4-OH ATV) to ATV.

* $p < 0.05$; ** $p < 0.01$ as compared to values for the same dosing route in the absence of RIF.

[§] Significantly different from comparable intravenous ratio ($p < 0.01$).

5.3.3 Effect of RIF on the oral bioavailability, gut and liver metabolic extractions of ATV

The estimated ER_H of ATV was 0.58 ± 0.13 (Table 5.3). Therefore, $F_H = 0.42 \pm 0.13$. From Eqn. (5.4), mean ($F_{abs} \times F_G$) is 0.14 ± 0.08 , assuming that ER_H is the same after intravenous and oral administration of ATV. As noted in Table 5.1, C_{max} and AUC ATV values following oral dosing with RIF did not exceed concentrations measured following intravenous control dosing. ATV concentrations following intravenous dosing with RIF were within the two-fold range in which we demonstrated dose linearity in our pilot intravenous studies. Therefore, we believe it is reasonable to assume that linearity was maintained when calculating ER_H, F_H and ($F_{abs} \times F_G$) for the studies when RIF was present. In studies with RIF present, oral bioavailability (F) was increased from 5.2 % to

14 % ($p < 0.001$). The ER_H calculated in the presence of RIF was significantly decreased by 28% compared to that in the absence of RIF (Table 5.3). Calculating F_H and substituting into Eqn. (5.4) allows estimation of ($F_{abs} \times F_G$), which is 71% greater than the control ($p < 0.05$) (Table 5.3), suggesting that intravenous RIF co-administration in the rat can affect both gut and liver bioavailability of ATV.

Table 5.3 Measures of ATV bioavailability and calculated hepatic and gut metabolic extraction based on Eqns. 5.1-5.4.

	F	ER_H	F_H	$F_{abs} \times F_G$
ATV alone	0.052 ± 0.020	0.58 ± 0.13	0.42 ± 0.13	0.14 ± 0.08
with RIF	$0.14 \pm 0.03^{***}$	$0.42 \pm 0.07^*$	$0.58 \pm 0.07^*$	$0.24 \pm 0.04^*$

Data are mean values \pm SD (n = 5); * $p < 0.05$; *** $p < 0.001$ compared to ATV alone.

F, measured oral bioavailability; ER_H : hepatic extraction ratio; F_H : hepatic availability;

$F_{abs} \times F_G$: gut processes affecting availability

5.3.4 Metabolic studies of ATV by rat small intestinal microsomes

The inhibitory effects of RIF (0-50 μ M) on the *in vitro* metabolism of ATV (initial concentration is 0.1 μ M) by rat small intestinal microsomes were also examined (Table 5.4), since we had not previously reported these values (Lau et al., 2006a). RIF did not alter the metabolism of ATV up to a concentration of 35 μ M and reduced it significantly, but less than 20%, at 50 μ M as reflected by the increase in ATV concentrations. As depicted in Fig. 5.3, RIF plasma concentrations following intravenous dosing were less than 50 μ M at all time points.

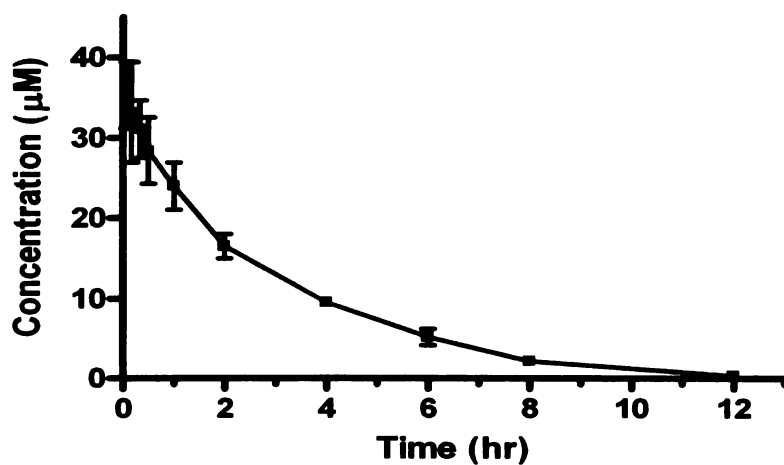
Table 5.4 Effects of RIF on the intestinal microsomal metabolism of ATV (0.1 μM).

RIF concentrations (μM)	ATV concentrations ^a (% of control)
0	100.0 \pm 7.4
10	101.9 \pm 1.8
20	110.9 \pm 6.6
35	112.2 \pm 8.5
50	118.3 \pm 5.6**

Data are mean values \pm SD ($n = 3$); ** $p < 0.01$ significantly different from ATV alone control.

^aATV concentrations at the end of a 15 min microsomal incubation study.

Fig. 5.3 Mean (\pm SD) plasma concentration of RIF following a single intravenous dose (20 mg/kg) in an ATV rat pharmacokinetic study with RIF co-administration ($n = 5$).



5.4 Discussion

Recently, we evaluated the interaction of ATV with hepatic uptake transporters, Oatps, *in vitro* in cellular systems and *ex situ* using the IPRL model (Chapter 3; Lau et al., 2006a). Hepatic uptake inhibition by an Oatp blocker, RIF, significantly increased the AUCs of ATV and OH ATVs with reduced amounts of all compounds in RIF-treatment livers, indicating a reduced partition of ATV into the liver compartment for subsequent metabolism. Both 2-OH ATV and 4-OH ATV were proven to be substrates of Oatp1b2, utilizing *in vitro* assays, thereby explaining their increased AUC values by RIF (Chapter 3; Lau et al., 2006a). Here, we studied the pharmacokinetics and metabolism of ATV under both intravenous and oral administration in rats. We had hoped that intravenous administration of RIF would have no gut effect, thereby allowing us to investigate the *in vivo* effect of hepatic Oatp on the drug-drug interaction between ATV and RIF following intravenous administration of both drugs.

As shown in Figs. 5.1A-C, intravenous coadministration of ATV and RIF led to a significant 4-fold increase in the AUC values for ATV's metabolites, consistent with our IPRL data (Chapter 3; Lau et al., 2006a). We also observed a significant 36% increase in ATV AUC_{0-∞} (Table 5.1). However, this increase was lower than our expectation, considering that RIF led to a significant 56% increase in ATV AUC when only 5 μM of RIF was co-administered with 1 μM ATV in our previous IPRL study (Chapter 3; Lau et al., 2006a). As depicted in Fig. 5.3, the plasma concentration of RIF reached a value of ~35 μM at 5 min after ATV dosing. At this concentration, RIF should be effective in inhibiting the hepatic uptake of ATV, considering that the K_i values of RIF inhibition on ATV's uptake obtained from *in vitro* cellular uptake assays were 2.88 μM for Oatp1a4

and 0.79 μM for Oatp1b2 (Chapter 3; Lau et al., 2006a). As indicated in Table 5.3, ATV has an ER_H value of 0.58, which would classify ATV as an intermediate hepatic extraction ratio drug (i.e. $0.3 \leq \text{intermediate ER}_\text{H} \leq 0.7$), where blood flow considerations can modify the effect of changes in intrinsic clearance on total clearance. That is, upon RIF treatment, total drug intrinsic clearance ($f_u \times \text{CL}_\text{int}$) decreased significantly by 53%, almost twice that observed for the 28% decrease in total hepatic clearance (CL_iv) (Table 5.2).

When ATV was administered orally at 10 mg/kg, there was a marked 3.5-fold increase in $\text{AUC}_{0-\infty}$ in the presence of RIF (Table 5.1; Fig. 5.2A), which was more extensive than for ($f_u \times \text{CL}_\text{int}$) observed after intravenous dosing. Since clearance following oral dosing (CL/F) is not affected by hepatic blood flow [i.e. $\text{CL}/F = (f_u \times \text{CL}_\text{int}) / (F_\text{abs} \times F_\text{G})$], the marked change in oral clearance suggests that ($F_\text{abs} \times F_\text{G}$) must also have been increased following intravenous RIF dosing.

It is likely that some hydroxy metabolites are formed by intestinal wall Cyp3a during the absorption phase when ATV was dosed orally. This can be examined by comparing AUC ratios of metabolites to parent ATV. The $\text{AUC}_\text{M}/\text{AUC}_\text{P}$ ratio was 7-fold higher for oral control versus i.v. control (Table 5.2), indicating a greater portion of metabolism under oral administration, due to first-pass metabolism from both intestine and liver, as supposed to that under i.v. route, where metabolism is assumed to occur only (or predominantly) in the liver. To obviate saturation of either transport or metabolic processes, the chosen doses for both routes of administration were within the linear dose-exposure range found in preliminary studies. As shown in Table 5.3 for ATV alone dosing, the estimated gut availability ($F_\text{abs} \times F_\text{G}$) was one-third of the liver availability

(F_H). Given that ATV has rapid and almost completed intestinal absorption (Lennernas, 2003), we suspect that the contribution of F_{abs} to the low value of estimated gut availability should be relatively minor compared with that of F_G . The significant gut metabolism is probably due to the high capacity of intestinal enzymes to metabolize ATV and/or increased drug exposure to metabolizing intestinal enzymes from the contribution of intestinal efflux transporters at the apical domain of the enterocyte, such as P-glycoprotein (P-gp), leading to recycling of drugs between the gut lumen and the enterocytes, thereby causing significant enzyme-transporter interplay (Benet et al., 1999; Johnson et al., 2001; Cummins et al., 2002a, 2004). Since ATV has the characteristics of a Class 2 compound according to the Biopharmaceutics Drug Disposition Classification System proposed by Wu and Benet (2005), its high permeability will allow ready access to the gut membrane but the low solubility will limit the concentrations coming into the enterocytes, thereby preventing saturation of efflux transporters.

The AUC_M/AUC_P ratio was significantly increased by RIF following i.v. dosing (Table 5.2). RIF caused a 310% increase in the total metabolites AUC_{0-2hr} , in contrast to the 36% increase in ATV AUC (and the 56% decrease in $f_u \times CL_{int}$). This finding is consistent with metabolites uptake also being inhibited by RIF. However, RIF has no significant effect on the AUC_M/AUC_P ratio following oral dosing. That is, RIF caused a parallel increase in metabolites and parent ATV. A number of hypotheses could be put forward to explain these results, but here we only report the observation, since we were unsuccessful in avoiding RIF gut effects, and therefore cannot experimentally differentiate liver versus gut inhibitory effects.

RIF is conventionally known for its induction effect on several drug metabolizing enzymes such as CYP3A4 and 2C9 as well as P-gp and MRP2 when given following a multiple dosage regimen (Schuetz et al., 1996; Fromm et al., 2000). More recently Kajosaari et al. (2005) reported that RIF also exhibits enzymatic inhibitory effect towards repaglinide CYP-mediated metabolism in hepatic microsomal studies. However, the potency of RIF inhibitory effect towards CYP enzymes is probably substrate specific as RIF did not exhibit substantial inhibition on the metabolism of ATV as reported in our rat hepatic microsomal studies (Chapter 3; Lau et al., 2006a). We show here that RIF also had no effect on intestinal microsomal metabolism (Table 5.4) at RIF concentrations comparable to those measured *in vivo*. We believe that the RIF effect on reducing hepatic metabolic extraction is most likely due to its inhibition on hepatic Oatps, which in turn led to reduction in the amount of parent drug getting into the hepatocytes for metabolism. Moreover, RIF could contribute to increased gut availability through inhibition of intestinal efflux transporters following oral dosing of ATV. Upon RIF treatment, ($F_{\text{abs}} \times F_G$) significantly increased from 0.14 ± 0.08 to 0.24 ± 0.04 in the present study. However, our previous work does not provide an adequate explanation of this finding. As shown by our IPR and transporter studies, ATV is subject to efflux transport by MRP2 in addition to P-gp (Chapter 3; Lau et al., 2006a). RIF was able to exhibit inhibitory effects on efflux of ATV (5 μM) mediated by MRP2, but not P-gp. But these effects were only observed at concentrations of 50 μM or higher using the human MRP2 or P-gp overexpressing cell lines. Cellular study using CYP3A4-transfected Caco-2 cells (Cummins et al., 2002a, 2004) did suggest significant reduction in metabolic extraction ratio from the apical to basolateral direction when the efflux of ATV was

inhibited by the concomitant GG918, a potent P-gp inhibitor with no inhibitory effect on CYP3A4-mediated metabolism (see Chapter 4).

In conclusion, these pharmacokinetic experiments reinforce our hypothesis that hepatic Oatp is one of the major determinants for drug elimination, especially for drugs that are mainly eliminated by the liver, and/or undergo hepatic metabolism. We have also shown that a single bolus dose of RIF might cause significant drug-drug interaction by impairing hepatic uptake. Additionally, ATV undergoes extensive gut metabolism besides hepatic metabolism and exhibits low oral bioavailability in rats, possibly due to transporter-enzyme interplay at both intestinal and hepatic level, but since intravenous RIF administration caused obvious changes in gut bioavailability we were unable to differentiate intestinal enzymatic and transporter effects *in vivo*.

Chapter 6

THE EFFECT OF OATP1B1 ON THE DISPOSITION OF ATORVASTATIN IN HEALTHY VOLUNTEERS

6.1 Introduction

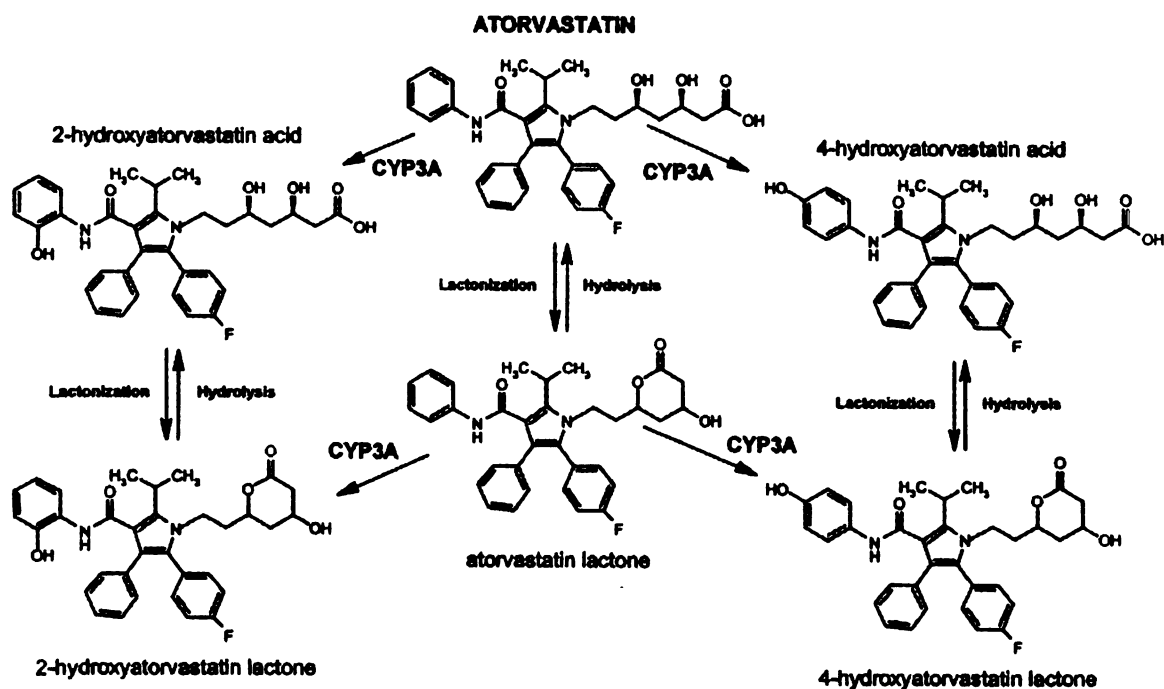
Members of the organic anion-transporting polypeptides (OATP), which belong to the solute carrier family SLCO, represent a family of important proteins involved in the membrane uptake of physiological substrates and drugs in human (Bossuyt et al., 1996; Abe et al., 1999; Takikawa, 2002; Mikkaichi et al., 2004). One of these uptake transporters, OATP1B1, previously known as liver specific transporter-1 (Abe et al., 1999) OATP2 (Hsiang et al., 1999) or OATP-C (Konig et al., 2000b) is the most abundant, with expression exclusively in the basolateral membrane of hepatocytes (Abe et al., 1999; Hsiang et al., 1999; Konig et al., 2000a, 2000b). OATP1B1 plays an important role in controlling the uptake of endogenous compounds and drugs, mostly anionic in nature, into hepatocytes, thereby increasing both the amount of drug available for metabolism by liver enzymes such as cytochromes P450 (CYP) and the subsequent biliary excretion of drugs.

There are many examples of drug-drug interactions due to inhibition or induction of enzymes expressed in both the intestine and the liver that can potentially result in drug toxicity or lack of drug efficacy. However, drug-drug interactions may also occur by

interference with the relevant uptake transporter protein(s) in the liver that are located upstream of the hepatic enzymes.

The widely used lipid-lowering agent, atorvastatin (acid), a member of the class of 3-hydroxy-3-methylglutaryl-coenzyme A (HMG-CoA) reductase inhibitors (statins), was studied here to investigate the contributions of OATP1B1 to overall drug disposition and metabolism. Atorvastatin is mainly excreted by hepatobiliary mechanisms with less than 1% of atorvastatin and derivatives eliminated in urine (Lennernas, 2003). In humans, atorvastatin is orally administered in the open hydroxy acid ring form but can biotransform to its inactive lactone form either via a coenzyme A-dependent and/or an acyl glucuronide intermediate pathway (Fig. 6.1).

Fig. 6.1. The proposed metabolic pathways of atorvastatin (Jacobsen et al., 2000).



Atorvastatin has been shown to be both a substrate (Chapter 3; Konig et al., 2000b; Kameyama et al., 2005; Lau et al., 2006a) and an inhibitor (Konig et al., 2000b; Chen et al., 2005) of OATP1B1, and subject to extensive first-pass metabolism both in the intestine and in the liver by CYP3A (CYP3A4 and CYP3A5) and to a smaller extent, CYP2C8 (Christians et al., 1998; Jacobsen et al., 2000), to form two major active metabolites, 2-hydroxy-atorvastatin acid and 4-hydroxy-atorvastatin acid. Both of these metabolites are pharmacologically equipotent with the parent drug (Lennernas, 2003). These long-lived active metabolites are responsible for the majority of circulating inhibitory activity of HMG-CoA reductase, the rate-limiting enzyme residing in the liver for the *de novo* synthesis of cholesterol (Lennernas, 2003). A reduction in the hepatic uptake of atorvastatin and the hepatic formation of its active metabolites would lead to a decrease in their therapeutic efficacy and an increase in atorvastatin's systemic exposure, which could predispose to adverse reactions such as rhabdomyolysis or myopathy (Lennernas, 2003). Therefore, better characterization of the mechanisms behind the drug interactions that may cause these adverse effects is needed.

In the present study, we chose to use the antituberculosis agent rifampicin as a model inhibitor of hepatic uptake. Rifampicin is a well-known inducer for CYP enzymes (Niemi et al., 2003) and efflux transporters such as P-glycoprotein (P-gp) and multidrug resistance-associated protein 2 (MRP2) (Schuetz et al., 1996; Fromm et al., 2000) upon multiple dosing, but following only a single dose, rifampicin is a potent OATP1B1 blocker and substrate (Vavricka et al., 2002; Tirona et al., 2003). Previous studies have indicated that a single intravenous infusion of rifampicin increased the level of bilirubin in blood (Acocella et al., 1965). Rifampicin also acutely reduced the hepatic elimination

of sulfobromophthalein to approximately one quarter of pretreatment values (Acocella et al., 1965). Both bilirubin and sulfobromophthalein are high affinity substrates of OATP1B1 (Konig et al., 2000b; Cui et al., 2001b; Vavricka et al., 2002). These observations indicate that rifampicin may inhibit the transporter-mediated uptake of organic anions into human liver via the OATP1B1 pathway.

Here, we have investigated the effects of a single intravenous short infusion of rifampicin on the kinetics of atorvastatin and its metabolites in healthy volunteers. The primary goal of the study is to demonstrate if competitive inhibition of OATP1B1 mediated uptake by rifampicin in the liver can influence the disposition of atorvastatin and its active metabolites *in vivo* in the same manner previously observed in our isolated perfused rat liver studies (Chapter 3; Lau et al., 2006a) and in whole animal rat pharmacokinetic studies (Chapter 5; Lau et al., 2006b). All volunteers participating in the study were genotyped for *SLCO1B1* (gene name for OATP1B1) variants that have been reported to exert clinical effects on drug exposure of OATP1B1 substrates (Tirona et al., 2001; Nishizato et al., 2003). The affinity of atorvastatin acid and the substrate specificity of hydroxy atorvastatin acids towards OATP1B1 were also investigated using *in vitro* cellular assays. The potency of rifampicin to inhibit the OATP1B1-mediated uptake of atorvastatin was studied as well, to provide a mechanistic explanation for the underlying kinetics when atorvastatin was co-administered with an acute dose of rifampicin in humans.

6.2 Methods

6.2.1 Clinical study

6.2.1.1 Subjects and study design

A prospective randomized, open-labeled, crossover study was conducted at the General Clinical Research Center, University of California at San Francisco (UCSF). The study protocol was approved by the Committee on Human Research and the General Clinical Research Center at UCSF. All subjects gave their written informed consent before enrollment.

Six men and six women were enrolled in the study. Subjects underwent a medical history and physical examination and blood and urine chemistries to check hepatic and renal function, and to insure that none of the subjects were anemic. Participants included 5 Caucasians, 4 Asians, 2 African American, and 1 Pacific Islander. Their mean age was 36 ± 12 years and their mean body height and weight were 170 ± 7 cm and 67 ± 11 kg, respectively. All subjects were nonsmokers. One subject withdrew from the study 12 hours after atorvastatin dosing during the rifampicin-treatment phase due to discomfort from venipuncture and anxiety from bruising. The data obtained from this subject up to 12 hour for both phases (control phase and rifampicin-treatment phase) were included in the pharmacokinetic analysis.

Each subject was enrolled for two study periods of atorvastatin: (A) one oral dose (one 40-mg tablet of *Lipitor*[®]; Pfizer, New York, NY) of atorvastatin and (B) one oral dose of atorvastatin (one 40-mg tablet of *Lipitor*[®]) preceded by a 30-minute intravenous infusion of rifampicin (one bottle of 600 mg *Rifadin*[®] powder for injection reconstituted

with 10 ml sterile saline; Sanofi-Aventis, Bridgewater, NJ). The two study periods were separated by a one-week washout.

Subjects were randomized to one of the two treatment groups, (A) or (B) on study day 1 (period 1) and study day 8 (period 2). In both treatments, venous blood samples (8 mL each) were drawn before and at 0.5, 1, 1.5, 2, 2.5, 3, 4, 6, 9, 12, 24, 36 and 48 hours after atorvastatin dosing (24, 36 and 48-hour samples were collected on study days 2 and 3 and study days 9 and 10). The study ended after the last blood collection at 48 hours. For treatment (B), rifampicin was infused at a rate of 20 mg/min for 30 minutes through a cannulated forearm vein of each subject and was given one-half hour before atorvastatin oral administration.

To minimize drug degradation, the blood samples were centrifuged within 30 minutes, and the plasma was separated and frozen at -80 °C. Food intake on atorvastatin dosing days was standardized and subjects were instructed to fast overnight the day before study days 1 and 8, and for 3 hours post-dosing. Alcohol or any non-study drugs were not allowed for 2 weeks before and during the study days. Citrus fruits and citrus beverages were also not allowed during the same time period due to their inhibitory effect on intestinal CYP3A4-mediated metabolism of atorvastatin (Lilja et al., 1999) and potentially on intestinal uptake transporters.

6.2.1.2 Sequencing analysis for *SLCO1B1* polymorphisms identification

DNA was extracted from blood samples by standard methods with a Puregene DNA Purification kit (Gentra Systems, Minneapolis, MN) and stored in aliquots (5 µg/30 µL) at 4°C. The sequencing method utilizes capillary electrophoresis and incorporation of

dye labeled dideoxyribonucleoside triphosphates (ddNTPs). Initially, the region containing the single nucleotide polymorphisms (SNPs) within the respective exons of interest was amplified by PCR. Two enzymes were added to the PCR products to remove some of the remaining reaction reagents: shrimp alkaline phosphatase (SAP) acts to remove the phosphate group from any remaining dNTPs, while exonuclease I (exoI) digests any remaining PCR primers. The cleaned product was added to the sequencing reaction, which contained polymerase, a single sequencing primer (usually it is either the forward or reverse PCR primer), and a mixture of fluorescently labeled ddNTPs and unlabeled dNTPs. The incorporation of a dNTP allows extension of the template copy, while ddNTP incorporation results in termination of extension. The products were run on a 3730xl DNA Analyzer (Applied Biosystems, Foster City, CA), where the products were separated by capillary electrophoresis according to their size (length) differences. After separation, the fluorescent tags attached onto the ddNTPs on the ends of the products were excited by a laser, leading to emission at a specific wavelength. The data were converted into an electronic format, where each labeled ddNTP signified a specific base (A, G, T or C) and was seen as a colored peak for the associated base. The string of bases forms the sequence of the product. SNPs were seen as different bases incorporated at the same particular position, while samples with heterozygous samples had two bases incorporated and seen as overlapping peaks on top of each other. Table 6.1 shows the primer sequences for the SNPs that were detected in the study subjects.

Table 6.1 Single-nucleotide polymorphism (SNP) primers for identification of *SLCO1B1* polymorphisms using sequencing.

<i>Primer Name</i>	<i>Primer Sequence</i>	<i>SNP</i>	<i>Exon</i>
SLCO1B1-5Fwd	ATCTCTTAAAACACATGCTGGGA	A388G	4
SLCO1B1-5Rev	GGTTTATCATCCAGTTCAGATGG	(Asn130Asp)	
SLCO1B1-6Fwd	CAGCATAAGAATGGACTAATACACC	T521C	5
SLCO1B1-6Rev	GCAATTTTACTAGATGCCAAGAA	(Val174Ala)	

6.2.1.3 Analytical drug assays

The concentrations of atorvastatin and its main metabolites were measured using a liquid chromatography/tandem mass spectrometry (LC/MS/MS) system, consisting of a 717 plus autosampler (Waters Corporation, Milford, MA), and a Quattro LC Ultima (Micromass, Manchester, UK) detector with electrospray positive ionization mode. The multiple reaction monitor (MRM) was set at 559.6 – 440.8 *m/z* for atorvastatin acid, 575.2 – 440.5 *m/z* for 2-hydroxy-atorvastatin acid and 4-hydroxy-atorvastatin acid, 541.2 – 448.2 for atorvastatin lactone, 557.2 – 448.2 *m/z* for 2-hydroxy-atorvastatin lactone and 4-hydroxy-atorvastatin lactone, 564.2 – 445.8 *m/z* for D₅-atorvastatin, the internal standard for atorvastatin and metabolites in the acid form and 546.2 – 451.2 *m/z* for D₅-atorvastatin lactone, the internal standard for atorvastatin and metabolites in the lactone form. The samples and standards were prepared as previously described (Jemal et al., 1999). Chromatography was performed on an Agilent, XDB C18 column (4.6 x 50 mm, 5 µm particle size, Agilent Technologies, Palo Alto, CA). The mobile phase A was 20% acetonitrile containing 0.05% acetic acid and 5 mM ammonium acetate and mobile phase B was 80% acetonitrile containing 0.05% acetic acid and 5 mM ammonium acetate. The gradient elution time program was set as follows: 0–1.5 min, B, 20–100%; 1.5–4.0 min,

B, 100%; 4.0-4.5 min, B, 100-20%; The flow rate was 1.0 ml/min from 0-4.5 min and increased to 1.5 ml/min at 4.6 min and kept at 1.5 ml/min from 4.6-6.5 min. The run time for each sample was 6.5 min. Twenty-five percent of the flow liquid was split into the mass system. The sample cone voltage and collision energy for all analytes and internal standard were set at 30 V and 20 eV, respectively.

MRM were set at 823.5 – 791.5 *m/z* and 721 – 689 *m/z* for rifampicin and the internal standard, rifamycin SV, respectively. The sample cone voltage and collision energy for rifampicin were set at 30 V and 18 eV, respectively. The corresponding values for rifamycin SV were 40 V and 35 eV, respectively. The analytical column was a BDS C18 (50 x 4.6 mm) from Hypersil-Keystone (Bellefonte, PA). The mobile phase consisted of 36% acetonitrile containing 0.05% acetic acid and 5 mM ammonium acetate. The flow rate was 1.0 ml/min and ¼ was split into the mass system.

The method for atorvastatin and metabolites was validated from 0.1 to 100 ng/ml in plasma. The intra- and inter-day coefficients of variation were below 15% at relevant concentrations (n = 10). Rifampicin did not interfere with the assay. Calculations were performed with MassLynx 3.5 software (Micromass, Manchester, UK).

6.2.1.4 Pharmacokinetic analysis

Pharmacokinetic parameters were estimated from plasma concentration data via noncompartmental analysis using WinNonlin Professional software (Version 3.1; Pharsight Corporation, Mountain View, CA). The total area under the plasma concentration-time curve (AUC) from time 0 to 48 hours (AUC₀₋₄₈) was estimated using the linear/logarithmic trapezoidal method (for the up/down portions of the curve,

respectively) up to the last measured concentration. This area was extrapolated to infinity ($AUC_{0-\infty}$) by the addition of the last measured concentration divided by the apparent terminal disposition rate constant λ_z , determined by regression analysis of the terminal portion of the log plasma concentration-time curve. The apparent terminal half-life ($t_{1/2}$) was estimated from the terminal rate constant as $t_{1/2} = \ln 2 / \lambda_z$. Oral clearance (CL/F) was calculated as $Dose / AUC_{0-\infty}$. The steady-state volume of distribution (V_{ss}/F) was calculated as $V_{ss}/F = MRT \times CL/F$. The mean residence time (MRT) was calculated as the ratio of the area under the first moment curve $AUMC_{0-\infty}$ divided by $AUC_{0-\infty}$ (Benet and Galeazzi, 1979), minus the estimated mean absorption time (MAT) [i.e. $MRT = (AUMC_{0-\infty} / AUC_{0-\infty}) - MAT$]. MAT was the reciprocal of first-order absorption rate constant, when fitting the oral data to 2-compartmental model with first-order absorption. The values of CL/F and V_{ss}/F were normalized by body weight.

6.2.1.5 Statistical analysis

The number of subjects ($n = 12$) was estimated to be sufficient to detect a 50% difference in $AUC_{0-\infty}$ (from time 0 to infinity) between the two study regimens with a statistical power of 80% (α level, 5%). Results are expressed as mean \pm SD. The pharmacokinetic variables were compared by use of paired t test across the two treatment periods except for t_{max} in which the Wilcoxon signed rank test was used. Logarithmic transformation of C_{max} , $t_{1/2}$, V_{ss}/F , CL/F and AUC values was performed before statistical analysis, and 95% confidence intervals were calculated for the geometric mean ratios (rifampicin phase value as a percentage of the control phase values) of these variables.

The data were analyzed with GraphPad Prism 4.0 (GraphPad Software, San Diego, CA).

Differences were considered statistically significant at $p < 0.05$.

6.2.2 In vitro study

6.2.2.1 Materials

Atorvastatin acid, 2-hydroxy-atorvastatin acid and 4-hydroxy-atorvastatin acid were obtained from Toronto Research Chemicals (North York, Ontario, Canada). Rifampicin and sodium butyrate were purchased from Sigma-Aldrich (St. Louis, MO). All other chemicals were reagent grade and purchased from either Sigma or Fisher Scientific (Pittsburg, PA, USA). Human OATP1B1 cDNA plasmid was kindly provided by Professor Richard Kim (Vanderbilt University, Nashville, TN). Human embryonic kidney cells (HEK293) and all cell culture media were obtained from the UCSF Cell Culture Facility (San Francisco, CA). Poly-D-lysine coated 12-well plates were obtained from BD Bioscience (Bedford, MA). The Lipofectamine 2000 transfection system and Opti-MEM buffer were purchased from Invitrogen (Carlsbad, CA).

6.2.2.2 Transient transfection and uptake transport studies

The protocol for the uptake experiments in our laboratory has been previously described (Chapter 3; Lau et al., 2006a). Briefly, HEK293 cells were cultured in Eagle's minimal essential medium with Eagle's balanced salt solution and *l*-glutamine plus 10% heat-inactivated fetal bovine serum (FBS), non-essential amino acids, sodium pyruvate, streptomycin and penicillin. Cells were seeded into poly-D-lysine coated 12-well plates at

a density of 0.5×10^6 cells per well one day prior to transient transfection with OATP1B1 plasmid or pEF/V5-His vector control (Invitrogen, Carlsbad, CA) using the Lipofectamine 2000 transfection system according to the manufacturer's directions. Culture medium was replaced 24 hour before the uptake studies with the same medium containing 10 mM sodium butyrate to induce the expression of transporter. Before initiation of the uptake study, cells were washed once with phosphate buffered saline (PBS) pre-warmed at 37 °C. The uptake study was initiated by adding 0.5 ml of Opti-MEM buffer containing substrates (atorvastatin acid or hydroxy-atorvastatin acids) and incubating at 37 °C for 3 min (within the linear time range). To assess the inhibitory potency of rifampicin towards OATP1B1-mediated uptake of atorvastatin acid, rifampicin (concentration range, 0.5 – 100 μ M) was added simultaneously with atorvastatin acid. At designated times, buffer was removed to terminate the reaction and the cells were washed three times with ice-cold PBS. The homogenate was centrifuged for 5 min at 13,000 g and the resulting supernatant was analyzed by LC/MS-MS. The protein concentrations in cell experiments were determined by the method of Lowry et al. (1951) using bovine serum albumin as a standard.

6.2.2.3 Data analysis

Kinetic parameters for the uptake of atorvastatin acid in the OATP1B1-expressing HEK293 cells were obtained by using the following equation,

$$v_0 = (V_{\max} \times S)/(K_m + S) + P_{\text{dif}} \times S \quad \text{Eqn. (6.1)}$$

where v_0 is the initial uptake rate, S is the substrate concentration, K_m is the Michaelis constant, V_{\max} is the maximal uptake rate, and P_{dif} is the nonsaturable uptake clearance.

Data were fitted to Eqn. (6.1), using a nonlinear least-square method by SigmaPlot (Version 5.0; SPSS Inc., Chicago, IL). To obtain the IC₅₀ value of rifampicin inhibitory effect on atorvastatin acid uptake, the data were fitted using WinNonlin (Version 3.1; Pharsight Corporation, Mountain View, CA). The K_i value was estimated as

$$K_i = IC_{50}/[1+S/K_m] \quad \text{Eqn. (6.2)}$$

Student's *t* test was used to analyze differences between two groups. Analysis of variance was used to analyze differences among more than two groups, and the significance of difference between two means in these groups was evaluated using Tukey's post hoc test. The data were analyzed with GraphPad Prism 4.0 (GraphPad Software, San Diego, CA). Differences were considered statistically significant at $p < 0.05$.

6.3 Results

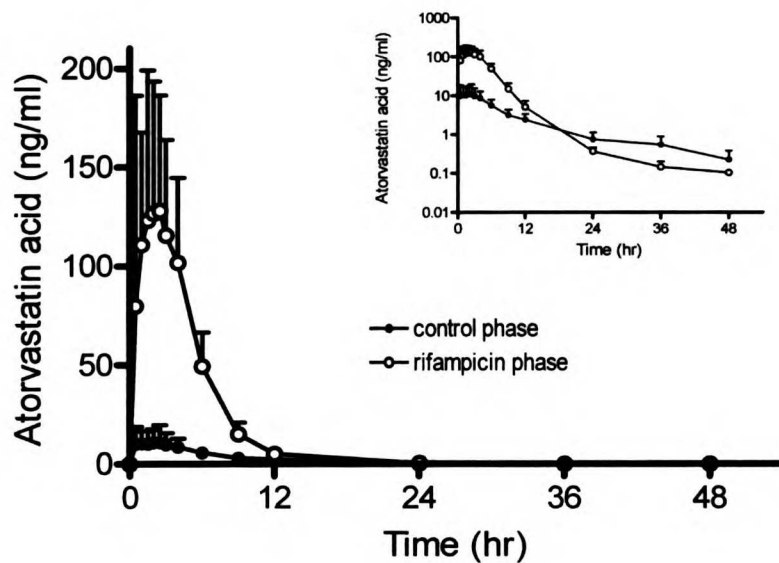
6.3.1 Clinical study

6.3.1.1 Effect of rifampicin on the pharmacokinetics of atorvastatin acid and lactone

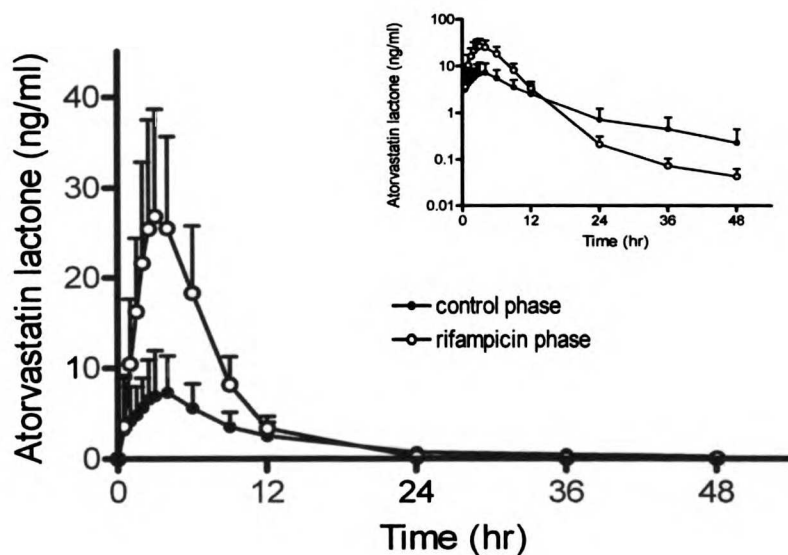
Rifampicin significantly increased the AUC_{0-∞} of atorvastatin acid by 567% ($p < 0.001$) and C_{max} by more than 930% ($p < 0.001$) compared with the control phase (Fig. 6.2A and Table 6.2). The AUC_{0-∞} of atorvastatin lactone was also increased 113% by rifampicin ($p < 0.001$) (Fig. 6.2B and Table 6.2) and C_{max} of the lactone was increased by 220% ($p < 0.001$). There was no apparent sex or ethnic differences in the pharmacokinetics of atorvastatin acid and lactone.

Fig. 6.2 Mean plasma concentration (\pm SD) of (A) atorvastatin acid and (B) atorvastatin lactone in 12 healthy volunteers after a single oral dose of 40 mg atorvastatin with and without intravenous rifampicin. *Inset:* depicts the same data on a semilogarithmic scale.

(A)



(B)



The lactone/acid AUC ratio of atorvastatin was decreased 68% ($p < 0.001$) by rifampicin (Fig. 6.3). Values of t_{\max} remained statistically unaltered by rifampicin, for both atorvastatin and its lactone.

Rifampicin considerably shortened the apparent terminal half-lives ($t_{1/2}$) of atorvastatin acid and its lactone form (by 54%, $p < 0.01$ and 26%, $p < 0.05$, respectively; Table 6.2), although there was no statistical difference between acid and lactone half-lives within each phase. The steady-state volume of distribution (V_{ss}/F) of atorvastatin acid was extensively decreased in the presence of rifampicin by 97% ($p < 0.001$), whereas the oral clearance (CL/F) was also markedly decreased from 6.17 ± 2.50 L/hr/kg to 0.88 ± 0.22 L/hr/kg (by 86%, $p < 0.001$).

Fig. 6.3 Individual $AUC_{0-\infty}$ ratios of atorvastatin lactone to atorvastatin acid in 12 healthy volunteers after a single oral dose of 40 mg atorvastatin with and without intravenous rifampicin. ***, $p < 0.001$ significantly different from control phase.

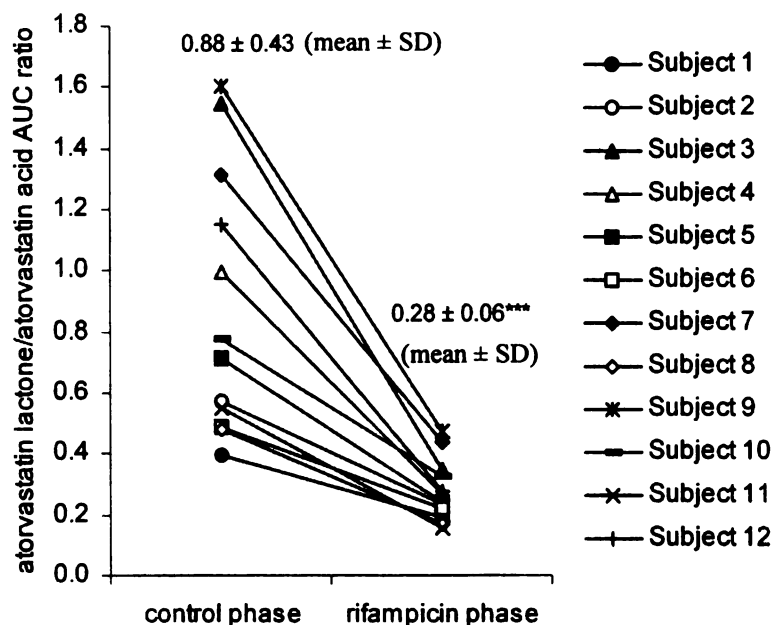


Table 6.2 Pharmacokinetic variables of atorvastatin acid and lactone in 12 healthy volunteers after a single oral dose of 40 mg atorvastatin with and without intravenous rifampicin.

variable	atorvastatin alone control phase ^a	rifampicin phase ^a	rifampicin phase (% of control)	
			mean and range	95% C.I.
atorvastatin (acid)				
C_{max} (ng/ml)	17.8 ± 8.4	184 ± 72‡	1030 (520 - 2730)	678 - 1606
t_{max}^b (hr)	1 (0.5 - 3)	2 (0.5 - 4)	—	—
$t_{1/2}$ (hr)	11.5 ± 4.5	5.24 ± 3.55†	46 (13 - 116)	33 - 71
$AUC_{0-48\text{ hr}}$ (ng/ml · hr)	103 ± 36	732 ± 214‡	711 (330 - 1190)	519 - 810
$AUC_{0-\infty}$ (ng/ml · hr)	110 ± 36	734 ± 215‡	667 (320 - 1170)	474 - 761
CL/F (L/hr/kg)	6.17 ± 2.50	0.88 ± 0.22‡	14 (9-31)	12 - 19
V_{ss}/F (L/kg)	66.2 ± 36.1	2.25 ± 0.94‡	3 (2-10)	3 - 6
atorvastatin lactone				
C_{max} (ng/ml)	9.07 ± 5.94	29.2 ± 11.9‡	320 (202 - 568)	294 - 449
t_{max}^b (hr)	3(0.5 - 4)	3(1 - 6)	—	—
$t_{1/2}$ (hr)	13.7 ± 4.0	10.2 ± 4.2*	75 (24 - 153)	47 - 98
$AUC_{0-48\text{ hr}}$ (ng/ml · hr)	87.1 ± 44.9	194 ± 62‡	223 (150 - 365)	201 - 293
$AUC_{0-\infty}$ (ng/ml · hr)	91.9 ± 48.7	196 ± 63‡	213 (135 - 354)	193 - 279

^a Values were shown in mean ± SD unless otherwise stated.

^b t_{max} data are given as median and range.

*, $p < 0.05$; †, $p < 0.01$; ‡, $p < 0.001$ significantly different from atorvastatin alone control phase.

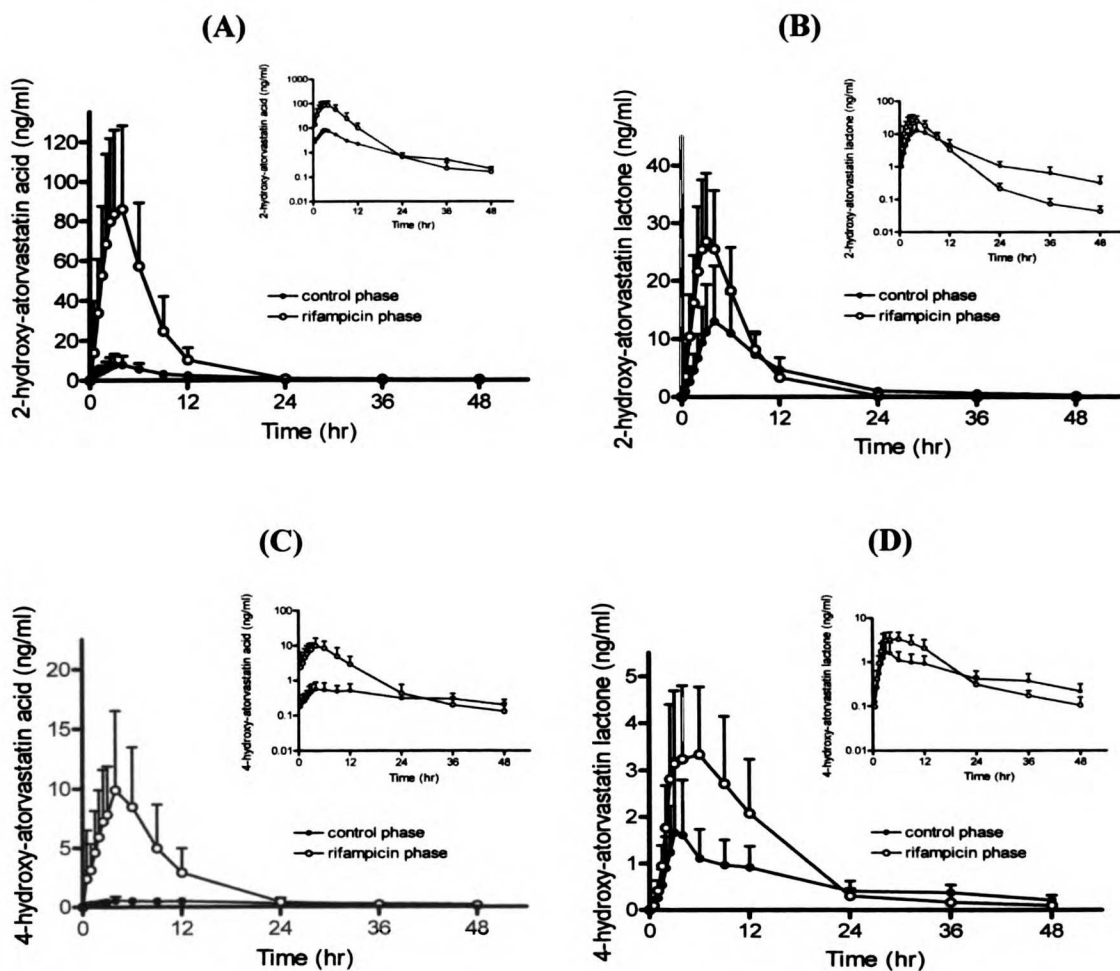
6.3.1.2 Effect of rifampicin on the pharmacokinetics of atorvastatin metabolites in acid and lactone forms

The $AUC_{0-\infty}$ values of the active metabolites, 2-hydroxy-atorvastatin acid and 4-hydroxy-atorvastatin acid, were 569% ($p < 0.001$) and 278% ($p < 0.001$) greater during the rifampicin phase than during the control phase, respectively (Fig. 6.4A and C; Table 6.3). C_{max} values were also significantly increased by 861% ($p < 0.001$) and 1680% ($p < 0.001$) for 2-hydroxy-atorvastatin acid and 4-hydroxy-atorvastatin acid, respectively (Table 6.3). Rifampicin also raised the plasma concentrations of the lactone form of 2-hydroxy and 4-hydroxy metabolites (Fig. 6.4B and D). The $AUC_{0-\infty}$ value of 2-hydroxy-atorvastatin lactone was 92% higher than the corresponding value during the control phase ($p < 0.001$). $AUC_{0-\infty}$ was increased by 52% during the rifampicin phase for 4-hydroxy-atorvastatin lactone ($p < 0.01$). Rifampicin increased the C_{max} of 2-hydroxy-atorvastatin lactone by 143% ($p < 0.001$) and that of 4-hydroxy-atorvastatin lactone by 101% ($p < 0.01$). The C_{max} values of both acid and lactone forms of 2-hydroxy-atorvastatin without rifampicin were about 11-fold and 5-fold higher, respectively, than the corresponding values of 4-hydroxy-atorvastatin, indicating that 2-hydroxy-atorvastatin, both acid and lactone forms (Table 6.3), are the major metabolites generated from atorvastatin in human.

There was no significant difference between 2-hydroxy-atorvastatin acid and lactone half-lives and the half-life for atorvastatin acid (or lactone) in each phase (Tables 6.2 and 6.3) indicating that the elimination of both metabolites and parent drug forms (acid and lactone) are rate-limited by the elimination of atorvastatin acid with or without rifampicin. In contrast, the half-lives for 4-hydroxy-atorvastatin acid (33.3 hours) and

lactone (27.2 hours) were approximately 2-3 fold those of the parent drug during the control phase ($p < 0.01$). In addition, the half-life for 4-hydroxy-atorvastatin acid was approximately 104% greater than the parent drug during the rifampicin phase ($p < 0.01$), indicating that this metabolite elimination is not rate limited by the parent drug.

Fig. 6.4 Mean plasma concentration (\pm SD) of (A) 2-hydroxy-atorvastatin acid; (B) 2-hydroxy-atorvastatin lactone; (C) 4-hydroxy-atorvastatin acid; and (D) 4-hydroxy-atorvastatin lactone in 12 healthy volunteers after a single oral dose of 40 mg atorvastatin with and without intravenous rifampicin. *Inset*: depicts the same data on a semilogarithmic scale.



The lactone/acid AUC ratios of 2-hydroxy-atorvastatin and 4-hydroxy-atorvastatin were decreased 71% ($p < 0.001$) and 62% ($p < 0.01$) by rifampicin, respectively (Fig. 6.5A and B), values very close to the 68% decrease shown for the lactone and acid of the parent drug, reflecting the greater increase in the concentrations of the acid forms caused by rifampicin.

Fig. 6.5 Individual AUC_{0-∞} ratios of (A) 2-hydroxy-atorvastatin lactone to 2-hydroxy-atorvastatin acid and (B) 4-hydroxy-atorvastatin lactone to 4-hydroxy-atorvastatin acid in 12 healthy volunteers after a single oral dose of 40 mg atorvastatin with and without intravenous rifampicin. **, $p < 0.01$; ***, $p < 0.001$ significantly different from control phase.

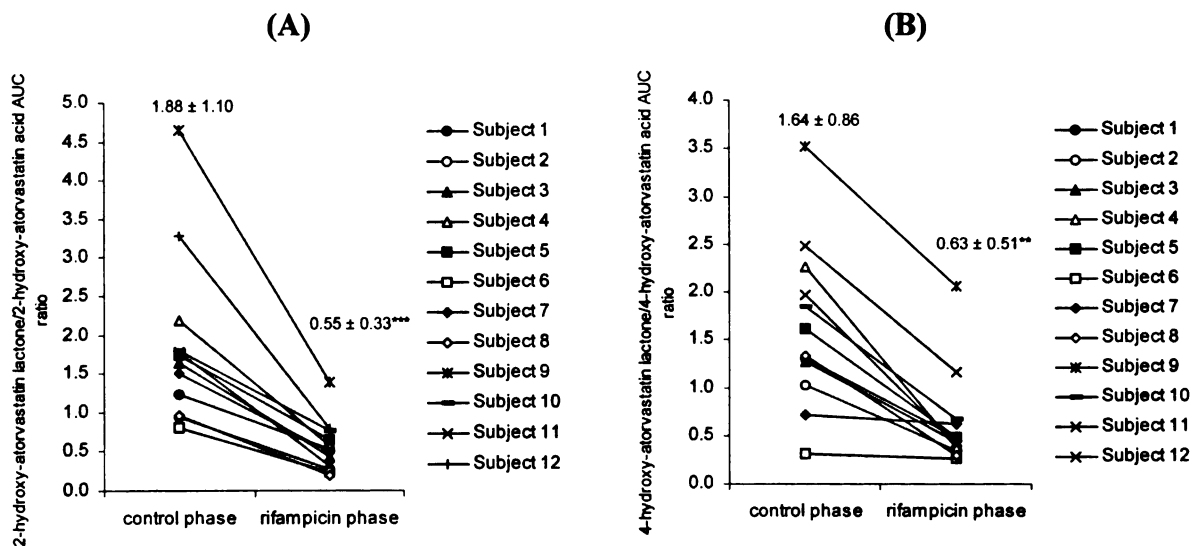


Table 6.3 Pharmacokinetic variables of 2- and 4-hydroxy-atorvastatin acid and lactone in 12 healthy volunteers after a single oral dose of 40 mg atorvastatin with and without intravenous rifampicin.

variable	atorvastatin alone control phase ^a	rifampicin phase ^a	rifampicin phase (% of control)	
			mean and range	95% C.I.
2-hydroxy- atorvastatin acid				
C_{max} (ng/ml)	10.1 ± 5.1	97.1 ± 45.2‡	961 (408- 1950)	694 - 1293
t_{max}^b (hr)	3(0.5 - 4)	3(1.5 - 6)	-	-
$t_{1/2}$ (hr)	14.5 ± 4.7	4.68 ± 2.80‡	32 (19 - 70)	23 - 41
AUC _{0-48 hr} (ng/ml · hr)	83.3 ± 32.9	609 ± 303‡	731 (342 - 1180)	508 - 817
AUC _{0-∞} (ng/ml · hr)	92.0 ± 35.3	615 ± 306‡	669 (309 - 1130)	453 - 738
2-hydroxy- atorvastatin lactone				
C_{max} (ng/ml)	12.8 ± 8.8	31.1 ± 15.2‡	243 (158 - 406)	220 - 331
t_{max}^b (hr)	4(2.5 - 6)	4(2.5 - 6)	-	-
$t_{1/2}$ (hr)	15.9 ± 7.5	5.95 ± 2.50‡	37 (13 - 86)	29 - 56
AUC _{0-48 hr} (ng/ml · hr)	142 ± 65	283 ± 113‡	199 (137 - 382)	168 - 251
AUC _{0-∞} (ng/ml · hr)	151 ± 65	290 ± 122‡	192 (131 - 370)	159 - 236
4-hydroxy- atorvastatin acid				
C_{max} (ng/ml)	0.84 ± 0.35	11.6 ± 6.1‡	1780 (604 - 2930)	1195 - 2365

t_{\max}^b (hr)	6(0.5 – 12)	4(0.5 – 6)	–	–
$t_{1/2}$ (hr)	33.3 ± 12.0	10.7 ± 5.5‡	32 (8 - 67)	23 - 48
AUC _{0-48 hr} (ng/ml · hr)	16.7 ± 7.3	94.3 ± 53.8‡	565 (339 - 1010)	449 - 720
AUC _{0-∞} (ng/ml · hr)	26.3 ± 10.2	99.3 ± 55.6‡	378 (206 - 693)	288 - 477
4-hydroxy- atorvastatin lactone				
C_{\max} (ng/ml)	2.01 ± 1.54	4.03 ± 1.59†	201 (79 - 721)	171 - 464
t_{\max}^b (hr)	3(0.5 – 9)	4(2.5 – 9)	–	–
$t_{1/2}$ (hr)	27.2 ± 12.8	11.1 ± 5.1†	41 (20 - 137)	27 - 66
AUC _{0-48 hr} (ng/ml · hr)	25.3 ± 10.8	45.9 ± 19.3‡	181 (91 - 278)	156 - 235
AUC _{0-∞} (ng/ml · hr)	34.0 ± 13.4	51.6 ± 23.6†	152 (85 - 270)	122 - 191

^a Values were shown in mean ± SD unless otherwise stated.

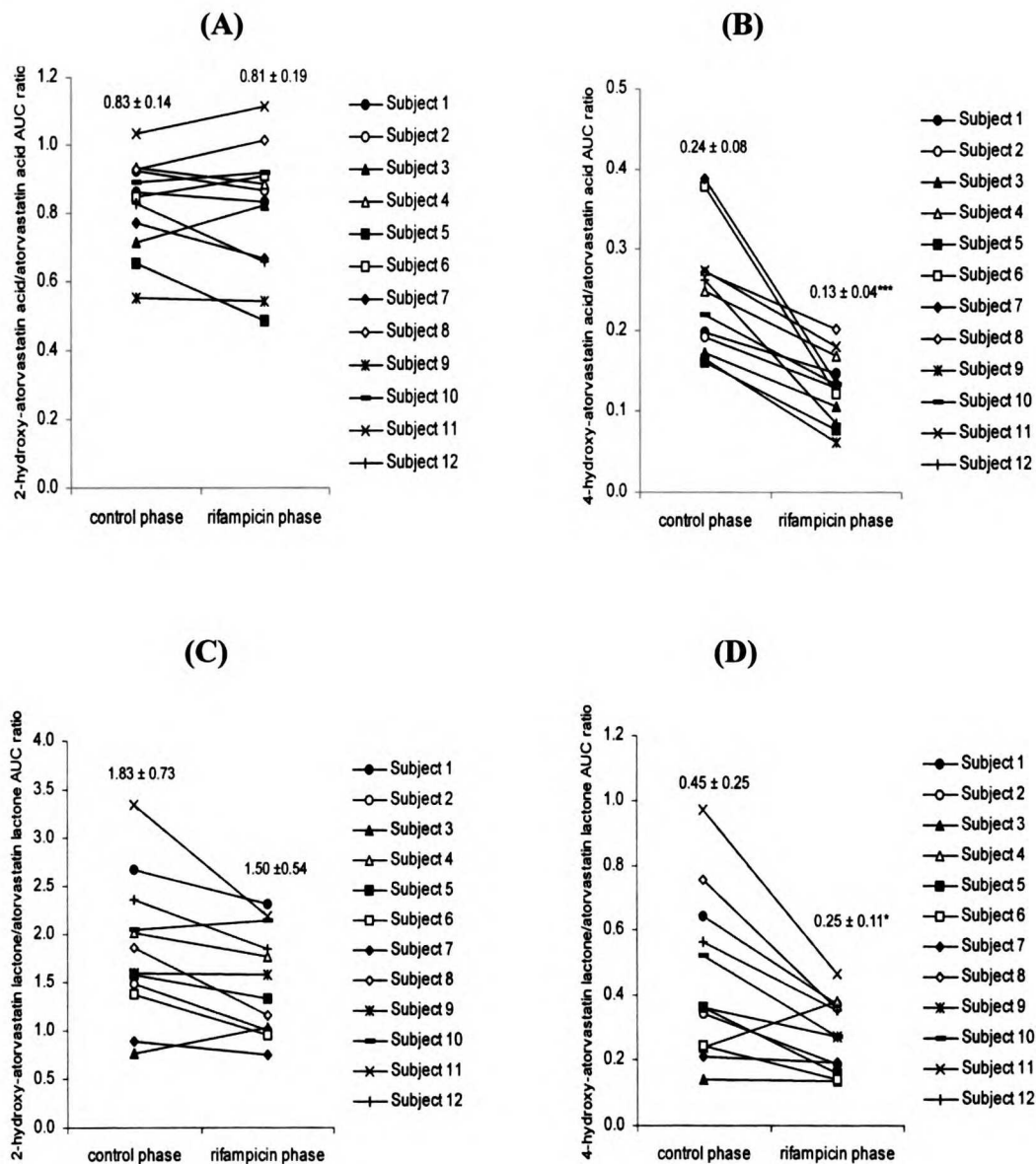
^b t_{\max} data are given as median and range.

†, $p < 0.01$; ‡, $p < 0.001$ significantly different from atorvastatin alone control phase.

6.3.1.3 Effect of rifampicin on the AUC ratios of each hydroxy-atorvastatin to atorvastatin (acid and lactone)

The AUC ratios of the 2-hydroxy metabolite to atorvastatin (in both acid and lactone forms) were statistically unchanged between the control phase and the rifampicin phase (Fig. 6.6A and C). However, significant reductions in the AUC ratios of 4-hydroxy metabolite (acid and lactone) to atorvastatin were observed (46% decrease for acid; $p < 0.001$ and 44% decrease for lactone; $p < 0.05$) (Fig. 6.6B and D).

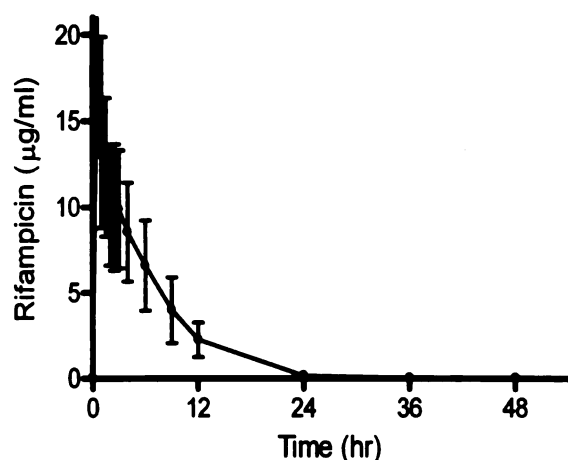
Fig. 6.6 Individual $AUC_{0-\infty}$ ratios of (A) 2-hydroxy-atorvastatin acid to atorvastatin acid; (B) 4-hydroxy-atorvastatin acid to atorvastatin acid; (C) 2-hydroxy-atorvastatin lactone to atorvastatin lactone; and (D) 4-hydroxy-atorvastatin lactone to atorvastatin lactone in 12 healthy volunteers after a single oral dose of 40 mg atorvastatin with and without intravenous rifampicin. *, $p < 0.05$; ***, $p < 0.001$ significantly different from control phase.



6.3.1.4 Rifampicin plasma concentrations

Rifampicin plasma levels were measurable up to 48 hours (Fig. 6.7). C_{max} for rifampicin was 17.2 $\mu\text{g/ml}$ half an hour after atorvastatin administration and declined steadily to 21 ng/ml at 48 hour, the last sampling time point.

Fig. 6.7 Mean plasma concentration (\pm SD) of a single intravenous infusion of rifampicin (600 mg) given half an hour before a single oral dose of atorvastatin in 12 healthy volunteers.



6.3.1.5 Comparisons of allelic and genotypic frequencies in study subjects

Previous studies have focused on two nonsynonymous variants of *SLCO1B1*, Asn130Asp (A388G) and Val174Ala (T521C), because they are frequently observed in all ethnic groups (Tirona et al., 2001; Nishizato et al., 2003). Nishizato et al. (2003) demonstrated that Val174Ala was tightly linked with Asn130Asp and formed a haplotype referred to as *15.

In view of the haplotype assignment previously described by Nishizato et al. (2003), we classified the subjects who participated in the present clinical study into 4 genotypic groups (Table 6.4), *OATP1B1**1a/*1a, *1a/*1b, *1a/*15 and *1b/*15 based on the genotyping results, where *1a allele represents the reference allele and has no polymorphisms at any SNP positions (Tirona et al., 2001), *1b for Asp130 and *15 for Asp130Ala174. We were not able to determine the genotype of subject number 10 due to failed PCR reaction while detecting the T521C variant.

The allelic frequencies of *OATP1B1**1a, *OATP1B1**1b and *OATP1B1**15 were 54.4%, 27.3% and 18.2% respectively, in 11 subjects (Table 6.4). The genotypic frequencies of *1a/*1a and *1a/*1b were 27.3% and 36.4%, respectively. Both *1a/*15 and *1b/*15 genotype groups had a frequency of 18.2%. None of our subjects were homozygous for *1b and *15 alleles.

Table 6.4 Haplotypes of *OATP1B1* gene in 11 subjects.

<i>Allele</i>	<i>Frequency (%) (n = 22)</i>	<i>Genotype</i>	<i>Frequency (n = 11)</i>	<i>Ethnicity</i>
OATP1B1*1a	54.5	*1a/*1a	27.3	3C
OATP1B1*1b	27.3	*1a/*1b	36.4	2A, 1AA, 1PI
OATP1B1*15	18.2	*1a/*15	18.2	1AA, 1C
		*1b/*15	18.2	2A

A: Asian; AA: African American; C: Caucasian; PI: Pacific Islander

6.3.1.6 Effects of OATP1B1 polymorphisms on the pharmacokinetics of atorvastatin and its metabolites with and without rifampicin treatment

Previously, Tirona et al. (2001) had demonstrated using an *in vitro* cellular uptake assay that no alteration in OATP1B1-mediated transport was associated with Asn130Asp, whereas Val174Ala led to a significant reduction in transport of the prototypical OATP1B1 substrate, estrone sulfate. Kameyama et al. (2005) also demonstrated that the uptakes of atorvastatin and other statins were significantly reduced in HEK293 cells transiently expressing OATP1B1 allelic variants *5 (Val174Ala) and *15 (Asn130Asp and Val174Ala) but not *1b (Asn130Asp). On the basis of this finding, we compared the AUC values between 2 groups: *OATP1B1**1a/*1a and *1a/*15.

As shown in Table 6.5 and Fig 6.8A, C, E, G, I and K, the AUC values for atorvastatin acid and all its metabolites (both acid and lactone forms) were higher in *1a/*15 genotypic group compared with the *1a/*1a wild-type group during the atorvastatin alone control phase. There was a 96%, 102% and 24% increase of AUC for atorvastatin acid, 2-hydroxy-atorvastatin acid and 4-hydroxy-atorvastatin acid, respectively in the *1a/*15 group. The percentage increase in AUC values for the corresponding lactone forms increased by 31% ($p < 0.05$), 43% and 48%, respectively.

A different trend was observed for the AUC changes during the rifampicin treatment phase, in which carriers for *1a/*15 either have a similar or lower AUC values relative to the wild-type group (Table 6.5; Fig 6.8B, D, F, H, J and L). Atorvastatin lactone, 2-hydroxy-atorvastatin lactone and 4-hydroxy-atorvastatin lactone all showed a decrease in AUC values for *15 carriers relative to wild-type, whereas atorvastatin acid,

2-hydroxy-atorvastatin acid and 4-hydroxy-atorvastatin acid only showed a minimal increases of 2%, 3% and 21%, respectively.

Table 6.5 AUC_{0-∞} values (ng/ml · hr) of atorvastatin and its metabolites after a single dose of atorvastatin with and without intravenous rifampicin in two OATP1B1 genotypic groups: *OATP1B1*1a/*1a* and **1a/*15*.

Variable	*1a/*1a (n = 3) ^a	*1a/*15 (n = 2) ^a	% increase of *1a/*15 from *1a/*1a
Atorvastatin acid (control phase)	74.4 ± 36.4	146 ± 37	96
Atorvastatin acid (rifampicin phase)	597 ± 130	607 ± 82	2
Atorvastatin lactone (control phase)	52.1 ± 5.5	68.4 ± 0.1*	31
Atorvastatin lactone (rifampicin phase)	162 ± 34	129 ± 36	-20
2-hydroxy-atorvastatin acid (control phase)	63.9 ± 31.2	129 ± 27	102
2-hydroxy-atorvastatin acid (rifampicin phase)	506 ± 182	517 ± 84	3
2-hydroxy-atorvastatin lactone (control phase)	99.3 ± 20.4	142 ± 57	43
2-hydroxy-atorvastatin lactone (rifampicin phase)	270 ± 138	197 ± 60	-27
4-hydroxy-atorvastatin acid (control phase)	22.8 ± 17.3	28.3 ± 7.8	24
4-hydroxy-atorvastatin acid (rifampicin phase)	69.2 ± 26.2	83.8 ± 4.2	21
4-hydroxy-atorvastatin lactone (control phase)	22.7 ± 8.2	33.7 ± 9.2	48
4-hydroxy-atorvastatin lactone (rifampicin phase)	40.7 ± 16.3	33.7 ± 6.6	-17

^a Values were shown in mean ± SD.

*, *p* < 0.05 significantly different from atorvastatin alone control phase.

Fig. 6.8 Mean plasma concentrations (\pm SD) of atorvastatin and metabolites (both acid and lactone forms) in 11 healthy volunteers after a single oral dose of 40 mg atorvastatin with and without intravenous rifampicin (B, D, F, H, J and L depict levels with rifampicin treatment) in two OATP1B1 genotypic groups: *OATP1B1**1a/*1a (n = 3) and *1a/*15 (n = 2).

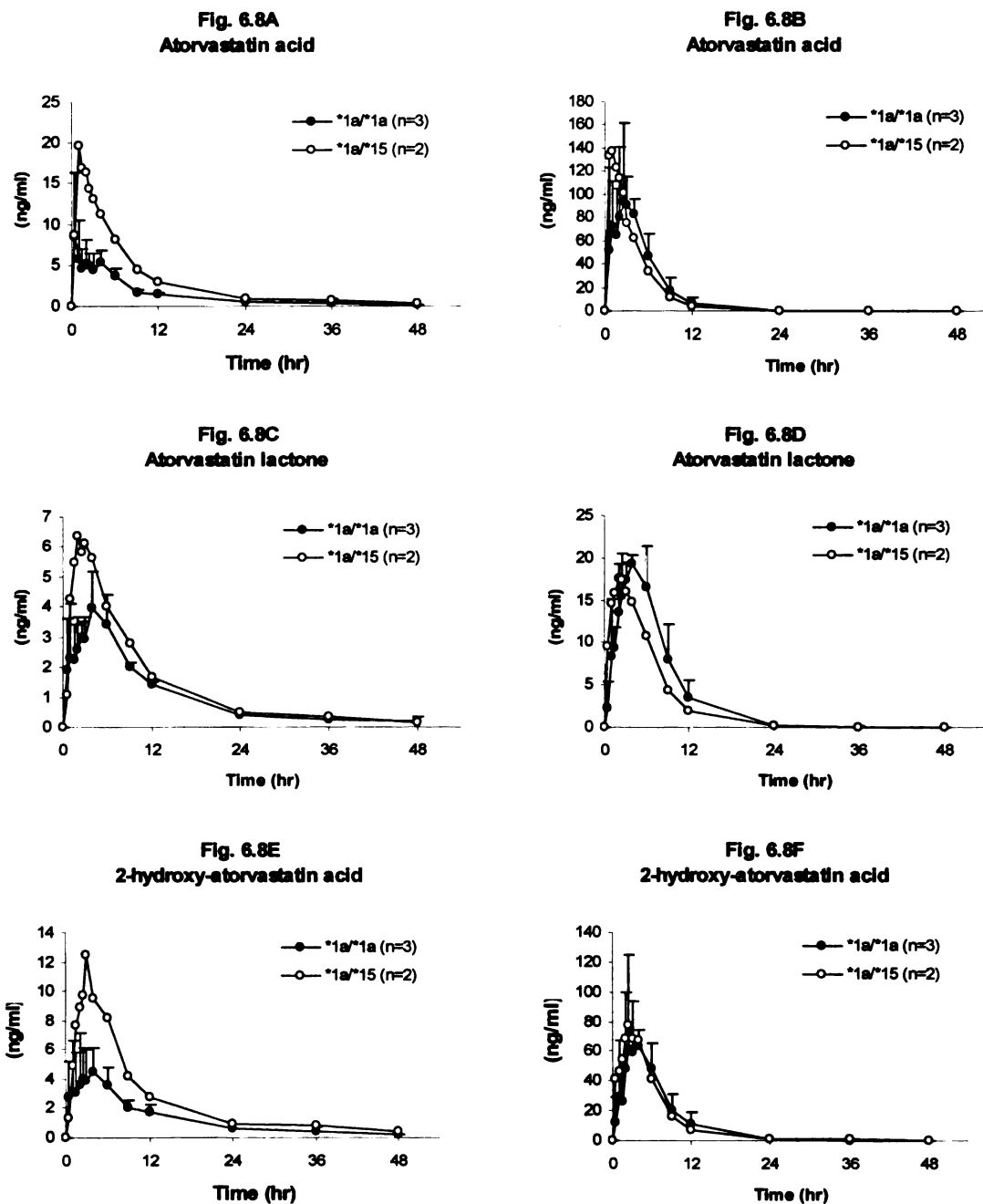


Fig. 6.8G
2-hydroxy-atorvastatin lactone

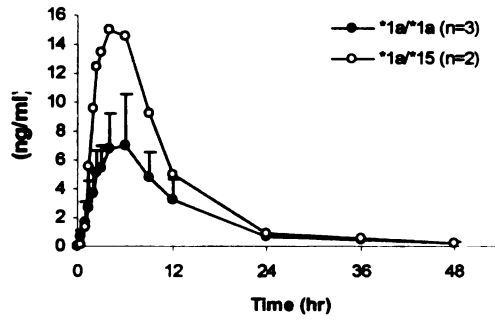


Fig. 6.8H
2-hydroxy-atorvastatin lactone

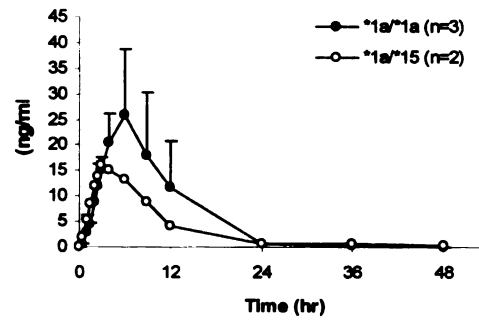


Fig. 6.8I
4-hydroxy-atorvastatin acid

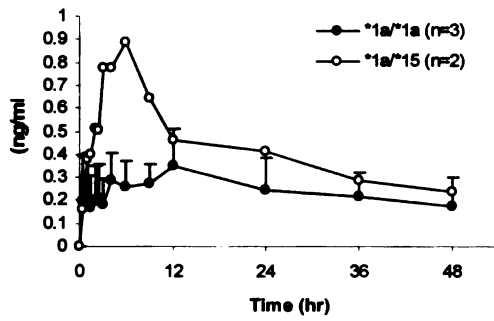


Fig. 6.8J
4-hydroxy-atorvastatin acid

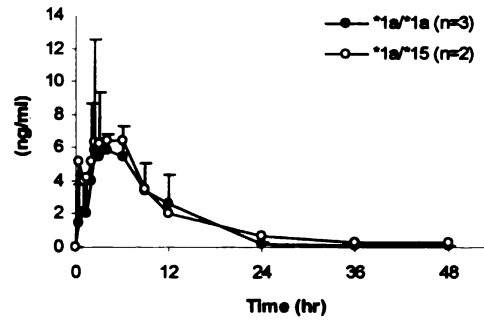


Fig. 6.8K
4-hydroxy-atorvastatin lactone

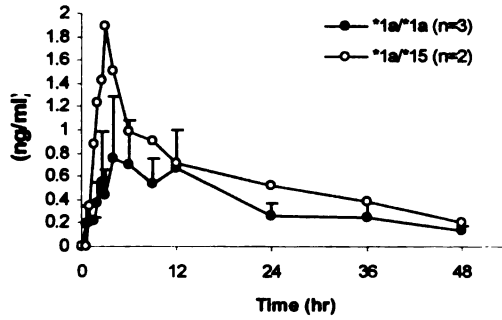
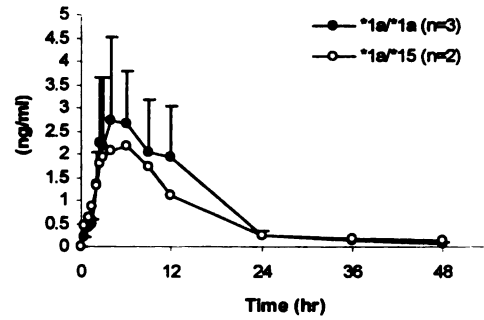


Fig. 6.8L
4-hydroxy-atorvastatin lactone



6.3.2 In vitro study

6.3.2.1 In vitro uptake kinetics of atorvastatin acid and rifampicin inhibitory effect on the uptake of atorvastatin in HEK293 cells transiently transfected with OATP1B1

The uptakes of atorvastatin acid, and metabolites 2- and 4-hydroxy-atorvastatin acid, were significantly higher in OATP1B1-transfected cells relative to that in vector-transfected cells (Fig. 6.9). Using the OATP1B1-transfected cell system, we demonstrated concentration-dependent uptake of atorvastatin acid (Fig. 6.10). Both a saturable (OATP1B1-mediated) and a linear nonsaturable (diffusion-mediated) component were observed.

Based on Eqn. (6.1), K_m , V_{max} and P_{dif} values for the uptake of atorvastatin in OATP1B1-transfected cells were $18.9 \pm 4.6 \mu\text{M}$ ($10.6 \pm 2.6 \mu\text{g/ml}$), 105 ± 15 pmole/min/mg protein ($58.7 \pm 8.4 \text{ ng/min/mg protein}$) and $0.40 \pm 0.08 \mu\text{l/min/mg protein}$, respectively. The saturable component estimated by V_{max}/K_m accounts for about 93% of the total uptake within the linear range of the total uptake curve. OATP1B1-mediated uptake of atorvastatin was inhibited by rifampicin in a concentration-dependent manner (Fig. 6.11). Using Eqn. (6.2), the estimated IC_{50} and K_i values for rifampicin inhibition on uptake of atorvastatin were $3.25 \pm 0.52 \mu\text{M}$ ($1.82 \pm 0.29 \mu\text{g/ml}$) and $3.08 \pm 0.49 \mu\text{M}$ ($1.72 \pm 0.27 \mu\text{g/ml}$), respectively.

Fig. 6.9 Uptake of atorvastatin (acid) and hydroxy-atorvastatin acids at 1 μ M into HEK293 cells with transient expression of OATP1B1 or vector control. Data are shown as the mean \pm SD. (n = 4). ***, $p < 0.001$ versus control.

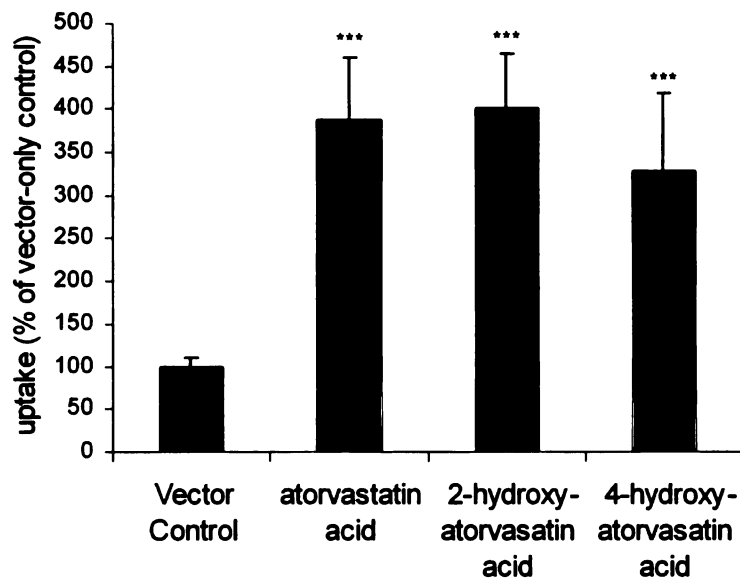


Fig. 6.10 Concentration-dependent uptake of atorvastatin (acid) into OATP1B1 transiently transfected HEK293 cells. Total uptake is the sum of the saturable OATP1B1-mediated uptake and the nonsaturable diffusion-mediated uptake. Each value represents mean \pm SD (n = 4).

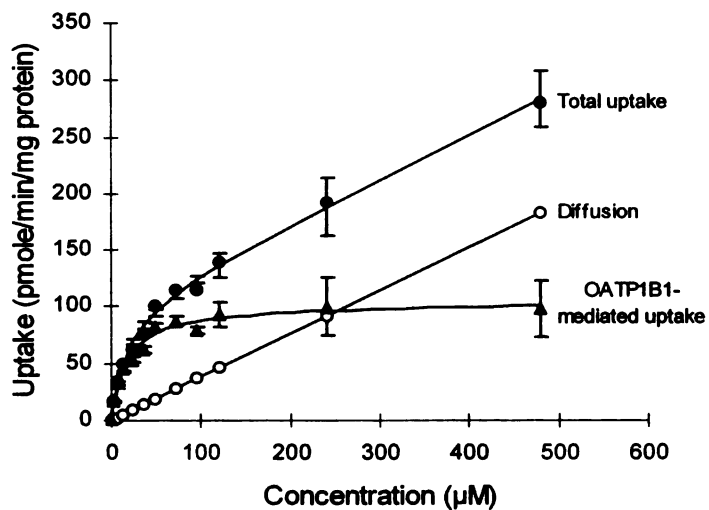
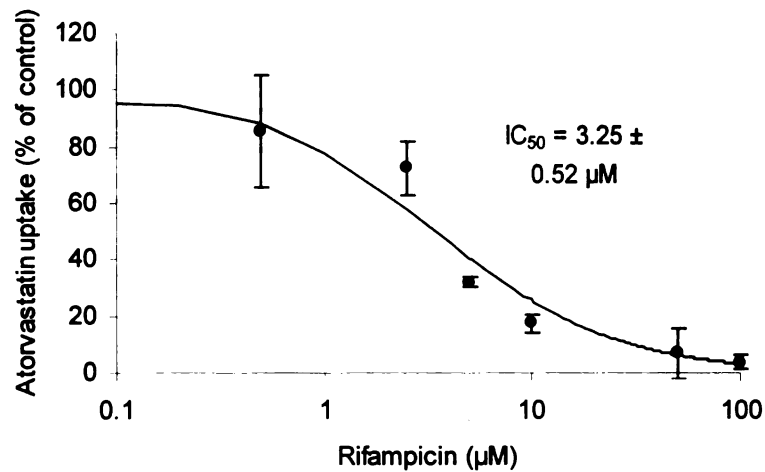


Fig. 6.11 Inhibition of the uptake of atorvastatin (acid) (1 μM) by rifampicin into OATP1B1 transiently transfected HEK293 cells. Each value represents mean \pm SD (n = 4). Net OATP1B1-mediated uptake was calculated by subtracting values obtained with vector-only HEK293 cells from those obtained with transfected HEK293 cells.



6.4 Discussion

Our present results demonstrate that rifampicin, given as a single intravenous infusion, significantly and markedly increased the plasma AUC and C_{\max} values of atorvastatin and its hydroxy metabolites, most probably due to inhibition of OATP1B1 by rifampicin (Figs. 6.2 & 6.4).

Atorvastatin and its two major active metabolites, 2-hydroxy-atorvastatin acid and 4-hydroxy-atorvastatin acid, formed after intestinal and hepatic metabolism, are mainly eliminated by biliary excretion (Lennernas, 2003). The substantial increase in AUC values observed for atorvastatin and its metabolites in the presence of rifampicin suggest a significant reduction in their hepatobiliary elimination mediated by hepatic transporters controlling the movement of drugs from blood to bile.

In the present clinical study, rifampicin, which is a potent OATP inhibitor (Vavricka et al., 2002; Tirona et al., 2003), was chosen to block the *in vivo* OATP1B1-mediated hepatic uptake of atorvastatin. We had hoped that the potential confounding interactions in the intestine either at the enzyme or transporter levels could be minimized when rifampicin was given intravenously. We are unable to determine if this is true, since in the rat our recently published atorvastatin pharmacokinetic study showed that intravenous rifampicin administration caused obvious changes in gut bioavailability (Chapter 5; Lau et al., 2006b).

Interestingly, as seen in Table 6.2, the 54% decrease in atorvastatin half-life ($t_{1/2}$) in the presence of rifampicin was markedly less than the 86% decrease in CL/F indicating that effects of rifampicin on volume of distribution at steady state (V_{ss}/F) was even more substantial (97% decrease). These results are very different than what we observed in rats

(Chapter 5; Lau et al., 2006b) where one may calculate that CL/F decreased 63% from 37.3 L/hr/kg control to 10.0 L/hr/kg with intravenous rifampicin and V_{ss}/F also decreased 63% from 196 L/kg to 53.6 L/kg. Thus, in rats the change in CL and V_{ss} was minimal (28% and 26% decreases respectively) and the effect of rifampicin was primarily an increase in bioavailability (5.2% control vs. 14% with rifampicin) (Chapter 5; Lau et al., 2006b). In contrast, in this human study CL/F and V_{ss}/F do not decrease in parallel suggesting that rifampicin decreases atorvastatin's uptake into tissues besides hepatocytes. It is likely that other tissues also have expression of transporters that are capable of mediating the uptake of atorvastatin and can be inhibited by rifampicin.

Another major difference between our rat and human studies is the high levels of the active 2-hydroxy metabolites observed in humans. Following oral dosing in rats, total active metabolites to parent drug were 0.2 both with and without rifampicin (lactone measurements could not be accurately determined in the rat studies due to analytical sensitivity). In humans, 2-hydroxy to parent ratios following oral dosing were also unchanged with rifampicin, but the ratios were 0.83 (Fig. 6.6A), four-fold higher than in rats. In contrast, the 4-hydroxy to parent ratios in humans were 0.24, comparable to rats, but the ratios decreased by 46% with rifampicin (Fig. 6.6B). This change of ratio for the 4-hydroxy metabolite reflects the fact that elimination of this metabolite is slower than parent or the 2-hydroxy metabolite, the latter being rate-limited by parent drug elimination. That is, both the parent and the 2-hydroxy metabolite are rate-limited by the parent and change in parent elimination by rifampicin affects both equally. While for the 4-hydroxy metabolite, apparently elimination of the metabolite is increased more by rifampicin than for the parent drug.

To explain the mechanism underlying the atorvastatin-rifampicin interaction mentioned above, we also conducted *in vitro* cellular studies in parallel. Atorvastatin acid and both hydroxy metabolites were subject to OATP1B1 mediated uptake using the OATP1B1-expressing HEK293 cells (Fig. 6.9). Atorvastatin acid is a fairly good substrate of OATP1B1 with an affinity constant (K_m) of $10.6 \pm 2.6 \mu\text{g/ml}$ (Fig. 6.10). We previously demonstrated in the isolated perfused rat liver system (Chapter 3; Lau et al., 2006a), that increasing concentrations of rifampicin effectively decreased the hepatic accumulation of atorvastatin acid via inhibition of rat Oatp1a4 and Oatp1b2. Here, rifampicin was able to inhibit the OATP1B1-mediated uptake of atorvastatin acid in a dose-dependent manner with an inhibition constant (K_i) of $1.72 \pm 0.27 \mu\text{g/ml}$ (Fig. 6.11).

Inhibition of hepatic efflux transporters belonging to the ATP-binding cassette family, such as P-gp and MRP2 located at the canalicular border of hepatocytes (Keppler and Arias, 1997) might also lead to increased AUCs for atorvastatin, since atorvastatin is a dual substrate for both of these active transporters (Chapter 3; Wu et al., 2000; Hochman et al., 2004; Chen et al., 2005; Lau et al., 2006a). However, considering the more distant location of efflux transporters compared with that of OATP1B1 relative to the sinusoidal blood, it is unlikely that an inhibitory effect of rifampicin on P-gp and MRP2 would lead to a greater AUC increase of atorvastatin than that on OATP1B1. We have previously demonstrated that rifampicin does not exert an inhibitory effect on P-gp mediated efflux of atorvastatin, and only moderately inhibits MRP2 at concentrations of $50 \mu\text{M}$ ($28 \mu\text{g/ml}$) or higher (Chapter 3; Lau et al., 2006a), concentrations higher than those measured here (Fig. 6.7).

The C_{\max} of atorvastatin acid obtained from the present clinical study was $17.8 \pm$

8.4 ng/ml during the control phase and 184 ± 72 ng/ml during the rifampicin phase; both values were well below the K_m value of OATP1B1-mediated uptake of atorvastatin determined *in vitro* (Fig. 6.10), indicating that there was no saturation of atorvastatin's hepatic uptake at all plasma concentrations. Given that atorvastatin is 98% bound to plasma protein (Lennernas, 2003), the free systemic concentration of atorvastatin at C_{max} would be as low as 0.36 ng/ml, even though the portal vein concentrations should be much higher than the systemic levels after oral administration. Rifampicin is 80% protein bound (Acocella, 1978) and the free concentration at C_{max} was 3.5 $\mu\text{g/ml}$ and dropped steadily to 2 ng/ml at 48 hours. These concentrations were far higher than those of atorvastatin and its metabolites at all time points. Since rifampicin is also a substrate of OATP1B1 with a K_m value of 1.2 $\mu\text{g/ml}$ (Tirona et al., 2003), it should effectively block the hepatic uptake of atorvastatin mediated by OATP1B1 in a competitive manner *in vivo*.

In vitro metabolic studies reported by Jacobsen et al. (2000) suggest the importance of atorvastatin metabolism by CYP3A, consistent with the increased plasma exposure of atorvastatin in humans following co-administration with erythromycin (Siedlik et al., 1999) and itraconazole (Kantola et al., 1998), both known inhibitors of this P450 subclass. In the present study, we evaluated the metabolic-mediated interaction between atorvastatin and rifampicin. The observed significant increase in the AUC values of the hydroxy metabolites in the presence of rifampicin (Fig. 6.4A and C; Table 6.3) ruled out the possibility of extensive inhibition of CYP3A-mediated metabolism by rifampicin, although moderate inhibition of enzymes was still possible. A recent study by Kajosaari et al. (2005) demonstrated that rifampicin exhibited enzymatic inhibitory effects towards the antidiabetic drug, repaglinide, another dual CYP3A and OATP1B1

substrate (Kajosaari et al., 2005; Niemi et al., 2005a).

In humans, atorvastatin is orally administered in the open hydroxy acid ring form but it can also biotransform to its inactive lactone form either via a coenzyme A-dependent and/or an acyl glucuronide intermediate pathway (Jacobsen et al., 2000; Prueksaritanont et al., 2002; Lennernas, 2003). Jacobsen et al. (2000) had demonstrated that atorvastatin lactone is more susceptible to metabolism by CYP3A compared to atorvastatin acid and had proposed that metabolism of the lactone is the relevant pathway for atorvastatin's metabolic-mediated drug interactions *in vivo*. In the present study, we monitored the pharmacokinetic changes of atorvastatin lactone and the lactone metabolites as well, in order to evaluate the effect of rifampicin on the lactonization of atorvastatin acid, as well as the hepatic uptake and metabolism of atorvastatin lactone. A recent study by Chen et al. (2005) comparing the differential substrate and inhibitor activities of the acid and lactone forms of various statins towards efflux mediated by P-gp and MRP2, and uptake mediated by OATP transporters demonstrate that the acid form of statins, including atorvastatin, exhibit a stronger inhibitory effect towards OATP1B1 compared to the more lipophilic lactone form. These findings suggest the lactone forms have weaker affinities for OATP compared with the acid forms, which might explain the difference in the extent of AUC increase for the acid and lactone forms of atorvastatin observed in our study: There was a 2-fold increase in the AUC values of atorvastatin lactone with rifampicin co-administration (Table 6.2), indicating that atorvastatin lactone might also be subject to uptake mediated by OATP1B1. However, compared with the 7-fold increase in the corresponding values of atorvastatin acid, the increase in lactone AUC values was much smaller. Although the lactone to acid AUC ratio was markedly

decreased for atorvastatin during the rifampicin treatment phase (Fig. 6.3), inhibition of lactonization was unlikely as the concentrations for the lactone forms of 2- and 4-hydroxy-atorvastatin were also increased by rifampicin (Fig. 6.4B and D; Table 6.3). Extensive inhibition of atorvastatin lactone metabolism was not probable either since the ratio of the total metabolites (summation of 2-hydroxy atorvastatin lactone and 4-hydroxy atorvastatin lactone) to parent drug in the lactone form remained statistically unaltered. We also investigated whether rifampicin might increase the extent of lactone hydrolysis to parent acid form by spiking atorvastatin lactone with and without rifampicin to human plasma *ex vivo* over a period of time. Our results indicate that the amount of atorvastatin acid detected over a 24-hour period remained unchanged with and without rifampicin (data not shown).

Conventionally, rifampicin is more well known for inducing drug metabolizing enzymes such as CYP3A4 and CYP2C9 (Schuetz et al., 1996; Niemi et al., 2003). Rifampicin also induces P-gp and MRP2 via the PXR-dependent mechanism (Schuetz et al., 1996; Greiner et al., 1999; Fromm et al., 2000). Many drugs, including the statins, which are co-substrates for cytochrome P450 enzymes and P-gp, exhibit clinically relevant drug-drug interactions due to the co-induction of *CYP3A4* and *MDR1* genes by rifampicin. For instance, a recent clinical study conducted by Backman et al. (2005) showed that rifampicin given 600 mg daily for 5 consecutive days significantly reduced the $AUC_{0-\infty}$ of atorvastatin by 80% and that of the active metabolites, 2- and 4-hydroxy-atorvastatin acid, by 43% and 81%, respectively. The above pharmacokinetic changes in the presence of rifampicin could be explained by a rifampicin co-induction effect on CYP3A4, which reduced the AUC of parent drug, as well as on P-gp and MRP2 in both

gut and liver, which enhanced the elimination of parent drug and metabolites. Notice that these changes in pharmacokinetic variables were exactly opposite to those observed in our current study. We believe that when given as a single intravenous infusion, rifampicin did not induce transporters and/or enzymes, but rather significantly inhibited OATP1B1, potentially leading to a clinically relevant drug-drug interaction at the hepatic uptake level. We chose rifampicin as a model inhibitor that could be administered intravenously to demonstrate the importance of inhibition of hepatic uptake transporters on drug pharmacokinetics.

The target for atorvastatin and its active metabolites is HMG-CoA reductase, the rate-limiting enzyme in the liver involved in cholesterol synthesis (Nawrocki et al., 1995). Inhibition of the hepatic uptake of atorvastatin and its active metabolites would lead to a reduction in their therapeutic efficacy, partly due to the decreased hepatic uptake of parent drug and metabolites formed pre-hepatically by CYP3A expressed in the gut wall (Christians et al., 1998), and partly due to the decreased extent of hepatic metabolism resulting from lower amounts of atorvastatin entering the liver for exposure to hepatic CYP3A. Reduction in hepatic uptake of atorvastatin might also increase the risk of rhabdomyolysis as excessive systemic exposure to atorvastatin might occur when atorvastatin cannot be efficiently eliminated via the hepatobiliary pathway. Certain common single nucleotide polymorphisms (SNPs) in the *SLOC1B1* gene encoding for OATP1B1 that are associated with a significant reduction in transporter activity *in vitro* (Tirona et al., 2001; Iwai et al., 2004; Kameyama et al., 2005) and lead to increased plasma levels of OATP1B1 substrates, including pravastatin (Nishizato et al., 2003; Niemi et al., 2004), repaglinide (Niemi et al., 2005a) and fexofenadine (Niemi et al.,

2005b) have been identified. To explore the importance of OATP1B1 towards the pharmacokinetic-pharmacodynamic relationship of atorvastatin, it will be worthwhile to conduct studies that aim to correlate certain OATP1B1 polymorphisms (equivalent to long-term OATP1B1 functional change) to the modulation of lipid parameters after atorvastatin administration to patient populations.

Our genotyping results in relation to the pharmacokinetics study revealed that there are functional differences between subjects with the *OATP1B1**1a reference allele and the *15 allele, which contains the nonsynonymous variant Val174Ala. The presence of *OATP1B1**15 greatly increased the plasma levels of atorvastatin acid and all its metabolites with AUC value increases ranging from 24 -102% (Table 6.5; Fig 6.8A, C, E, G, I and K). These results further confirm the importance of OATP1B1 in mediating the biliary elimination of atorvastatin metabolites, both acid and lactone forms. We also observed that the effects of genotypic difference for the *1a/*1a-*1a/*15 comparison decreased under conditions of OATP1B1 inhibition by rifampicin, given as an intravenous 30-min infusion (Table 6.5; Fig 6.8B, D, F, H, J and L), due to the compromising effect of *15 genotypic pattern on rifampicin inhibitory effect on OATP1B1-mediated uptake of atorvastatin and its metabolites. In this study the 12 healthy volunteers were not selected for a specific genotype for OATP1B1. For a better understanding of the potential effects of genetic variation, a statistically significant number of subjects should be included in each genotype group. This will remain as a future study.

In conclusion, our single-dose study of the atorvastatin-rifampicin interaction in healthy volunteers demonstrates that an intravenous infusion of rifampicin could

significantly increase the plasma levels of both atorvastatin and its metabolites most likely via inhibition of hepatic uptake transport mediated by OATP1B1. The results from this study imply that drugs that are substrates and/or inhibitors of a liver uptake transporter should be co-administered with caution together with another known substrate and/or inhibitor of transporters to prevent excess systemic exposure. Equal attention should be given to drugs that interact with hepatic uptake transporters as to drugs that interact with metabolizing enzymes.

Chapter 7

CONCLUSION AND PERSPECTIVES

7.1 Overview

Throughout the course of this dissertation, the synergistic role of metabolizing enzymes and hepatic transporters (both uptake and efflux) in modulating drug disposition and metabolism has been explored. Literature reveals that many CYP3A substrates are also subject to transport mediated by organic anion transporting polypeptide (OATP), P-glycoprotein (P-gp) and multidrug resistance associated protein 2 (MRP2) (Table 1.2). We have used multiple experimental tools, including *in vitro* cellular assays, *ex situ* single-organ perfusion, as well as *in vivo* studies in both rat and human, to investigate how digoxin (Dg3) and atorvastatin (ATV) metabolism can be altered by changes that occur only in hepatic transporters, either uptake or efflux. Specifically, we have used relatively selective transporter inhibitors to explore how inhibition of OATP/Oatp (human/rodent) and MRP2 by rifampicin (RIF), P-gp by quinidine and GG918, can modify the distribution of drug into the eliminating organ, and hence the extent of metabolism.

Results presented in this thesis have provided strong evidence demonstrating how hepatic transporters can modulate drug disposition by altering the drug exposure to CYP3A without apparently affecting enzymatic activity.

7.2 Cellular studies

We have shown through a series of studies in cells, as illustrated in Chapter 3, the influence of OATP, P-gp and MRP2 on the disposition of ATV in various cell lines. ATV is recognized by rat Oatp1a4 and Oatp1b2 in cells overexpressing various Oatp transporters (Lau et al., 2006a). Bidirectional transport studies also indicate that ATV is a dual substrate of both P-gp and MRP2. Upon co-administration of RIF, a competitive inhibitor of both Oatp and MRP2, the Oatp-mediated uptake and MRP2-mediated efflux was inhibited, though RIF shows a much higher affinity for blocking Oatps than MRP2, as indicated by the high concentrations needed to inhibit MRP2 in cellular assays utilizing MRP2-overexpressing MII-cMOAT cells (Lau et al., 2006a).

We also utilized the CYP3A4-transfected Caco-2 cellular system to investigate the role of P-gp in affecting CYP3A4-mediated metabolism (Chapter 4). The application of this system led us to recognize the potential for translating basolateral to apical transport experiments as a model for studying the interplay of P-gp and CYP3A4 in affecting ATV metabolism in the liver. Calculation of the extent of metabolism was carried out using the extraction ratio (ER) equation proposed by Cummins et al. (2002a), which defines the fraction of drug that is metabolized relative to the amount of drug coming in contact with the CYP3A4 enzyme. As expected, incubation with cyclosporine (CsA) resulted in decreased ER for ATV from either transport direction, as CsA is a known potent CYP3A4 blocker. In the presence of GG918, a potent inhibitor of P-gp but not CYP3A4, the ER was significantly increased by 140% following a basolateral dose, revealing the role of P-gp in limiting metabolism by facilitating efflux out of the cells.

7.3 Ex situ studies

The specific objectives of the *ex situ* isolated perfused rat liver (IPRL) study, detailed in Chapters 2 and 3, was to illustrate that blockage of transporters, either basolateral uptake or apical efflux, can alter the extent of metabolism by changing the access of drug to rat CYP3A. IPRL is a useful physiological-based model for examining the hepatobiliary disposition of drugs at the organ level. The cardiotonic drug digoxin, Dg3, was chosen as the first compound to study the transporter-enzyme interplay in the liver because of the existence of *in vitro* data for its substrate specificity towards rat Cyp3a (Salphati and Benet, 1999) as well as Oatp1a4 (Shitara et al., 2002) and P-gp (de Lannoy and Silverman, 1992). The changes in the pharmacokinetic parameters for digoxin with and without Oatp1a4 and P-gp inhibitors were summarized in Table 7.1. In the presence of quinidine, the AUC for digoxin was reduced, that is, when the efflux transporter is inhibited, more drugs is available to be metabolized by the enzyme and AUC decreased due to increased total hepatic clearance. These results are in agreement with that obtained from tacrolimus (Table 7.1) (Wu and Benet, 2003), in which concomitant GG918 reduced the AUC of tacrolimus in the IPRL system. In the presence of RIF, on the other hand, the AUC of Dg3 was increased with reduced metabolism due to decreased amount of Dg3 in the liver when its hepatic uptake was blocked by RIF, hence leading to reduced exposure to enzyme.

We then studied ATV using this system because ATV's metabolism by CYP3A in the liver leads to two primary active hydroxy metabolites. The sequential transport of ATV governed by hepatic uptake (Oatp) and efflux (P-gp and Mrp2) transporters as validated by *in vitro* studies is important for ATV disposition and metabolism. The

Table 7.1 Pharmacokinetics of tacrolimus, digoxin and atorvastatin in perfused rat liver preparation with and without transporter inhibitors.

	<i>Inhibitors</i>	<i>Biliary Clearance</i>	<i>Metabolism</i>	<i>AUC</i>	<i>Total hepatic clearance</i>	<i>Reference</i>
Tacrolimus	+ GG918 (P-gp inhibitor)	Not measured	Not measured	↓	↑	Wu and Benet (2003)
Digoxin (Dg3)	+ Rifampicin (Oatp1a4 inhibitor)	Not measured	↓	↑	↓	Chapter 2
	+ Quinidine (P-gp inhibitor)	Not measured	↑	↓	↑	Lau et al. (2004)
Atorvastatin (ATV)	+ Rifampicin (Oatp1a4 & Oatp1b2 inhibitor)	↓	↓	↑	↓	Chapter 3 Lau et al. (2006a)

pharmacokinetic profile of ATV was examined alone and in the presence of RIF (5, 10 and 50 μ M). We found a concentration-dependent increase in the AUC of ATV, together with decreased levels of both ATV and metabolites in the liver tissues, indicating that the extent of metabolism was decreased when the upstream hepatic uptake was inhibited (Chapter 3; Lau et al., 2006a). However, the bile to liver amount ratio for ATV was significantly decreased when 50 μ M of RIF was coadministered, indicating that efflux by Mrp2 was inhibited at this concentration of RIF. This is not surprising, as Oatp and Mrp2 often share similar substrates and inhibitors. One of the major findings from our ATV IPRL study is the fact that the active hydroxy metabolites of ATV were also subject to

Oatp-mediated uptake. These results have revealed that the formed active metabolites are also influenced by transport processes.

7.4 In vivo studies

Our *ex situ* rat perfusion studies, using the strategy of concomitant RIF inhibition, demonstrated that hepatic Oatp is the major player in determining the hepatobiliary excretion of ATV and its active metabolites. We then attempted to translate what was observed at the single organ level to whole animals (Chapter 5; Lau et al., 2006b). Clinically, ATV is only given as an oral formulation. It was likely that ATV undergoes extensive metabolism in both the gut and the liver, given the presence of CYP3A at both locations. A pharmacokinetic study was designed to evaluate if a single intravenous dose of RIF could lead to increased exposure of ATV and its metabolites. ATV was administered via both oral and intravenous routes in an attempt to compare drug metabolism in the liver versus gut (Chapter 5; Lau et al., 2006b).

RIF markedly increased the plasma concentrations of ATV and its metabolites when ATV was administered orally. The AUC for ATV also increased significantly after intravenous dosing of ATV with RIF, but the extent was much less than that observed for oral ATV dosing since in rat ATV approaches high extraction categorization and blood flow considerations dampen the effect of the marked changes in intrinsic clearance on total clearance. Significant increases in plasma levels were observed for both metabolites as well. The 7-fold higher AUC ratio of metabolites to parent drug following oral versus intravenous ATV dosing suggests that ATV undergoes extensive gut metabolism. Both hepatic and intestinal metabolism contribute to the low oral bioavailability of ATV in

rats. In the presence of RIF, the liver metabolic extraction ratio was significantly reduced, most likely due to RIF's inhibitory effect on Oatp-mediated uptake, which in turn leads to reduced hepatic amounts of parent drug available for subsequent metabolism. These studies reinforce our hypothesis that hepatic uptake is a major contributor to the elimination of ATV and its metabolites *in vivo*.

7.5 Clinical study

To investigate the potential involvement of human liver-specific transporter, OATP1B1, during hepatic drug elimination of ATV, and as an extension of the *in vivo* pharmacokinetic study performed in rats, an interaction study between ATV and RIF, a potent competitive inhibitor of OATP1B1, was studied in a randomized, crossover study (Chapter 6). Twelve subjects received two 40 mg oral ATV doses, one dose in study period 1 and one dose in study period 2, separated by a 1-week washout. An intravenous 30-min infusion of 600 mg RIF was administered to each subject either in study period 1 or study period 2. In this study, RIF was chosen to block the *in vivo* OATP1B1-mediated hepatic uptake of ATV.

Our clinical results demonstrate that RIF, given as a single intravenous infusion, significantly increased the plasma AUC and C_{\max} values of ATV and its active hydroxy metabolites, 2-hydroxy-atorvastatin acid (2-OH ATV) and 4-hydroxy-atorvastatin acid (4-OH ATV). These three active species are mainly eliminated by biliary excretion. The substantial increases in AUC observed for ATV and its metabolites in the presence of RIF suggest a significant reduction in their hepatobiliary elimination mediated by hepatic transporters controlling the movement of drugs from blood to bile. To clarify the

mechanism underlying the ATV-RIF interaction, we also conducted *in vitro* cellular studies in parallel. ATV and its two hydroxy metabolites were subject to OATP1B1 uptake with only 7% of ATV attributable to passive diffusion at clinically relevant concentrations. In humans, ATV is orally administered in the open hydroxy acid ring form but it can be biotransformed to its inactive lactone form via a coenzyme A-dependent and/or an acyl glucuronide intermediate pathway (Jacobsen et al., 2000; Prueksaritanont et al., 2002; Lennernas, 2003). In this study, we monitored the pharmacokinetic changes of ATV lactone and the lactone metabolites as well, in order to evaluate the effect of RIF on the lactonization of ATV acid and hepatic uptake of ATV lactone. We observed a 2-fold increase in the AUC values of ATV lactone by concomitant RIF, indicating that ATV lactone might also be subject to uptake mediated by OATP1B1, even though it is lipophilic in nature. However, compared with the 6.7-fold increase in the corresponding value of ATV acid, the increase in lactone AUC was much less. Although the lactone to acid AUC ratio was markedly decreased for ATV during the RIF treatment phase, inhibition of lactonization was unlikely as the concentrations for the lactone forms of 2- and 4-OH ATV were also increased by RIF. Extensive inhibition of ATV lactone metabolism is not a probable cause since the ratio of the total metabolites to parent drug in the lactone form remained statistically unaltered.

Conventionally, RIF is more well known for its induction effect on drug metabolizing enzymes such as cytochrome P450 and efflux transporters such as P-gp and MRP2 (Schuetz et al., 1996; Niemi et al., 2003). Many drugs, including statins, which are co-substrates for CYP3A and P-gp, exhibit clinically relevant interactions due to co-induction of CYP3A and MDR1 genes by RIF. A recent clinical study conducted by

Backman et al. (2005) showed that multiple-doses of RIF significantly reduced the AUCs of ATV and its metabolites due to RIF's induction effects. As expected, these changes in pharmacokinetic variables are exactly opposite to what we have observed in our current study. We believe that when given as a single intravenous infusion, RIF did not exhibit induction effects on transporters and/or enzymes, but displays significant inhibition towards OATP1B1. We chose to study single doses of RIF as a model inhibitor since it can be dosed intravenously, to demonstrate that inhibitors of uptake transporters in the liver can lead to significant drug-drug interactions at the hepatic uptake level.

7.6 Concluding remarks

In addition to drug metabolizing enzymes, hepatic transporters are now recognized as major players contributing to drug-drug interactions and drug adverse effects. Results presented in this thesis provide strong evidence demonstrating how hepatic transporters can modulate drug disposition by altering the drug exposure to CYP3A without apparently affecting enzymatic activity. In addition to drug metabolizing enzymes, hepatic transporters are now recognized as major players contributing to drug-drug interactions and drug adverse effects. This thesis work endeavors to understand the effect of hepatic OATP, P-gp and MRP2 involvement in the metabolism and disposition of Dg3 and ATV, as well as the active metabolites of ATV. Among these transporters, OATP, guarding the entrance of drugs into hepatocytes, seems to play a dominant role in controlling the hepatobiliary elimination of many bulky amphipathic compounds that are anionic in nature. Our understanding of the importance of transporters in altering drug metabolism has also led us to incorporate hepatic transport processes in predicting drug

clearance from *in vitro* systems such as the isolated hepatocytes that retain transporter expressions and have been demonstrated to be a more accurate tool for measuring metabolic intrinsic clearance compared with microsomes (Lam and Benet, 2004).

Though our knowledge of hepatic transport has increased considerably over the past decade, many important questions remain to be answered from a physiological perspective. For instance, we still do not understand how some metabolites traverse across the basolateral membrane into the sinusoidal blood leading to renal elimination. We have successfully characterized the role of basolateral uptake in mediating hepatic excretion of drug and metabolites. However we believe that basolateral efflux, either mediated by an ATP-mediated efflux pump such as MRP3 or the bi-directional Oatps, are equally important, particularly for the elimination of polar metabolites that are formed in the liver. This remains as a new and exciting aspect for future research in our laboratory. It is obvious that drug-drug interaction at the transporter level can also occur via induction as the upstream nuclear receptor such as pregnane X receptor (PXR) and constitutive androstane receptor (CAR) are often involved in the co-regulation of multiple proteins, both enzymes and transporters in the detoxification pathway. Fundamental understanding regarding the regulatory pathway controlling multiple transporter expressions at the molecular level needs to be addressed. Finally, we are aware of the existence of variations in the expression levels and activity of hepatic transport proteins due to genetic polymorphisms that may result in altered disposition of some drugs. The effects of polymorphisms in the liver-specific OATP1B1 (*SLCO1B1*) gene has been extensively studied and several reports have found a correlation between the kinetics of clinically used compounds and certain SNPs identified in European and

Japanese populations (Tirona et al., 2001; Nishizato et al., 2003; Niemi et al., 2005a).

Elucidation of genetic polymorphisms in hepatic transport genes, determination of their functional significance and conduction of clinical study to identify clinically significant polymorphisms is an important area of research that may impact the use of drugs that are substrates for transporters.

Chapter 8

REFERENCES

- Abe T, Kakyo M, Tokui T, Nakagomi R, Nishio T, Nakai D, Nomura H, Unno M, Suzuki M, Naitoh T, Matsuno S and Yawo H (1999) Identification of a novel gene family encoding human liver-specific organic anion transporter LST-1. *J Biol Chem* **274**:17159-17163.
- Abe T, Unno M, Onogawa T, Tokui T, Kondo TN, Nakagomi R, Adachi H, Fujiwara K, Okabe M, Suzuki T, Nunoki K, Sato E, Kakyo M, Nishio T, Sugita J, Asano N, Tanemoto M, Seki M, Date F, Ono K, Kondo Y, Shiiba K, Suzuki M, Ohtani H, Shimosegawa T, Iinuma K, Nagura H, Ito S and Matsuno S (2001) LST-2, a human liver-specific organic anion transporter, determines methotrexate sensitivity in gastrointestinal cancers. *Gastroenterology* **120**:1689-1699.
- Acocella G (1978) Clinical pharmacokinetics of rifampicin. *Clin Pharmacokinet* **3**:108-127.
- Acocella G, Nicolis FB and Tenconi LT (1965) The effect of an intravenous infusion of rifamycin SV on the excretion of bilirubin, bromsulphalein, and indocyanine green in man. *Gastroenterology* **49**:521-525.
- Allikmets R, Schriml LM, Hutchinson A, Romano-Spica V and Dean M (1998) A human placenta-specific ATP-binding cassette gene (ABCP) on chromosome 4q22 that is involved in multidrug resistance. *Cancer Res* **58**:5337-5339.

- Ambudkar SV, Dey S, Hrycyna CA, Ramachandra M, Pastan I and Gottesman MM (1999) Biochemical, cellular, and pharmacological aspects of the multidrug transporter. *Annu Rev Pharmacol Toxicol* **39**:361-398.
- Amidon GL, Lennernas H, Shah VP and Crison JR (1995) A theoretical basis for a biopharmaceutic drug classification: the correlation of in vitro drug product dissolution and in vivo bioavailability. *Pharm Res* **12**:413-420.
- Backman JT, Luurila H, Neuvonen M and Neuvonen PJ (2005) Rifampin markedly decreases and gemfibrozil increases the plasma concentrations of atorvastatin and its metabolites. *Clin Pharmacol Ther* **78**:154-167.
- Baldwin SJ, Clarke SE and Chenery RJ (1999) Characterization of the cytochrome P450 enzymes involved in the in vitro metabolism of rosiglitazone. *Br J Clin Pharmacol* **48**:424-432.
- Benet LZ and Cummins CL (2001) The drug efflux-metabolism alliance: biochemical aspects. *Adv Drug Deliv Rev* **50 Suppl 1**:S3-11.
- Benet LZ and Galeazzi RL (1979) Noncompartmental determination of the steady-state volume of distribution. *J Pharm Sci* **68**:1071-1074.
- Benet LZ, Izumi T, Zhang Y, Silverman JA and Wacher VJ (1999) Intestinal MDR transport proteins and P-450 enzymes as barriers to oral drug delivery. *J Control Release* **62**:25-31.
- Benet LZ, Cummins CL and Wu CY (2003) Transporter-enzyme interactions: implications for predicting drug-drug interactions from in vitro data. *Curr Drug Metab* **4**:393-398.

- Benet LZ, Cummins CL and Wu CY (2004) Unmasking the dynamic interplay between efflux transporters and metabolic enzymes. *Int J Pharm* **277**:3-9.
- Bidstrup TB, Bjornsdottir I, Sidelmann UG, Thomsen MS and Hansen KT (2003) CYP2C8 and CYP3A4 are the principal enzymes involved in the human in vitro biotransformation of the insulin secretagogue repaglinide. *Br J Clin Pharmacol* **56**:305-314.
- Bigger JT, Jr. and Leahey EB, Jr. (1982) Quinidine and digoxin. An important interaction. *Drugs* **24**:229-239.
- Black AE, Hayes RN, Roth BD, Woo P and Woolf TF (1999) Metabolism and excretion of atorvastatin in rats and dogs. *Drug Metab Dispos* **27**:916-923.
- Borst P, Evers R, Kool M and Wijnholds J (1999) The multidrug resistance protein family. *Biochim Biophys Acta* **1461**:347-357.
- Bosma PJ, Seppen J, Goldhoorn B, Bakker C, Oude Elferink RP, Chowdhury JR, Chowdhury NR and Jansen PL (1994) Bilirubin UDP-glucuronosyltransferase 1 is the only relevant bilirubin glucuronidating isoform in man. *J Biol Chem* **269**:17960-17964.
- Bossuyt X, Muller M and Meier PJ (1996) Multispecific amphipathic substrate transport by an organic anion transporter of human liver. *J Hepatol* **25**:733-738.
- Boyer JL (1980) New concepts of mechanisms of hepatocyte bile formation. *Physiol Rev* **60**:303-326.

- Buchler M, Konig J, Brom M, Kartenbeck J, Spring H, Horie T and Keppler D (1996) cDNA cloning of the hepatocyte canalicular isoform of the multidrug resistance protein, cMrp, reveals a novel conjugate export pump deficient in hyperbilirubinemic mutant rats. *J Biol Chem* **271**:15091-15098.
- Bussey HI (1982) The influence of quinidine and other agents on digitalis glycosides. *Am Heart J* **104**:289-302.
- Cattori V, van Montfoort JE, Stieger B, Landmann L, Meijer DK, Winterhalter KH, Meier PJ and Hagenbuch B (2001) Localization of organic anion transporting polypeptide 4 (Oatp4) in rat liver and comparison of its substrate specificity with Oatp1, Oatp2 and Oatp3. *Pflugers Arch* **443**:188-195.
- Cavet ME, West M and Simmons NL (1996) Transport and epithelial secretion of the cardiac glycoside, digoxin, by human intestinal epithelial (Caco-2) cells. *Br J Pharmacol* **118**:1389-1396.
- Cha SH, Sekine T, Kusuhara H, Yu E, Kim JY, Kim DK, Sugiyama Y, Kanai Y and Endou H (2000) Molecular cloning and characterization of multispecific organic anion transporter 4 expressed in the placenta. *J Biol Chem* **275**:4507-4512.
- Chandra P and Brouwer KL (2004) The complexities of hepatic drug transport: current knowledge and emerging concepts. *Pharm Res* **21**:719-735.
- Chang JH and Benet LZ (2005) Glucuronidation and the transport of the glucuronide metabolites in LLC-PK1 cells. *Mol Pharm* **2**:428-434.
- Chen C, Mireles RJ, Campbell SD, Lin J, Mills JB, Xu JJ and Smolarek TA (2005) Differential interaction of 3-hydroxy-3-methylglutaryl-coa reductase inhibitors with ABCB1, ABCC2, and OATP1B1. *Drug Metab Dispos* **33**:537-546.

- Cheng X, Maher J, Dieter MZ and Klaassen CD (2005) Regulation of mouse organic anion-transporting polypeptides (oatps) in liver by prototypical microsomal enzyme inducers that activate distinct transcription factor pathways. *Drug Metab Dispos* **33**:1276-1282.
- Childs S, Yeh RL, Georges E and Ling V (1995) Identification of a sister gene to P-glycoprotein. *Cancer Res* **55**:2029-2034.
- Christians U, Jacobsen W and Floren LC (1998) Metabolism and drug interactions of 3-hydroxy-3-methylglutaryl coenzyme A reductase inhibitors in transplant patients: are the statins mechanistically similar? *Pharmacol Ther* **80**:1-34.
- Christians U, Jacobsen W, Serkova N, Benet LZ, Vidal C, Sewing KF, Manns MP and Kirchner GI (2000) Automated, fast and sensitive quantification of drugs in blood by liquid chromatography-mass spectrometry with on-line extraction: immunosuppressants. *J Chromatogr B Biomed Sci Appl* **748**:41-53.
- Cole SP, Sparks KE, Fraser K, Loe DW, Grant CE, Wilson GM and Deeley RG (1994) Pharmacological characterization of multidrug resistant MRP-transfected human tumor cells. *Cancer Res* **54**:5902-5910.
- Cordon-Cardo C, O'Brien JP, Casals D, Rittman-Grauer L, Biedler JL, Melamed MR and Bertino JR (1989) Multidrug-resistance gene (P-glycoprotein) is expressed by endothelial cells at blood-brain barrier sites. *Proc Natl Acad Sci U S A* **86**:695-698.
- Cui Y, Konig J and Keppler D (2001a) Vectorial transport by double-transfected cells expressing the human uptake transporter SLC21A8 and the apical export pump ABCC2. *Mol Pharmacol* **60**:934-943.

- Cui Y, Konig J, Leier I, Buchholz U and Keppler D (2001b) Hepatic uptake of bilirubin and its conjugates by the human organic anion transporter SLC21A6. *J Biol Chem* **276**:9626-9630.
- Cummins CL, Jacobsen W and Benet LZ (2002a) Unmasking the dynamic interplay between intestinal P-glycoprotein and CYP3A4. *J Pharmacol Exp Ther* **300**:1036-1045.
- Cummins CL, Wu CY and Benet LZ (2002b) Sex-related differences in the clearance of cytochrome P450 3A4 substrates may be caused by P-glycoprotein. *Clin Pharmacol Ther* **72**:474-489.
- Cummins CL, Salphati L, Reid MJ and Benet LZ (2003) In vivo modulation of intestinal CYP3A metabolism by P-glycoprotein: studies using the rat single-pass intestinal perfusion model. *J Pharmacol Exp Ther* **305**:306-314.
- Cummins CL, Jacobsen W, Christians U and Benet LZ (2004) CYP3A4-transfected Caco-2 cells as a tool for understanding biochemical absorption barriers: studies with sirolimus and midazolam. *J Pharmacol Exp Ther* **308**:143-155.
- Cvetkovic M, Leake B, Fromm MF, Wilkinson GR and Kim RB (1999) OATP and P-glycoprotein transporters mediate the cellular uptake and excretion of fexofenadine. *Drug Metab Dispos* **27**:866-871.
- Davies B and Morris T (1993) Physiological parameters in laboratory animals and humans. *Pharm Res* **10**:1093-1095.
- de Lannoy IA and Silverman M (1992) The MDR1 gene product, P-glycoprotein, mediates the transport of the cardiac glycoside, digoxin. *Biochem Biophys Res Commun* **189**:551-557.

- de Lannoy IA, Koren G, Klein J, Charuk J and Silverman M (1992) Cyclosporin and quinidine inhibition of renal digoxin excretion: evidence for luminal secretion of digoxin. *Am J Physiol* **263**:F613-622.
- de Waziers I, Cugnenc PH, Yang CS, Leroux JP and Beaune PH (1990) Cytochrome P 450 isoenzymes, epoxide hydrolase and glutathione transferases in rat and human hepatic and extrahepatic tissues. *J Pharmacol Exp Ther* **253**:387-394.
- Depeille P, Cuq P, Mary S, Passagne I, Evrard A, Cupissol D and Vian L (2004) Glutathione S-transferase M1 and multidrug resistance protein 1 act in synergy to protect melanoma cells from vincristine effects. *Mol Pharmacol* **65**:897-905.
- Doyle LA, Yang W, Abruzzo LV, Krogmann T, Gao Y, Rishi AK and Ross DD (1998) A multidrug resistance transporter from human MCF-7 breast cancer cells. *Proc Natl Acad Sci U S A* **95**:15665-15670.
- Eckhardt U, Schroeder A, Stieger B, Hochli M, Landmann L, Tynes R, Meier PJ and Hagenbuch B (1999) Polyspecific substrate uptake by the hepatic organic anion transporter Oatp1 in stably transfected CHO cells. *Am J Physiol* **276**:G1037-1042.
- Evans WH (1980) A biochemical dissection of the functional polarity of the plasma membrane of the hepatocyte. *Biochim Biophys Acta* **604**:27-64.
- Evans WE and Relling MV (2004) Moving towards individualized medicine with pharmacogenomics. *Nature* **429**:464-468.
- Evers R, Kool M, van Deemter L, Janssen H, Calafat J, Oomen LC, Paulusma CC, Oude Elferink RP, Baas F, Schinkel AH and Borst P (1998) Drug export activity of the human canalicular multispecific organic anion transporter in polarized kidney MDCK cells expressing cMOAT (MRP2) cDNA. *J Clin Invest* **101**:1310-1319.

- Fardel O, Lecureur V, Loyer P and Guillouzo A (1995) Rifampicin enhances anti-cancer drug accumulation and activity in multidrug-resistant cells. *Biochem Pharmacol* **49**:1255-1260.
- Fardel O, Jigorel E, Le Vee M and Payen L (2005) Physiological, pharmacological and clinical features of the multidrug resistance protein 2. *Biomed Pharmacother* **59**:104-114.
- Fattinger K, Cattori V, Hagenbuch B, Meier PJ and Stieger B (2000) Rifamycin SV and rifampicin exhibit differential inhibition of the hepatic rat organic anion transporting polypeptides, Oatp1 and Oatp2. *Hepatology* **32**:82-86.
- Flanagan SD, Cummins CL, Susanto M, Liu X, Takahashi LH and Benet LZ (2002) Comparison of furosemide and vinblastine secretion from cell lines overexpressing multidrug resistance protein (P-glycoprotein) and multidrug resistance-associated proteins (MRP1 and MRP2). *Pharmacology* **64**:126-134.
- Friesema EC, Docter R, Moerings EP, Stieger B, Hagenbuch B, Meier PJ, Krenning EP, Hennemann G and Visser TJ (1999) Identification of thyroid hormone transporters. *Biochem Biophys Res Commun* **254**:497-501.
- Fromm MF, Kim RB, Stein CM, Wilkinson GR and Roden DM (1999) Inhibition of P-glycoprotein-mediated drug transport: A unifying mechanism to explain the interaction between digoxin and quinidine. *Circulation* **99**:552-557.
- Fromm MF, Kauffmann HM, Fritz P, Burk O, Kroemer HK, Warzok RW, Eichelbaum M, Siegmund W and Schrenk D (2000) The effect of rifampin treatment on intestinal expression of human MRP transporters. *Am J Pathol* **157**:1575-1580.

- Gerloff T, Stieger B, Hagenbuch B, Madon J, Landmann L, Roth J, Hofmann AF and Meier PJ (1998) The sister of P-glycoprotein represents the canalicular bile salt export pump of mammalian liver. *J Biol Chem* **273**:10046-10050.
- Gibson DM, Stern RH and Abel RB (1997) Absolute bioavailability of atorvastatin in man. *Pharm Res* **14**: S253
- Gomez DY, Wachter VJ, Tomlanovich SJ, Hebert MF and Benet LZ (1995) The effects of ketoconazole on the intestinal metabolism and bioavailability of cyclosporine. *Clin Pharmacol Ther* **58**:15-19.
- Gottesman MM and Pastan I (1993) Biochemistry of multidrug resistance mediated by the multidrug transporter. *Annu Rev Biochem* **62**:385-427.
- Gottesman MM, Fojo T and Bates SE (2002) Multidrug resistance in cancer: role of ATP-dependent transporters. *Nat Rev Cancer* **2**:48-58.
- Gray IC, Nobile C, Muresu R, Ford S and Spurr NK (1995) A 2.4-megabase physical map spanning the CYP2C gene cluster on chromosome 10q24. *Genomics* **28**:328-332.
- Greiner B, Eichelbaum M, Fritz P, Kreichgauer HP, von Richter O, Zundler J and Kroemer HK (1999) The role of intestinal P-glycoprotein in the interaction of digoxin and rifampin. *J Clin Invest* **104**:147-153.
- Grundemann D, Gorboulev V, Gambaryan S, Veyhl M and Koepsell H (1994) Drug excretion mediated by a new prototype of polyspecific transporter. *Nature* **372**:549-552.
- Guillemette C (2003) Pharmacogenomics of human UDP-glucuronosyltransferase enzymes. *Pharmacogenomics J* **3**:136-158.

- Hagenbuch B and Meier PJ (2004) Organic anion transporting polypeptides of the OATP/SLC21 family: phylogenetic classification as OATP/SLCO superfamily, new nomenclature and molecular/functional properties. *Pflugers Arch* **447**:653-665.
- Harrison LI and Gibaldi M (1976) Pharmacokinetics of digoxin in the rat. *Drug Metab Dispos* **4**:88-93.
- Hedman A, Angelin B, Arvidsson A, Dahlqvist R and Nilsson B (1990) Interactions in the renal and biliary elimination of digoxin: stereoselective difference between quinine and quinidine. *Clin Pharmacol Ther* **47**:20-26.
- Hirano M, Maeda K, Hayashi H, Kusuhara H and Sugiyama Y (2005a) Bile salt export pump (BSEP/ABCB11) can transport a nonbile acid substrate, pravastatin. *J Pharmacol Exp Ther* **314**:876-882.
- Hirano M, Maeda K, Matsushima S, Nozaki Y, Kusuhara H and Sugiyama Y (2005b) Involvement of BCRP (ABCG2) in the biliary excretion of pitavastatin. *Mol Pharmacol* **68**:800-807.
- Hirohashi T, Suzuki H, Ito K, Ogawa K, Kume K, Shimizu T and Sugiyama Y (1998) Hepatic expression of multidrug resistance-associated protein-like proteins maintained in eisai hyperbilirubinemic rats. *Mol Pharmacol* **53**:1068-1075.
- Hirohashi T, Suzuki H, Takikawa H and Sugiyama Y (2000) ATP-dependent transport of bile salts by rat multidrug resistance-associated protein 3 (Mrp3). *J Biol Chem* **275**:2905-2910.
- Hochman JH, Pudvah N, Qiu J, Yamazaki M, Tang C, Lin JH and Prueksaritanont T (2004) Interactions of human P-glycoprotein with simvastatin, simvastatin acid, and atorvastatin. *Pharm Res* **21**:1686-1691.

- Hori R, Okamura N, Aiba T and Tanigawara Y (1993) Role of P-glycoprotein in renal tubular secretion of digoxin in the isolated perfused rat kidney. *J Pharmacol Exp Ther* **266**:1620-1625.
- Hsiang B, Zhu Y, Wang Z, Wu Y, Sasseville V, Yang WP and Kirchgessner TG (1999) A novel human hepatic organic anion transporting polypeptide (OATP2). Identification of a liver-specific human organic anion transporting polypeptide and identification of rat and human hydroxymethylglutaryl-CoA reductase inhibitor transporters. *J Biol Chem* **274**:37161-37168.
- Huang L, Hoffman T and Vore M (1998) Adenosine triphosphate-dependent transport of estradiol-17beta(beta-D-glucuronide) in membrane vesicles by MDR1 expressed in insect cells. *Hepatology* **28**:1371-1377.
- Ismair MG, Stieger B, Cattori V, Hagenbuch B, Fried M, Meier PJ and Kullak-Ublick GA (2001) Hepatic uptake of cholecystinin octapeptide by organic anion-transporting polypeptides OATP4 and OATP8 of rat and human liver. *Gastroenterology* **121**:1185-1190.
- Ito K, Suzuki H, Hirohashi T, Kume K, Shimizu T and Sugiyama Y (1997) Molecular cloning of canalicular multispecific organic anion transporter defective in EHBR. *Am J Physiol* **272**:G16-22.
- Iwai M, Suzuki H, Ieiri I, Otsubo K and Sugiyama Y (2004) Functional analysis of single nucleotide polymorphisms of hepatic organic anion transporter OATP1B1 (OATP-C). *Pharmacogenetics* **14**:749-757.

- Iwatsubo T, Hirota N, Ooie T, Suzuki H, Shimada N, Chiba K, Ishizaki T, Green CE, Tyson CA and Sugiyama Y (1997) Prediction of in vivo drug metabolism in the human liver from in vitro metabolism data. *Pharmacol Ther* **73**:147-171.
- Jacobsen W, Kuhn B, Soldner A, Kirchner G, Sewing KF, Kollman PA, Benet LZ and Christians U (2000) Lactonization is the critical first step in the disposition of the 3-hydroxy-3-methylglutaryl-CoA reductase inhibitor atorvastatin. *Drug Metab Dispos* **28**:1369-1378.
- Jacobson TA (2004) Comparative pharmacokinetic interaction profiles of pravastatin, simvastatin, and atorvastatin when coadministered with cytochrome P450 inhibitors. *Am J Cardiol* **94**:1140-1146.
- Jemal M, Ouyang Z, Chen BC and Teitz D (1999) Quantitation of the acid and lactone forms of atorvastatin and its biotransformation products in human serum by high-performance liquid chromatography with electrospray tandem mass spectrometry. *Rapid Commun Mass Spectrom* **13**:1003-1015.
- Johnson BM, Charman WN and Porter CJ (2001) The impact of P-glycoprotein efflux on enterocyte residence time and enterocyte-based metabolism of verapamil. *J Pharm Pharmacol* **53**:1611-1619.
- Jonker JW and Schinkel AH (2004) Pharmacological and physiological functions of the polyspecific organic cation transporters: OCT1, 2, and 3 (SLC22A1-3). *J Pharmacol Exp Ther* **308**:2-9.
- Jonker JW, Smit JW, Brinkhuis RF, Maliepaard M, Beijnen JH, Schellens JH and Schinkel AH (2000) Role of breast cancer resistance protein in the bioavailability and fetal penetration of topotecan. *J Natl Cancer Inst* **92**:1651-1656.

- Kajosaari LI, Laitila J, Neuvonen PJ and Backman JT (2005) Metabolism of repaglinide by CYP2C8 and CYP3A4 in vitro: effect of fibrates and rifampicin. *Basic Clin Pharmacol Toxicol* **97**:249-256.
- Kakumoto M, Takara K, Sakaeda T, Tanigawara Y, Kita T and Okumura K (2002) MDR1-mediated interaction of digoxin with antiarrhythmic or antianginal drugs. *Biol Pharm Bull* **25**:1604-1607.
- Kakyo M, Unno M, Tokui T, Nakagomi R, Nishio T, Iwasashi H, Nakai D, Seki M, Suzuki M, Naitoh T, Matsuno S, Yawo H and Abe T (1999) Molecular characterization and functional regulation of a novel rat liver-specific organic anion transporter rlst-1. *Gastroenterology* **117**:770-775.
- Kameyama Y, Yamashita K, Kobayashi K, Hosokawa M and Chiba K (2005) Functional characterization of SLCO1B1 (OATP-C) variants, SLCO1B1*5, SLCO1B1*15 and SLCO1B1*15+C1007G, by using transient expression systems of HeLa and HEK293 cells. *Pharmacogenet Genomics* **15**:513-522.
- Kanai N, Lu R, Bao Y, Wolkoff AW and Schuster VL (1996a) Transient expression of oatp organic anion transporter in mammalian cells: identification of candidate substrates. *Am J Physiol* **270**:F319-325.
- Kanai N, Lu R, Bao Y, Wolkoff AW, Vore M and Schuster VL (1996b) Estradiol 17 beta-D-glucuronide is a high-affinity substrate for oatp organic anion transporter. *Am J Physiol* **270**:F326-331.
- Kantola T, Kivisto KT and Neuvonen PJ (1998) Effect of itraconazole on the pharmacokinetics of atorvastatin. *Clin Pharmacol Ther* **64**:58-65.

- Kawabe T, Chen ZS, Wada M, Uchiumi T, Ono M, Akiyama S and Kuwano M (1999) Enhanced transport of anticancer agents and leukotriene C4 by the human canalicular multispecific organic anion transporter (cMOAT/MRP2). *FEBS Lett* **456**:327-331.
- Keitel V, Nies AT, Brom M, Hummel-Eisenbeiss J, Spring H and Keppler D (2003) A common Dubin-Johnson syndrome mutation impairs protein maturation and transport activity of MRP2 (ABCC2). *Am J Physiol Gastrointest Liver Physiol* **284**:G165-174.
- Keppler D and Arias IM (1997) Hepatic canalicular membrane. Introduction: transport across the hepatocyte canalicular membrane. *FASEB J* **11**:15-18.
- Kirchheiner J, Kudlicz D, Meisel C, Bauer S, Meineke I, Roots I and Brockmoller J (2003) Influence of CYP2C9 polymorphisms on the pharmacokinetics and cholesterol-lowering activity of (-)-3S,5R-fluvastatin and (+)-3R,5S-fluvastatin in healthy volunteers. *Clin Pharmacol Ther* **74**:186-194.
- Klopman G, Shi LM and Ramu A (1997) Quantitative structure-activity relationship of multidrug resistance reversal agents. *Mol Pharmacol* **52**:323-334.
- Kodawara T, Masuda S, Wakasugi H, Uwai Y, Futami T, Saito H, Abe T and Inu K (2002) Organic anion transporter oatp2-mediated interaction between digoxin and amiodarone in the rat liver. *Pharm Res* **19**:738-743.
- Konig J, Nies AT, Cui Y, Leier I and Keppler D (1999) Conjugate export pumps of the multidrug resistance protein (MRP) family: localization, substrate specificity, and MRP2-mediated drug resistance. *Biochim Biophys Acta* **1461**:377-394.

- Konig J, Cui Y, Nies AT and Keppler D (2000a) Localization and genomic organization of a new hepatocellular organic anion transporting polypeptide. *J Biol Chem* **275**:23161-23168.
- Konig J, Cui Y, Nies AT and Keppler D (2000b) A novel human organic anion transporting polypeptide localized to the basolateral hepatocyte membrane. *Am J Physiol Gastrointest Liver Physiol* **278**:G156-164.
- Kool M, van der Linden M, de Haas M, Scheffer GL, de Vree JM, Smith AJ, Jansen G, Peters GJ, Ponne N, Scheper RJ, Elferink RP, Baas F and Borst P (1999) MRP3, an organic anion transporter able to transport anti-cancer drugs. *Proc Natl Acad Sci U S A* **96**:6914-6919.
- Kuehl P, Zhang J, Lin Y, Lamba J, Assem M, Schuetz J, Watkins PB, Daly A, Wrighton SA, Hall SD, Maurel P, Relling M, Brimer C, Yasuda K, Venkataramanan R, Strom S, Thummel K, Boguski MS and Schuetz E (2001) Sequence diversity in CYP3A promoters and characterization of the genetic basis of polymorphic CYP3A5 expression. *Nat Genet* **27**:383-391.
- Kullak-Ublick GA, Ismail MG, Stieger B, Landmann L, Huber R, Pizzagalli F, Fattinger K, Meier PJ and Hagenbuch B (2001) Organic anion-transporting polypeptide B (OATP-B) and its functional comparison with three other OATPs of human liver. *Gastroenterology* **120**:525-533.
- Kuroda M, Kobayashi Y, Tanaka Y, Itani T, Mifuji R, Araki J, Kaito M and Adachi Y (2004) Increased hepatic and renal expressions of multidrug resistance-associated protein 3 in Eisai hyperbilirubinuria rats. *J Gastroenterol Hepatol* **19**:146-153.

- Lam JL and Benet LZ (2004) Hepatic microsome studies are insufficient to characterize in vivo hepatic metabolic clearance and metabolic drug-drug interactions: studies of digoxin metabolism in primary rat hepatocytes versus microsomes. *Drug Metab Dispos* **32**:1311-1316.
- Lampen A, Zhang Y, Hackbarth I, Benet LZ, Sewing KF and Christians U (1998) Metabolism and transport of the macrolide immunosuppressant sirolimus in the small intestine. *J Pharmacol Exp Ther* **285**:1104-1112.
- Lasker JM, Wester MR, Aramsombatdee E and Raucy JL (1998) Characterization of CYP2C19 and CYP2C9 from human liver: respective roles in microsomal tolbutamide, S-mephenytoin, and omeprazole hydroxylations. *Arch Biochem Biophys* **353**:16-28.
- Lau YY, Wu CY, Okochi H and Benet LZ (2004) Ex situ inhibition of hepatic uptake and efflux significantly changes metabolism: hepatic enzyme-transporter interplay. *J Pharmacol Exp Ther* **308**:1040-1045.
- Lau YY, Okochi H, Huang Y and Benet LZ (2006a) Multiple transporters affect the disposition of atorvastatin and its two active hydroxy metabolites: application of in vitro and ex situ systems. *J Pharmacol Exp Ther* **316**:762-771.
- Lau YY, Okochi H, Huang Y and Benet LZ (2006b) Pharmacokinetics of atorvastatin and its hydroxy metabolites in rats and the effects of concomitant rifampicin single doses: Relevance of first-pass effect from hepatic uptake transporters, intestinal and hepatic metabolism. *Drug Metab Dispos* [Fast Forward April 19, 2006]

- Leahey EB, Jr., Reiffel JA, Drusin RE, Heissenbuttel RH, Lovejoy WP and Bigger JT, Jr. (1978) Interaction between quinidine and digoxin. *Jama* **240**:533-534.
- Lecureur V, Sun D, Hargrove P, Schuetz EG, Kim RB, Lan LB and Schuetz JD (2000) Cloning and expression of murine sister of P-glycoprotein reveals a more discriminating transporter than MDR1/P-glycoprotein. *Mol Pharmacol* **57**:24-35.
- Lennernas H (2003) Clinical pharmacokinetics of atorvastatin. *Clin Pharmacokinet* **42**:1141-1160.
- Lewis DF, Eddershaw PJ, Goldfarb PS and Tarbit MH (1996) Molecular modelling of CYP3A4 from an alignment with CYP102: identification of key interactions between putative active site residues and CYP3A-specific chemicals. *Xenobiotica* **26**:1067-1086.
- Lewis DF, Jacobs MN and Dickins M (2004a) Compound lipophilicity for substrate binding to human P450s in drug metabolism. *Drug Discov Today* **9**:530-537.
- Lewis DF, Lake BG, Dickins M and Goldfarb PS (2004b) Homology modelling of CYP3A4 from the CYP2C5 crystallographic template: analysis of typical CYP3A4 substrate interactions. *Xenobiotica* **34**:549-569.
- Li L, Lee TK, Meier PJ and Ballatori N (1998) Identification of glutathione as a driving force and leukotriene C4 as a substrate for oatp1, the hepatic sinusoidal organic solute transporter. *J Biol Chem* **273**:16184-16191.
- Lilja JJ, Kivisto KT and Neuvonen PJ (1999) Grapefruit juice increases serum concentrations of atorvastatin and has no effect on pravastatin. *Clin Pharmacol Ther* **66**:118-127.

- Lindahl A, Persson B, Ungell AL and Lennernas H (1999) Surface activity and concentration dependent intestinal permeability in the rat. *Pharm Res* **16**:97-102.
- Litman T, Zeuthen T, Skovsgaard T and Stein WD (1997) Structure-activity relationships of P-glycoprotein interacting drugs: kinetic characterization of their effects on ATPase activity. *Biochim Biophys Acta* **1361**:159-168.
- Lowry OH, Rosebrough NJ, Farr AL and Randall RJ (1951) Protein measurement with the Folin phenol reagent. *J Biol Chem* **193**:265-275.
- Matsushima S, Maeda K, Kondo C, Hirano M, Sasaki M, Suzuki H and Sugiyama Y (2005) Identification of the hepatic efflux transporters of organic anions using double-transfected Madin-Darby canine kidney II cells expressing human organic anion-transporting polypeptide 1B1 (OATP1B1)/multidrug resistance-associated protein 2, OATP1B1/multidrug resistance 1, and OATP1B1/breast cancer resistance protein. *J Pharmacol Exp Ther* **314**:1059-1067.
- Meier PJ, Eckhardt U, Schroeder A, Hagenbuch B and Stieger B (1997) Substrate specificity of sinusoidal bile acid and organic anion uptake systems in rat and human liver. *Hepatology* **26**:1667-1677.
- Meyer-Wentrup F, Karbach U, Gorboulev V, Arndt P and Koepsell H (1998) Membrane localization of the electrogenic cation transporter rOCT1 in rat liver. *Biochem Biophys Res Commun* **248**:673-678.
- Mikkaichi T, Suzuki T, Tanemoto M, Ito S and Abe T (2004) The organic anion transporter (OATP) family. *Drug Metab Pharmacokinet* **19**:171-179.
- Miners JO and Birkett DJ (1998) Cytochrome P4502C9: an enzyme of major importance in human drug metabolism. *Br J Clin Pharmacol* **45**:525-538.

- Mordel A, Halkin H, Zulty L, Almog S and Ezra D (1993) Quinidine enhances digitalis toxicity at therapeutic serum digoxin levels. *Clin Pharmacol Ther* **53**:457-462.
- Morimoto K, Oishi T, Ueda S, Ueda M, Hosokawa M and Chiba K (2004) A novel variant allele of OATP-C (SLCO1B1) found in a Japanese patient with pravastatin-induced myopathy. *Drug Metab Pharmacokinet* **19**:453-455.
- Motohashi H, Sakurai Y, Saito H, Masuda S, Urakami Y, Goto M, Fukatsu A, Ogawa O and Inui K (2002) Gene expression levels and immunolocalization of organic ion transporters in the human kidney. *J Am Soc Nephrol* **13**:866-874.
- Mwinyi J, Johne A, Bauer S, Roots I and Gerloff T (2004) Evidence for inverse effects of OATP-C (SLC21A6) 5 and 1b haplotypes on pravastatin kinetics. *Clin Pharmacol Ther* **75**:415-421.
- Naritomi Y, Terashita S, Kimura S, Suzuki A, Kagayama A and Sugiyama Y (2001) Prediction of human hepatic clearance from in vivo animal experiments and in vitro metabolic studies with liver microsomes from animals and humans. *Drug Metab Dispos* **29**:1316-1324.
- Nawrocki JW, Weiss SR, Davidson MH, Sprecher DL, Schwartz SL, Lupien PJ, Jones PH, Haber HE and Black DM (1995) Reduction of LDL cholesterol by 25% to 60% in patients with primary hypercholesterolemia by atorvastatin, a new HMG-CoA reductase inhibitor. *Arterioscler Thromb Vasc Biol* **15**:678-682.
- Nezasa K, Higaki K, Takeuchi M, Nakano M and Koike M (2003) Uptake of rosuvastatin by isolated rat hepatocytes: comparison with pravastatin. *Xenobiotica* **33**:379-388.

- Niemi M, Backman JT, Fromm MF, Neuvonen PJ and Kivisto KT (2003)
Pharmacokinetic interactions with rifampicin : clinical relevance. *Clin Pharmacokinet* **42**:819-850.
- Niemi M, Schaeffeler E, Lang T, Fromm MF, Neuvonen M, Kyrklund C, Backman JT, Kerb R, Schwab M, Neuvonen PJ, Eichelbaum M and Kivisto KT (2004) High plasma pravastatin concentrations are associated with single nucleotide polymorphisms and haplotypes of organic anion transporting polypeptide-C (OATP-C, SLCO1B1). *Pharmacogenetics* **14**:429-440.
- Niemi M, Backman JT, Kajosaari LI, Leathart JB, Neuvonen M, Daly AK, Eichelbaum M, Kivisto KT and Neuvonen PJ (2005a) Polymorphic organic anion transporting polypeptide 1B1 is a major determinant of repaglinide pharmacokinetics. *Clin Pharmacol Ther* **77**:468-478.
- Niemi M, Kivisto KT, Hofmann U, Schwab M, Eichelbaum M and Fromm MF (2005b) Fexofenadine pharmacokinetics are associated with a polymorphism of the SLCO1B1 gene (encoding OATP1B1). *Br J Clin Pharmacol* **59**:602-604.
- Nishizato Y, Ieiri I, Suzuki H, Kimura M, Kawabata K, Hirota T, Takane H, Irie S, Kusuhara H, Urasaki Y, Urae A, Higuchi S, Otsubo K and Sugiyama Y (2003) Polymorphisms of OATP-C (SLC21A6) and OAT3 (SLC22A8) genes: consequences for pravastatin pharmacokinetics. *Clin Pharmacol Ther* **73**:554-565.
- Noe B, Hagenbuch B, Stieger B and Meier PJ (1997) Isolation of a multispecific organic anion and cardiac glycoside transporter from rat brain. *Proc Natl Acad Sci U S A* **94**:10346-10350.

- Pastan I, Gottesman MM, Ueda K, Lovelace E, Rutherford AV and Willingham MC (1988) A retrovirus carrying an MDR1 cDNA confers multidrug resistance and polarized expression of P-glycoprotein in MDCK cells. *Proc Natl Acad Sci U S A* **85**:4486-4490.
- Paulusma CC, Bosma PJ, Zaman GJ, Bakker CT, Otter M, Scheffer GL, Scheper RJ, Borst P and Oude Elferink RP (1996) Congenital jaundice in rats with a mutation in a multidrug resistance-associated protein gene. *Science* **271**:1126-1128.
- Paulusma CC, Kool M, Bosma PJ, Scheffer GL, ter Borg F, Scheper RJ, Tytgat GN, Borst P, Baas F and Oude Elferink RP (1997) A mutation in the human canalicular multispecific organic anion transporter gene causes the Dubin-Johnson syndrome. *Hepatology* **25**:1539-1542.
- Prueksaritanont T, Hoener BA and Benet LZ (1992) Effects of low-density lipoprotein and ethinyl estradiol on cyclosporine metabolism in isolated rat liver perfusions. *Drug Metab Dispos* **20**:547-552.
- Prueksaritanont T, Subramanian R, Fang X, Ma B, Qiu Y, Lin JH, Pearson PG and Baillie TA (2002) Glucuronidation of statins in animals and humans: a novel mechanism of statin lactonization. *Drug Metab Dispos* **30**:505-512.
- Rahman A, Korzekwa KR, Grogan J, Gonzalez FJ and Harris JW (1994) Selective biotransformation of taxol to 6 alpha-hydroxytaxol by human cytochrome P450 2C8. *Cancer Res* **54**:5543-5546.
- Rendic S and Di Carlo FJ (1997) Human cytochrome P450 enzymes: a status report summarizing their reactions, substrates, inducers, and inhibitors. *Drug Metab Rev* **29**:413-580.

- Roberts MS, Magnusson BM, Burczynski FJ and Weiss M (2002) Enterohepatic circulation: physiological, pharmacokinetic and clinical implications. *Clin Pharmacokinet* **41**:751-790.
- Rodin SM and Johnson BF (1988) Pharmacokinetic interactions with digoxin. *Clin Pharmacokinet* **15**:227-244.
- Rowland M, Benet LZ and Graham GG (1973) Clearance concepts in pharmacokinetics. *J Pharmacokinet Biopharm* **1**:123-136.
- Sakai K, Yamazaki T and Hinohara Y (1988) Effects of AN-132 and quinidine, antiarrhythmic agents, on plasma digoxin concentrations in rats. *J Pharm Pharmacol* **40**:68-69.
- Salphati L and Benet LZ (1999) Metabolism of digoxin and digoxigenin digitoxosides in rat liver microsomes: involvement of cytochrome P4503A. *Xenobiotica* **29**:171-185.
- Sasaki M, Suzuki H, Ito K, Abe T and Sugiyama Y (2002) Transcellular transport of organic anions across a double-transfected Madin-Darby canine kidney II cell monolayer expressing both human organic anion-transporting polypeptide (OATP2/SLC21A6) and Multidrug resistance-associated protein 2 (MRP2/ABCC2). *J Biol Chem* **277**:6497-6503.
- Sasaki M, Suzuki H, Aoki J, Ito K, Meier PJ and Sugiyama Y (2004) Prediction of in vivo biliary clearance from the in vitro transcellular transport of organic anions across a double-transfected Madin-Darby canine kidney II monolayer expressing both rat organic anion transporting polypeptide 4 and multidrug resistance associated protein 2. *Mol Pharmacol* **66**:450-459.

- Satlin LM, Amin V and Wolkoff AW (1997) Organic anion transporting polypeptide mediates organic anion/HCO₃⁻ exchange. *J Biol Chem* **272**:26340-26345.
- Schaub TP, Kartenbeck J, Konig J, Spring H, Dorsam J, Staehler G, Storkel S, Thon WF and Keppler D (1999) Expression of the MRP2 gene-encoded conjugate export pump in human kidney proximal tubules and in renal cell carcinoma. *J Am Soc Nephrol* **10**:1159-1169.
- Schinkel AH (1997) The physiological function of drug-transporting P-glycoproteins. *Semin Cancer Biol* **8**:161-170.
- Schinkel AH, Mayer U, Wagenaar E, Mol CA, van Deemter L, Smit JJ, van der Valk MA, Voordouw AC, Spits H, van Tellingen O, Zijlmans JM, Fibbe WE and Borst P (1997) Normal viability and altered pharmacokinetics in mice lacking mdr1-type (drug-transporting) P-glycoproteins. *Proc Natl Acad Sci U S A* **94**:4028-4033.
- Schmid D, Ecker G, Kopp S, Hitzler M and Chiba P (1999) Structure-activity relationship studies of propafenone analogs based on P-glycoprotein ATPase activity measurements. *Biochem Pharmacol* **58**:1447-1456.
- Schmoldt A and Ahsendorf B (1980) Cleavage of digoxigenin digitoxosides by rat liver microsomes. *Eur J Drug Metab Pharmacokinet* **5**:225-232.
- Schuetz EG, Schinkel AH, Relling MV and Schuetz JD (1996) P-glycoprotein: a major determinant of rifampicin-inducible expression of cytochrome P4503A in mice and humans. *Proc Natl Acad Sci U S A* **93**:4001-4005.

- Schuetz EG, Relling MV, Kishi S, Yang W, Das S, Chen P, Cook EH, Rosner GL, Pui CH, Blanco JG, Edick MJ, Hancock ML, Winick NJ, Dervieux T, Amylon MD, Bash RO, Behm FG, Camitta BM, Raimondi SC, Goh BC, Lee SC, Wang LZ, Fan L, Guo JY, Lamba J, Lim R, Lim HL, Ong AB, Lee HS, Kuehl P, Zhang J, Lin Y, Assem M, Schuetz J, Watkins PB, Daly A, Wrighton SA, Hall SD, Maurel P, Brimer C, Yasuda K, Venkataramanan R, Strom S, Thummel K and Boguski MS (2004) PharmGKB update: II. CYP3A5, cytochrome P450, family 3, subfamily A, polypeptide 5. *Pharmacol Rev* **56**:159.
- Seelig A (1998) A general pattern for substrate recognition by P-glycoprotein. *Eur J Biochem* **251**:252-261.
- Sekine T, Cha SH, Tsuda M, Apiwattanakul N, Nakajima N, Kanai Y and Endou H (1998) Identification of multispecific organic anion transporter 2 expressed predominantly in the liver. *FEBS Lett* **429**:179-182.
- Shimada T, Yamazaki H, Mimura M, Inui Y and Guengerich FP (1994) Interindividual variations in human liver cytochrome P-450 enzymes involved in the oxidation of drugs, carcinogens and toxic chemicals: studies with liver microsomes of 30 Japanese and 30 Caucasians. *J Pharmacol Exp Ther* **270**:414-423.
- Shitara Y, Sugiyama D, Kusuhara H, Kato Y, Abe T, Meier PJ, Itoh T and Sugiyama Y (2002) Comparative inhibitory effects of different compounds on rat oatpl (slc21a1)- and Oatp2 (Slc21a5)-mediated transport. *Pharm Res* **19**:147-153.
- Shitara Y, Itoh T, Sato H, Li AP and Sugiyama Y (2003) Inhibition of transporter-mediated hepatic uptake as a mechanism for drug-drug interaction between cerivastatin and cyclosporin A. *J Pharmacol Exp Ther* **304**:610-616.

- Shitara Y, Hirano M, Sato H and Sugiyama Y (2004) Gemfibrozil and its glucuronide inhibit the organic anion transporting polypeptide 2 (OATP2/OATP1B1:SLC21A6)-mediated hepatic uptake and CYP2C8-mediated metabolism of cerivastatin: analysis of the mechanism of the clinically relevant drug-drug interaction between cerivastatin and gemfibrozil. *J Pharmacol Exp Ther* **311**:228-236.
- Shu Y, Bello CL, Mangravite LM, Feng B and Giacomini KM (2001) Functional characteristics and steroid hormone-mediated regulation of an organic cation transporter in Madin-Darby canine kidney cells. *J Pharmacol Exp Ther* **299**:392-398.
- Siedlik PH, Olson SC, Yang BB and Stern RH (1999) Erythromycin coadministration increases plasma atorvastatin concentrations. *J Clin Pharmacol* **39**:501-504.
- Simonson SG, Raza A, Martin PD, Mitchell PD, Jarcho JA, Brown CD, Windass AS and Schneck DW (2004) Rosuvastatin pharmacokinetics in heart transplant recipients administered an antirejection regimen including cyclosporine. *Clin Pharmacol Ther* **76**:167-177.
- Smith NF, Acharya MR, Desai N, Figg WD and Sparreboom A (2005) Identification of OATP1B3 as a High-Affinity Hepatocellular Transporter of Paclitaxel. *Cancer Biol Ther* **4**.
- Smitherman PK, Townsend AJ, Kute TE and Morrow CS (2004) Role of multidrug resistance protein 2 (MRP2, ABCC2) in alkylating agent detoxification: MRP2 potentiates glutathione S-transferase A1-1-mediated resistance to chlorambucil cytotoxicity. *J Pharmacol Exp Ther* **308**:260-267.

- Spears KJ, Ross J, Stenhouse A, Ward CJ, Goh LB, Wolf CR, Morgan P, Ayrton A and Friedberg TH (2005) Directional trans-epithelial transport of organic anions in porcine LLC-PK1 cells that co-express human OATP1B1 (OATP-C) and MRP2. *Biochem Pharmacol* **69**:415-423.
- Stedman CA, Liddle C, Coulter SA, Sonoda J, Alvarez JG, Moore DD, Evans RM and Downes M (2005) Nuclear receptors constitutive androstane receptor and pregnane X receptor ameliorate cholestatic liver injury. *Proc Natl Acad Sci U S A* **102**:2063-2068.
- Stieger B and Meier PJ (1998) Bile acid and xenobiotic transporters in liver. *Curr Opin Cell Biol* **10**:462-467.
- Strautnieks SS, Bull LN, Knisely AS, Kocoshis SA, Dahl N, Arnell H, Sokal E, Dahan K, Childs S, Ling V, Tanner MS, Kagalwalla AF, Nemeth A, Pawlowska J, Baker A, Mieli-Vergani G, Freimer NB, Gardiner RM and Thompson RJ (1998) A gene encoding a liver-specific ABC transporter is mutated in progressive familial intrahepatic cholestasis. *Nat Genet* **20**:233-238.
- Su SF and Huang JD (1996) Inhibition of the intestinal digoxin absorption and exsorption by quinidine. *Drug Metab Dispos* **24**:142-147.
- Sun H, Huang Y, Frassetto L and Benet LZ (2004) Effects of uremic toxins on hepatic uptake and metabolism of erythromycin. *Drug Metab Dispos* **32**:1239-1246.
- Sun H, Frassetto L and Benet LZ (2006) Effects of renal failure on drug transport and metabolism. *Pharmacol Ther* **109**:1-11.
- Suzuki H and Sugiyama Y (1999) Transporters for bile acids and organic anions. *Pharm Biotechnol* **12**:387-439.

- Suzuki H and Sugiyama Y (2000) Role of metabolic enzymes and efflux transporters in the absorption of drugs from the small intestine. *Eur J Pharm Sci* **12**:3-12.
- Suzuki M, Suzuki H, Sugimoto Y and Sugiyama Y (2003) ABCG2 transports sulfated conjugates of steroids and xenobiotics. *J Biol Chem* **278**:22644-22649.
- Synold TW, Dussault I and Forman BM (2001) The orphan nuclear receptor SXR coordinately regulates drug metabolism and efflux. *Nat Med* **7**:584-590.
- Takano M, Yumoto R and Murakami T (2006) Expression and function of efflux drug transporters in the intestine. *Pharmacol Ther* **109**:137-161.
- Takenaka O, Horie T, Suzuki H and Sugiyama Y (1995) Different biliary excretion systems for glucuronide and sulfate of a model compound; study using Eisai hyperbilirubinemic rats. *J Pharmacol Exp Ther* **274**:1362-1369.
- Takikawa H (2002) Hepatobiliary transport of bile acids and organic anions. *J Hepatobiliary Pancreat Surg* **9**:443-447.
- Tam D, Sun H and Pang KS (2003) Influence of P-glycoprotein, transfer clearances, and drug binding on intestinal metabolism in Caco-2 cell monolayers or membrane preparations: a theoretical analysis. *Drug Metab Dispos* **31**:1214-1226.
- Tamai I, Nezu J, Uchino H, Sai Y, Oku A, Shimane M and Tsuji A (2000) Molecular identification and characterization of novel members of the human organic anion transporter (OATP) family. *Biochem Biophys Res Commun* **273**:251-260.
- Tanaka E (1998) Clinically important pharmacokinetic drug-drug interactions: role of cytochrome P450 enzymes. *J Clin Pharm Ther* **23**:403-416.

- Tanigawara Y, Okamura N, Hirai M, Yasuhara M, Ueda K, Kioka N, Komano T and Hori R (1992) Transport of digoxin by human P-glycoprotein expressed in a porcine kidney epithelial cell line (LLC-PK1). *J Pharmacol Exp Ther* **263**:840-845.
- Thiebaut F, Tsuruo T, Hamada H, Gottesman MM, Pastan I and Willingham MC (1987) Cellular localization of the multidrug-resistance gene product P-glycoprotein in normal human tissues. *Proc Natl Acad Sci U S A* **84**:7735-7738.
- Tirona RG, Leake BF, Merino G and Kim RB (2001) Polymorphisms in OATP-C: identification of multiple allelic variants associated with altered transport activity among European- and African-Americans. *J Biol Chem* **276**:35669-35675.
- Tirona RG, Leake BF, Wolkoff AW and Kim RB (2003) Human organic anion transporting polypeptide-C (SLC21A6) is a major determinant of rifampin-mediated pregnane X receptor activation. *J Pharmacol Exp Ther* **304**:223-228.
- Tokui T, Nakai D, Nakagomi R, Yawo H, Abe T and Sugiyama Y (1999) Pravastatin, an HMG-CoA reductase inhibitor, is transported by rat organic anion transporting polypeptide, oatp2. *Pharm Res* **16**:904-908.
- Trauner M and Boyer JL (2003) Bile salt transporters: molecular characterization, function, and regulation. *Physiol Rev* **83**:633-671.
- Treiber A, Schneiter R, Delahaye S and Clozel M (2004) Inhibition of organic anion transporting polypeptide-mediated hepatic uptake is the major determinant in the pharmacokinetic interaction between bosentan and cyclosporin A in the rat. *J Pharmacol Exp Ther* **308**:1121-1129.

- Tukey RH and Strassburg CP (2000) Human UDP-glucuronosyltransferases: metabolism, expression, and disease. *Annu Rev Pharmacol Toxicol* **40**:581-616.
- Vavricka SR, Van Montfoort J, Ha HR, Meier PJ and Fattinger K (2002) Interactions of rifamycin SV and rifampicin with organic anion uptake systems of human liver. *Hepatology* **36**:164-172.
- Wacher VJ, Wu CY and Benet LZ (1995) Overlapping substrate specificities and tissue distribution of cytochrome P450 3A and P-glycoprotein: implications for drug delivery and activity in cancer chemotherapy. *Mol Carcinog* **13**:129-134.
- Wacher VJ, Silverman JA, Zhang Y and Benet LZ (1998) Role of P-glycoprotein and cytochrome P450 3A in limiting oral absorption of peptides and peptidomimetics. *J Pharm Sci* **87**:1322-1330.
- Wang JS, Neuvonen M, Wen X, Backman JT and Neuvonen PJ (2002) Gemfibrozil inhibits CYP2C8-mediated cerivastatin metabolism in human liver microsomes. *Drug Metab Dispos* **30**:1352-1356.
- Watkins PB, Wrighton SA, Maurel P, Schuetz EG, Mendez-Picon G, Parker GA and Guzelian PS (1985) Identification of an inducible form of cytochrome P-450 in human liver. *Proc Natl Acad Sci U S A* **82**:6310-6314.
- Watkins PB, Wrighton SA, Schuetz EG, Molowa DT and Guzelian PS (1987) Identification of glucocorticoid-inducible cytochromes P-450 in the intestinal mucosa of rats and man. *J Clin Invest* **80**:1029-1036.
- Wilkinson GR and Shand DG (1975) Commentary: a physiological approach to hepatic drug clearance. *Clin Pharmacol Ther* **18**:377-390.

- Wilkinson GR (1983) Plasma and tissue binding considerations in drug disposition. *Drug Metab Rev* 14:427-465.
- Wu CY, Benet LZ, Hebert MF, Gupta SK, Rowland M, Gomez DY and Wachter VJ (1995) Differentiation of absorption and first-pass gut and hepatic metabolism in humans: studies with cyclosporine. *Clin Pharmacol Ther* 58:492-497.
- Wu CY and Benet LZ (2003) Disposition of tacrolimus in isolated perfused rat liver: influence of troleandomycin, cyclosporine, and gg918. *Drug Metab Dispos* 31:1292-1295.
- Wu CY and Benet LZ (2005) Predicting drug disposition via application of BCS: transport/absorption/ elimination interplay and development of a biopharmaceutics drug disposition classification system. *Pharm Res* 22:11-23.
- Wu X, Whitfield LR and Stewart BH (2000) Atorvastatin transport in the Caco-2 cell model: contributions of P-glycoprotein and the proton-monocarboxylic acid co-transporter. *Pharm Res* 17:209-215.
- Zelcer N, van de Wetering K, Hillebrand M, Sarton E, Kuil A, Wielinga PR, Tephly T, Dahan A, Beijnen JH and Borst P (2005) Mice lacking multidrug resistance protein 3 show altered morphine pharmacokinetics and morphine-6-glucuronide antinociception. *Proc Natl Acad Sci U S A* 102:7274-7279.
- Zhang L, Dresser MJ, Gray AT, Yost SC, Terashita S and Giacomini KM (1997) Cloning and functional expression of a human liver organic cation transporter. *Mol Pharmacol* 51:913-921.

Zhang L, Gorset W, Dresser MJ and Giacomini KM (1999) The interaction of n-tetraalkylammonium compounds with a human organic cation transporter, hOCT1. *J Pharmacol Exp Ther* **288**:1192-1198.

Zhang Y and Benet LZ (2001) The gut as a barrier to drug absorption: combined role of cytochrome P450 3A and P-glycoprotein. *Clin Pharmacokinet* **40**:159-168.

Zong J and Pollack GM (2003) Modulation of P-glycoprotein transport activity in the mouse blood-brain barrier by rifampin. *J Pharmacol Exp Ther* **306**:556-562.

[Faint, illegible text, likely bleed-through from the reverse side of the page]

UNIVERSITY OF MICHIGAN



UNIVERSITY OF MICHIGAN

7542072



3 1378 00754 2072

SAN FRANCISCO

For reference

Not to be taken
from the room.

